



**HAL**  
open science

# Etude d'acteurs moléculaires et cellulaires dans le métabolisme du cholestérol

Thierry Huby

► **To cite this version:**

Thierry Huby. Etude d'acteurs moléculaires et cellulaires dans le métabolisme du cholestérol. Sciences du Vivant [q-bio]. SORBONNE UNIVERSITE, 2022. tel-04034820

**HAL Id: tel-04034820**

**<https://hal.sorbonne-universite.fr/tel-04034820>**

Submitted on 24 Mar 2023

**HAL** is a multi-disciplinary open access archive for the deposit and dissemination of scientific research documents, whether they are published or not. The documents may come from teaching and research institutions in France or abroad, or from public or private research centers.

L'archive ouverte pluridisciplinaire **HAL**, est destinée au dépôt et à la diffusion de documents scientifiques de niveau recherche, publiés ou non, émanant des établissements d'enseignement et de recherche français ou étrangers, des laboratoires publics ou privés.

**Sorbonne Université**

Mémoire pour l'obtention de l'  
**Habilitation à Diriger les Recherches**

Présenté par

Thierry HUBY

Le 15 Juin 2022

**Etude d'acteurs moléculaires et cellulaires dans le  
métabolisme du cholestérol**

**Jury**

Dr Muriel Laffargue, INSERM, IC2M toulouse

Dr David Masson, INSERM, Université de Bourgogne

Dr Xavier Collet, INSERM, IC2M toulouse

Dr Hélène Duez, INSERM, Université de Lille

Dr Fabienne Foufelle, INSERM, Sorbonne Université Paris

# Table des matières

<b><u>TABLE DES MATIÈRES.....</u></b>	<b><u>2</u></b>
<b><u>CURRICULUM VITAE.....</u></b>	<b><u>3</u></b>
<b><u>ENCADREMENT, FORMATION ET DIRECTION SCIENTIFIQUE .....</u></b>	<b><u>7</u></b>
<b><u>PUBLICATIONS .....</u></b>	<b><u>11</u></b>
<b><u>MEMOIRE .....</u></b>	<b><u>17</u></b>
<b>1. LA LIPOPROTEINE (A). .....</b>	<b>17</b>
<b>2. APOA5 ET METABOLISME DES TRIGLYCERIDES. ....</b>	<b>19</b>
<b>3. ÉTUDE DU RECEPTEUR SR-B1 DANS LE METABOLISME DU CHOLESTEROL ET COMME FACTEUR DE RISQUE DE L'ATHEROSCLEROSE.....</b>	<b>20</b>
3.1- REGULATIONS MOLECULAIRE ET CELLULAIRE DE SR-B1 AU NIVEAU HEPATIQUE.....	21
3.2- ETUDE DE L'ACTIVITE DU RECEPTEUR SR-B1 POUR FACILITER L'EFFLUX CELLULAIRE DU CHOLESTEROL .....	21
3.3- <i>ROLE DE SR-B1 DANS LA VOIE DU TRANSPORT INVERSE DU CHOLESTEROL (RCT) IN VIVO ET COMME FACTEUR DE RISQUE DE L'ATHEROSCLEROSE. ....</i>	<i>22</i>
3.4- <i>EXPLORATION DU ROLE ANTI-ATHEROGENE DE SR-B1 EXPRIME PAR LE MACROPHAGE. ....</i>	<i>25</i>
<b>4 ROLE DE SR-B1 DANS L'APPORT DE CHOLESTEROL POUR LA PRODUCTION ENDOGENE DE GLUCOCORTICOÏDES PAR LA GLANDE SURRENALE ET LA PROTECTION CONTRE LE CHOC SEPTIQUE .....</b>	<b>26</b>
<b><u>RESEARCH PROJECT .....</u></b>	<b><u>29</u></b>
<b><u>SELECTED PUBLICATIONS .....</u></b>	<b><u>35</u></b>

## Curriculum Vitae

### Thierry Huby, PhD

ORCID # 0000-0001-6634-551X

Researcher ID: E-6768-2017

#### **UMR-S 1166**

Team 5 / Mononuclear phagocytes in cardiometabolic diseases

Faculté de médecine Pierre et Marie Curie

Bureau 421 - 4ème étage

91, Boulevard de l'hôpital

75013 Paris

Né le 20 Octobre 1969

Nationalité : Française

Marié, 4 enfants

Tél : 33 (1) 40 77 95 04

[thierry.huby@universite-sorbone.fr](mailto:thierry.huby@universite-sorbone.fr)

[thierry.huby@inserm.fr](mailto:thierry.huby@inserm.fr)

### ✓ Diplômes

- 1991 - 1992 :** DEA (Master) " Structure, fonctions et ingénierie des protéines"  
Université PARIS VII / Institut Pasteur
- 1992 - 1993 :** Service National
- 1993 - 1997 :** Thèse de Doctorat de l'Université Paris VII. (Mention "Très Honorable")  
Spécialité : " Structure, fonctions et ingénierie des protéines".  
Titre du mémoire : "Relation Structure-Fonction de la Lipoprotéine (a) :  
Etude des Domaines Structuraux de l'Apolipoprotéine (a) et de leur  
Liaison à la Fibrine".
- 2000 :** Certificat d'Autorisation d'expérimenter sur Animaux Vertébrés, Niveau 1.
- 2000 :** Formation à la chirurgie expérimentale

### ✓ Expérience professionnelle

- 1991/92 – 1993-97 :** DEA puis thèse à l'Unité INSERM 321 "Lipoprotéines et Athérogénèse"  
Directeur du laboratoire : Dr John CHAPMAN
- 1997 – 1999** American Heart Association post-doctoral fellow au Lawrence Berkeley  
National laboratory, CA, USA  
Genome Sciences Department  
Directeur du laboratoire : Dr Edward RUBIN
- Oct 1999-2008** UMR\_S 551 "Dyslipoprotéïnémies et Athérosclérose"  
Directeur du laboratoire : Dr John CHAPMAN

Chargé de Recherche INSERM CR2 (1999-2003) ; CR1 (2004-)

- 2009-2014**      **UMR\_S 939** - "Dyslipidémies, inflammation et athérosclérose dans les maladies métaboliques"  
Directeur du laboratoire : Dr Philippe LESNIK  
Chargé de Recherche INSERM CR1
- 2014-2018**      **UMR\_S 1166** – Equipe 4  
Dir. du laboratoire: Dr Stéphane Hatem ; Resp équipe : P. Lesnik  
-Chargé de Recherche INSERM CR1
- 2014-2021**      Responsable scientifique de la Plateforme préclinique PreclinICAN d'exploration CardioMétabolique de l'IHU ICAN.
- 2019-présent**      **UMR\_S 1166\_Equipe 5**  
[Site web: recherche-cardiovasculaire-metabolique.fr/teams/teams/mononuclear-phagocytes-in-cardiometabolic-diseases/](http://recherche-cardiovasculaire-metabolique.fr/teams/teams/mononuclear-phagocytes-in-cardiometabolic-diseases/)  
Dir. du laboratoire : Dr Stéphane Hatem ; Resp. équipe : P. Lesnik  
- Chargé de Recherche INSERM CRHC

## √ Bourses

- 1993-96**      Allocation de recherche par le **Ministère de l'Enseignement Supérieur et de la Recherche**
- 1996**      Bourse de la **Fondation Phillippe**
- 1997**      Bourse post-doctorale **Parke Davis/Arcol**
- 1998 et 1999** Bourse post-doctorale de l'**American Heart Association**, Western Affiliate

## √ Appartenance à des sociétés savantes, groupes de réflexion

Membre de la **NSFA** (Nouvelle Société Française d'athérosclérose)

Membre du comité d'éthique pour l'expérimentation animale **Charles Darwin** (CE5)

## √ Activités de revues

Activité comme membre examinateur de jury de thèse : Université Paris 6, 2007; Université de Leiden, Netherlands, 2011; - Université Paris 6, 2014; Université Paris 7, 2015, Sorbonne Université, 2019 & 2020

Activité en tant que 'reviewer' scientifique pour les revues : The Journal of Vascular Research (1); Arteriosclerosis, Thrombosis, and Vascular Biology (14); PlosOne (2); Atherosclerosis (12); Anesthesiology (1)

## ✓ Financements / Prix

- 2003-05** **HDL International Research Award** "Hepatic versus non hepatic SRBI expression: relevance to the role of macrophages in atherogenesis" (Lesnik P., co-lauréat Huby T.) -
- 2005-07** **HDL International Research Award** "Impact of peripheral versus hepatic expression of scavenger receptor SR-B1 on reverse cholesterol transport, atherosclerosis and cardiovascular disease" (Huby T.,) -
- 2007-2010** Appel d'offre **ANRS 2007** - Programme collaboratif de recherche avec le Dr Agata Budkowska (porteur) de l'Institut Pasteur (Unité Hépacivirus) portant sur le rôle de la lipoprotéine lipase et lipoprotéines associées aux virus dans l'infection par le virus de l'hépatite C.
- 2007-10** **Fondation Cœur et Artères:** "Modulation thérapeutique du transport Inverse du Cholestérol dans des modèles murins d'athérosclérose et d'infarctus" - Co-lauréats : Huby T., Lesnik P. et Le Goff W.
- 2007-2010** Programme de recherche collaboratif avec le groupe pharmaceutique **GlaxoSmithKline** portant sur "Pharmacological modulation of myocardial infarction events in mouse models". Co-responsables Huby T. & Lesnik P
- 2008-12** **Bénéficiaire d'un contrat d'interface vers l'Hôpital**  
Les Lipoprotéines de haute densité HDL et leur relation au risque cardiovasculaire: Recherche des déterminants génétiques, épigénétiques et identification de nouveaux marqueurs diagnostiques.
- 2009-12** **ANR GENOPATH** –"Lipoprotéines de Haute Densité et protection contre les maladies cardiovasculaires" – Porteur : Huby T.
- 2011-13** **Fondation de France** " Impact de la sécrétion des glucocorticoïdes endogènes en réponse à un stress lipidique chronique dans le développement du syndrome métabolique et l'athérosclérose" - Porteur : Huby T.
- 2011-13** Contrat de Recherche / **Roche** –"Evaluation de nouveaux inhibiteurs de la CETP et d'activateurs du transport Inverse du Cholestérol ". Porteur : Huby T.
- 2013-15** Projet DeNoMAtE - **IHU ICAN**. Porteurs Drs P. Couvert et A. Carrié. Partenaire Huby T. pour l'évaluation du rôle de la méthylation de Novo sur la fonctionnalité et l'adaptation à l'environnement de la cellule dendritique.
- 2015-17** **Labex Lermite** Porteur V. Dice (CEA), Partenaires Inserm (co-porteurs : Huby, Lesnik, Le Goff, Gautier)
- 2018-22** **ANR AAPG 2017**. Projet Rephago: Identification of new receptors at the RPE apical cell surface for the diurnal regulation of retinal phagocytosis  
Porteur : E. Nandrot (IDV) ; partenaire : Huby T.
- 2019-22** **Fondation de France**. "Rôle des cellules de Kupffer dans l'homéostasie du cholestérol et l'athérosclérose" - Porteur : Huby T.
- 2021-23** **Sorbonne University programme Emergence 2021**. Kupffer cells at the interface of cholesterol and iron homeostasis. Porteur : Huby T.

**2021-25**     **ANR AAPG 2021.** Projet ROKHY ; Porteur : Huby T ; Partenaires : Carole Peyssonnaud (UMRS\_1016) et Alexandre Boissonnas (UMRS\_1235).

## Encadrement, Formation et Direction Scientifique

### Techniciens/Ingénieurs

- 2000–2007** M<sup>me</sup> Chantal Doucet (**Technicienne TRE INSERM**; Départ en retraite 06/2007);
- 2001-2003** M<sup>me</sup> Christiane Dachet (**Ingénieure d'Etude INSERM** ; Départ en retraite 06/2003);
- 2007-2008** M<sup>lle</sup> Betty Ouzilleau (**Technicienne** recrutée en CDD; Financement Fondation Cœur et Artères)
- 2009-2010** M<sup>me</sup> Jacqueline Polyte (**Ingénieure d'Etude** recrutée en CDD; Financement Fondation Cœur et Artères).
- 2012-2015** M<sup>lle</sup> Raphaëlle Ballaire (**Ingénieure d'Etude** recrutée en CDD; Contrat de Recherche avec ROCHE).
- 2002-2021** M<sup>me</sup> Martine Moreau (**Assistante Ingénieure INSERM**)
- 2014-2021** M<sup>me</sup> Amélie Lacombe (**Ingénieure d'Etude IHU ICAN**), plateforme préclinique
- 2021-2022** M<sup>me</sup> Cheima Benbida (**Ingénieure d'Etude** recrutée en CDD; projet ANR)

### Étudiants de Licence et M1 (Maîtrise)

- 05-06/2003** M<sup>lle</sup> Magalie Niasme – **Licence** de Biologie Cellulaire et Physiologie de l'Université Paris Sud; Projet : "Mise au point d'un protocole de purification de l'apolipoprotéine APO-AV".
- 04-05/2005** M<sup>lle</sup> Aurélie Guislain - **Master1 Recherche** "Biologie Cellulaire, Physiologie et Pathologie" (BCPP) de l'Université Paris 7 Diderot"; Projet: "Atténuation de l'expression du récepteur scavenger Cla-1 par ARN interférence dans les lignées cellulaires CHO-K1 et Huh7".
- 04-06/2008** M<sup>r</sup> Chan Kessara - **Master 1 Recherche** "Biologie Intégrative et Physiologique" (BIP) de l'Université Paris 6-Pierre et Marie Curie; Projet: "Expression et purification de protéines APO-A1 recombinantes humaines à partir de souches de levure *pichia pastoris* génétiquement modifiées".
- 05-06/2010** M<sup>lle</sup> Julie Soulié - **Master 1 Recherche** "Biologie Intégrative et Physiologique" (BIP) de l'Université Paris 6-Pierre et Marie Curie; Projet: "Etude du rôle de SR-B1 au niveau endothélial: mise au point d'une culture primaire de cellules endothéliales d'aorte de souris".



- 05-06/2010** M<sup>r</sup> Florian Gondelle - **Master 1 Recherche** "Biologie Intégrative et Physiologique" (BIP) de l'Université Paris 6-Pierre et Marie Curie; Projet: "Effet de la vitamine D sur l'expression des récepteurs scavenger de macrophages murins".
- 06-07/2012** M<sup>lle</sup> Meriem Sahli – **Licence L3** "Génie Biologique et Informatique" de l'Université d'Evry Val Essone Projet: "Mise au point de protocoles de génotypage".
- 04-06/2017** M<sup>r</sup> Alexis Casciato – **Master 1 Recherche** "Biologie Intégrative et Physiologique" (BIP) de l'Université Paris 6-Pierre et Marie Curie  
Projet: "Impact du cholestérol exogène sur les cellules de Kupffer".
- 02-03/2017** M<sup>r</sup> Thomas Huby – Étudiant en Pharmacie, filière PHBMR (5<sup>ème</sup> année) de l'Université Paris Saclay. Stage équivalent **Master 1**
- 05-06/2018** M<sup>lle</sup> Gabrielle Dupuis – **Master 1 Recherche** "Biologie Intégrative et Physiologique" (BIP) de l'Université Paris 6-Pierre et Marie Curie  
Projet: "Impact de l'hypercholestérolémie sur le métabolisme des érythrocytes".
- 11/18-02/19** M<sup>lle</sup> Sankeetha Vickneswaran - **DUT** Génie Biologique Université Paris 13  
Projet: "Validation d'un nouveau modèle de souris pour l'étude des cellules de Kupffer"
- 02/20-08/20** M<sup>lle</sup> Elsa Bernard – **Licence Pro** Biotechnologies et Bio-industries Université Paris Saclay  
Projet: "Exploration du rôle du récepteur éboueur Colec12 dans l'élimination des lipoprotéines oxydées par les macrophages"

### Etudiants de M2 (DEA) et Ingénieur CNAM

- 2000-2001** M<sup>lle</sup> Morgan Tréguier – **Master 2 Recherche** "Endocrinologie et signalisation cellulaires" de l'Université Paris XI– Projet: "Régulation moléculaire et cellulaire du récepteur scavenger Cla-1 dans la cellule hépatique".
- 2003-2005** M<sup>lle</sup> Guilaine Grémy – Diplôme d'**Ingénieur** du Conservatoire National des Arts et Métiers (Paris), Spécialité Sciences et Techniques du Vivant, Option Génie Biologique; Projet : "Expression hépatique par transfert de gène du récepteur scavenger humain SR-B1/CLA-I chez la souris : impact sur le profil lipoprotéique".
- 2005-2006** M<sup>lle</sup> Majda El Bouhassani - **Master 2 Recherche** "Biologie Intégrative et Physiologie" (BIP) de l'Université Paris 6-Pierre et Marie Curie, Spécialité Physiologie et Physiopathologie – Projet: "Relation entre la protéine de transfert des esters de cholestérol CETP et le récepteur SR-B1 dans l'homéostasie du cholestérol".

- 08-11/2006** M<sup>r</sup> Nour-Eddine Sellak - Stage pratique pour le Diplôme *d'Etudes Supérieures et Techniques* (DEST) du Conservatoire National des Arts et Métiers (Paris); Projet : "Etude du profil d'expression de la protéine de transfert des esters de cholestérol (CETP) chez la souris transgénique".
- 2010-2011** M<sup>lle</sup> Lauriane Galle - **Master 2 Recherche** Biologie Cellulaire, Physiologie et Pathologie" (BCPP) de l'Université Paris 7 Diderot, Spécialité Nutrition Métabolisme Signalisation (Numési) – Projet: "Caractérisation du rôle anti-inflammatoire de SR-B1 dans le macrophage".
- 12/13-06/14** M<sup>lle</sup> Cécile Scimeca - **Master 2 Recherche** Biologie Intégrative et Physiologie" (BIP) de l'Université Paris 6-Pierre et Marie Curie, Spécialité Physiologie et Physiopathologie – Projet: "Implication de l'axe HDL-C, SR-B1 dans la production circadienne des glucocorticoïdes et dans le contrôle périphérique du cycle nyctéméral".
- 12/14-06/15** M<sup>r</sup> Zakarya El Mohtassem - **Master 2 Recherche** Biologie Intégrative et Physiologie" (BIP) de l'Université Paris 6-Pierre et Marie Curie, Spécialité : Physiologie, métabolisme et physiopathologies humaines – Projet: " Impact of targeted deletion of *de novo* DNA methylation by DNMT3A in dendritic (CD11c<sup>+</sup>) cells *in vivo* "
- 03/17-09/17** M<sup>r</sup> Tommaso Mancini – **Master student; Erasmus+** Programme d'échange (Higher Education Learning agreement) avec l'Université de Parme (Italie). Projet: "Métabolisme du cholestérol et macrophages".
- 12/17-06/18** M<sup>lle</sup> Rebecca Fima – **Master 2 Recherche** Biologie Intégrative et Physiologie" (BIP) de l'Université Paris 6-Pierre et Marie Curie. Projet: " Réponse des Cellules de Kupffer à l'hypercholestérolémie".
- 01/20-06/20** M<sup>lle</sup> Hiba Yazbek – **Master 2 Recherche** Sciences, Technologie et Santé de l'Université Claude Bernard Lyon1. Projet: "Interaction of lipid and iron metabolism in Kupffer cells".
- 01/21-06/21** M<sup>lle</sup> Cheima Benbida – **Master 2 Recherche** Biologie Intégrative et Physiologie" (BIP) de Sorbonne Université. Projet : "Métabolisme des lipides et du fer dans les cellules de Kupffer".
- 03/21-08/21** M<sup>lle</sup> Claudia Brambilla – **Corso di Laurea Magistrale in Farmacia\_Tesi Sperimentale** avec l'Université de Parme (Italie). Projet : "Liver Immune Zonation Kupffer response to hypercholesterolemia".
- 01/22-06/22** M<sup>lle</sup> Merve Guler – **Master 2 Recherche** Biologie Intégrative et Physiologie" (BIP) de Sorbonne Université. Projet: "Exploration du rôle du facteur de transcription Bhlhe40 dans l'homéostasie des cellules de Kupffer".

## Doctorant(e)s

- 2002-2006** M<sup>lle</sup> Morgan Tréguier - Ecole doctorale "Signalisations, Neurosciences, Endocrinologie, Reproduction" de l'Université Paris XI. Lauréate d'une allocation du Ministère de la Recherche. Projet : « Etude la régulation de l'expression du récepteur SR-B1/Cla1 par le cholestérol et caractérisation de sa fonction d'efflux cellulaire de cholestérol ». Thèse soutenue le 28 Juin 2006. Directeur de thèse officiel : John Chapman
- 2007** M<sup>r</sup> Francesco Poti: Programme d'échange avec le laboratoire du Prof. Franco Bernini et l'Université de Parme (Italie), Faculté de Pharmacie. Encadrement de la 3<sup>ème</sup> année de thèse intitulée "Pharmacological approaches for modulating the Reverse Cholesterol Transport (RCT)". Thèse soutenue en Italie le 3 Mars 2008.
- 2009** M<sup>lle</sup> Sara Costa: Programme d'échange avec le laboratoire du Prof. Franco Bernini et l'Université de Parme (Italie), Faculté de Pharmacie. Encadrement de la 3<sup>ème</sup> année de thèse intitulée "Endothelial cells and atherosclerosis: in vitro and in vivo studies.". Thèse soutenue en Italie le 3 Avril 2010.
- 2007 – 2010** M<sup>lle</sup> Majda El Bouhassani - Ecole doctorale (394) de Physiologie et Physiopathologie de l'Université Paris 6-Pierre et Marie Curie. Lauréate d'une allocation du Ministère de la Recherche. Projet : "Impact de la CETP sur le transport inverse du cholestérol et l'athérosclérose chez la souris déficiente en SR-B1". Thèse soutenue le 12 Juillet 2010. Directeur de thèse officiel : John Chapman
- 2011 – 2015** M<sup>lle</sup> Lauriane Galle - Ecole doctorale (394) de Physiologie et Physiopathologie de l'Université Paris 6-Pierre et Marie Curie. Lauréate d'une allocation du CODDIM (région Ile de France). Projet : " Implication du récepteur Scavenger SR-B1 dans la réponse immuno-inflammatoire – relation au risque cardio-vasculaire". Directrice de thèse officielle : J. Thillet/P. Lesnik
- 2019 – 2022** M<sup>lle</sup> Rebecca Fima - École doctorale (394) de Physiologie et Physiopathologie de l'Université Sorbonne. Lauréate d'une allocation du Ministère de la Recherche. Projet : " Rôle des cellules de Kupffer dans l'homéostasie du cholestérol". Directeur de thèse officielle : A. Carrié
- 2022 – 2025** M<sup>lle</sup> Margault Blanchet - École doctorale (394) de Physiologie et Physiopathologie de l'Université Sorbonne. Projet : " Kupffer cells at the interface of cholesterol and iron homeostasis ". Directeur de thèse officielle : G. Helft

## Post-doctorant(e)s

- 2000-2002** Dr Andrei Sposito M.D., Ph.D. – Médecin Cardiologue Brésilien; Stage post-doctoral effectué dans le cadre d'un poste vert INSERM

**2009-2013** Dr Sophie Gilibert, Ph.D. – Stage post-doctoral effectué dans le cadre d'un projet financé par l'Agence National pour la Recherche dans le cadre de l'appel d'offre GENOPATH 2008. Projet : "Contribution du récepteur scavenger SR-B1 endothélial dans l'athérosclérose – étude in vivo".

## Publications

(Étudiant(e)s encadré(e)s indiqués en bleu \_ ITA encadré(e)s en vert)

1. **Huby T**, Le Goff W. Macrophage SR-B1 in atherosclerotic cardiovascular disease Curr Opin Lipidol 2022, 33
2. **Huby T**, Gautier EL. Immune cell-mediated features of non-alcoholic steatohepatitis. Nat Rev Immunol. 2021 Nov 5:1–15.
3. Lécuyer E, Le Roy T, Gestin A, **Lacombe A**, Philippe C, Ponnaiah M, Huré JB, Fradet M, Ichou F, Boudebouze S, **Huby T**, Gautier E, Rhimi M, Maguin E, Kapel N, Gérard P, Venteclef N, Garlatti M, Chassaing B, Lesnik P. Tolerogenic Dendritic Cells Shape a Transmissible Gut Microbiota That Protects From Metabolic Diseases. Diabetes. 2021 Sep;70(9):2067-2080.
4. Ma F, Darabi M, Lhomme M, Tubeuf E, Canicio A, Brerault J, Medadje N, Rached F, Lebreton S, Frisdal E, Brites F, Serrano C, Santos R, Gautier E, **Huby T**, El Khoury P, Carrié A, Abifadel M, Bruckert E, Guerin M, Couvert P, Giral P, Lesnik P, Le Goff W, Guillas I, Kontush A. Phospholipid transfer to high-density lipoprotein (HDL) upon triglyceride lipolysis is directly correlated with HDL-cholesterol levels and is not associated with cardiovascular risk. Atherosclerosis. 2021 May;324:1-8.
5. Tran-Dinh A, Levoye A, Couret D, **Galle-Treger L**, **Moreau M**, Delbosc S, Hoteit C, Montravers P, Amarenco P, **Huby T**, Meilhac O. High-Density Lipoprotein Therapy in Stroke: Evaluation of Endothelial SR-B1-Dependent Neuroprotective Effects. Int J Mol Sci. 2020 Dec 24;22(1):106.
6. Langlois AC, Manzoni G, Vincensini L, Coppée R, Marinach C, Guérin M, **Huby T**, Carrière V, Cosset FL, Dreux M, Rubinstein E, Silvie O. Molecular determinants of SR-B1-dependent Plasmodium sporozoite entry into hepatocytes. Sci Rep. 2020 Aug 11;10(1):13509.
7. Tran S, Baba I, Poupel L, Dussaud S, **Moreau M**, Gélinau A, Marcelin G, Magréau-Davy E, Ouhachi M, Lesnik P, Boissonnas A, Le Goff W, Clausen BE, Yvan-Charvet L, Sennlaub F, **Huby T**, Gautier EL. Impaired Kupffer Cell Self-Renewal Alters the Liver Response to Lipid Overload during Non-alcoholic Steatohepatitis. Immunity. 2020 Sep 15;53(3):627-640.e5
8. **Galle-Treger L**, **Moreau M**, **Ballaire R**, Poupel L, **Huby T**, Sasso E, Troise F, **Poti F**, Lesnik P, Le Goff W, Gautier EL, **Huby T**. Targeted invalidation of SR-B1 in macrophages reduces macrophage apoptosis and accelerates atherosclerosis. Cardiovasc Res. 2020 Mar 1;116(3):554-565.

9. Feng M, Darabi M, Tubeuf E, Canicio A, Lhomme M, Frisdal E, Lanfranchi-Lebreton S, Matheron L, Rached F, Ponnaiah M, Serrano CV Jr, Santos RD, Brites F, Bolbach G, Gautier E, **Huby T**, Carrie A, Bruckert E, Guerin M, Couvert P, Giral P, Lesnik P, Le Goff W, Guillas I, Kontush A. Free cholesterol transfer to high-density lipoprotein (HDL) upon triglyceride lipolysis underlies the U-shape relationship between HDL-cholesterol and cardiovascular disease. *Eur J Prev Cardiol*. 2019 doi: 10.1177/2047487319894114.
10. Le Roy T, Lécuyer E, Chassaing B, Rhimi M, Lhomme M, Boudebouze S, Ichou F, Haro Barceló J, **Huby T**, Guerin M, Giral P, Maguin E, Kapel N, Gérard P, Clément K, Lesnik P. The intestinal microbiota regulates host cholesterol homeostasis. *BMC Biol*. 2019 Nov 27;17(1):94.
11. Kautbally S, Lepropre S, Onselaer MB, Le Rigoleur A, Ginion A, De Meester de Ravenstein C, Ambroise J, Boudjeltia KZ, Octave M, Wéra O, Hego A, Pincemail J, Cheramy-Bien JP, **Huby T**, Giera M, Gerber B, Pouleur AC, Guigas B, Vanoverschelde JL, Kefer J, Bertrand L, Oury C, Horman S, Beauloye C. Platelet Acetyl-CoA Carboxylase Phosphorylation: A Risk Stratification Marker That Reveals Platelet-Lipid Interplay in Coronary Artery Disease Patients. *JACC Basic Transl Sci*. 2019 Sep 11;4(5):596-610.
12. Beliard S, Le Goff W, Saint-Charles F, Poupel L, Deswaerte V, Bouchareychas L, **Huby T**, Lesnik P. Modulation of Gr1(low) monocyte subset impacts insulin sensitivity and weight gain upon high-fat diet in female mice. *Int J Obes (Lond)* 2017;**41**:1805-1814.
13. Manzoni G, Marinach C, Topcu S, Briquet S, Grand M, Tolle M, Gransagne M, Lescar J, Andolina C, Franetich JF, Zeisel MB, **Huby T**, Rubinstein E, Snounou G, Mazier D, Nosten F, Baumert TF, Silvie O. Plasmodium P36 determines host cell receptor usage during sporozoite invasion. *Elife* 2017;**6**.
14. Vancraeynest D, Roelants V, Bouzin C, Hanin FX, Walrand S, Bol V, Bol A, Pouleur AC, Pasquet A, Gerber B, Lesnik P, **Huby T**, Jamar F, Vanoverschelde JL. alphaVbeta3 integrin-targeted microSPECT/CT imaging of inflamed atherosclerotic plaques in mice. *EJNMMI Res* 2016;**6**:29.
15. Jacobsen MJ, Mentzel CM, Olesen AS, **Huby T**, Jorgensen CB, Barres R, Fredholm M, Simar D. Altered Methylation Profile of Lymphocytes Is Concordant with Perturbation of Lipids Metabolism and Inflammatory Response in Obesity. *J Diabetes Res* 2016;**2016**:8539057.
16. El Khoury P, Waldmann E, **Huby T**, Gall J, Couvert P, Lacorte JM, Chapman J, Frisdal E, Lesnik P, Parhofer KG, Le Goff W, Guerin M. Extended-Release Niacin/Laropiprant Improves Overall Efficacy of Postprandial Reverse Cholesterol Transport. *Arterioscler Thromb Vasc Biol* 2016;**36**:285-294.
17. Pant SD, Karlskov-Mortensen P, Jacobsen MJ, Cirera S, Kogelman LJ, Bruun CS, Mark T, Jorgensen CB, Grarup N, Appel EV, Galijatovic EA, Hansen T, Pedersen O, Guerin M, **Huby T**, Lesnik P, Meuwissen TH, Kadarmideen HN, Fredholm M. Comparative Analyses of QTLs Influencing Obesity and Metabolic Phenotypes in Pigs and Humans. *PLoS One* 2015;**10**:e0137356.
18. Hescot S, Seck A, Guerin M, Cockenpot F, **Huby T**, Broutin S, Young J, Paci A, Baudin E, Lombes M. Lipoprotein-Free Mitotane Exerts High Cytotoxic Activity in Adrenocortical Carcinoma. *J Clin Endocrinol Metab* 2015;**100**:2890-2898.

19. Bouchareychas L, Pirault J, Saint-Charles F, Deswaerte V, Le Roy T, Jessup W, Giral P, Le Goff W, **Huby** T, Gautier EL, Lesnik P. Promoting macrophage survival delays progression of pre-existing atherosclerotic lesions through macrophage-derived apoE. *Cardiovasc Res* 2015;**108**:111-123.
20. Frisdal E, Le Lay S, Hooton H, Poupel L, Olivier M, Alili R, Plengpanich W, Villard EF, **Gilibert S**, Lhomme M, Superville A, Miftah-Alkhair L, Chapman MJ, Dallinga-Thie GM, Venteclef N, Poitou C, Tordjman J, Lesnik P, Kontush A, **Huby** T, Dugail I, Clement K, Guerin M, Le Goff W. Adipocyte ATP-binding cassette G1 promotes triglyceride storage, fat mass growth, and human obesity. *Diabetes* 2015;**64**:840-855.
21. **Gilibert S**, Galle-Treger L, Moreau M, Saint-Charles F, Costa S, Ballaire R, Couvert P, Carrie A, Lesnik P, **Huby** T. Adrenocortical scavenger receptor class B type I deficiency exacerbates endotoxic shock and precipitates sepsis-induced mortality in mice. *J Immunol* 2014;**193**:817-826.
22. Shearn AI, Deswaerte V, Gautier EL, Saint-Charles F, Pirault J, Bouchareychas L, Rucker EB, 3rd, Beliard S, Chapman J, Jessup W, **Huby** T, Lesnik P. Bcl-x inactivation in macrophages accelerates progression of advanced atherosclerotic lesions in Apoe(-/-) mice. *Arterioscler Thromb Vasc Biol* 2012;**32**:1142-1149.
23. Maillard P, Walic M, Meuleman P, Roohvand F, **Huby** T, Le Goff W, Leroux-Roels G, Pecheur EI, Budkowska A. Lipoprotein lipase inhibits hepatitis C virus (HCV) infection by blocking virus cell entry. *PLoS One* 2011;**6**:e26637.
24. Zhao Y, Pennings M, Vrins CL, Calpe-Berdiel L, Hoekstra M, Kruijt JK, Ottenhoff R, Hildebrand RB, van der Sluis R, Jessup W, Le Goff W, Chapman MJ, **Huby** T, Groen AK, Van Berkel TJ, Van Eck M. Hypocholesterolemia, foam cell accumulation, but no atherosclerosis in mice lacking ABC-transporter A1 and scavenger receptor BI. *Atherosclerosis* 2011;**218**:314-322.
25. Frisdal E, Lesnik P, Olivier M, Robillard P, Chapman MJ, **Huby** T, Guerin M, Le Goff W. Interleukin-6 protects human macrophages from cellular cholesterol accumulation and attenuates the proinflammatory response. *J Biol Chem* 2011;**286**:30926-30936.
26. El Bouhassani M, **Gilibert S**, Moreau M, Saint-Charles F, Treguier M, Poti F, Chapman MJ, Le Goff W, Lesnik P, **Huby** T. Cholesteryl ester transfer protein expression partially attenuates the adverse effects of SR-B1 receptor deficiency on cholesterol metabolism and atherosclerosis. *J Biol Chem* 2011;**286**:17227-17238.
27. Fabre AC, Malaval C, Ben Addi A, Verdier C, Pons V, Serhan N, Lichtenstein L, Combes G, **Huby** T, Briand F, Collet X, Nijstad N, Tietge UJ, Robaye B, Perret B, Boeynaems JM, Martinez LO. P2Y13 receptor is critical for reverse cholesterol transport. *Hepatology* 2010;**52**:1477-1483.
28. Catanese MT, Ansuini H, Graziani R, **Huby** T, Moreau M, Ball JK, Paonessa G, Rice CM, Cortese R, Vitelli A, Nicosia A. Role of scavenger receptor class B type I in hepatitis C virus entry: kinetics and molecular determinants. *J Virol* 2010;**84**:34-43.
29. Gautier EL, **Huby** T, Saint-Charles F, Ouzilleau B, Pirault J, Deswaerte V, Ginhoux F, Miller ER, Witztum JL, Chapman MJ, Lesnik P. Conventional dendritic cells at the crossroads between immunity and cholesterol homeostasis in atherosclerosis. *Circulation* 2009;**119**:2367-2375.

30. Prieur X, Lesnik P, Moreau M, Rodriguez JC, Doucet C, Chapman MJ, Huby T. Differential regulation of the human versus the mouse apolipoprotein AV gene by PPARalpha. Implications for the study of pharmaceutical modifiers of hypertriglyceridemia in mice. *Biochim Biophys Acta* 2009;**1791**:764-771.
31. Gautier EL, Huby T, Witztum JL, Ouzilleau B, Miller ER, Saint-Charles F, Aucouturier P, Chapman MJ, Lesnik P. Macrophage apoptosis exerts divergent effects on atherogenesis as a function of lesion stage. *Circulation* 2009;**119**:1795-1804.
32. Couvert P, Giral P, Dejager S, Gu J, Huby T, Chapman MJ, Bruckert E, Carrie A. Association between a frequent allele of the gene encoding OATP1B1 and enhanced LDL-lowering response to fluvastatin therapy. *Pharmacogenomics* 2008;**9**:1217-1227.
33. Yalaoui S, Huby T, Franetich JF, Gego A, Rametti A, Moreau M, Collet X, Siau A, van Gemert GJ, Sauerwein RW, Luty AJ, Vaillant JC, Hannoun L, Chapman J, Mazier D, Froissard P. Scavenger receptor BI boosts hepatocyte permissiveness to Plasmodium infection. *Cell Host Microbe* 2008;**4**:283-292.
34. Gautier EL, Huby T, Saint-Charles F, Ouzilleau B, Chapman MJ, Lesnik P. Enhanced dendritic cell survival attenuates lipopolysaccharide-induced immunosuppression and increases resistance to lethal endotoxic shock. *J Immunol* 2008;**180**:6941-6946.
35. Komori H, Arai H, Kashima T, Huby T, Kita T, Ueda Y. Coexpression of CLA-1 and human PDZK1 in murine liver modulates HDL cholesterol metabolism. *Arterioscler Thromb Vasc Biol* 2008;**28**:1298-1303.
36. Out R, Jessup W, Le Goff W, Hoekstra M, Gelissen IC, Zhao Y, Kritharides L, Chimini G, Kuiper J, Chapman MJ, Huby T, Van Berkel TJ, Van Eck M. Coexistence of foam cells and hypocholesterolemia in mice lacking the ABC transporters A1 and G1. *Circ Res* 2008;**102**:113-120.
37. Kockx M, Guo DL, Huby T, Lesnik P, Kay J, Sabaretnam T, Jary E, Hill M, Gaus K, Chapman J, Stow JL, Jessup W, Kritharides L. Secretion of apolipoprotein E from macrophages occurs via a protein kinase A and calcium-dependent pathway along the microtubule network. *Circ Res* 2007;**101**:607-616.
38. Catanese MT, Graziani R, von Hahn T, Moreau M, Huby T, Paonessa G, Santini C, Luzzago A, Rice CM, Cortese R, Vitelli A, Nicosia A. High-avidity monoclonal antibodies against the human scavenger class B type I receptor efficiently block hepatitis C virus infection in the presence of high-density lipoprotein. *J Virol* 2007;**81**:8063-8071.
39. Gautier EL, Huby T, Ouzilleau B, Doucet C, Saint-Charles F, Gremy G, Chapman MJ, Lesnik P. Enhanced immune system activation and arterial inflammation accelerates atherosclerosis in lupus-prone mice. *Arterioscler Thromb Vasc Biol* 2007;**27**:1625-1631.
40. Treguier M, Moreau M, Sposito A, Chapman MJ, Huby T. LDL particle subspecies are distinct in their capacity to mediate free cholesterol efflux via the SR-B1/Cla-1 receptor. *Biochim Biophys Acta* 2007;**1771**:129-138.
41. Grove J, Huby T, Stamatakis Z, Vanwolleghem T, Meuleman P, Farquhar M, Schwarz A, Moreau M, Owen JS, Leroux-Roels G, Balfe P, McKeating JA. Scavenger receptor BI and BII expression levels modulate hepatitis C virus infectivity. *J Virol* 2007;**81**:3162-3169.

42. **Huby T, Doucet C, Dachet C**, Ouzilleau B, Ueda Y, Afzal V, Rubin E, Chapman MJ, Lesnik P. Knockdown expression and hepatic deficiency reveal an atheroprotective role for SR-B1 in liver and peripheral tissues. *J Clin Invest* 2006;**116**:2767-2776.
43. Maillard P, **Huby T**, Andreo U, **Moreau M**, Chapman J, Budkowska A. The interaction of natural hepatitis C virus with human scavenger receptor SR-B1/Cla1 is mediated by ApoB-containing lipoproteins. *FASEB J* 2006;**20**:735-737.
44. Prieur X, **Huby T**, Coste H, Schaap FG, Chapman MJ, Rodriguez JC. Thyroid hormone regulates the hypotriglyceridemic gene APOA5. *J Biol Chem* 2005;**280**:27533-27543.
45. **Treguier M, Doucet C, Moreau M, Dachet C**, Thillet J, Chapman MJ, **Huby T**. Transcription factor sterol regulatory element binding protein 2 regulates scavenger receptor Cla-1 gene expression. *Arterioscler Thromb Vasc Biol* 2004;**24**:2358-2364.
46. **Huby T**, Afzal V, **Doucet C**, Lawn RM, Gong EL, Chapman MJ, Thillet J, Rubin EM. Regulation of the expression of the apolipoprotein(a) gene: evidence for a regulatory role of the 5' distal apolipoprotein(a) transcription control region enhancer in yeast artificial chromosome transgenic mice. *Arterioscler Thromb Vasc Biol* 2003;**23**:1633-1639.
47. Schoonjans K, Annicotte JS, **Huby T**, Botrugno OA, Fayard E, Ueda Y, Chapman J, Auwerx J. Liver receptor homolog 1 controls the expression of the scavenger receptor class B type I. *EMBO Rep* 2002;**3**:1181-1187.
48. **Huby T, Dachet C**, Lawn RM, Wickings J, Chapman MJ, Thillet J. Functional analysis of the chimpanzee and human apo(a) promoter sequences: identification of sequence variations responsible for elevated transcriptional activity in chimpanzee. *J Biol Chem* 2001;**276**:22209-22214.
49. Chenivesse X, **Huby T**, Wickins J, Chapman J, Thillet J. Molecular cloning of the cDNA encoding the carboxy-terminal domain of chimpanzee apolipoprotein(a): An asp57 --> asn mutation in kringle IV-10 is associated with poor fibrin binding. *Biochemistry* 1999;**38**:1950.
50. **Huby T**, Chapman J, Thillet J. Pathophysiological implication of the structural domains of lipoprotein(a). *Atherosclerosis* 1997;**133**:1-6.
51. Chenivesse X, **Huby T**, Chapman J, Franco D, Thillet J. Expression of a recombinant kringle V of human apolipoprotein(a): antibody characterization and species specificity. *Protein Expr Purif* 1996;**8**:145-150.
52. Doucet C, **Huby T**, Ruiz J, Chapman MJ, Thillet J. Non-enzymatic glycation of lipoprotein(a) in vitro and in vivo. *Atherosclerosis* 1995;**118**:135-143.
53. **Huby T**, Schroder W, Doucet C, Chapman J, Thillet J. Characterization of the N-terminal and C-terminal domains of human apolipoprotein(a): relevance to fibrin binding. *Biochemistry* 1995;**34**:7385-7393.
54. Chapman MJ, **Huby T**, Nigon F, Thillet J. Lipoprotein (a): implication in atherothrombosis. *Atherosclerosis* 1994;**110 Suppl**:S69-75.
55. Ruiz J, Thillet J, **Huby T**, James RW, Erlich D, Flandre P, Froguel P, Chapman J, Passa P. Association of elevated lipoprotein(a) levels and coronary heart disease in NIDDM patients. Relationship with apolipoprotein(a) phenotypes. *Diabetologia* 1994;**37**:585-591.



56. **Huby** T, Doucet C, Dieplinger H, Chapman J, Thillet J. Structural domains of apolipoprotein(a) and its interaction with apolipoprotein B-100 in the lipoprotein(a) particle. *Biochemistry* 1994;**33**:3335-3341.
57. Doucet C, **Huby** T, Chapman J, Thillet J. Lipoprotein[a] in the chimpanzee: relationship of apo[a] phenotype to elevated plasma Lp[a] levels. *J Lipid Res* 1994;**35**:263-270.

# Mémoire

## 1. La Lipoprotéine (a).

La Lp(a) est une lipoprotéine très similaire aux lipoprotéines de basse densité LDL qui se distingue de celles-ci par la présence d'une glycoprotéine de haute masse moléculaire appelée apo(a), qui est liée à l'apoB100 par un pont disulfure. Le rôle pro-athérogène de cette lipoprotéine est encore aujourd'hui débattu.

Mes travaux de thèse ont principalement porté sur l'étude de la conformation des constituants protéiques de la lipoprotéine (a) et des relations structure/fonction de la Lp(a) dans son interaction avec le système fibrinolytique. J'ai ainsi mis en évidence la présence de deux domaines structuraux dans l'apo(a) et montré qu'ils pouvaient avoir des fonctions différentes. Des études de liaison ont ainsi montré que le domaine C-terminal de l'apo(a) possède le site de liaison à la fibrine. Le domaine C-terminal joue également un rôle fondamental dans la formation de la Lp(a) puisqu'il contient la cystéine impliquée dans le pont disulfure avec l'apo B100 et les kringles impliqués dans la liaison non covalente de l'apo(a) avec l'apo B100. En ce qui concerne le domaine N-terminal de l'apo(a), aucune propriété de liaison ne lui a été attribuée jusqu'à présent. Son action pourrait être indirecte. En effet, sa taille semble influencer sur la capacité maximale de liaison de la Lp(a) à la fibrine in vitro. Par ailleurs, il pourrait également moduler l'affinité du domaine C-terminal pour la fibrine. Une relation inverse entre la taille de l'apo(a) et l'affinité de la Lp(a) pour la fibrine a par ailleurs été démontrée et semble soutenir un tel mécanisme d'action.

Ces travaux originaux ont donné lieu aux publications [Pub56](#), **Huby** et al. Biochemistry 1994 et [Pub53](#), **Huby** et al. Biochemistry 1995.

Au début de mon recrutement à l'Inserm, j'ai concrétisé un travail initié dans le laboratoire du Dr Rubin (Genome Science dept., CA, USA) pendant mon stage post-doctoral. J'ai poursuivi la caractérisation de souris transgéniques pour le gène humain de l'apo(a). La caractérisation des mécanismes régulant la synthèse d'apo(a) est importante puisque ceux-ci vont déterminer pour une grande part le taux plasmatique de Lp(a) et donc le risque vasculaire associé. L'analyse de 40 kb de la région 5' du gène de l'apo(a) a mis en évidence 4 sites hypersensibles à la DNase-I

hépato-spécifiques. La caractérisation *in vitro* de ces régions suggère que le site DH III pouvait jouer un rôle essentiel dans le contrôle de l'activité transcriptionnelle du gène de l'apo(a). Cet élément DH III (300 pb), appelé également ACR ("apo(a) transcription control region"), se situe à environ 20 kb du site d'initiation de la transcription du gène de l'apo(a). Il stimule *in vitro* l'activité basale du promoteur minimal du gène de l'apo(a) d'un facteur 10 à 15 lorsqu'il est placé en amont de celui-ci et quel que soit son orientation. L'analyse fonctionnelle de l'ACR indique que son activité "enhanceur" est essentiellement dépendante de sites de liaison pour les facteurs de transcription ubiquitaires Sp1 et Ets. Bien que l'analyse de la région ACR *in vitro* soit très encourageante, celle-ci ne constitue pas une preuve absolue de l'aspect fonctionnel de cette région *in vivo*. Nous avons donc évalué le rôle joué par la région ACR dans la régulation de l'expression du gène de l'apo(a) *in vivo*. Pour réaliser cette étude j'ai généré deux lignées de souris transgéniques ne différant que par la présence ou l'absence de l'élément enhanceur en amont d'un transgène humain apo(a). Les souris transgéniques apo(a) ont été créées à partir d'un chromosome artificiel de levure (YAC) de 270 kilobases (kb) contenant un gène humain de l'apo(a) (110 kb) ainsi que l'intégralité des régions 3' (~20 kb) et 5' (~40 kb) entourant ce gène. J'ai modifié le YAC apo(a) par recombinaison homologue dans la levure de manière à introduire des sites LoxP en orientation directe autour de l'enhanceur ACR. Ce YAC apo(a) ainsi modifié a été introduit dans le génome d'une cellule embryonnaire pluripotente ES de souris par fusion entre levure et cellule ES. Des cellules ES ayant intégré le YAC apo(a) dans leur génome et issues d'un même clone ont ensuite été utilisées pour générer des souris chimères puis, par transmission germinale, la lignée de souris transgéniques YAC apo(a). J'ai ensuite croisé des souris YAC apo(a) avec des souris transgéniques pour la recombinaison Cre, afin d'obtenir des souris simple-transgéniques YAC apo(a) et des souris double transgéniques YAC apo(a) et Cre. Pour ces dernières, l'expression de la recombinaison Cre entraîne la délétion spécifique de l'ACR au niveau du transgène par interaction avec les sites Lox P l'encadrant et ceci dans toutes les cellules. Cette approche a donc permis d'obtenir, deux lignées de souris possédant un site d'intégration identique pour le YAC et ne différant que par la présence ou l'absence de l'élément enhanceur en amont du gène de l'apo(a). L'analyse des deux groupes de souris a révélé que la délétion de la séquence ACR est associée avec une diminution de 30% du taux plasmatique basal d'apo(a) que ce soit chez les femelles ou les mâles. Par ailleurs, les souris avec ou sans ACR ne diffèrent pas en ce qui concerne différents aspects de régulation du gène de l'apo(a), dont son expression spécifique au niveau du foie, et les régulations précédemment décrites au cours

de la maturation sexuelle des animaux ou en réponse à un régime riche en cholestérol et en lipides. L'ensemble des résultats obtenus *in vivo* est en accord avec la caractérisation de l'élément ACR faite *in vitro* et soutient l'hypothèse que cet enhanceur participe à l'expression optimale du gène de l'apo(a). Ces données ont permis d'identifier pour la première fois un élément de cis-régulation du gène de l'apo(a) *in vivo*. Enfin, l'élément ACR est situé dans une séquence répétée appartenant à la famille des rétrotransposons Line1. Les résultats de cette étude fournissent donc le premier exemple, à notre connaissance, d'un élément Line 1 capable d'affecter l'expression d'un gène voisin. Cette observation suggère que les éléments line mobiles peuvent également participer à l'évolution du génome en tant qu'éléments potentiellement modulateur de l'expression de gènes ([pub46](#), **Huby** et al ATVB 2003 ; fourni en annexe).

## 2. ApoA5 et métabolisme des triglycérides.

Identifiée en 2001, l'apolipoprotéine AV (apoAV) apparaissait comme un acteur clef du métabolisme des triglycérides (TG). Nous avons démontré dans l'équipe avec le Dr Xavier Prieur (ancien étudiant en thèse de l'unité) des différences de régulations inter-espèces (homme, souris) de ce gène *ApoA5* par les fibrates. Pour cela, nous avons utilisé des approches d'étude de l'activité des promoteurs par transfections transitoires, ainsi que l'utilisation de souris transgéniques pour le gène humain de l'apoA5 (souris générées par le Laboratoire du Dr Rubin, Genome Science Department, LBNL, Berkeley, USA). *In vitro* et *in vivo*, nos résultats ont permis de montrer que le gène humain est activé par les agonistes des facteurs de transcription PPARalpha tandis que le gène homologue murin est réprimé. Cette régulation espèce spécifique de l'APOAV parallèle celle observée pour les gènes humain et murin de l'*ApoA-1* ([pub30](#), **Prieur X**, et al Biochim Biophys Acta. 2009 ; fourni en annexe).

### 3. Étude du récepteur SR-B1 dans le métabolisme du cholestérol et comme facteur de risque de l'athérosclérose.

Les études épidémiologiques ont clairement établi que les concentrations plasmatiques des HDL sont corrélées négativement avec l'incidence des maladies cardiovasculaires. Les propriétés anti-athérogènes des particules HDL résultent de plusieurs activités biologiques et notamment de leur implication dans le transport inverse du cholestérol ou RCT (Reverse Cholesterol Transport). Ce processus correspond au transport du cholestérol des tissus périphériques vers le foie pour son excrétion et est actuellement considéré comme une des voies métaboliques majeures permettant de maintenir l'homéostasie du cholestérol au sein de l'organisme.

Découvert en 1994, le récepteur SR-B1 (ou SCARB1) fait partie de la famille des récepteurs scavengers de classe B (Acton, S.L., et al., *J.Biol.Chem.*,1994. 269:21003-21009). Initialement isolé par sa capacité à lier les LDL acétylées, SR-B1 lie aussi les LDL natives et oxydées, les VLDL mais également certains phospholipides anioniques. Un intérêt grandissant a été porté sur ce récepteur puisqu'il a aussi été identifié comme un récepteur capable de lier les lipoprotéines HDL et de transférer les esters de cholestérol des HDL vers la cellule sans internalisation de la particule lipoprotéique (Acton, S., et al., *Science*, 1996. 271:518-520). Caractérisé depuis longtemps, ce transfert sélectif semble particulièrement important, non seulement pour fournir les tissus stéroïdogènes (glande surrénale, ovaire, testicule) en cholestérol où il est transformé en hormones stéroïdiennes, mais également dans l'étape finale du RCT à savoir la captation du cholestérol au niveau hépatique où il est excrété sous forme d'acides biliaires ou utilisé pour la synthèse de lipoprotéines naissantes telles que les VLDL. Le développement de modèles de souris génétiquement modifiées a permis de démontrer que SR-B1 participe activement à ces processus chez les rongeurs (Rigotti, A., et al., *Proc Natl Acad Sci U S A*, 1997. 94(23):12610-5; Wang, N., et al., *J Biol Chem*, 1998. 273(49): p. 32920-6; Ueda, Y., et al., *J Biol Chem*, 1999. 274(11): p. 7165-71; Trigatti, B., et al., *Proc Natl Acad Sci U S A*, 1999. 96(16): p. 9322-7). En effet, les souris totalement déficientes pour SR-B1 ont des taux élevés de HDL-cholestérol et le contenu de cholestérol de leurs glandes surrénales est diminué. A l'inverse, les souris qui surexpriment SR-B1 au niveau hépatique ont une captation sélective de HDL-cholestérol accrue au niveau hépatique tandis que leurs taux plasmatiques de HDL-cholestérol sont fortement réduits. Enfin, SR-B1 facilite également *in vitro* l'efflux cellulaire du cholestérol vers les particules HDL.

Une grande partie de mes travaux de recherche a été focalisée sur l'étude de ce récepteur scavenger SR-B1.

### 3.1- Régulations moléculaire et cellulaire de SR-B1 au niveau hépatique

L'homéostasie du cholestérol est assurée par de nombreuses voies métaboliques finement régulées. Notamment, la captation du cholestérol plasmatique par la voie du LDL-récepteur (LDL-r) et la biosynthèse intracellulaire *de novo* du cholestérol sont rétro-régulées par la concentration intracellulaire du cholestérol. Des évidences indirectes ont suggéré que l'expression du récepteur SR-B1 était dépendante du contenu intracellulaire en cholestérol. Par conséquent, afin de déterminer le mécanisme moléculaire sous-jacent à cette régulation potentielle du gène, nous avons évalué si *SR-B1* était un gène cible de la famille des facteurs de transcription sterol regulatory element binding protein (SREBP).

Par transfections transitoires, nous avons pu montrer que les facteurs SREBP activent le promoteur du gène humain *SR-B1*; l'isoforme SREBP2 activant préférentiellement le promoteur du gène par rapport à l'isoforme SREBP1a. Une analyse par délétion séquentielle de la région 5' flanquante du gène, combinée à des approches de mutagenèse dirigée et d'EMSA nous ont permis d'identifier un site de liaison SRE fonctionnel capable de lier les facteurs SREBP. La régulation du gène *hSR-B1* par les facteurs SREBP a été confirmée par la création de cellules stablement transfectées pour la forme nucléaire active SREBP2. Dans ces lignées, nous avons démontré que les taux d'ARNm et de protéine SR-B1 augmentent en proportion directe avec le taux intracellulaire du facteur recombinant nSREBP2. Ces travaux démontrent que le facteur SREBP2, un acteur clé qui contrôle la captation du cholestérol plasmatique en modulant la voie du LDL-récepteur, peut également influencer l'homéostasie cellulaire du cholestérol en régulant l'expression du gène *SR-B1* (Pub45, Tréguier et al. ATVB 2004 ; fourni en annexe).

### 3.2- Etude de l'activité du récepteur SR-B1 pour faciliter l'efflux cellulaire du cholestérol

Afin de caractériser l'activité de SR-B1 en tant que récepteur membranaire permettant l'efflux cellulaire de cholestérol vers les lipoprotéines ou la captation sélective d'esters de cholestérol à partir de lipoprotéines, nous avons développé des lignées clonales de cellules CHO exprimant de façon stable SR-B1 à différents niveaux. Nous avons utilisé ces lignées afin de mieux

comprendre dans quelles proportions relatives les particules lipoprotéiques LDL et HDL, et leurs sous-fractions respectives, permettent l'efflux cellulaire de cholestérol par l'intermédiaire du récepteur humain SR-B1. Nos résultats ont montré que l'efflux cellulaire de cholestérol facilité par SR-B1 vers les lipoprotéines LDL est variable selon le type de sous-fraction de LDL utilisée. En particulier, les sous-fractions petites et denses LDL-4 et LDL-5 (regroupées sous l'appellation sdLDL) par rapport aux autres sous-fractions de LDL apparaissent comme de très mauvais accepteurs de cholestérol transporté par SR-B1. De plus, nous observons que les sdLDL réduisent l'efflux de cholestérol facilité par SR-B1 vers les lipoprotéines LDL larges et légères et ceci d'une manière dose dépendante. A l'inverse, les sdLDL n'influencent pas l'efflux vers les HDL2. Les LDL sont des particules lipoprotéiques hétérogènes qui diffèrent de par leurs propriétés chimiques et physiques mais également de par leurs pouvoirs athérogènes. A cet égard les LDL-4 et -5, sont considérées comme les LDL les plus athérogènes car elles sont notamment plus susceptibles à l'oxydation et interagissent moins bien avec le récepteur LDL. A l'heure actuelle, il ne peut pas être exclu que les LDL participent avec les HDL à l'efflux cellulaire de cholestérol dans la voie du transport inverse du cholestérol. Nos données suggèrent donc que les individus possédant des profils de lipoprotéines LDL avec une prépondérance de LDL petites et denses auraient une capacité d'"efflux" cellulaire de cholestérol par la voie SR-B1 réduite par rapport à des individus possédant des profils de lipoprotéines LDL avec une prépondérance de LDL plus légères. Un tel mécanisme pourrait participer au risque accru de maladie cardiovasculaire observé chez les patients possédant une prévalence de LDL petites et denses (Pub40, Tréguier et al. BBA 2007; fourni en annexe).

### *3.3- Rôle de SR-B1 dans la voie du transport inverse du cholestérol (RCT) in vivo et comme facteur de risque de l'athérosclérose.*

Les premières démonstrations d'un rôle pro-athérogène exercé par le récepteur SR-B1 ont été établies au début des années 2000 en étudiant les effets d'une déficience totale du récepteur dans des modèles murins. Afin d'étudier plus spécifiquement le rôle de SR-B1 dans différents organes/types cellulaires, j'ai développé un modèle d'inactivation conditionnelle du gène basé sur l'utilisation du système Cre-Lox (modèle créé au cours de mon stage post-doctoral). Nos résultats ont montré que les souris déficientes en SR-B1 spécifiquement au niveau du foie présentent une augmentation similaire des taux plasmatiques de cholestérol par rapport aux souris avec une déficience totale (SR-B1 KO). Parmi, les différences phénotypiques majeures

nous avons observé que la déficience hépatique de SR-B1 n'était pas associée à une sous-fertilité des femelles comme cela a été reporté pour les souris SR-B1 KO. Un rôle de SR-B1 dans l'apport de lipides, et notamment de cholestérol, au sein des ovaires pour la production de progestérone pourrait être impliqué. D'autres différences phénotypiques peuvent être également observées au niveau des tissus périphériques entre les souris SR-B1 KO et les souris présentant une déficience hépatique de SR-B1. Notamment, si les glandes surrénales des souris SR-B1 KO ont leur contenu en cholestérol diminué celui-ci est doublé dans les glandes surrénales des souris SR-B1 "foie" KO. Ces travaux soutiennent très fortement le rôle prépondérant du récepteur SR-B1 dans l'homéostasie du cholestérol au niveau de ce tissu stéroïdogène. Nos travaux de délétion spécifique de SR-B1 dans la glande surrénale l'ont confirmé par la suite (voir plus bas, [pub21](#) ; fourni en annexe).

Les données chez la souris suggéraient fortement que SR-B1 joue un rôle protecteur contre l'athérosclérose, mais les mécanismes responsables de cette protection étaient à préciser. Au niveau du tissu hépatique, l'étude de modèles de souris surexprimant SR-B1 a permis de démontrer un rôle important de SR-B1 dans la captation du HDL-cholestérol et son action anti-athérogène. Toutefois de nombreuses autres activités, dont l'importance physiologique n'est pas encore clairement établie, sont attribuées à SR-B1 et pourraient également contribuer à son rôle protecteur (activité d'efflux cellulaire de cholestérol dans les macrophages; captation de lipides oxydés et participation à la transformation du macrophage en cellule spumeuse au sein de la plaque; action de remodelage intravasculaire des lipoprotéines; activité d'échange d'autres classes de lipides incluant la vitamine E anti-oxydante, transfert cellulaire d'oestradiol associé aux HDL induisant la production d'oxyde nitrique (puissant médiateur anti-inflammatoire et vasodilatateur) au niveau des cellules endothéliales). Afin, de démontrer l'importance du rôle extra-hépatique de SR-B1 dans son rôle athéroprotecteur, nous avons comparé la formation d'athérosclérose chez des souris avec une expression hypomorphe de SR-B1, une déficience totale (SR-B1 KO) et des souris avec une déficience hépatique de SR-B1 (SR-B1 "foie" KO). Les résultats ont confirmé très clairement le rôle athéroprotecteur de SR-B1 au niveau hépatique mais démontrent également que l'expression de SR-B1 au niveau périphérique exerce une action protectrice, potentiellement anti-inflammatoire ([pub42](#), Huby et al J Clin Invest 2006 ; fourni en annexe).



Nous avons ensuite confirmé ce rôle majeur de SRB1 hépatique dans le métabolisme du HDL-cholestérol, le transport inverse du cholestérol (RCT) et l'athérosclérose dans un contexte où le transport du cholestérol était humanisé par l'expression de la protéine de transfert des esters de cholestérol, CETP. En effet, l'Homme transporte son cholestérol au niveau plasmatique principalement sous forme de LDL et VLDL, contrairement aux souris chez lesquelles les HDL sont les lipoprotéines circulantes majoritaires. Par ailleurs, les rongeurs ne possèdent pas l'enzyme CETP (Cholesteryl Ester Transfer Protein) qui redistribue chez l'homme le cholestérol des HDL vers les lipoprotéines athérogènes contenant de l'apoB100, les VLDL et LDL. Ainsi, afin de déterminer plus spécifiquement le rôle physiologique et physiopathologique de SR-B1, nous avons développé des modèles de souris (SR-B1 KO, SR-B1 hypomorphique, SR-B1 KO<sup>foie</sup>) ayant un métabolisme lipidique plus proche de l'homme par expression de la CETP à un taux physiologique (souris NFR-CETP transgéniques développées par A.Tall). Nos résultats démontrent que l'expression de la CETP réduit les taux plasmatiques de cholestérol, restaure la distribution du HDL-cholestérol et diminue significativement l'athérosclérose à la fois chez les souris SR-B1 KO<sup>foie</sup> et les souris totalement déficientes en SR-B1. Toutefois, le rôle athéroprotecteur hépatique et extra-hépatique de SR-B1 que nous avons démontré précédemment ([pub42](#), Huby JCI 2006) est également observé dans ce contexte métabolique où la CETP est présente et fonctionnelle. Nous avons également pu démontrer que si SR-B1 contribue très significativement à l'apport de cholestérol pour la synthèse de glucocorticoïdes dans la glande surrénale (assurant un rôle primordial pour le maintien de la fonction endocrine de cette glande), la CETP n'avait aucun impact sur le métabolisme du cholestérol dans celle-ci. Nous avons également mis en évidence que la CETP ne restaurait que partiellement la thrombocytopénie et les défauts de maturation des réticulocytes en érythrocytes associés à la déficience en SR-B1. Enfin, nos résultats démontrent que le transport inverse du cholestérol (RCT), lorsque celui-ci est sécrété à partir de macrophages, est fortement affecté lorsque SR-B1 est absent au niveau hépatique mais ne semble pas restauré en présence de la CETP ; ces données ayant été reproduites dans des conditions de normo- et d'hypercholestérolémie mais également en présence d'un inhibiteur de l'absorption intestinale du cholestérol (Ezétimibe). L'ensemble de ces travaux soutiennent très fortement l'hypothèse d'un rôle déterminant de SR-B1 dans le métabolisme du cholestérol et le risque cardiovasculaire chez l'Homme ([Pub 26](#), [El Bouhassani](#) et al. J Biol Chem 2011 ; fourni en annexe). En complément de ces travaux, le modèle de souris KO conditionnel pour le gène SRB1 a été utilisé par l'équipe du Dr Martinez

(UMR 1048) pour démontrer que le récepteur P2Y13 participe également au processus de RCT mais d'une manière indépendante de la voie SRB1 hépatique (Pub 27, Fabre et al. Hepatology 2010). Enfin, avec le Dr Ueda (Japon), nous avons démontré l'implication du récepteur SRB1 humain dans le RCT dans un modèle de souris humanisée exprimant les formes humaines de l'ApoA1, de SRB1 et de la protéine d'assemblage PDZK1 qui joue un rôle critique dans l'expression protéique de SR-B1 (Pub 35, Komori et al. ATVB 2008).

### 3.4- Exploration du rôle anti-athérogène de SR-B1 exprimé par le macrophage.

Les études menées sur les souris déficientes en SR-B1 ont clairement mis en évidence une action globalement anti-athérogène de ce récepteur. Toutefois, l'activité de SR-B1 est multiple et ce rôle bénéfique semble s'opposer à la découverte récente que SR-B1 peut également être pro-athérogène au niveau de l'endothélium en facilitant la transcytose des lipoprotéines vers l'intima artériel (Huang L *et al*, Nature. 2019). Cependant, nos travaux comparatifs menés entre des souris déficientes en SR-B1 dans les hépatocytes et des souris totalement déficientes pour le récepteur ont aussi permis d'établir que SR-B1 exerce globalement un rôle anti-athérogène dans les tissus extra-hépatiques (Pub26 ; pub42). Ainsi, plusieurs études anciennes et plus récentes utilisant des approches de transfert de moelle osseuse de souris SRB1 KO dans des modèles de souris susceptibles à l'athérosclérose (LDLr KO (Covey et al, ATVB 2003; Tao et al, J Lipid Res 2015; Van Eck et al, Am J Pathol 2004) et ApoE KO (Zhang et al, Circulation 2003)) ont suggéré que ce récepteur exerçait une activité athéroprotectrice dans les cellules d'origine hématopoïétique. Dans ce contexte, des travaux ont suggéré que l'action athéroprotectrice des HDL sur la prolifération et la différenciation des cellules souches/progénitrices hématopoïétiques de la moelle osseuse pour contrôler la leucocytose et l'inflammation était dépendante du récepteur SR-B1 (Gao *et al*, ATVB 2014). Cependant, le rôle athéroprotecteur de SR-B1 le plus mis en avant pour les cellules d'origine hématopoïétique était celui que pouvait jouer SR-B1 au sein du macrophage lésionnel. Toutefois, aucune approche de délétion spécifique dans le macrophage n'avait été conduite. C'est donc ce que nous avons cherché à faire en utilisant notre modèle de souris SR-B1 KO conditionnel (SR-B1<sup>f/f</sup>). La caractérisation de l'expression de SR-B1 dans les globules blancs circulants de souris SR-B1<sup>f/f</sup> a montré que l'expression la plus élevée se trouvait dans les monocytes, mais aucune expression n'était mesurable dans les neutrophiles et les éosinophiles. L'analyse des souris Lysm-Cre x SR-B1<sup>f/f</sup> a

démontré une absence totale d'expression de SR-B1 dans les macrophages et une délétion partielle dans les monocytes sanguins (effet en accord avec d'autres publications utilisant le modèle Lysm-Cre). Par transplantation de moëlle osseuse de souris Lysm-Cre x SR-B1<sup>f/f</sup>, de souris SR-B1<sup>-/-</sup> et de souris contrôles SR-B1<sup>f/f</sup> nos résultats démontrent sans ambiguïté que pour les cellules d'origine hématopoïétique, c'est la délétion spécifique de SR-B1 dans le macrophage qui prédomine comme effet pro-athérogène. De plus, nous observons que la délétion spécifique de SR-B1 dans le macrophage est associée à une réduction marquée des macrophages apoptotiques dans le développement de lésions aortiques et cela dans deux modèles différents de souris susceptibles à l'athérosclérose. D'un point de vue mécanistique, nous démontrons que les macrophages déficients en SR-B1 sont moins sensibles à l'apoptose induite par la charge de cholestérol libre. Cet effet s'accompagne d'une activation réduite de p38MAPK et STAT1 qui sont des facteurs critiques de l'apoptose des macrophages induite par le cholestérol libre. De plus, nous observons que la résistance des macrophages déficients en SR-B1 à l'apoptose est associée à l'induction du facteur anti-apoptotique AIM (CD5L) *in vitro* dans des macrophages humains et murins mais également au sein des macrophages de la plaque d'athérosclérose. Par approche siRNA, par blocage du récepteur avec des anticorps neutralisants et en utilisant des inhibiteurs spécifiques, nous démontrons que cette induction de AIM est bien dépendante de la présence d'un SR-B1 fonctionnel et de la voie STAT3. Dans l'ensemble, ces résultats suggèrent un effet pro-survie de l'AIM dans les macrophages déficients en SR-B1, entraînant une augmentation de la cellularité de la plaque et une expansion précoce des lésions d'athérosclérose ([Pub8](#), [Galle-Treger et al. Cardiovasc Res 2020](#); [Review Pub 1 Huby et al 2022](#) ; fournis en annexe).

#### 4. Rôle de SR-B1 dans l'apport de cholestérol pour la production endogène de glucocorticoïdes par la glande surrénale et la protection contre le choc septique

Un certain nombre d'études avaient mis en évidence que les souris SR-B1 KO présentent un phénotype extrême avec une réponse systémique hyper-inflammatoire suite à un choc endotoxique, mais aussi à un sepsis. Ces souris ont par ailleurs une mortalité très élevée après un choc endotoxique provoqué au LPS (Cai, *et al* J. Clin. Invest. 2008; Li *et al* Circ. Res. 2006) ou suite à l'induction d'une septicémie (Guo *et al*, J Biol Chem 2009). Plusieurs mécanismes

différents pour expliquer ce phénomène avaient ainsi été proposés. Notamment, il avait été suggéré que SR-B1 protège du choc septique 1/en facilitant la clairance hépatique du LPS (Cai J Clin Invest 2008), 2/par son action anti-inflammatoire dans le macrophage (Guo et al J. Biol. Chem. 2009, Cai J. Lipid Res. 2011), 3/en facilitant la survie des bactéries dans les granulocytes (Leelahavanichkul, J. Immunol. 2012) 4/ en protégeant de la cytotoxicité du NO, potentiellement au niveau endothélial (Li et al Circ Res 2006), 5/ en contribuant à la production des glucocorticoïdes endogènes via l'apport de cholestérol à partir des HDL dans la glande surrénale (Cai J Clin Invest 2008), 6/en assurant la captation hépatique des HDL, qui jouent un rôle neutralisant important du LPS circulant. Grâce à notre modèle de souris *Srb1* conditionnel KO, nous avons pu explorer ces mécanismes. Ainsi nous avons démontré que restaurer la concentration plasmatique de HDL, qui sont des lipoprotéines essentielles pour la neutralisation du LPS, par expression de la CETP n'a pas amélioré les résultats aigus de l'injection de LPS chez les souris SR-B1 KO. La déficience de SR-B1 dans les hépatocytes (*Alb-Cre X SR-B1<sup>f/f</sup>*), dans les cellules endothéliales (*Tie2-Cre X SR-B1<sup>f/f</sup>*) ou bien encore dans les cellules myéloïdes (*Lysm-Cre X SR-B1<sup>f/f</sup>*) n'a pas augmenté la susceptibilité de ces animaux à la mort induite par endotoxémie au LPS. Cependant si l'ablation du SR-B1 dans les hépatocytes a conduit à une augmentation modérée de marqueurs pro-inflammatoires, le déficit en SR-B1 dans les cellules myéloïdes a été associé à un effet anti-inflammatoire. Enfin, les souris déficientes en SR-B1 dans le cortex surrénalien, où le récepteur fournit du cholestérol dérivé des lipoprotéines, présentaient une sécrétion altérée de glucocorticoïdes en réponse au stress. En réponse à l'injection de LPS en dose normalement sous-léthale, ces souris ont présenté une réponse inflammatoire systémique et locale exacerbées, une activation réduite des gènes d'atrophie dans le muscle et une létalité extrêmement élevée. De manière concordante, l'induction d'une septicémie polymicrobienne (modèle de ligature et ponction cæcal) a entraîné une mort accélérée de ces animaux. Notre étude démontre clairement que le SR-B1 corticosurrénalien est un élément essentiel de l'axe hypothalamo-hypophysio-surrénalien pour fournir une défense efficace de l'hôte dépendante des glucocorticoïdes après un choc endotoxique ou une infection bactérienne. La pertinence de nos résultats chez l'homme reste inconnue. Toutefois, les orthologues humains et murins partagent les mêmes ligands et semblent exercer les mêmes propriétés. Une élévation du HDL-C chez les membres d'une famille porteur de la mutation fonctionnelle P297S à l'état hétérozygote du gène humain SR-B1 apporte un soutien solide à une contribution de SR-B1 hépatique dans le métabolisme des lipoprotéines/cholestérol chez

l'homme (Vergeer et al N. Engl. J. Med. 2011). Cette élévation du HDL-C a également été retrouvée pour une patiente homozygote pour la mutation rare P376L du gène (Zanoni et al ;Science 2016). Par ailleurs, une diminution de la stéroïdogénèse surrénalienne observée chez les porteurs hétérozygotes de la mutation P297S suggère que l'apport de cholestérol par SR-B1 au niveau du cortex surrénalien puisse aussi être important dans la régulation de la fonction endocrinienne de la glande. Au total, ces études soulignent la pertinence potentielle de la recherche de mutations du gène SR-B1 chez les patients diagnostiqués avec une insuffisance surrénalienne primaire dont l'étiologie moléculaire n'a pas été identifiée ([Pub21](#), [Gilibert S, Galle-Treger L et al/ J Immunol 2014](#) ; fourni en annexe).

## Research project

### Role of Kupffer cells in hypercholesterolemia-driven cardiovascular risk

#### *Scientific context and research hypotheses*

Atherosclerotic cardiovascular disease (ASCVD) and its clinical outcomes such as myocardial infarction are a leading cause of morbidity and mortality worldwide. Multiple lines of evidence have established that cholesterol-rich LDL lipoproteins and their oxidatively damaged forms (oxLDL) are implicated in ASCVD<sup>1,2</sup>. Cholesterol is an essential component of vertebrate cell membranes. It is supplied by the diet or can be synthesized by all cells but red blood cells (RBCs). Reverse cholesterol transport (RCT), the process of removing excess cholesterol from peripheral tissues for excretion by the intestine, is critical to maintain cholesterol balance and, as such, has been an area of intense research as it bears the potential to reduce CVD risk<sup>3,4</sup>. Notably, we established that hepatic-SRB1-mediated cholesterol uptake was critical to fuel the RCT, decrease plasma cholesterol and atherosclerosis<sup>5,6</sup>. Although lipoproteins ensure plasma cholesterol transport, RBCs carry also large amount of cholesterol and may also contribute to RCT<sup>7</sup>. Inversely, impairment of RCT leads to noticeable modifications in RBCs cholesterol pool and blood concentrations<sup>6</sup>.

Beside liver and intestine as major organs in regulating plasma cholesterol levels, several lines of evidence suggest the immune system could also participate. Indeed, we earlier revealed that **modulation of tissue-resident macrophage (trMac) pools resulted in remarkable changes in plasma cholesterol in hypercholesterolemic mice**<sup>8,9</sup>. Those trMac are best known for their immune roles relying on their phagocytic activity, which is necessary to maintain tissue homeostasis by clearing dead cells or pathogens. However, trMac are now increasingly recognized as serving accessory roles in tissue development, homeostasis and repair<sup>10</sup>. Reducing<sup>8</sup> or increasing<sup>9</sup> trMac survival capacities by modulation of anti-apoptotic *Bcl2l1* and *Bcl2* gene expressions associated with plasma cholesterol elevation or reduction, respectively.

Yet, the mechanisms and the specific tissue Macs involved remain to be identified. Nonetheless, these two models shared in common a modulation in the hepatic trMacs, Kupffer cells (KCs), arguing for their role in the control of cholesterolemia.

Located in the hepatic sinusoids, KCs are the largest trMac population in direct contact with blood, and thus with RBCs and lipoproteins. They are seeded from various progenitor waves during embryogenesis and maintain by self-renewal independently from circulating monocytes in the steady-state adult liver<sup>11-13</sup>. However, when the embryonic KC (emKC) network is altered during pathological conditions such as those occurring during non-alcoholic steatohepatitis (NASH)<sup>14-16</sup>, excessive intravascular hemolysis<sup>17</sup>, bacterial<sup>18</sup> or parasitic<sup>19</sup> infections, or experimentally<sup>20</sup>, blood monocytes can be recruited to the liver and differentiate into KCs. These monocyte-derived KCs (moKCs) exhibit an overall similar transcriptomic profile, but may display altered functions with pathological consequences as we recently demonstrated in NASH<sup>15</sup>. In the sinusoids, KCs closely interact with liver sinusoidal endothelial cells (LSECs), hepatic stellate cells (HSCs) and hepatocytes in order to acquire their tissue-imprinted signature as well as the signals allowing them to self-maintain<sup>21</sup>. Notably, Notch signals from LSECs synchronize with BMP9 produced from stellate cells to induce the transcription factor (TF) LXR- $\alpha$ <sup>21</sup>, a nuclear receptor that controls cellular cholesterol export in the macrophage<sup>22</sup> and that is essential for KCs survival<sup>23,24</sup>. LSECs-derived Notch ligands act also on developing KCs to induce the expression of SPI-C, a TF required for the development of iron-scavenging red pulp macrophages in the spleen<sup>25</sup>. One of the SPIC-inducible genes is Ferroportin (Slc40a1 or Fpn1) that promotes iron export to pass it on to hepatocytes, the main iron storage cell of the body. Indeed, apart from their role in clearing blood-borne pathogens, KCs play an important role in the elimination of aged or damaged RBCs<sup>17</sup>. Such well-defined function of KCs in erythrophagocytosis (EPC) plays a critical role in systemic iron recycling and prevents damage from excess iron, heme, and hemoglobin deposition in organs<sup>17</sup>. However, EPC-mediated by KCs might also participate to the elimination of circulating cholesterol pools.

Overall, there are several pieces of evidence pointing at KCs as a key cell type involved in cholesterol homeostasis. The corollary being that hypercholesterolemia could in turn disturb KCs homeostasis and self-maintenance.

## Objectives

We propose to investigate how KCs specifically contribute to cholesterol homeostasis and could as such participate to atherosclerosis development in condition of hypercholesterolemia. Using mouse models of diet-induced hypercholesterolemia and models specifically targeting KCs among other Mac populations, we will evaluate the role played by embryonically-derived KCs, but equally by monocyte-derived KCs that engraft in livers of hypercholesterolemic mice (preliminary findings). Moreover, we will also evaluate how RBC metabolism and cellular iron fluxes influence KCs' homeostasis and functions in the context of hypercholesterolemia.

## Preliminary data

Our preliminary experiments revealed **KCs are markedly impacted by hypercholesterolemia**. We have submitted LDL-receptor (LDLr) KO mice to a 1% cholesterol-rich diet for 4 days to induce hypercholesterolemia. KCs analysis by flow cytometry revealed a doubling in KCs as compared to chow-fed controls. KCs expansion was due to enhanced proliferation. In addition, bodipy staining showed KCs were heavily loaded with lipids, that lipidomic analyses identified as being primarily cholesteryl-esters. These effects were totally absent when hypercholesterolemia was blunted by addition of Ezetimibe, a drug that blocks intestinal cholesterol absorption. Such rapid response to hypercholesterolemia appeared specific to KCs and was not observed in the other trMacs analyzed in the spleen, kidney and gut.

RNAseq analyses of cell-sorted KCs from normo- and hypercholesterolemic mice confirmed hypercholesterolemia induced KC cycling. We also observed a **clear modulation of genes involved in heme/iron cellular metabolism**, suggesting increased EPC by KCs under hypercholesterolemia. This was associated with a transient increase in plasma levels of erythropoietin (EPO, the main hormone controlling erythropoiesis) and enhanced erythropoiesis in the spleen. These effects potentially reflected compensatory mechanisms to counterbalance increased EPC. In agreement, we demonstrated an enhanced propensity of RBCs isolated from hypercholesterolemic mice to Mac phagocytosis *in vitro*.

Analysis of LDLr KO mice for longer periods on cholesterol-rich diet (3 weeks) revealed that 1/3



of KCs were monocyte-derived KCs (moKCs), as opposed to embryonically-derived KCs (emKCs) that reside in the liver at the steady state. The recruitment of monocytes that can convert into moKCs and engraft the KC pool has been recently reported in various conditions<sup>20,21,24</sup>, including our recent study in NASH<sup>15</sup>. While having an overall similar transcriptomic profile than their emKCs counterparts, moKCs potentially displayed altered functions<sup>14,15</sup>. Along these lines, our preliminary data demonstrated that **moKCs found within the livers of hypercholesterolemic mice were significantly less lipid-loaded than emKCs**. In addition, we observed that **replacement of emKCs by moKCs favors hypercholesterolemia**.

### *Specific aims*

#### **1) Mechanisms controlling KCs proliferation in response to hypercholesterolemia**

We will explore the Csf1/Csf1-R signaling pathway known to control trMac proliferation and maintenance. Neutralizing Abs and pharmacological inhibitors of Csf1-R kinase activity will be used to assess their impact on KCs proliferation in LDLr KO mice fed 1% chol diet. Csf1-R ligands Il-34 and Csf1 gene expressions will be monitored in livers upon induction of hypercholesterolemia. KCs express the EPO-receptor and proliferate following administration of Epo *in vivo*<sup>26</sup>. Thus, following on the transient increase in plasma EPO we observed, we will evaluate the effect of anti-EPO neutralizing Abs on KCs cycling and population doubling. Moreover, the transcription factor (TF) *Bhlhe40* was significantly upregulated (our RNAseq) in proliferative KCs following induction of hypercholesterolemia. This TF was recently shown to control peritoneal Mac proliferation<sup>27</sup> but also able to bind to the cholesterol sensor LXR $\alpha$ <sup>28</sup>, a key regulator of KCs survival<sup>23</sup>. The role of *Bhlhe40* will be assessed in *Cd207-cre x Bhlhe40<sup>f/f</sup>* mice to generate *Bhlhe40*-deficient KC mice.

#### **2) Impact of hypercholesterolemia on KCs homeostasis and ontogeny**

##### a) Determinants of a differential lipid loading between emKCs and moKCs.

Lipidomic and RNAseq analyses will be performed on cell-sorted moKCs and emKCs from hypercholesterolemic mice to uncover differentially regulated cellular lipid-related pathways between the two KC subsets. Fluorescently labeled native- or oxidized-LDL will be injected to mice followed by flow cytometry (FC) analysis of emKC and moKC to evaluate whether they exhibit differential uptake capacities depending on the nature of the lipoproteins injected.

b) Determine whether moKCs can maintain in the long term.

Hypercholesterolemia will be induced in LDLr KO mice for 3 weeks, then mice will be switched to chow diet for 4 or 8 weeks. We will then determine by FC whether moKCs generated during hypercholesterolemia are maintained within the KC pool when the disease regresses. To more accurately trace moKCs, we will also perform these studies with bone-marrow (BM) chimeras allowing fate mapping of GFP+ monocyte-derived cells, as we published<sup>15</sup>. Hepatic engrafting and localization of moKCs will be analyzed by IHC and multiphoton imaging microscopy.

c) Impact of increased survival of emKCs to cell death on moKCs generation.

We recently reported that protecting emKCs from cell death by overexpression of the anti-apoptotic *Bcl2* gene limited moKCs generation in the context of steatohepatitis<sup>15</sup>. To evaluate whether similar mechanisms are operative in the hypercholesterolemic context, BM chimeras will be generated as published<sup>15</sup> using Cd68-Bcl2 x CCR2-KO or CCR2-KO mice as recipients of GFP+ BM cells. The proportion of engrafted moKCs will be evaluated in the 2 groups after prolonged exposure of the mice to hypercholesterolemia (induced by cholesterol feeding and overexpression of PCSK9<sup>29</sup> to inactivate the LDL-receptor using AAV-PCSK9 administration).

d) Determine the impact of hypercholesterolemia on RBC metabolism and iron fluxes.

We observed diminished iron liver store in livers of hypercholesterolemic mice. We will further characterize perturbation in iron metabolism induced by hypercholesterolemia by measuring iron tissue and plasma levels, expression levels of main iron transporters and circulating regulators. Cytometry and intravital two-photons microscopy imaging will be used to investigate *in vivo* the differential clearance by KCs of RBCs from normo- or hypercholesterolemic mice. We will use fluorescent reporter mice for KCs and RBCs (CSF1R-AppleFP, UBI-GFP) in combination with CARS to quantify lipid content<sup>30</sup>. Impact of hypercholesterolemia on RBCs half-life will be monitored by biotin-labeling of RBCs. We will seek for potential determinants favoring RBCs phagocytosis by evaluating phosphatidylserine exposure (apoptosis marker) and CD47 expression ("don't eat me" signal protecting cells from phagocytosis) on RBCs. We will also perform lipidomic analyses of RBCs to search for changes in lipid content following induction of hypercholesterolemia such as enrichment in membrane cholesterol (that can rigidify membranes), or in sphingosine 1-P ("find-me" signal promoting dying cell clearance by Macs<sup>31</sup>).

e) Influence of cellular iron fluxes on KCs' homeostasis.

Iron supplementation will be given to hypercholesterolemic LDLr KO mice to measure the consequences on KCs numbers, lipid-loading, inflammatory status, production of lipid reactive oxygen species (characteristic of ferroptosis, an iron-dependent cell death) and moKCs engraftment. We will evaluate the impact of increasing cellular iron efflux by repressing hepcidin (*Hamp*) expression. This hormone controls cellular iron efflux by binding to the iron exporter Fpn1 and inducing its degradation. Mice with genetic deletion of *hamp* in the hepatocyte (*Alb-cre* x *Hamp*<sup>f/f</sup>), the main site production<sup>32</sup> will be analyzed in a hypercholesterolemic context. As recently demonstrated<sup>33</sup>, Macs-derived hepcidin can also exert autocrine activities. Thus, we will also evaluate the impact of targeted deletion of hepcidin in KCs (*CD207-cre* x *Hamp*<sup>f/f</sup>) under hypercholesterolemic conditions.

**3) KCs contribution to cholesterol homeostasis and atherosclerosis**

a) Evaluating the pro-atherogenic potential of moKCs.

We will generate LDLr KO mice exhibiting similar KC numbers but various proportions of moKCs and emKCS in their livers using *Cd207-DTR* x LDLr KO mice treated either with active or inactivated DT, as observed in our preliminary data. Mice will be fed a cholesterol-rich diet for 2-months and analyzed for liver and systemic inflammation, impact on RCT and atherosclerosis. Plasma cholesterol levels will be followed over the time course of the study. To uncover the mechanisms responsible for differences in plasma cholesterol levels, hepatic VLDL production and lipoproteins plasma clearance will be measured.

b) Anti-atherogenic impact of protecting KCs to cell death-

Building on our studies in which overexpression of the anti-apoptotic *bcl2* gene under the control of the CD68 myeloid promoter increased KC numbers<sup>9</sup>, we will characterize triple transgenic *CD207-Cre* x *CAGs-LSL-rtTA3* x *tetO-Bcl2* mice under hypercholesterolemia. KC-specific cre-mediated deletion of the floxed-Stop cassette allows inducible *Bcl2* gene expression by administration of doxycycline to the mice. We will investigate whether increasing KCs numbers impacts on cholesterol homeostasis and atherosclerosis.

## Project references

1. Ference, B. A. *et al.* Low-density lipoproteins cause atherosclerotic cardiovascular disease. 1. Evidence from genetic, epidemiologic, and clinical studies. A consensus statement from the European Atherosclerosis Society Consensus Panel. *Eur. Heart J.* **38**, 2459–2472 (2017).
2. Que, X. *et al.* Oxidized phospholipids are proinflammatory and proatherogenic in hypercholesterolaemic mice. *Nature* **558**, 301–306 (2018).
3. Guerin, M. *et al.* Association of Serum Cholesterol Efflux Capacity With Mortality in Patients With ST-Segment Elevation Myocardial Infarction. *Journal of the American College of Cardiology* **72**, 3259–3269 (2018).
4. Shea, S. *et al.* Cholesterol Mass Efflux Capacity, Incident Cardiovascular Disease, and Progression of Carotid Plaque: The Multi-Ethnic Study of Atherosclerosis. *ATVB* **39**, 89–96 (2019).
5. Huby, T. *et al.* Knockdown expression and hepatic deficiency reveal an atheroprotective role for SR-BI in liver and peripheral tissues. *J. Clin. Invest.* **116**, 2767–2776 (2006).
6. El Bouhassani, M. *et al.* Cholesteryl ester transfer protein expression partially attenuates the adverse effects of SR-BI receptor deficiency on cholesterol metabolism and atherosclerosis. *J. Biol. Chem.* **286**, 17227–17238 (2011).
7. Hung, K. T., Berisha, S. Z., Ritchey, B. M., Santore, J. & Smith, J. D. Red blood cells play a role in reverse cholesterol transport. *Arterioscler. Thromb. Vasc. Biol.* **32**, 1460–1465 (2012).
8. Shearn, A. I. U. *et al.* Bcl-x inactivation in macrophages accelerates progression of advanced atherosclerotic lesions in ApoE(-/-) mice. *Arterioscler. Thromb. Vasc. Biol.* **32**, 1142–1149 (2012).
9. Bouchareychas, L. *et al.* Promoting macrophage survival delays progression of pre-existing atherosclerotic lesions through macrophage-derived apoE. *Cardiovasc. Res.* **108**, 111–123 (2015).
10. Wynn, T. A. & Vannella, K. M. Macrophages in Tissue Repair, Regeneration, and Fibrosis. *Immunity* **44**, 450–462 (2016).
11. Sawai, C. M. *et al.* Hematopoietic Stem Cells Are the Major Source of Multilineage Hematopoiesis in Adult Animals. *Immunity* **45**, 597–609 (2016).
12. Hoeffel, G. *et al.* C-Myb(+) erythro-myeloid progenitor-derived fetal monocytes give rise to adult tissue-resident macrophages. *Immunity* **42**, 665–78 (2015).
13. Liu, Z. *et al.* Fate Mapping via Ms4a3-Expression History Traces Monocyte-Derived Cells. *Cell* **178**, 1509-1525.e19 (2019).
14. Remmerie, A. *et al.* Osteopontin Expression Identifies a Subset of Recruited Macrophages Distinct from Kupffer Cells in the Fatty Liver. *Immunity* **53**, 641-657.e14 (2020).
15. Tran, S. *et al.* Impaired Kupffer Cell Self-Renewal Alters the Liver Response to Lipid Overload during Non-alcoholic Steatohepatitis. *Immunity* **53**, 627-640.e5 (2020).
16. Seidman, J. S. *et al.* Niche-Specific Reprogramming of Epigenetic Landscapes Drives Myeloid Cell Diversity in Nonalcoholic Steatohepatitis. *Immunity* **52**, 1057-1074.e7 (2020).
17. Theurl, I. *et al.* On-demand erythrocyte disposal and iron recycling requires transient macrophages in the liver. *Nat. Med.* **22**, 945–951 (2016).
18. Bleriot, C. *et al.* Liver-resident macrophage necroptosis orchestrates type 1 microbicidal inflammation and type-2-mediated tissue repair during bacterial infection. *Immunity* **42**, 145–58 (2015).
19. Lai, S. M. *et al.* Organ-Specific Fate, Recruitment, and Refilling Dynamics of Tissue-Resident Macrophages during Blood-Stage Malaria. *Cell Reports* **25**, 3099-3109.e3 (2018).
20. Scott, C. L. *et al.* Bone marrow-derived monocytes give rise to self-renewing and fully differentiated Kupffer cells. *Nat Commun* **7**, 10321 (2016).
21. Bonnardel, J. *et al.* Stellate Cells, Hepatocytes, and Endothelial Cells Imprint the Kupffer Cell Identity on Monocytes Colonizing the Liver Macrophage Niche. *Immunity* **51**, 638-654.e9 (2019).
22. Venkateswaran, A. *et al.* Control of cellular cholesterol efflux by the nuclear oxysterol receptor LXRA. *Proceedings of the National Academy of Sciences* **97**, 12097–12102 (2000).
23. Scott, C. L. *et al.* The Transcription Factor ZEB2 Is Required to Maintain the Tissue-Specific Identities of Macrophages. *Immunity* **49**, 312-325.e5 (2018).

24. Sakai, M. *et al.* Liver-Derived Signals Sequentially Reprogram Myeloid Enhancers to Initiate and Maintain Kupffer Cell Identity. *Immunity* **51**, 655-670.e8 (2019).
25. Kohyama, M. *et al.* Role for Spi-C in the development of red pulp macrophages and splenic iron homeostasis. *Nature* **457**, 318–321 (2009).
26. Gilboa, D. *et al.* Erythropoietin enhances Kupffer cell number and activity in the challenged liver. *Sci Rep* **7**, 10379 (2017).
27. Jarjour, N. N. *et al.* Bhlhe40 mediates tissue-specific control of macrophage proliferation in homeostasis and type 2 immunity. *Nat. Immunol.* **20**, 687–700 (2019).
28. Tian, J. *et al.* BHLHE40, a third transcription factor required for insulin induction of SREBP-1c mRNA in rodent liver. *Elife* **7**, (2018).
29. Goettsch, C. *et al.* A single injection of gain-of-function mutant PCSK9 adeno-associated virus vector induces cardiovascular calcification in mice with no genetic modification. *Atherosclerosis* **251**, 109–118 (2016).
30. Boissonnas, A. *et al.* Imaging resident and recruited macrophage contribution to Wallerian degeneration. *Journal of Experimental Medicine* **217**, e20200471 (2020).
31. Luo, B. *et al.* Erythropoietin Signaling in Macrophages Promotes Dying Cell Clearance and Immune Tolerance. *Immunity* **44**, 287–302 (2016).
32. Zumerle, S. *et al.* Targeted disruption of hepcidin in the liver recapitulates the hemochromatotic phenotype. *Blood* **123**, 3646–3650 (2014).
33. Zlatanova, I. *et al.* Iron Regulator Hepcidin Impairs Macrophage-Dependent Cardiac Repair After Injury. *Circulation* **139**, 1530–1547 (2019).

## Selected publications

# Regulation of the Expression of the Apolipoprotein(a) Gene Evidence for a Regulatory Role of the 5' Distal Apolipoprotein(a) Transcription Control Region Enhancer in Yeast Artificial Chromosome Transgenic Mice

Thierry Huby, Veena Afzal, Chantal Doucet, Richard M. Lawn, Elaine L. Gong, M. John Chapman,  
Joëlle Thillet, Edward M. Rubin

**Objective**—The apolipoprotein(a) [apo(a)] gene locus is the major determinant of the circulating concentration of the atherothrombogenic lipoprotein Lp(a). In vitro analysis of the intergenic region between the apo(a) and plasminogen genes revealed the presence of a putative apo(a) transcription control region (ACR) approximately 20 kb upstream of the apo(a) gene that significantly increases the minimal promoter activity of the human apo(a) gene.

**Methods and Results**—To examine the function of the ACR in its natural genomic context, we used the Cre-loxP recombination system to generate 2 nearly identical apo(a)-yeast artificial chromosome transgenic mouse lines that possess a single integration site for the human apo(a) transgene in the mouse genome but differ by the presence or absence of the ACR enhancer. Analysis of the 2 groups of animals revealed that the deletion of the ACR was associated with 30% reduction in plasma and mRNA apo(a) levels. Apo(a)-yeast artificial chromosome transgenic mice with and without the ACR sequence were similar in all other aspects of apo(a) regulation, including liver-specific apo(a) expression and alteration in expression levels in response to sexual maturation and a high-fat diet.

**Conclusions**—This study provides the first experimental in vivo evidence for a functional role of the ACR enhancer in determining levels of apo(a) expression. (*Arterioscler Thromb Vasc Biol.* 2003;23:1633-1639.)

**Key Words:** apolipoprotein(a) ■ gene expression ■ enhancer ■ yeast artificial chromosome ■ transgenic mice

Lipoprotein(a) [Lp(a)] is a cholesterol-rich particle that differs from LDL by the presence of the highly glycosylated apolipoprotein (apo) apo(a), which is covalently linked by a disulfide bond to apoB100.<sup>1,2</sup> Clinical interest in Lp(a) lies in its potential role as a proatherogenic and prothrombogenic risk factor.<sup>3</sup> Despite some conflicting results, numerous prospective studies have demonstrated an association between elevated levels of Lp(a) and coronary heart disease.<sup>4</sup>

The plasma concentration of Lp(a) is an inherited quantitative trait and remains fairly constant throughout life in a given individual. Nevertheless, Lp(a) levels may differ over a thousand-fold range between individuals. The apo(a) gene is the major determinant of lipoprotein(a) concentration. It has been estimated that the apo(a) gene locus explain from 74% to more than 90% of the intraindividual variability in Lp(a) levels in the white population.<sup>5,6</sup> The size polymorphism of apo(a) affects apo(a) protein processing<sup>7</sup> and clearly accounts for a significant portion of the total variability in Lp(a) levels seen in human populations.<sup>5,8,9</sup> However, other *cis*-sequences

that influence apo(a) expression are also believed to contribute to variance in plasma Lp(a) levels.<sup>10-12</sup>

In addition to humans, the apo(a) gene is naturally present only in Old World monkeys and the hedgehog. Because of the paucity of model organisms with an apo(a) orthologue, the regulation of apo(a) synthesis has been difficult to assess in vivo. Yeast artificial chromosome (YAC) genomic clones carrying human apo(a) alleles with significant 5' and 3' human flanking DNA have been used to generate transgenic mouse lines.<sup>13,14</sup> These transgenic mice, expressing apo(a) in an appropriate liver-specific manner, have provided information regarding the regulation of apo(a) mRNA synthesis most notably by the effect on its expression of ovarian sex steroid hormones<sup>15</sup> and growth hormone.<sup>16</sup> The transcriptional control elements that participate in basal apo(a) expression and in the above regulatory processes are yet to be characterized.

Functional analysis of the plasminogen apo(a) intergenic 40-kb sequence has revealed the presence of 2 candidate regions that possess enhancer activities in transient transfection assays.<sup>17,18</sup> These regions coincide with liver-specific

Received February 25, 2003; revision accepted May 15, 2003.

From Institut National de la Santé et de la Recherche Médicale (T.H., C.D., M.J.C., J.T.), INSERM Unit 551, Dyslipemias and Atherosclerosis: Genetics, Metabolism and Therapeutics, Hôpital de la Pitié, Paris, France; Genome Sciences Department (V.A., E.L.G., E.M.R.), Lawrence Berkeley National Laboratory, Berkeley, Calif; and CV Therapeutics (R.M.L.), Palo Alto, Calif.

Correspondence to Thierry Huby, INSERM Unit 551, Hôpital de la Pitié, Pavillon Benjamin Delessert, 83 Boulevard de l'Hôpital, 75651, Paris Cedex 13, France. E-mail thuby@infobiogen.fr

© 2003 American Heart Association, Inc.

*Arterioscler Thromb Vasc Biol.* is available at <http://www.atvbaha.org>

DOI: 10.1161/01.ATV.0000084637.01883.CA

DNase I–hypersensitive sites (DHII and DHIII) characterized previously and suggest that they likely correspond to open chromatin domains accessible to nuclear transcription factors. The DHII region is located approximately 26 kb away from the apo(a) promoter, and its activity is repressed in vitro by estrogen, suggesting that it may correspond to the *cis*-regulatory element mediating estrogen-dependent repression of apo(a) expression.<sup>19</sup> The DHIII core element, also called the apo(a) transcription control region (ACR), exhibits the highest stimulating activity (10- to 15-fold) of the 2 enhancers when ligated to the apo(a) proximal promoter. Of note is the observation that the ACR is located within the 5' untranslated region of a line 1 retrotransposon element, nearly 20 kb upstream of the transcription start site of the apo(a) gene.

To evaluate the functional role of the ACR enhancer in its natural genomic context, we created 2 mouse lines containing a 270-kb human apo(a) transgene that differs only by the presence or the absence of the ACR element. Analysis of apo(a) expression in these animals suggests that whereas the targeted deletion of the ACR sequence in apo(a) transgenic mice does not affect various aspects of the regulation of the apo(a) gene, it does impact basal apo(a) plasma levels. These findings provide the first experimental evidence that the ACR actively participates in apo(a) gene expression in vivo.

## Methods

### ACR Targeting Vector, Replacement of the ACR Element by a Floxed ACR in the apo(a)-YAC, Analysis of apo(a)-YAC Modifications, and apo(a)-YAC Integration Into Mouse Embryonic Stem (ES) Cells

Please see the expanded Methods section, available online at <http://atvb.ahajournals.org>.

### Generation of Transgenic Mice

Two positive ES clones containing the apo(a)-YAC were injected into C57BL/6J blastocysts, which were implanted into recipient females. Chimeric mice were obtained and mated with C57BL/6J mice. Germ line transmission was evaluated in the F1 agouti progeny by polymerase chain reaction (PCR) analysis. Plasma from PCR-tested positive animals were subjected to immunoblot analysis using a polyclonal anti-apo(a) antibody to evaluate apo(a) production. MMTV-Cre transgenic mice (>95% FVB genetic background) were bred with apo(a) transgenic mice to produce littermate mice of the desired genotypes used in this study. Genotyping of the animals for the MMTV-Cre transgene was done by PCR using the primer pair Cre-F (5'-GGTCGATGCAACGAGTGATG) and Cre-R (5'-CAGCATTGCTGTCACCTGGTC) (293 bp). The animals were housed in a conventional animal facility on a 6 AM to 6 PM dark/light cycle. They were weaned at 21 days and fed ad libitum a normal mouse chow diet (Purina No. 5001). For the high-fat diet experiment, 14- to 20-week-old female transgenic mice were placed on a Western-type diet consisting of 1.25% cholesterol, 0.5% cholic acid, and 15% fat for 2 weeks. Plasma samples were collected before and after the diet.

### RNA Preparation and Reverse Transcription-PCR Methods

Please see the expanded Methods section, available online at <http://atvb.ahajournals.org>.

## Immunoblotting and Quantification of Plasma apo(a)

Blood samples were collected in heparinized capillary tubes from the retro-orbital sinus at the specified age and centrifuged, and plasma was stored at  $-80^{\circ}\text{C}$ . Samples were electrophoresed on 4.5% SDS-polyacrylamide gel under reducing conditions. Proteins were subsequently transferred onto nitrocellulose membranes (Hybond ECL, Amersham Pharmacia Biotech) for Western blot analysis using a peroxidase-conjugated sheep polyclonal anti-apo(a) antibody.<sup>20</sup> The revelation was performed by chemiluminescence using Hyperfilm ECL (Amersham Pharmacia Biotech) for signal capture. Deviation from a linear response of the film to the emitted signal intensity was controlled for by using low film exposures. Films were digitized with a desktop scanner, and densitometry was performed with the image processing and analysis program Scion image. For normalization and quantification purposes, a pool of plasma collected from several apo(a) transgenic mice was included in all Western blots. The apo(a) concentration of the plasma pool was determined by densitometric analysis of a Western blot loaded with known quantities of a purified recombinant apo(a)<sup>21</sup> along with the pool. The presence of aliquots of the plasma pool in all Western blots allowed the conversion of the measured peak areas into apo(a) quantities. For each plasma sample, at least 3 independent Western blot experiments were performed to calculate a mean value  $\pm$  SD. This normalization and quantification procedure gave a mean interassay CV of 29% calculated on the basis of all Western blots performed. The mean CV calculated on intraassays without normalizing to the pool was 17%. One animal exhibiting an atypical apo(a) plasma level relative to the other members of its group [value above the mean apo(a) level plus  $3 \times \text{SD}$ ] was considered as an outlier and excluded from the study. At the indicated time points, apo(a) plasma levels between groups of mice were compared using Student's *t* test.

## Results

### Creation of apo(a)-YAC Transgenic Mice With or Without the ACR

The general strategy to modify the apo(a)-YAC by flanking the ACR with *loxP* sequences (floxed ACR) is presented as supplementary data (Figure I, please see <http://atvb.ahajournals.org>). To generate apo(a) transgenic (tg) mice, ES clones that had integrated the apo(a)-YAC through polyethylene glycol (PEG)-mediated spheroplast fusion were injected into C57BL/6 blastocysts. The introduction of YACs into mammalian cells by spheroplast fusion has been shown in numerous studies to result in the stable integration of single-copy, unrearranged YAC transgenes.<sup>22–24</sup> Chimeric mice had variable plasma apo(a) levels, as documented by Western blot analysis. When immunodetectable, the size of the apo(a) protein secreted was identical in every animal, suggesting that the apo(a)-YAC present in the selected ES clones had not been rearranged. The apparent molecular mass of the apo(a) isoform expressed was consistent with the YAC containing a 12 kringle 4 type-2 repeats apo(a) allele, as originally reported for this human apo(a) YAC.<sup>13</sup> Two of 5 chimeric males derived from the same ES clone gave germ-line transmission of the apo(a)-YAC when mated with C57BL/6 females and were used to establish transgenic lines. The apo(a)-YAC transgene was maintained in an hemizygous state by repeated breeding with C57BL/6 mice. Males from the F2 generation offspring were mated with MMTV-Cre transgenic females to produce littermate mice that were either hemizygous for the apo(a) transgene or doubly hemizygous with both transgenes. Cre-mediated recombination of floxed constructs using this specific Cre recombinase-expressing



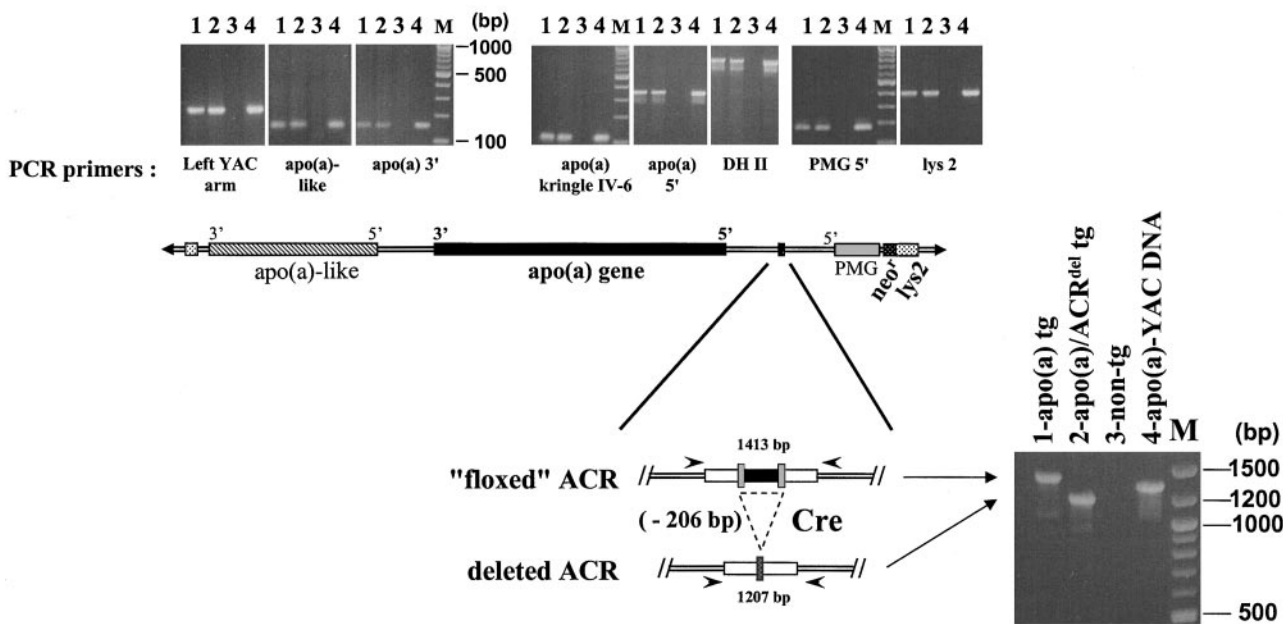


**Figure 1.** Comprehensive PCR analysis of the apo(a)-YAC transgene in apo(a) and apo(a)/ACR<sup>del</sup> tg mice. Genomic DNA prepared from apo(a) transgenic (lane 1) or apo(a)/ACR<sup>del</sup> transgenic (lane 2) mice were subjected to PCR amplification using specific primer sets spanning the entire apo(a)-YAC length. DNA prepared from a nontransgenic mouse (lane 3) and from the pLys2-neo retrofitted apo(a)-YAC (lane 4) were included as negative and positive controls, respectively. M is the molecular-weight DNA marker. Top, PCR amplifications for the left YAC arm, apo(a)-like 5' region, apo(a) 3', apo(a) kringle IV type 6, apo(a) 5', apo(a) DHII enhancer, plasminogen (PMG) 5' region, and yeast lys2 gene. Bottom, PCR amplification of the ACR region. The sizes of the PCR products corresponding to the floxed ACR [apo(a) tg, lane 1], the cre-deleted ACR [apo(a)/ACR<sup>del</sup> tg, lane 2], and the nonmodified ACR region [apo(a)-YAC, lane 4] are 1413, 1207, and 1337 bp, respectively.

line has been shown to occur in every tissue examined and notably the female germ line.<sup>25</sup> We were able to conclude based on PCR analysis that transmission of the cre transgene was systematically accompanied by the deletion of the floxed ACR element in the apo(a)-YAC transgene. Recombination appeared to be total, because amplification of the PCR fragment corresponding to the nonrecombined floxed ACR was not observed in any of the tissues analyzed (liver or tail) of the double apo(a)/MMTV-cre progeny (Figure 1). These animals were designated apo(a)/ACR<sup>del</sup> tg mice. Comprehensive PCR analysis covering the entire apo(a)-YAC was run on both apo(a) and apo(a)/ACR<sup>del</sup> tg mice and showed the presence of all PCR products of the expected size for both genotypes (Figure 1). Taken together, these data are consistent with the presence of the apo(a)-YAC in its entirety in all apo(a)-YAC transgenic mice but differing solely in the apo(a)/ACR<sup>del</sup> progeny by the absence of the ACR.

**Apo(a) Transgene Tissue Expression**

Although small amounts of apo(a) mRNA were detected in testes and brain of rhesus monkeys, the liver is the major site of apo(a) synthesis in humans and Old World monkeys.<sup>26,27</sup> To investigate whether deletion of the ACR could affect the tissue specificity of apo(a) mRNA synthesis, we examined the tissue distribution of apo(a) expression in apo(a) and apo(a)/ACR<sup>del</sup> tg mice by subjecting total RNA preparations from several tissues (adrenal, kidney, heart, spleen, brain, and liver) to reverse transcription (RT)-PCR analysis (Figure 2). Apo(a) mRNA was detected only in the liver for the various lines of mice independent of whether their apo(a) transgene contained the ACR.

**Apo(a) Expression Levels**

Apo(a) plasma levels in transgenic mice were determined by densitometric analysis of immunoblots performed with a polyclonal anti-apo(a) antibody. Plasmas of apo(a) and apo(a)/ACR<sup>del</sup> mice were analyzed at different time points over an 8-week period (Figure 3). Although male and female mice exhibited similar levels at the 28-day time point (compare band intensities against the pool lane in Figure 3), apo(a) expression decreased after 4 weeks of age in male mice containing both apo(a) and apo(a)/ACR<sup>del</sup> transgenes. This decrease associated with the sexual maturation of the animals has been previously reported in transgenic mice carrying the same apo(a)-YAC transgene clone<sup>13</sup> as well as in another line of transgenic mice containing a different human apo(a) genomic transgene.<sup>14</sup> Such a reduction in plasma apo(a) levels has been previously shown to associate with decreases in expression of the human apo(a) transgene. In contrast, we observed a 2- to 3-fold increase of plasma levels of apo(a) after 4 weeks in female mice.

To evaluate whether the deletion of the ACR influenced the level of apo(a) synthesis, we compared apo(a) plasma concentrations in apo(a) and apo(a)/ACR<sup>del</sup> littermate mice (Figure 4A). In young animals (28-day time point), there was a clear interindividual variability (2- to 3-fold) in the plasma levels of apo(a) in female and male mice for both genotypes. It is noteworthy that similar variability was also observed in the other apo(a)-YAC transgenic line developed by Acquati et al.<sup>14</sup> The mean apo(a) level in female mice containing the apo(a)/ACR<sup>del</sup> transgene was some 30% ( $P=0.01$ ) lower than that in female mice containing an intact apo(a) transgene

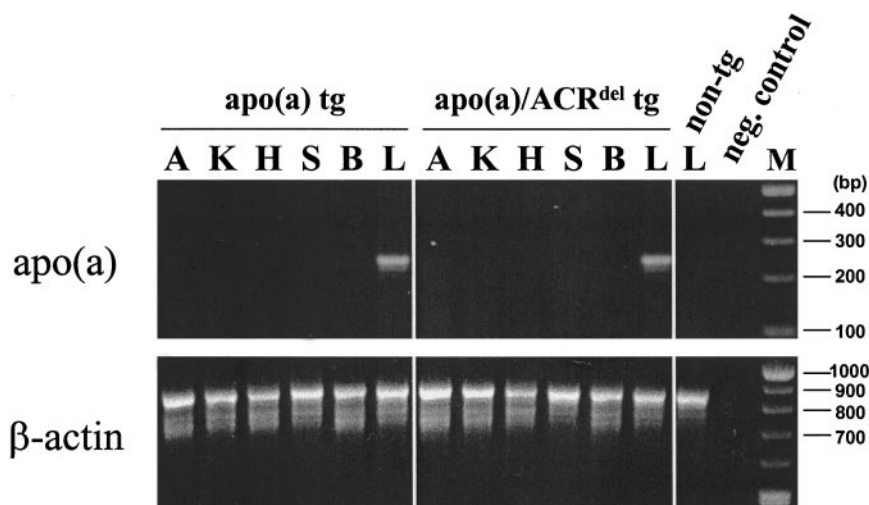


**Figure 2.** Tissue expression of the apo(a) transgene. Total RNA isolated from the adrenals (A), kidney (K), heart (H), spleen (S), brain (B), and liver (L) of apo(a) and apo(a)/ACR<sup>del</sup> tg mice was subjected to RT, followed by PCR amplification using apo(a) gene and β-actin gene-specific primer pairs. PCR analysis of cDNA prepared from the liver of a non-tg mouse and from non-reverse-transcribed RNA was used as control. Molecular weight DNA markers (M) are present at right.

(1.4±0.5 versus 2.0±0.8 μg/mL, respectively). After sexual maturity (day 84), apo(a) concentration varied noticeably between individuals among the 2 groups of female mice. Similarly to day 28, a statistically significant decrease (27%; *P*=0.04) in mean plasma apo(a) level was noted in female mice containing an apo(a)/ACR<sup>del</sup> transgene compared with those containing an intact apo(a) transgene (4.0±2.0 versus 5.5±2.0 μg/mL, respectively). Likewise, comparison of the amounts of hepatic apo(a) mRNA between both genotypes using real-time quantitative RT-PCR revealed the same decrease as that seen by comparing plasma apo(a) protein concentrations (Figure 4B). These results provide good support for a role of the ACR in determining the level of apo(a) gene expression and thereby apo(a) plasma levels. Assessing the impact of deleting the ACR from the apo(a) transgene was more complicated in male mice because of diminished expression of apo(a) as the males aged. Because of the extremely low concentrations of apo(a) in postpubertal males, the comparison of apo(a) levels could not be performed after puberty. In young apo(a) transgenic males, the loss of the ACR element was associated with a 21% reduction in apo(a) plasma levels, a difference that did not quite achieve statistical significance (Figure 4A).

### Changes in apo(a) Expression After a High-Fat Diet

Cholesterol- and cholate-containing high-fat diet has previously been demonstrated to affect apo(a) mRNA levels in apo(a) transgenic mice.<sup>14</sup> To address the role of the ACR enhancer in this transcriptional regulation of apo(a) expression, adult apo(a) and apo(a)/ACR<sup>del</sup> female mice (n=4 in each group) were fed a Western-type diet for 2 weeks. As illustrated in Figure 5A, whereas apo(a) plasma concentrations in both groups of mice before the diet were in the same range as those observed at 84 days (Figure 4), a marked decrease (≈3-fold) in the plasma levels of apo(a) was clearly observed after the Western diet. However, densitometric analyses of the Western blots indicated a similar reduction in the apo(a) plasma concentrations in either apo(a) tg or apo(a)/ACR<sup>del</sup> tg mice. Comparison of hepatic apo(a) mRNA levels from female mice fed a chow or the high-fat diet showed that, as previously reported,<sup>14</sup> the pronounced fall in apo(a) plasma levels in mice receiving the high-fat diet was associated with a similar reduction in apo(a) mRNA levels (Figure 5B). Interestingly, despite this important decline in the amount of apo(a) transcript after the high-fat diet, the apo(a)/ACR<sup>del</sup> tg mice still displayed an approximately 30%

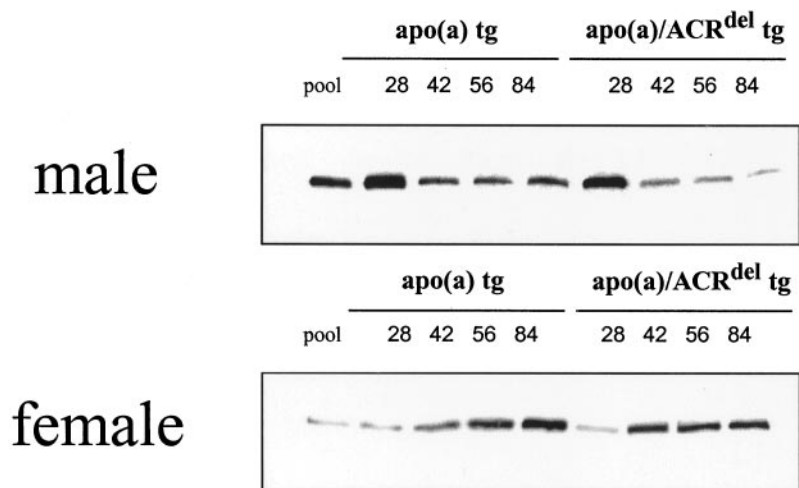


**Figure 3.** Time course of apo(a) plasma levels. Plasma samples were collected from male and female apo(a) and apo(a)/ACR<sup>del</sup> transgenic animals at the age of 28, 42, 56, and 84 days and analyzed on reducing SDS-PAGE followed by immunoblotting with an anti-apo(a) antibody. A pool of plasma collected from several apo(a) transgenic mice was included in all Western blots for normalization and quantification purposes as described under Methods. To clearly reveal the respective increase or decrease in apo(a) plasma levels over time in female and in male mice, a short exposure time for the Western blots was used for females and a longer one for males.

**A. Apo(a) plasma levels**

	Apo(a) tg		Apo(a)/ACRdel tg		% decrease
	plasma apo(a) (µg/ml)				
<b>28 days-old</b>					
Female	2.0 ± 0.80 (15)	1.4 ± 0.5 (16)			30 %*
Male	1.4 ± 0.6 (8)	1.1 ± 0.5 (11)			21 %
<b>84 days-old</b>					
Female	5.5 ± 2.0 (14)	4.0 ± 2.0 (20)			27 %¶

**B. Apo(a) mRNA levels**

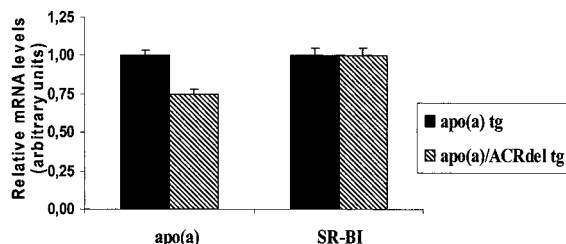


**Figure 4.** A, Apo(a) plasma levels in apo(a) and apo(a)/ACR<sup>del</sup> tg mice. Apo(a) levels were determined before (28 days old) or after (84 days old) sexual maturity for females and only at pre-pubertal age (28 days) for males. For each group of mice analyzed, the number (n) of animals and the calculated mean apo(a) levels ±SD are indicated. Comparison of apo(a) plasma levels between apo(a) and apo(a)/ACR<sup>del</sup> tg mice in age- and sex-related groups was performed using Student's *t* test (statistical significance: \**P* = 0.01; ¶*P* = 0.04). The decrease (%) in plasma levels observed in apo(a)/ACR<sup>del</sup> tg mice compared with apo(a) tg mice is indicated for each group. B, apo(a) mRNA expression levels in liver tissue of apo(a) and apo(a)/ACR<sup>del</sup> tg mice. Total RNA from the livers of adult female mice (n = 4 for both genotypes) was pooled, reverse-transcribed, and subjected to real-time PCR quantification as described in Methods. β-glucuronidase (β-GUS) was used as the reference gene to normalize the data. Values (±SD) represent the amount of mRNA relative to that measured in apo(a) tg mice, which was set arbitrarily to 1. As an additional control for the normalization procedure, the expression level of another gene (SR-BI) in both groups is shown.

decrease in apo(a) mRNA levels compared with apo(a) tg mice (Figure 5B).

**Discussion**

Recent in vitro studies that allowed identification of the enhancer element ACR located in a L1 retrotransposon upstream of the apo(a) gene have raised the possibility that apo(a) expression is partly determined by this element. Transgenic mice created for this study have enabled us to evaluate in vivo whether the enhancer is only an inherent element of the L1 or whether it actively influences apo(a) expression. Our findings are consistent with prior in vitro characterization of the ACR and add support to the hypothesis that the ACR participates in optimal transcriptional expression of the apo(a) gene. This observation represents a rare example of an L1 element affecting the expression of a nearby gene and particularly illustrates the manner in which L1s may contribute to genome evolution as potential mobile gene-control elements.

To date, 2 apo(a)-YAC clones, including the one used in this study, have successfully been used to create transgenic mice, and both constructs exhibit liver-specific expression of

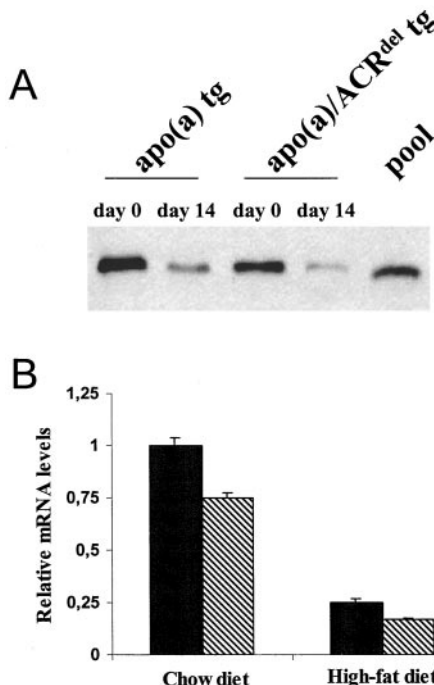


**Figure 5.** A, apo(a) plasma levels after a high-fat diet. apo(a) and apo(a)/ACR<sup>del</sup> female mice were fed with a cholesterol- and cholate-containing high-fat diet for 2 weeks. Plasma samples were collected before (day 0) and after (day 14) the diet, and apo(a) plasma concentrations were compared by Western blot densitometric analyses. Plasma pool, same as in Figure 3. B, Quantitative real-time PCR of liver apo(a) mRNA from apo(a) and apo(a)/ACR<sup>del</sup> female mice fed a chow or a high-fat diet. Total RNA from the livers of female mice (n = 4 in each group) was pooled and subjected to real-time PCR quantification. β-GUS was used as the reference gene to normalize the data. Apo(a) mRNA levels in each group are presented relative to the amount of apo(a) transcript in the chow-fed apo(a) tg mice, which was set arbitrarily to 1.

the human apo(a) transgene.<sup>13,14</sup> In this study, we observed a similar restricted tissue specificity of apo(a) expression in mice both with and without the ACR element. It is important to note that in the earlier description<sup>13</sup> of the 4 separate lines of transgenic mice carrying a single copy of the same apo(a)-YAC that we used, a large range of apo(a) plasma concentrations (1 to 75 mg/dL) was detected, the transgenic line generated in the present study being in the lower expression range. These data suggest that the important *cis*-acting elements providing liver-specific apo(a) gene transcription are present in the YAC clone; however, this region of genomic DNA is likely to some extent to be subject to chromosomal site integration effect that can influence apo(a) transgene expression. This problem was largely circumvented in the present comparative study, because the apo(a) and apo(a)/ACR<sup>del</sup> transgenes mapped to the exact same genomic location being derived from the same transgenic line.

Several studies have suggested that deletion of individual regulatory elements/enhancers that are part of a locus control region (LCR) may not necessarily result in marked reduction in gene expression, because, at least partially, functionally redundant elements may be present and may compensate for the loss of activity.<sup>24,28</sup> Of particular relevance have been

studies describing the  $\beta$ -globin LCR that consists of several DNase I-hypersensitive chromatin domains spread over a region of 20 to 30 kb.<sup>29</sup> Targeted deletions of murine 5'HS2 or HS3 sites that demonstrated important LCR activities when tested individually in various expression assays caused only a 30% reduction of murine globin gene expression.<sup>30,31</sup> Likewise, in our study, apo(a) plasma levels were only moderately altered on deletion of the ACR in vivo, whereas in vitro the enhancer exhibited robust stimulation of apo(a) promoter activity.<sup>17,18</sup> We cannot exclude, however, the possibility that integration site-specific silencing effects may have dampened the ACR activity or that the presence of other functional LCR activities contribute along with the ACR element to general transcriptional activation at the apo(a) genomic locus. Notably, in the 40-kb intergenic region that separates the 5' regions of the apo(a) and plasminogen genes, 3 other DNase I-hypersensitive sites are present,<sup>32</sup> including the apo(a) enhancer DHIII<sup>19</sup>; these regions represent important candidate regions. Recent findings have also suggested that elements that lie outside the 5' region of the apo(a) gene may also be required for its expression.<sup>14</sup>

The ACR region colocalizes with a DNase I-hypersensitive site that was initially identified exclusively in hepatoma cell types in vitro<sup>32</sup> and in vivo in the liver of apo(a)-YAC transgenic mice.<sup>18</sup> Although these observations may indicate that the ACR acts as a hepatic control region of apo(a) expression, in vitro the enhancer does not exhibit tissue specificity.<sup>17,18</sup> Besides, ACR enhancer function depends on the Ets and Sp1 transcription factors that are ubiquitously expressed. Taken together, these findings indicate that the ACR is not likely to contribute to the liver-restricted expression of apo(a). The absence of ectopic expression of the apo(a) transgene in apo(a)/ACR<sup>del</sup> observed in this study is consistent with the latter hypothesis.

Apo(a)-YAC transgenic mice constitute a valuable model in which to assess the regulation of the human apo(a) gene. However, major differences in apo(a) expression have clearly been observed in this model compared with that seen in humans. For example, marked decrease in apo(a) levels occurs when the animals are fed a high-fat diet<sup>14</sup>; by contrast, variation in the type of dietary fat consumed is associated with none to only moderate variations in Lp(a) levels in humans.<sup>33,34</sup> The profound reduction in apo(a) mRNA levels previously reported in male apo(a) tg mice during puberty<sup>13</sup> is equally not observed in humans. The results of the present study exclude the possibility that such apo(a) transcriptional regulation in mice is mediated through the ACR element, because apo(a) and apo(a)/ACR<sup>del</sup> tg behaved similarly with respect to these effects. The understanding of such regulations in apo(a) tg mice may, however, shed light on metabolic pathways that influence Lp(a) levels in humans. Recently, it has been demonstrated that the fall in apo(a) serum levels associated with puberty in apo(a)-YAC transgenic males is determined by the secretory pattern of growth hormone (GH) in mice; this pattern is distinct from that in females, which results in a sexually dimorphic regulation of apo(a) expression.<sup>16</sup> Indeed, the latter study offered insights into the mechanisms responsible for the GH-associated increase in plasma levels of Lp(a) observed in humans<sup>35</sup> by revealing that

GH regulates apo(a) expression. However, it is noteworthy that the sex-specific pattern of apo(a) expression in adult apo(a) tg mouse liver that we presently observed was distinct [apo(a) plasma levels decreased in males during puberty but increased in females] from that previously reported in apo(a)-YAC transgenic lines. Differences in genetic background between transgenic lines in the expression of GH-dependent transcription factors that modulate apo(a) transcription, and that remain to be identified, may account for this finding.

Investigation of the regulation of the expression of genes for which there is no murine orthologue in transgenic mice is beset with problems of relevance, as in the case of apo(a), for which there is a paucity of alternative experimental in vivo systems. Nonetheless, our present findings have demonstrated the impact of targeted deletion of the ACR on apo(a) expression levels in an in vivo model; moreover, such in vivo data are consistent with earlier in vitro results. Finally, the large interindividual variability in Lp(a) concentrations observed in human populations is thought to result in a large part from the combined action of multiple factors that govern apo(a) levels.<sup>36</sup> From the experimental data presented here and from a recent study in which associations between sequence variations in the ACR enhancer and plasma Lp(a) concentrations were reported in human subjects,<sup>37</sup> the ACR sequence may appear as one of these functional regulatory elements that warrants additional analysis.

### Acknowledgments

These studies were supported by INSERM and the American Heart Association (98-03) and performed under Department of Energy Contract DE-AC0376SF00098, University of California, Berkeley. Research was conducted at the E.O. Lawrence Berkeley National Laboratory and at INSERM U551, France. We would like to thank Dr K. Peterson for providing the pLys2neo vector and Dr K.U. Wagner for sharing MMTV-Cre transgenic mice. We also thank Philip N. Cooper for excellent technical assistance.

### References

- Gaubatz JW, Heideman C, Gotto AM, Morrisett JD, Dahlen GH. Human plasma lipoprotein [a]: structural properties. *J Biol Chem*. 1983;258:4582-4589.
- Utermann G. The mysteries of lipoprotein(a). *Science*. 1989;246:904-910.
- Marcovina SM, Koschinsky ML. Lipoprotein(a) as a risk factor for coronary artery disease. *Am J Cardiol*. 1998;82:57U-66U.
- Danesh J, Collins R, Peto R. Lipoprotein(a) and coronary heart disease: meta-analysis of prospective studies. *Circulation*. 2000;102:1082-1085.
- Boerwinkle E, Leffert CC, Lin J, Lackner C, Chiesa G, Hobbs HH. Apolipoprotein(a) gene accounts for greater than 90% of the variation in plasma lipoprotein(a) concentrations. *J Clin Invest*. 1992;90:52-60.
- Scholz M, Kraft HG, Lingenhel A, Delpont R, Vorster EH, Bickeboller H, Utermann G. Genetic control of lipoprotein(a) concentrations is different in Africans and Caucasians. *Eur J Hum Genet*. 1999;7:169-178.
- White AL, Guerra B, Lanford RE. Influence of allelic variation on apolipoprotein(a) folding in the endoplasmic reticulum. *J Biol Chem*. 1997;272:5048-5055.
- Sandholzer C, Hallman DM, Saha N, Sigurdsson G, Lackner C, Csaszar A, Boerwinkle E, Utermann G. Effects of the apolipoprotein(a) size polymorphism on the lipoprotein(a) concentration in 7 ethnic groups. *Hum Genet*. 1991;86:607-614.
- Kraft HG, Lingenhel A, Pang RW, Delpont R, Trommsdorff M, Vermaak H, Janus ED, Utermann G. Frequency distributions of apolipoprotein(a) kringle IV repeat alleles and their effects on lipoprotein(a) levels in Caucasian, Asian, and African populations: the distribution of null alleles is non-random. *Eur J Hum Genet*. 1996;4:74-87.

10. Suzuki K, Kuriyama M, Saito T, Ichinose A. Plasma lipoprotein(a) levels and expression of the apolipoprotein(a) gene are dependent on the nucleotide polymorphisms in its 5'-flanking region. *J Clin Invest.* 1997;99:1361-1366.
11. Kraft HG, Windegger M, Menzel HJ, Utermann G. Significant impact of the +93 C/T polymorphism in the apolipoprotein(a) gene on Lp(a) concentrations in Africans but not in Caucasians: confounding effect of linkage disequilibrium. *Hum Mol Genet.* 1998;7:257-264.
12. Brazier L, Tired L, Luc G, Arveiler D, Ruidavets JB, Evans A, Chapman J, Cambien F, Thillet J. Sequence polymorphisms in the apolipoprotein(a) gene and their association with lipoprotein(a) levels and myocardial infarction: the ECTIM study. *Atherosclerosis.* 1999;144:323-333.
13. Frazer KA, Narla G, Zhang JL, Rubin EM. The apolipoprotein(a) gene is regulated by sex hormones and acute-phase inducers in YAC transgenic mice. *Nat Genet.* 1995;9:424-431.
14. Acquati F, Hammer R, Ercoli B, Mooser V, Tao R, Ronicke V, Michalich A, Chiesa G, Taramelli R, Hobbs HH, Muller HJ. Transgenic mice expressing a human apolipoprotein[a] allele. *J Lipid Res.* 1999;40:994-1006.
15. Zysow BR, Kauser K, Lawn RM, Rubanyi GM. Effects of estrus cycle, ovariectomy, and treatment with estrogen, tamoxifen, and progesterone on apolipoprotein(a) gene expression in transgenic mice. *Arterioscler Thromb Vasc Biol.* 1997;17:1741-1745.
16. Tao R, Acquati F, Marcovina SM, Hobbs HH. Human growth hormone increases apo(a) expression in transgenic mice. *Arterioscler Thromb Vasc Biol.* 1999;19:2439-2447.
17. Yang Z, Boffelli D, Boonmark N, Schwartz K, Lawn R. Apolipoprotein(a) gene enhancer resides within a LINE element. *J Biol Chem.* 1998;273:891-897.
18. Wade DP, Puckey LH, Knight BL, Acquati F, Mihalich A, Taramelli R. Characterization of multiple enhancer regions upstream of the apolipoprotein(a) gene. *J Biol Chem.* 1997;272:30387-30399.
19. Boffelli D, Zajchowski DA, Yang Z, Lawn RM. Estrogen modulation of apolipoprotein(a) expression: identification of a regulatory element. *J Biol Chem.* 1999;274:15569-15574.
20. Doucet C, Huby T, Chapman J, Thillet J. Lipoprotein[a] in the chimpanzee: relationship of apo[a] phenotype to elevated plasma Lp[a] levels. *J Lipid Res.* 1994;35:263-270.
21. Hoover-Plow JL, Boonmark N, Skocir P, Lawn R, Plow EF. A quantitative immunoassay for the lysine-binding function of lipoprotein(a): application to recombinant apo(a) and lipoprotein(a) in plasma. *Arterioscler Thromb Vasc Biol.* 1996;16:656-664.
22. Jakobovits A, Moore AL, Green LL, Vergara GJ, Maynard-Currie CE, Austin HA, Klapholz S. Germ-line transmission and expression of a human-derived yeast artificial chromosome. *Nature.* 1993;362:255-258.
23. Davies NP, Rosewell IR, Richardson JC, Cook GP, Neuberger MS, Brownstein BH, Norris ML, Bruggemann M. Creation of mice expressing human antibody light chains by introduction of a yeast artificial chromosome containing the core region of the human immunoglobulin kappa locus. *Biotechnology (N Y).* 1993;11:911-914.
24. Lien LL, Lee Y, Orkin SH. Regulation of the myeloid-cell-expressed human gp91-phox gene as studied by transfer of yeast artificial chromosome clones into embryonic stem cells: suppression of a variegated cellular pattern of expression requires a full complement of distant cis elements. *Mol Cell Biol.* 1997;17:2279-2290.
25. Wagner KU, Wall RJ, St-Onge L, Gruss P, Wynshaw-Boris A, Garrett L, Li M, Furth PA, Hennighausen L. Cre-mediated gene deletion in the mammary gland. *Nucleic Acids Res.* 1997;25:4323-4330.
26. Tomlinson JE, McLean JW, Lawn RM. Rhesus monkey apolipoprotein(a): sequence, evolution, and sites of synthesis. *J Biol Chem.* 1989;264:5957-5965.
27. Kraft HG, Menzel HJ, Hoppichler F, Vogel W, Utermann G. Changes of genetic apolipoprotein phenotypes caused by liver transplantation: implications for apolipoprotein synthesis. *J Clin Invest.* 1989;83:137-142.
28. Bulger M, Groudine M. Looping versus linking: toward a model for long-distance gene activation. *Genes Dev.* 1999;13:2465-2477.
29. Hardison R, Slightom JL, Gumucio DL, Goodman M, Stojanovic N, Miller W. Locus control regions of mammalian beta-globin gene clusters: combining phylogenetic analyses and experimental results to gain functional insights. *Gene.* 1997;205:73-94.
30. Fiering S, Epner E, Robinson K, Zhuang Y, Telling A, Hu M, Martin DI, Enver T, Ley TJ, Groudine M. Targeted deletion of 5'HS2 of the murine beta-globin LCR reveals that it is not essential for proper regulation of the beta-globin locus. *Genes Dev.* 1995;9:2203-2213.
31. Hug BA, Wesselschmidt RL, Fiering S, Bender MA, Epner E, Groudine M, Ley TJ. Analysis of mice containing a targeted deletion of beta-globin locus control region 5' hypersensitive site 3. *Mol Cell Biol.* 1996;16:2906-2912.
32. Magnaghi P, Mihalich A, Taramelli R. Several liver specific DNase hypersensitive sites are present in the intergenic region separating human plasminogen and apoprotein(A) genes. *Biochem Biophys Res Commun.* 1994;205:930-935.
33. Almendingen K, Jordal O, Kierulf P, Sandstad B, Pedersen JI. Effects of partially hydrogenated fish oil, partially hydrogenated soybean oil, and butter on serum lipoproteins and Lp[a] in men. *J Lipid Res.* 1995;36:1370-1384.
34. Clevidence BA, Judd JT, Schaefer EJ, Jenner JL, Lichtenstein AH, Muesing RA, Wittes J, Sunkin ME. Plasma lipoprotein (a) levels in men and women consuming diets enriched in saturated, cis-, or trans-monounsaturated fatty acids. *Arterioscler Thromb Vasc Biol.* 1997;17:1657-1661.
35. Mooser V, Hobbs HH. Lipoprotein(a) and growth hormone: is the puzzle solved? *Eur J Endocrinol.* 1997;137:450-452.
36. Utermann G. Genetic architecture and evolution of the lipoprotein(A) trait. *Curr Opin Lipidol.* 1999;10:133-141.
37. Puckey LH, Knight BL. Sequence and functional changes in a putative enhancer region upstream of the apolipoprotein(a) gene. *Atherosclerosis.* 2003;166:119-127.

# Transcription Factor Sterol Regulatory Element–Binding Protein 2 Regulates Scavenger Receptor Cla-1 Gene Expression

Morgan Tréguier, Chantal Doucet, Martine Moreau, Christiane Dachet, Joëlle Thillet, M. John Chapman, Thierry Huby

**Objective**—The human scavenger receptor class B type I (Cla-1) plays a key role in cellular cholesterol movement in facilitating transport of cholesterol between cells and lipoproteins. Indirect evidence has suggested that Cla-1 gene expression is under the feedback control of cellular cholesterol content. To define the molecular mechanisms underlying such putative regulation, we evaluated whether Cla-1 is a target gene of the sterol regulatory element–binding protein (SREBP) transcription factor family.

**Methods and Results**—Transient transfections demonstrated that SREBP factors induce Cla-1 promoter activity and that SREBP-2 is a more potent inducer than the SREBP-1a isoform. The 5′-deletion analysis of 3 kb of the 5′-flanking sequence of the Cla-1 gene, combined with site-directed mutagenesis and electrophoretic mobility shift assay, allowed identification of a unique sterol responsive element. SREBP-mediated Cla-1 regulation was confirmed in stably transfected human embryonic kidney 293 cells expressing the active form of SREBP-2 at incremental levels. In these cell lines, Cla-1 mRNA and protein levels were increased in direct proportion to the level of SREBP-2 expression.

**Conclusions**—These findings provide evidence that SREBP-2, a key regulator of cellular cholesterol uptake through modulation of the expression of the low-density lipoprotein receptor gene, may influence cellular cholesterol homeostasis via regulation of Cla-1 gene expression. (*Arterioscler Thromb Vasc Biol.* 2004;24:1-7.)

**Key Words:** SR-BI ■ SREBP ■ cholesterol homeostasis ■ regulation of gene expression ■ transcription factor

The scavenger receptor class B type I (SR-BI) has attracted considerable interest since the demonstration in vitro that it interacts with low-density lipoprotein (LDL) and high-density lipoprotein (HDL) to facilitate the bidirectional movement of cholesterol between these lipoprotein particles and SR-BI-expressing cells. On one hand, SR-BI mediates the selective uptake of cholesteryl esters (CEs) from HDL or LDL to cells; on the other, SR-BI can promote cellular efflux of free cholesterol to lipoprotein acceptor particles.<sup>1</sup> A major role of SR-BI-mediated cellular cholesterol uptake in cholesterol metabolism is strongly supported by SR-BI gene manipulation in mice. Mice totally deficient for SR-BI display elevated plasma levels of HDL-cholesterol and decreased cholesterol content in adrenal glands.<sup>2</sup> Conversely, mice that overexpress SR-BI in the liver exhibit a significant reduction in plasma HDL-cholesterol levels, concomitant with an increase in hepatic selective cholesterol uptake and cholesterol secretion in bile.<sup>3</sup>

The human homolog of SR-BI, termed Cla-1, exhibits similar tissue distribution, binding properties for a wide spectrum of plasma lipoproteins, and identical cholesterol

transfer capacities as those of murine SR-BI. Whereas SR-BI appears as a physiologically relevant HDL receptor intimately involved in HDL metabolism in rodents, the role of Cla-1 in LDL- and HDL-mediated cholesterol homeostasis in man remains incompletely understood. However, in a human hepatic cell model, Cla-1 is responsible for the major part of the selective uptake of CE from HDL and LDL particles.<sup>4</sup> This finding suggests that Cla-1 may play a pivotal role in metabolism of the cholesterol component of both lipoprotein classes in humans. Indeed, recent epidemiological studies have identified single-nucleotide polymorphisms (SNPs) in the Cla-1 gene that are associated with plasma lipid levels and lipoprotein composition.<sup>5,6</sup> Interestingly, these associations between SNPs or combinations of SNPs and HDL-cholesterol or LDL-cholesterol levels appear to be influenced by gender.

Cellular cholesterol and fatty acid metabolism is tightly regulated in animal cells and involves a family of transcription factors designated as sterol regulatory element–binding proteins (SREBPs). SREBP-1a and SREBP-1c are synthesized from a single gene through the use of alternate promoters and exons, whereas SREBP-2 is synthesized from a

Original received June 8, 2004; final version accepted September 8, 2004.

From the National Institute for Health and Medical Research (INSERM), Dyslipoproteinemia and Atherosclerosis Research Unit, Hôpital de la Pitié, Paris Cedex 13, France.

Correspondence to Thierry Huby, INSERM, Unit 551, Pavillon Benjamin Delessert, Hôpital de la Pitié, 83 Boulevard de la Pitié, 75651 Paris Cedex 13. E-mail thuby@infobiogen.fr

© 2004 American Heart Association, Inc.

*Arterioscler Thromb Vasc Biol.* is available at <http://www.atvbaha.org>

DOI: 10.1161/01.ATV.0000147896.69299.85

separate gene. All 3 are produced as precursors inserted into the membrane of the endoplasmic reticulum (ER). Proteolytic activation of the precursor form and subsequent release of the active Nter domain of the SREBP (nSREBP) is tightly regulated and occurs when the ER membrane becomes depleted in cholesterol. The soluble active nSREBP then enters the nucleus and activates transcription by binding either to 10-bp repeats known as sterol response elements (SREs), or to E-box sequences located in the promoter region of target genes. Use of transgenic mice overexpressing either of the active nuclear SREBP isoforms has demonstrated that the SREBP-1 isoforms are more relevant to fatty acid metabolism, whereas SREBP-2 is more selective in regulating cholesterol metabolism.<sup>7,8</sup>

Expression of the LDL-receptor, a key component of the cellular pathway for cholesterol uptake, is modulated as a function of cellular cholesterol content through SREBP-mediated transcriptional regulation. Indirect evidence suggests that SR-BI, which may modulate membrane cholesterol content and cellular cholesterol pool size through a pathway distinct from that of the LDL-receptor, may also be a target gene for SREBP factors. Indeed, SREBP-1a can induce the transcriptional activity of the rat SR-BI promoter through 2 SRE-binding sites *in vitro*.<sup>9</sup> Feedback control of SR-BI expression dependent on cellular cholesterol status has also been suggested *in vitro* in human keratinocytes<sup>10</sup> and *in vivo* in mouse adrenal glands<sup>11</sup> and rat ovaries.<sup>12</sup> However, in contrast, microarray analyses of RNA from livers of transgenic mice overexpressing SREBP isoforms 1a and 2 did not reveal changes in SR-BI mRNA levels.<sup>13</sup>

In this study, we evaluated the question of whether expression of the human SR-BI/Cla-1 gene is regulated via SREBP factors. Analysis of the 5'-proximal region of the Cla-1 gene allowed identification of a functional SRE-binding site through which SREBP-2 modulates Cla-1 promoter activity. Moreover, stable overexpression of nSREBP-2 in a human cell line is associated with significant upregulation of both levels of Cla-1 endogenous mRNA and protein. These findings strongly suggest that Cla-1 is a target gene for SREBP-mediated transcriptional regulation and imply that intracellular cholesterol status is implicated in regulation of its expression.

## Methods

### Plasmid Constructs and Site-Directed Mutagenesis

The Cla-1 promoter luciferase reporter plasmid p-2913 cloned into pGL3 basic vector (Promega), the corresponding 5'-deletion constructs p-258 and p-58 and the luciferase reporter plasmid for the mouse SR-BI promoter were described previously.<sup>14</sup> The expression vectors pCMV5-SREBP-1a and pCMV5-SREBP-2 were provided by K. Schoonjans (IGBMC, Illkirch, France). To generate the luciferase reporter plasmid for the LDL-receptor promoter, the proximal region (-171 to +57) of the gene was amplified by polymerase chain reaction (PCR) using human genomic DNA as template and cloned into pGL3 basic vector. The sequence was then verified in the final construct by DNA sequencing.

Site-directed mutants were prepared from construct p-258 using the GeneEditor *in vitro* Site-Directed Mutagenesis System (Promega). The synthetic complementary oligonucleotides SRE1 (5'-CAG CGG CAG CAA CCC GGG GCT TGT C-3'), SRE2 (5'-CTG CCC GTC CGT AGT GCG CCC CGC CCC GTC-3'), SRE3

(5'-CCC GCC CCG TGG CCG CCC CGG GCC CGC-3'), and the E-box sequence (5'-ACC ACT GGC CTG CTG CCG GGC TGC T-3') containing mismatched bases (underlined) were used to mutate the respective putative binding sites in the Cla-1 promoter sequence. The presence of the mutation was confirmed by sequencing.

### Stable Transfection of Human Embryonic Kidney 293 Cells With nSREBP-2

The cDNA encoding for nSREBP-2 (amino acids 1–481) was subcloned into the pcDNA3.1 expression vector (Invitrogen) containing the neomycin resistance gene. Human embryonic kidney 293 (HEK293) cells were grown for 24 hours in serum-free medium and then incubated with 4  $\mu$ g plasmid DNA and 5  $\mu$ g Lipofectamine (Invitrogen). After 6 hours of incubation, cells were trypsinized, and a serial dilution in complete medium was performed. Selective medium (complete medium supplemented with 0.5 g/L G418-sulfate) was applied 2 days later. After 2 weeks, wells containing 1 surviving colony were selected, and HEK-nSREBP-2 clones were expanded in selective medium.

### Transient Transfections, Electrophoretic Mobility Shift Assay, Immunoblot Analysis, RNA Preparation, and Real-Time Quantitative RT-PCR

Please see the expanded Methods section, available online at <http://atvb.ahajournals.org>.

## Results

### Statin and SREBP-Mediated Induction of Cla-1 Promoter Activity

Because an earlier report demonstrated that rat SR-BI promoter activity was upregulated *in vitro* by statin treatment and the SREBP-1a transcription factor,<sup>9</sup> we investigated whether the Cla-1 gene was regulated in a similar manner. The possibility that Cla-1 promoter activity could be modulated by intracellular sterol content was initially examined by transient transfection studies performed in HepG2 cells cultured in the absence or presence of cerivastatin, a potent 3-hydroxy-3-methylglutaryl-coenzyme A reductase inhibitor. Figure 1 shows that addition of cerivastatin for 24 hours resulted in differential activation of Cla-1 promoter/reporter constructs carrying  $\approx$ 3 kb (p-2913),  $\approx$ 0.4 kb (p-258), or  $\approx$ 0.2 kb (p-58) of 5'-flanking sequence of the Cla-1 gene. Whereas p-2913 and p-258 promoter activities were similarly and significantly increased 1.8-fold and 1.7-fold, respectively, by statin treatment, the activity of the p-58 construct remained unchanged. To ascertain whether the increase in Cla-1 promoter activity of p-2913 and p-258 induced by cerivastatin treatment was the result of SREBP-dependent promoter activation after cellular cholesterol depletion and not the result of a cholesterol-independent effect of statin, we performed cotransfection studies of Cla-1 promoter constructs and expression vectors coding for either nSREBP-1a or nSREBP-2 (Figure 1). As seen for the cerivastatin experiments, a statistically significant upregulation of promoter activity was observed with the p-2913 and p-258 constructs with either of the SREBP isoforms, whereas no activation occurred with the shortest p-58 construct. These data indicated that the Cla-1 promoter is a target for SREBP-dependent transactivation.

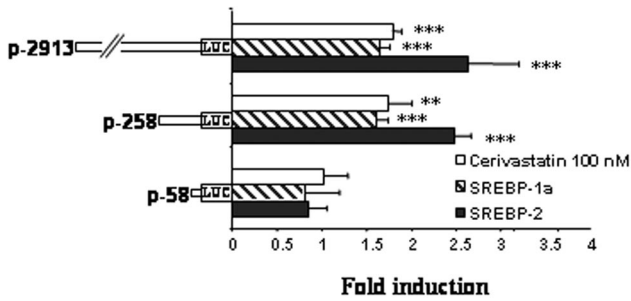


**Figure 1.** Comparison of transcriptional activation of 5'-deletion Cla-1 promoter constructs by statin or by cotransfection of SREBP-1a or SREBP-2 plasmids in HepG2 cells. The 5'-deletion Cla-1 constructs p-2913, p-258, or p-58 were cotransfected with pSVGal as reference plasmid. Statin effect (white columns), Cerivastatin was added to a concentration of 100 nM in serum-free DMEM 16 hours after transfection. Luciferase and  $\beta$ -galactosidase activities were assayed 24 hours later. SREBP cotransfection experiments, Cla-1 promoter constructs were transfected with expression vectors (20 ng) for SREBP-1a (striped columns) or SREBP-2 (black columns). Results are expressed as fold induction relative to normalized luciferase activities obtained with the respective control cells (no statin treatment or cotransfection with pCMV5 empty vector). Statistically significant differences from the controls \*\* $P < 0.01$ ; \*\*\* $P < 0.001$ .

### Differential Activation of mSR-BI and Cla-1 Promoter Activities by SREBP-1a and SREBP-2

It has been reported that SREBP-1a, SREBP-1c, and SREBP-2 may exhibit distinct efficacy in promoting transcriptional induction of target promoters.<sup>15–17</sup> Comparison of the level of transcriptional activation of p-2913 and p-258 constructs by 20 ng of pCMV5-SREBP expression vectors revealed a greater induction with the SREBP-2 encoding plasmid than with the SREBP-1a form (statistical difference  $P = 0.04$  and  $P = 0.02$  for p-2913 and p-258, respectively; Figure 1). Indeed, cotransfection of p-258 with increasing amounts of either pCMV5-SREBP-1a or pCMV5-SREBP-2 in HepG2 cells demonstrated a similar dose-dependent induction with both nSREBP forms using 1 and 5 ng of expression vectors (Figure 2A). However, whereas a 2.5-fold increase in Cla-1 promoter activity was obtained with 20 ng of the SREBP-2 plasmid (dose-dependent promoter induction was maintained up to 100 ng of SREBP-2 vector; data not shown), no further increase was observed when similar amounts of SREBP-1a vector were used (plateau induction at  $\approx 1.6$ -fold; Figure 2A). Similar results, with an identical fold increase, were obtained using the full-length p-2913 construct in place of p-258 (data not shown). To validate the capacity of SREBP-1a and SREBP-2 to transactivate target promoters in our luciferase assay, we evaluated the SREBP-mediated induction of the activity of a control reporter construct containing the proximal promoter ( $-171$  to  $+57$ ) of the human LDL-receptor gene. Under identical conditions of transfection as those used for the Cla-1 promoter plasmids, the promoter activity of the LDL-receptor reporter construct responded in a dose-dependent and similar manner when stimulated either by SREBP-1a or SREBP-2 over the range of the concentrations tested (1 to 20 ng of plasmid per well; Figure 2B). Furthermore, we evaluated the capacity of SREBP-1a and SREBP-2 to induce the activity of the mouse

SR-BI promoter ( $\approx 2.1$  kb of 5'-flanking sequence). Surprisingly, a marked increase in promoter activity was observed with both SREBP forms; however, as seen for the human promoter constructs, there was a clear differential activation of transcriptional activity of the mouse SR-BI promoter by cotransfection of either pCMV5-SREBP-1a or SREBP-2 (3.2-fold and 17.6-fold increase with SREBP-1a and SREBP-2, respectively; Figure 2C). Together, these data demonstrate that under the experimental conditions tested, SREBP-2 activates human and mouse SR-BI promoters with greater efficiency than SREBP-1a.

### Identification and Characterization of a Functional SREBP-2 Binding Site in the Promoter of the Cla-1 Gene

Data in Figure 1 revealed that p-2913 and p-258 responded in a similar manner to cerivastatin and to SREBP-mediated increase of luciferase activity. These data suggested that the 5'-deleted region between positions  $-2913$  and  $-258$  was not involved in the SREBP-specific response. Additionally, the lack of response of the p-58 plasmid to statin or SREBPs indicated that the DNA motif(s) required for the SREBP-mediated response lies in the region between positions  $-258$  and  $-58$ . Analysis of this region revealed 3 putative SREs (SRE1, SRE2, and SRE3), identified according to their homology with the consensus SRE sequence (ATC ACC CCA C). The functionality of these DNA sequences as an SRE was evaluated by site-directed mutagenesis. Whereas the induction of p-258 promoter activity by SREBP-2 was not affected by mutation of the putative SRE1 and SRE3, mutation of the SRE2 sequence resulted in the complete loss of SREBP-2 transcriptional induction of Cla-1 promoter activity (Figure 1, available online at <http://atvb.ahajournals.org>).

SREBP-2 affinity for the SRE2 sequence was evaluated by electrophoretic mobility shift assay (EMSA) analysis (Figure

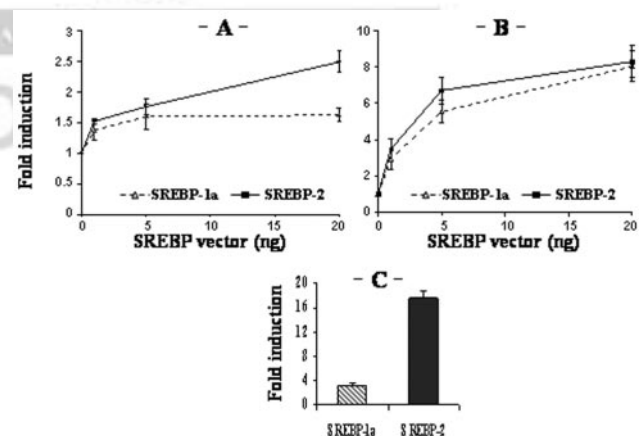


**Figure 2.** Dose-dependent activation of Cla-1 and LDL-receptor promoters by SREBP-1a and SREBP-2. The Cla-1 promoter construct p-258 (A) or the human LDL-receptor promoter construct (B) were transiently transfected in HepG2 cells in the presence of increasing amounts (1, 5, and 20 ng) of SREBP-1a and SREBP-2 expression vectors. C, Transactivation of the mouse SR-BI promoter by SREBP-1a and SREBP-2. The mouse SR-BI promoter construct was cotransfected in HepG2 cells with SREBP-1a or SREBP-2 expression vectors (20 ng). Results were expressed as fold induction relative to normalized luciferase activities in control cells.



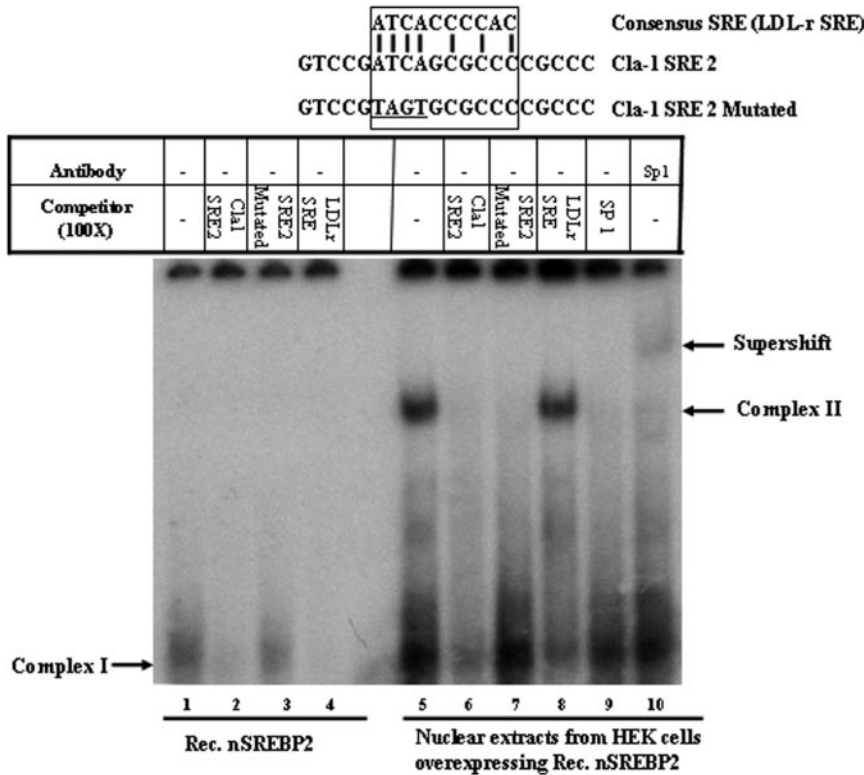


**Figure 3.** Characterization of SREBP-2 binding to the Cla-1 SRE2 sequence by EMSA. Labeled Cla-1 SRE2 probe was incubated with either SREBP-2 obtained by in vitro translation (lanes 1 through 4) or nuclear extracts (6 μg) prepared from HEK293 cells overexpressing nSREBP-2 (lanes 5 through 10). Specific complex I corresponding to SREBP-2 binding to the Cla-1 SRE2 probe (lanes 1 and 5) was competed out by the addition of an excess of cold Cla-1 SRE2 (lanes 2 and 6) and LDL-receptor SRE (lanes 4 and 8) oligonucleotides but not by mutated Cla-1 SRE2 (lanes 3 and 7) or Sp1 (lane 9) oligonucleotides. In the presence of HEK293 nuclear extracts, a second specific complex (II) was formed (lane 5), which was competed out by the addition of cold Sp1 oligonucleotide (lane 9). The specificity of Sp1 binding to the Cla-1 SRE2 probe was confirmed by supershifting of the band after addition of an anti-Sp1 antibody (lane 10).

3) using either in vitro-translated nSREBP-2 or nuclear extracts prepared from HEK293 cells overexpressing nSREBP-2 (see below). A retarded protein-DNA complex was detected in the presence of recombinant nSREBP-2 and HEK293 nuclear extracts (complex I, lanes 1 and 5). This complex appeared to be specific because the addition of an excess of unlabeled SRE2 probe prevented its formation (lanes 2 and 6), whereas an unlabeled mutated SRE2 oligonucleotide did not (lanes 3 and 7). The consensus SRE sequence identified in the promoter of the LDL-receptor gene was used as a control. The addition of an excess of unlabeled LDL-receptor SRE specifically competed with the SRE2-protein complex I (lanes 4 and 8). We equally observed that incubation of the SRE2 probe with nuclear extracts from HEK293 cells overexpressing nSREBP-2 produced another DNA-protein complex (complex II, lane 5). Because the SRE2 oligoprobe sequence is GC-rich, we tested the possibility that the protein involved in this second complex could be Sp1, a transcription factor that binds to such DNA motifs. Addition of a molar excess of an unlabeled oligomer containing an Sp1 binding sequence specifically prevented formation of complex II but not that of complex I (lane 9). Complex II was also competed out by the addition of an excess of unlabeled wild-type (lane 6) or mutated (lane 7) SRE2 oligonucleotides but not by that of cold LDL-receptor SRE (lane 8). These results suggest that Sp1 binds to a site adjacent to that of SREBP-2 on the SRE2 probe and may act as an SREBP cofactor. Further confirmation of the implication of Sp1 in this Cla-1 SRE2/protein complex II was provided by the disappearance of this complex and the formation of a supershifted band after addition of anti-Sp1 antibody (lane 10).

### Cla-1 Gene Expression Is Activated as a Function of nSREBP-2 Levels in Stably Transfected HEK293 Cells

To further evaluate whether Cla-1 gene expression is regulated by SREBP-2, we established stably transfected HEK293 cells expressing the human nuclear active form nSREBP-2. Stable HEK293 clones were assayed for the level of recombinant nSREBP-2 (rec.nSREBP-2) mRNA expression by quantitative RT-PCR using primer pairs that discriminate rec.nSREBP-2 cDNA from endogenous SREBP-2 cDNA (Table I, available online at <http://atvb.ahajournals.org>). Figure 4A shows the results of 4 clones that express very low (clone 1), moderate (clone 2), or high levels (clones 3 and 4) of rec.nSREBP-2. As reported previously in transgenic SREBP mouse models<sup>7</sup> or in in vitro cell systems,<sup>18</sup> graded overexpression of rec.nSREBP-2 was associated with a concomitant increase in the mRNA level of target genes of SREBPs, including the LDL-receptor (Figure II, available online at <http://atvb.ahajournals.org>). Cla-1 mRNA levels were equally increased incrementally as a function of the level of expression of rec.nSREBP-2 in the cell clone (Figure 4B, 1.5-fold, 3.4-fold, and 4.1-fold changes for clone 2, 3, and 4, respectively). Changes in protein levels were assessed by densitometric analysis of Western blots (Figure 4C). Although HEK293 cells normally express Cla-1 protein at low levels, comparison of Cla-1 protein expression between HEK-nSREBP-2 high expressor clones (clones 3 and 4) and 2 clones expressing nSREBP-2 at very low levels (clones 1 and 5) revealed greater Cla-1 protein levels in both high expressor clones (1.5-fold and 1.9-fold increase for clones 3 and 4, respectively;  $P < 0.0002$ ; Figure 4C). It is noteworthy that the fold changes measured at the mRNA level were

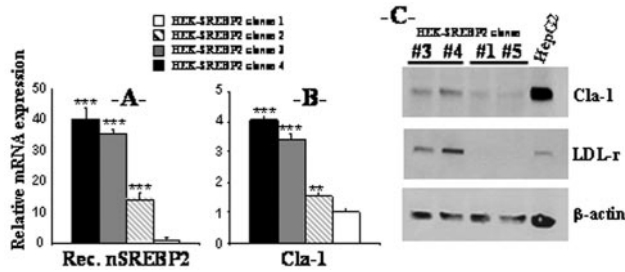


**Figure 4.** Quantification of Cla-1 expression in HEK-SREBP-2 clones. Total RNA from 4 HEK-SREBP-2 clones was extracted and subjected to quantitative RT-PCR using specific primers for rec.nSREBP-2 (A) and Cla-1 (B). For both genes, data ( $\pm$ SD) represent the amount of mRNA relative to that measured in HEK-SREBP-2 clone 1, which was set arbitrarily to 1. Statistical differences from clone 1 are indicated (Student *t* test; \*\* $P < 0.01$ ; \*\*\* $P < 0.001$ ). C, Total protein extracts prepared from HEK-SREBP-2 clones 3 and 4 expressing high levels of rec.nSREBP-2, from clones 1 and 5 expressing very low amounts of nSREBP-2, and from control HepG2 cells were analyzed by Western blotting. Immunoblot was performed with anti-SR-BI/Cla-1, anti-human LDL-receptor and mouse monoclonal anti- $\beta$ -actin. Data are representative of 3 independent experiments.

2-fold greater than those observed at the protein level, suggesting a potential control of Cla-1 expression at a post-transcriptional level. In this context, it is relevant that PDZK1, a PDZ domain containing protein essential for SR-BI protein expression,<sup>19</sup> could not be detected by quantitative RT-PCR in HEK293 cells; therefore, PDZK1 does not appear to be implicated in this potential post-transcriptional effect.

As a control for the Western blots, the use of an anti-LDL-receptor antibody revealed, as expected, a greater expression of LDL-receptor in high expressor clones than in very low expressor clones.

## Discussion

We established that the promoter regions of the mouse SR-BI gene and of its human homolog Cla-1 are transactivated by SREBP factors and preferentially by SREBP-2 compared with SREBP-1a. The significance of such regulation was highlighted by the analysis of HEK293 cells expressing the nuclear active nSREBP-2 at incremental levels, in which Cla-1 gene expression was increased as a function of that of nSREBP-2. The demonstration that SREBP-2 regulates Cla-1 gene expression, a receptor that mediates the bidirectional movement of cholesterol between cells and lipoproteins, is physiologically relevant with regard to the central role of SREBP-2 in the regulation of cellular cholesterol homeostasis. Indeed, SREBP-2 activates genes involved not only in cholesterol biosynthesis but also in the control of cellular cholesterol uptake via the LDL-receptor.

Promoter studies of mouse, rat, and human SR-BI genes have shown that they share important *cis*-regulatory elements and are modulated in a similar manner, as demonstrated for SF-1-mediated<sup>9,20</sup> and LRH-1-mediated<sup>14</sup> regulation of SR-BI expression. In the present work, mouse and human SR-BI promoters were shown to respond to SREBP-1a and SREBP-2. These data corroborate those of Lopez et al<sup>9</sup> on the induction of rat SR-BI promoter activity by SREBP-1a. Whereas 2 SREs

have been identified in the rat promoter,<sup>9</sup> analysis of 3 kb of 5'-flanking sequence of the Cla-1 gene revealed the presence of a unique functional SRE (at least 2 SREBP responsive regions could be detected in the mouse SR-BI promoter; data not shown). Based on site-directed mutation and EMSA analyses, this SRE element is most likely 5'-ATCAGCGCCC-3', thereby resembling the human LDL-receptor SRE-1 (5'-ATCACCCAC-3') and the SRE identified in the rat SR-BI proximal promoter<sup>9</sup> (5'-AGCACCGCCC-3'). Preferential activation of different target promoters by either of the SREBP isoforms has been reported;<sup>15-17</sup> indeed, such a mechanism has been proposed to partially account for the differential *in vivo* regulation of genes involved in fatty acid metabolism and cholesterol biosynthesis by SREBP-1 and SREBP-2, respectively. To date, no specific base change in SREBP recognition sites has been firmly identified that provides greater specificity in binding to individual SREBPs. However, it has been postulated that SREBP-2 could possibly display higher affinity for DNA motifs typified by the LDL-receptor SRE-1.<sup>15</sup> Conversely, it has also been suggested that differences in the first 2 5' nucleotides of the LDL-receptor SRE-1 could explain the exclusive binding of SREBP-2 to the human squalene synthase SRE (8/10) 5'-TCCACCCAC-3'.<sup>17,21</sup> The Cla-1 SRE2 site, as presently identified shares an identical 5' end but diverges in its 3' end from that of the LDL-receptor SRE-1, and on the basis of the aforementioned hypotheses, would not therefore correspond to a preferential target of the SREBP-2 form. Greater promoter activation by SREBP-2 than by SREBP-1a, as observed in the present study for human and mouse SR-BI promoters, has rarely been reported previously. Therefore, the Cla-1 SRE2 site may constitute an interesting sequence to analyze, along with the SREBP-responsive element(s) of the mouse SR-BI promoter; such analysis may lead to identification of key nucleotides in SRE motifs for preferential binding specificity/affinity of SREBP-2 versus SREBP-1a.

The general transcription factors NF-Y and Sp1 are co-regulatory transcription factors that are critical to high levels of SREBP-mediated activation of promoters.<sup>22,23</sup> In this study, we observed that the GC-box 3' of the Cla-1 SRE2 sequence interacts with the Sp1 transcription factor. The presence of this functional Sp1-binding site adjacent to the Cla-1 SRE2 site further supports the notion that Cla-1 is a member of the gene family activated by SREBP factors. It is relevant that an 11-bp deletion in the Cla-1 gene, which corresponds to this Sp1-binding sequence, has been identified recently in a Taiwanese Chinese population.<sup>24</sup> It would be of interest to evaluate whether this deletion, which was shown to be associated with reduced basal Cla-1 promoter activity *in vitro* but also with increased HDL-cholesterol levels in the aforementioned population, may affect SREBP-2-mediated regulation of Cla-1 gene expression.

A recent analysis of microarrays hybridized with RNA from livers of SREBP-1a and SREBP-2 transgenic mice failed to identify SR-BI as a target gene for SREBP.<sup>13</sup> One explanation for this apparent discrepancy with the current study resides in the fact that changes in SR-BI gene expression in the livers of these SREBP transgenic mice may be modest and therefore could not meet the criteria ( $>2.5$ -fold change) required to qualify SR-BI as an SREBP target.

Absence or moderate transcriptional activation of SR-BI expression may also underpin the complex regulation of this gene in hepatic tissue. Indeed, whereas SR-BI expression has been reported to be reduced in liver parenchymal cells of rats fed a high-cholesterol diet,<sup>25</sup> thereby suggesting cholesterol-mediated feedback control of SR-BI expression, concomitant increased expression was reported in liver Kupffer cells.<sup>25</sup> Alternatively, minor changes in the transcription levels of the cholesterol 7 $\alpha$ -hydroxylase gene, as reported in SREBP-2 transgenic mice,<sup>13</sup> may increase bile acid biosynthesis in the hepatocyte. On binding to bile acids, FXR activates transcription of the *Shp* gene, a repressor of the orphan nuclear receptor LRH-1, which we identified recently as a positively acting transcription factor of SR-BI/Cla-1 expression in mouse liver.<sup>14</sup> Whether such regulation of the SR-BI gene is relevant when SREBP action is maintained constant as in SREBP transgenic mouse models remains indeterminate.

Long-term treatment of hypercholesterolemic patients with statins has proven efficacious in reducing plasma LDL-cholesterol levels (up to 35%), whereas baseline values of HDL-cholesterol generally remain unchanged or may be slightly increased ( $\leq 10\%$ ). However, early and transitory reduction of HDL-cholesterol levels after high-dose atorvastatin has been reported in patients with heterozygous<sup>26</sup> or homozygous familial hypercholesterolemia (HFH; up to 21% reduction after 4 weeks treatment).<sup>27</sup> Such an effect could be partially related to an early response to statin-induced cellular cholesterol deprivation, which may result in SREBP-mediated upregulation of hepatic Cla-1 expression and subsequent increase in selective uptake of HDL-cholesterol with concomitant reduction in plasma HDL-cholesterol levels. In HFH patients, the transient effect of atorvastatin on HDL-cholesterol levels was 2-fold greater in patients with total LDL-receptor deficiency compared with receptor-defective HFH subjects, thereby suggesting a direct link to the degree of LDL-receptor deficiency.<sup>27</sup> This observation emphasizes the fact that metabolic processes influencing HDL-cholesterol levels are responsive to statin treatment and that these processes may be dependent on the presence of functional LDL-receptors. Indeed, atorvastatin therapy has been shown to decrease the mass and activity of the CE transfer protein<sup>28,29</sup> and also to decrease hepatic lipase activity;<sup>30</sup> both effects favor elevation of HDL-cholesterol and may be directly influenced by plasma concentrations of very LDL and LDL particles. Thus, in HFH patients treated with high-dose atorvastatin, intravascular remodeling of HDL particles could be partially altered because of LDL-receptor deficiency, revealing a statin-induced upregulation of Cla-1 expression with a subsequent lowering impact on HDL-cholesterol levels. This mechanistic hypothesis requires further studies to confirm it but suggests that 1 additional beneficial action of statins may involve minor changes in the hepatic expression of Cla-1, a low-affinity but high-capacity receptor that may positively influence the dynamic flux of the reverse cholesterol transport pathway.

### Acknowledgments

This study was supported by National Institute for Health and Medical Research (INSERM) and by a research grant from Bayer

HealthCare (Wuppertal, Germany). M.T. was the recipient of a young investigator award of the XIII International Symposium on Atherosclerosis (Kyoto, Japan, October 2003) and of a doctoral fellowship from the French government. It is a pleasure to acknowledge stimulating discussion with Dr K.D. Bremm.

### References

1. Ji Y, Jian B, Wang N, Sun Y, Moya ML, Phillips MC, Rothblat GH, Swaney JB, Tall AR. Scavenger receptor BI promotes high density lipoprotein-mediated cellular cholesterol efflux. *J Biol Chem.* 1997;272:20982–20985.
2. Rigotti A, Trigatti BL, Penman M, Rayburn H, Herz J, Krieger M. A targeted mutation in the murine gene encoding the high density lipoprotein (HDL) receptor scavenger receptor class B type I reveals its key role in HDL metabolism. *Proc Natl Acad Sci U S A.* 1997;94:12610–12615.
3. Kozarsky KF, Donahee MH, Rigotti A, Iqbal SN, Edelman ER, Krieger M. Overexpression of the HDL receptor SR-BI alters plasma HDL and bile cholesterol levels. *Nature.* 1997;387:414–417.
4. Rhoads D, Brodeur M, Lapointe J, Charpentier D, Falstra L, Brissette L. The role of human and mouse hepatic scavenger receptor class B type I (SR-BI) in the selective uptake of low-density lipoprotein-cholesteryl esters. *Biochemistry.* 2003;42:7527–7538.
5. Acton S, Osgood D, Donoghue M, Corella D, Pocovi M, Cenario A, Mozas P, Keilty J, Squazzo S, Woolf EA, Ordovas JM. Association of polymorphisms at the SR-BI gene locus with plasma lipid levels and body mass index in a white population. *Arterioscler Thromb Vasc Biol.* 1999;19:1734–1743.
6. Osgood D, Corella D, Demissie S, Cupples LA, Wilson PW, Meigs JB, Schaefer EJ, Coltell O, Ordovas JM. Genetic variation at the scavenger receptor class B type I gene locus determines plasma lipoprotein concentrations and particle size and interacts with type 2 diabetes: the Framingham Study. *J Clin Endocrinol Metab.* 2003;88:2869–2879.
7. Horton JD, Shimomura I, Brown MS, Hammer RE, Goldstein JL, Shimano H. Activation of cholesterol synthesis in preference to fatty acid synthesis in liver and adipose tissue of transgenic mice overproducing sterol regulatory element-binding protein-2. *J Clin Invest.* 1998;101:2331–2339.
8. Shimano H, Horton JD, Shimomura I, Hammer RE, Brown MS, Goldstein JL. Isoform 1c of sterol regulatory element binding protein is less active than isoform 1a in livers of transgenic mice and in cultured cells. *J Clin Invest.* 1997;99:846–854.
9. Lopez D, McLean MP. Sterol regulatory element-binding protein-1a binds to cis elements in the promoter of the rat high density lipoprotein receptor SR-BI gene. *Endocrinology.* 1999;140:5669–5681.
10. Tsuruoka H, Khovidhunkit W, Brown BE, Fluhr JW, Elias PM, Feingold KR. Scavenger receptor class B type I is expressed in cultured keratinocytes and epidermis. Regulation in response to changes in cholesterol homeostasis and barrier requirements. *J Biol Chem.* 2002;277:2916–2922.
11. Wang N, Weng W, Breslow JL, Tall AR. Scavenger receptor BI (SR-BI) is up-regulated in adrenal gland in apolipoprotein A-I and hepatic lipase knock-out mice as a response to depletion of cholesterol stores. In vivo evidence that SR-BI is a functional high density lipoprotein receptor under feedback control. *J Biol Chem.* 1996;271:21001–21004.
12. Landschulz KT, Pathak RK, Rigotti A, Krieger M, Hobbs HH. Regulation of scavenger receptor, class B, type I, a high density lipoprotein receptor, in liver and steroidogenic tissues of the rat. *J Clin Invest.* 1996;98:984–995.
13. Horton JD, Shah NA, Warrington JA, Anderson NN, Park SW, Brown MS, Goldstein JL. Combined analysis of oligonucleotide microarray data from transgenic and knockout mice identifies direct SREBP target genes. *Proc Natl Acad Sci U S A.* 2003;100:12027–12032.
14. Schoonjans K, Annicotte JS, Huby T, Botrugno OA, Fayard E, Ueda Y, Chapman J, Auwerx J. Liver receptor homolog 1 controls the expression of the scavenger receptor class B type I. *EMBO Rep.* 2002;3:1181–1187.
15. Amemiya-Kudo M, Shimano H, Hasty AH, Yahagi N, Yoshikawa T, Matsuzaka T, Okazaki H, Tamura Y, Iizuka Y, Ohashi K, Osuga J, Harada K, Gotoda T, Sato R, Kimura S, Ishibashi S, Yamada N. Transcriptional activities of nuclear SREBP-1a, -1c, and -2 to different target promoters of lipogenic and cholesterogenic genes. *J Lipid Res.* 2002;43:1220–1235.
16. Guan G, Dai P, Shechter I. Differential transcriptional regulation of the human squalene synthase gene by sterol regulatory element-binding

- proteins (SREBP) 1a and 2 and involvement of 5' DNA sequence elements in the regulation. *J Biol Chem.* 1998;273:12526–12535.
17. Shechter I, Dai P, Huo L, Guan G. IDH1 gene transcription is sterol regulated and activated by SREBP-1a and SREBP-2 in human hepatoma HepG2 cells: evidence that IDH1 may regulate lipogenesis in hepatic cells. *J Lipid Res.* 2003;44:2169–2180.
  18. Pai JT, Guryev O, Brown MS, Goldstein JL. Differential stimulation of cholesterol and unsaturated fatty acid biosynthesis in cells expressing individual nuclear sterol regulatory element-binding proteins. *J Biol Chem.* 1998;273:26138–26148.
  19. Kocher O, Yesilaltay A, Cirovic C, Pal R, Rigotti A, Krieger M. Targeted disruption of the PDZK1 gene in mice causes tissue-specific depletion of the high density lipoprotein receptor scavenger receptor class B type I and altered lipoprotein metabolism. *J Biol Chem.* 2003;278:52820–52825.
  20. Cao G, Garcia CK, Wyne KL, Schultz RA, Parker KL, Hobbs HH. Structure and localization of the human gene encoding SR-BI/CLA-1. Evidence for transcriptional control by steroidogenic factor 1. *J Biol Chem.* 1997;272:33068–33076.
  21. Guan G, Dai PH, Osborne TF, Kim JB, Shechter I. Multiple sequence elements are involved in the transcriptional regulation of the human squalene synthase gene. *J Biol Chem.* 1997;272:10295–10302.
  22. Sanchez HB, Yieh L, Osborne TF. Cooperation by sterol regulatory element-binding protein and Sp1 in sterol regulation of low density lipoprotein receptor gene. *J Biol Chem.* 1995;270:1161–1169.
  23. Jackson SM, Ericsson J, Osborne TF, Edwards PA. NF-Y has a novel role in sterol-dependent transcription of two cholesterologenic genes. *J Biol Chem.* 1995;270:21445–21448.
  24. Hsu LA, Ko YL, Wu S, Teng MS, Peng TY, Chen CF, Lee YS. Association between a novel 11-base pair deletion mutation in the promoter region of the scavenger receptor class B type I gene and plasma HDL cholesterol levels in Taiwanese Chinese. *Arterioscler Thromb Vasc Biol.* 2003;23:1869–1874.
  25. Fluiter K, van der Westhuijzen DR, van Berkel TJ. In vivo regulation of scavenger receptor BI and the selective uptake of high density lipoprotein cholesteryl esters in rat liver parenchymal and Kupffer cells. *J Biol Chem.* 1998;273:8434–8438.
  26. Wierzbicki AS, Lumb PJ, Chik G, Crook MA. Comparison of therapy with simvastatin 80 mg and atorvastatin 80 mg in patients with familial hypercholesterolaemia. *Int J Clin Pract.* 1999;53:609–611.
  27. Sposito AC, Gonbert S, Bruckert E, Atassi M, Beucler I, Amsellem S, Khallouf O, Benlian P, Turpin G. Magnitude of HDL cholesterol variation after high-dose atorvastatin is genetically determined at the LDL receptor locus in patients with homozygous familial hypercholesterolemia. *Arterioscler Thromb Vasc Biol.* 2003;23:2078–2082.
  28. Guerin M, Lassel TS, Le Goff W, Farnier M, Chapman MJ. Action of atorvastatin in combined hyperlipidemia: preferential reduction of cholesteryl ester transfer from HDL to VLDL1 particles. *Arterioscler Thromb Vasc Biol.* 2000;20:189–197.
  29. van Venrooij FV, Stolk RP, Banga JD, Sijmonsma TP, van Tol A, Erkelens DW, Dallinga-Thie GM. Common cholesteryl ester transfer protein gene polymorphisms and the effect of atorvastatin therapy in type 2 diabetes. *Diabetes Care.* 2003;26:1216–1223.
  30. Berk P, II, Hoogerbrugge N, Stolk RP, Bootsma AH, Jansen H. Atorvastatin dose-dependently decreases hepatic lipase activity in type 2 diabetes: effect of sex and the LIPC promoter variant. *Diabetes Care.* 2003;26:427–432.



# Arteriosclerosis, Thrombosis, and Vascular Biology

JOURNAL OF THE AMERICAN HEART ASSOCIATION

FIRST PROOF ONLY

# Knockdown expression and hepatic deficiency reveal an atheroprotective role for SR-BI in liver and peripheral tissues

Thierry Huby,<sup>1</sup> Chantal Doucet,<sup>1</sup> Christiane Dacet,<sup>1</sup> Betty Ouzilleau,<sup>1</sup> Yukihiko Ueda,<sup>2</sup> Veena Afzal,<sup>3</sup> Edward Rubin,<sup>3</sup> M. John Chapman,<sup>1</sup> and Philippe Lesnik<sup>1</sup>

<sup>1</sup>INSERM U551, Université Pierre et Marie Curie–Paris 6, Dyslipoproteinemia and Atherosclerosis Research Unit, Hôpital de la Pitié, Paris, France. <sup>2</sup>Horizontal Medical Research Organization, Graduate School of Medicine, Kyoto University, Shogoin, Sakyo-ku, Kyoto, Japan. <sup>3</sup>Lawrence Berkeley National Laboratory, Genomics Division, Berkeley, California, USA.

**Scavenger receptor SR-BI has been implicated in HDL-dependent atheroprotective mechanisms. We report the generation of an SR-BI conditional knockout mouse model in which SR-BI gene targeting by *loxP* site insertion produced a hypomorphic allele (hypomSR-BI). Attenuated SR-BI expression in hypomSR-BI mice resulted in 2-fold elevation in plasma total cholesterol (TC) levels. Cre-mediated SR-BI gene inactivation of the hypomorphic SR-BI allele in hepatocytes (hypomSR-BI-KO<sup>liver</sup>) was associated with high plasma TC concentrations, increased plasma free cholesterol/TC (FC/TC) ratio, and a lipoprotein-cholesterol profile typical of *SR-BI*<sup>-/-</sup> mice. Plasma TC levels were increased 2-fold in hypomSR-BI and control mice fed an atherogenic diet, whereas hypomSR-BI-KO<sup>liver</sup> and *SR-BI*<sup>-/-</sup> mice developed severe hypercholesterolemia due to accumulation of FC-rich, VLDL-sized particles. Atherosclerosis in hypomSR-BI mice was enhanced (2.5-fold) compared with that in controls, but to a much lower degree than in hypomSR-BI-KO<sup>liver</sup> (32-fold) and *SR-BI*<sup>-/-</sup> (48-fold) mice. The latter models did not differ in either plasma lipid levels or in the capacity of VLDL-sized lipoproteins to induce macrophage cholesterol loading. However, reduced atherosclerosis in hypomSR-BI-KO<sup>liver</sup> mice was associated with decreased lesional macrophage content as compared with that in *SR-BI*<sup>-/-</sup> mice. These data imply that, in addition to its major atheroprotective role in liver, SR-BI may exert an antiatherogenic role in extrahepatic tissues.**

## Introduction

Plasma concentrations of HDL cholesterol (HDL-C) are inversely proportional to the risk for premature development of atherosclerosis. One of the major atheroprotective actions of HDL particles involves the transport of excess cholesterol from peripheral tissues to the liver for excretion, a process known as reverse cholesterol transport (RCT). Understanding of the molecular events implicated in the formation and intravascular recycling of HDL particles, as well as the identification of key factors that control cholesterol flux through the plasma HDL pool, is critical to the development of innovative therapeutic strategies to enhance HDL-mediated RCT.

Scavenger receptor class B type 1, a physiologically relevant HDL receptor expressed in a variety of tissues, including vascular endothelial cells (1, 2), smooth muscle cells (3), and macrophages (4), mediates selective cellular uptake of HDL-associated cholesteryl esters (CEs) in the liver but also in adrenals (reviewed in ref. 5). Indeed, SR-BI is a major determinant of HDL metabolism in rodents. Hepatic overexpression of SR-BI in mice markedly reduces plasma HDL-C levels and increases biliary secretion of cholesterol (6–9). Conversely, partial to complete deficiency of this receptor results in an SR-BI dose-dependent elevation in plasma HDL-C with the appearance of large cholesterol-rich HDL particles (10, 11).

In humans, naturally occurring mutations that affect SR-BI function and that clearly establish the relevance of this receptor to HDL-C levels and RCT have not been detected to date. However, the human homolog of SR-BI, Cla-1, exhibits tissue distribution similar to and selective HDL-CE uptake identical to those of murine SR-BI (reviewed in 5). Moreover, epidemiological studies have identified polymorphisms in the *Cla-1* gene that are associated not only with plasma HDL-C or LDL cholesterol (LDL-C) levels, but also with lipoprotein particle size and coronary artery disease, suggesting that SR-BI may be intimately involved in HDL metabolism in humans (12–14).

A substantial body of evidence supports an atheroprotective role for SR-BI in mice. Thus, complete deficiency of SR-BI was associated with significantly increased atherosclerosis in mice fed a high-fat/cholesterol diet (15) as well as with accelerated atherosclerosis development in the atherosclerosis-prone apoE-KO mouse model (16). Conversely, hepatic overexpression of SR-BI led to reduction in murine atherosclerosis (6, 17, 18). The antiatherogenic impact of SR-BI expressed in the liver most likely involves its role in the final step of RCT, with potential elevation in cholesterol flux to the liver (19). However, additional mechanisms may contribute to this effect, as SR-BI transgene-mediated reduction of atherosclerosis in the human apoB100 transgenic mouse model was primarily associated with reduction in plasma non-HDL cholesterol levels (17). It has been difficult to gain a clear understanding of the tissue-specific contribution of SR-BI to protection against atherogenesis because of the multifunctional properties attributed to this receptor and the wide spectrum of ligands to which SR-BI binds; these

**Nonstandard abbreviations used:** CE, cholesteryl ester; FC, free cholesterol; HDL-C, HDL cholesterol; HFC, high-fat, high-cholesterol, and cholic acid-containing; PDZK1, PDZ domain containing 1-deficient; RCT, reverse cholesterol transport; SR-BI, scavenger receptor class B type 1; TC, total cholesterol; TG, triglyceride.

**Conflict of interest:** The authors have declared that no conflict of interest exists.

**Citation for this article:** *J. Clin. Invest.* doi:10.1172/JCI26893.

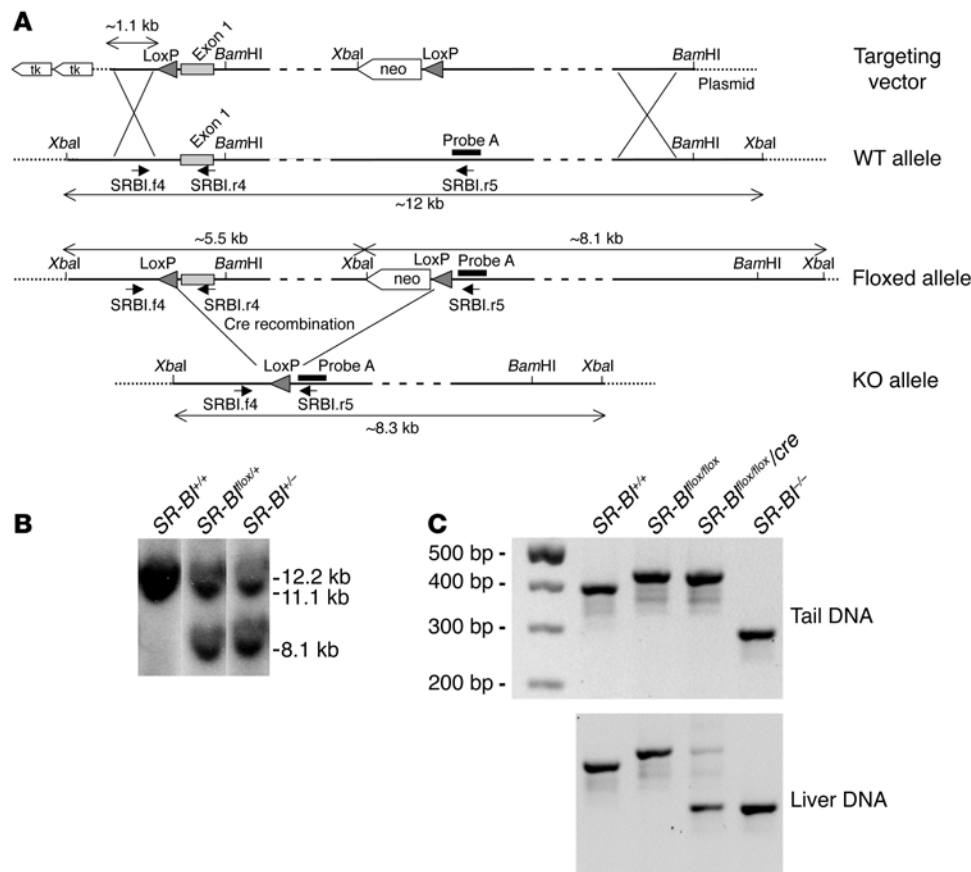


**Figure 1**

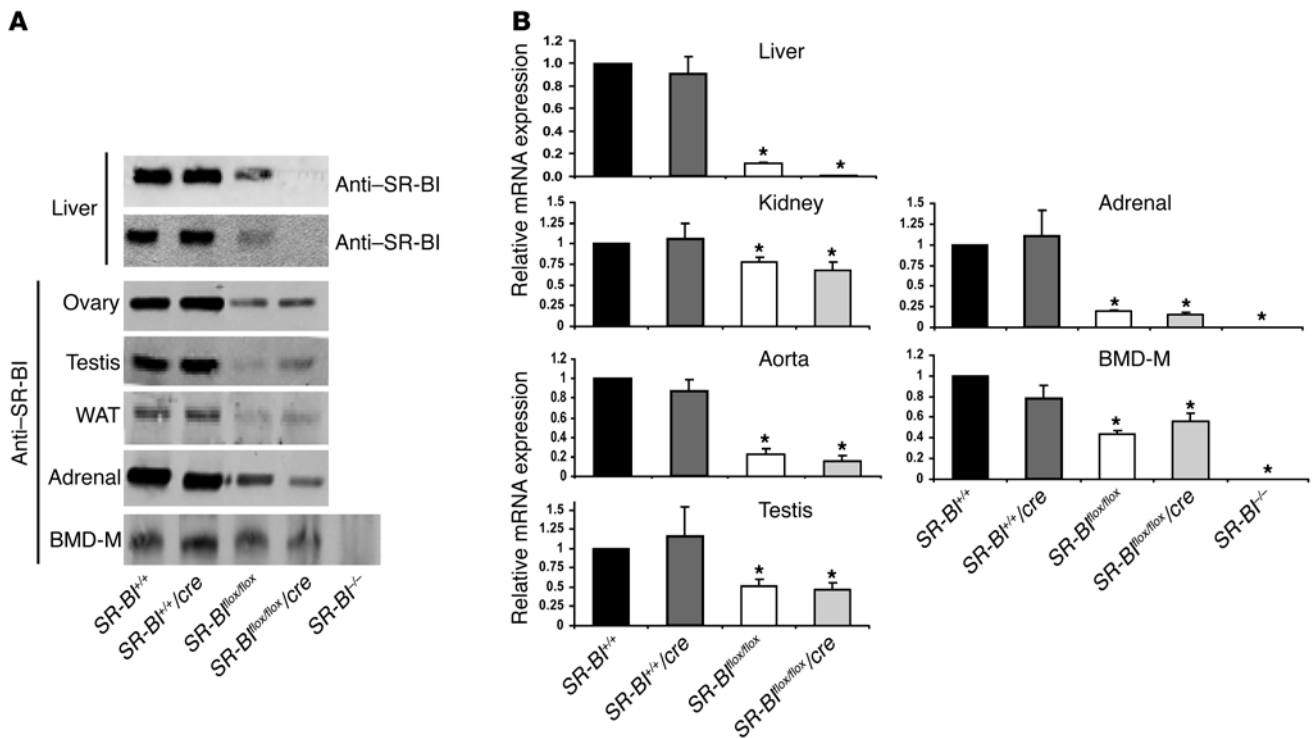
Targeting strategy and conditional deletion of the SR-BI<sup>lox</sup> allele. **(A)** Structural organization of the 5' region of the wild-type, floxed, and knockout SR-BI allele. The 2 loxP sites flanking the SR-BI exon 1 are shown as arrowheads. The relative positions of probe A used for Southern blot analysis, primers (short arrows) used for PCR screening, and endonuclease sites for BamHI and XbaI are indicated. XbaI-restricted fragments for each allele are depicted by double-headed arrows. Cre-mediated deletion of the SR-BI<sup>lox</sup> allele to generate the SR-BI-KO allele was achieved by transfection of the Cre recombinase cDNA in SR-BI<sup>lox/+</sup> ES cells. SR-BI<sup>-/-</sup> ES cells were then used to generate SR-BI-KO mice. Mice with hepatic SR-BI deficiency were generated by interbreeding of SR-BI<sup>lox/lox</sup> mice with Alb-Cre mice, which express the Cre recombinase in hepatocytes. **(B)** Southern blot analysis of XbaI-digested ES cell genomic DNA using probe A. **(C)** PCR analysis of tail and liver genomic DNA using a mix of SRBI.f4, SRBI.r4, and SRBI.r5 primers. Primer pair SRBI.f4 and SRBI.r4 discriminates for the presence or absence of the 5' loxP sequence upstream SR-BI exon 1. The sizes of the PCR products for the WT and SR-BI floxed alleles are 391 bp and 427 bp, respectively. Primer pair SRBI.f4 and SRBI.r5 identifies the SR-BI-KO allele (288 bp).

include not only HDL and oxidized LDL, but also anionic phospholipids, apoptotic cells, and the acute-phase protein serum amyloid A, all of which are relevant to atherogenesis. In addition to its capacity to facilitate selective cellular HDL-CE uptake, other tissue-specific mechanisms underlying the antiatherogenic properties of SR-BI may include: (a) activation of eNOS, and thus production of antiatherogenic nitric oxide in the vascular endothelium (2, 20); (b) contribution to the first step of RCT by mediation of cellular free cholesterol (FC) efflux from peripheral tissues, including macrophages (21–23); (c) induction of apoptosis in damaged endothelial cells (24); (d) recognition and phagocytosis of apoptotic cells by macrophages (25); and (e) cellular uptake of lipoprotein-associated  $\alpha$ -tocopherol, thereby contributing to increased antioxidant bioavailability in cells of the arterial wall (26, 27).

**Results**

*Generation of conditional SR-BI-deficient and SR-BI<sup>-/-</sup> mice.* Conditional targeting of the mouse SR-BI gene was achieved by flanking exon 1 with Cre recombinase loxP sites following homologous recombination in 129/Sv ES cells (Figure 1A). The SR-BI floxed region includes 85 bp of untranslated sequence, the entire coding region of the first exon, and approximately 3.5 kb of intron 1. SR-BI exon 1 was previously deleted in mice and resulted in a null allele (10). Thus, Cre-mediated deletion of SR-BI floxed exon 1 was appropriate for achieving SR-BI inactivation. Several ES cell clones that were found to be correctly targeted by PCR and Southern blot analysis and that contained a floxed SR-BI allele (SR-BI<sup>lox/+</sup> ES clones) were transfected with a vector encoding for the Cre recombinase in order to generate ES clones with an SR-BI-null allele

Earlier studies in PDZ domain containing 1-deficient (PDZK1-deficient) mice have provided insight into the impact of tissue-specific ablation of the SR-BI isoform in the hepatocyte (95%) and small intestine (50%) on cholesterol homeostasis (28). In order to evaluate the relative contributions of hepatic versus extrahepatic SR-BI expression to cholesterol homeostasis and atherogenesis, we developed an SR-BI conditional knockout mouse model by Cre/loxP technology. However, loxP targeting of the SR-BI gene resulted in reduced SR-BI expression in all tissues, generating a hypomorphic SR-BI mouse line in which SR-BI can be specifically deleted by Cre/loxP recombination. Our data reveal that while atherosclerosis was enhanced in mice with reduced expression of SR-BI (hypomSR-BI mice), aortic lesion formation was dramatically accelerated in mice with Cre-mediated deletion of hepatic SR-BI (hypomSR-BI-KO<sup>liver</sup> mice). Marked accumulation of atherogenic VLDL-sized lipoproteins enriched in FC most probably accounted for increased atherosclerosis in hypomSR-BI-KO<sup>liver</sup> mice. However, whereas hypomSR-BI-KO<sup>liver</sup> and SR-BI<sup>-/-</sup> mice exhibited similar atherogenic lipid levels and lipoprotein-cholesterol distribution, the latter developed 1.5-fold more arterial lesions, supporting the proposal that expression of SR-BI in peripheral tissues may fulfill an atheroprotective function.

**Figure 2**

Levels of SR-BI expression. (A) For each SR-BI genotype, total protein extracts were prepared from the indicated tissues and loaded onto SDS-PAGE, followed by immunoblotting with an anti-SR-BI antibody (or with an anti-SR-BII antibody for liver extracts) directed against the C-terminal domain of the protein. WAT, white adipose tissue; BMD-M, BM-derived macrophages. (B) Relative SR-BI mRNA levels. Total RNAs extracted from tissues were pooled (4–8 mice per group), reverse-transcribed, and subjected to real-time PCR quantification. Values (mean  $\pm$  SD) represent the amount of SR-BI mRNA relative to that measured in control mice, which was set arbitrarily to 1. Data for BM-derived macrophages were generated from 1 representative RNA preparation for each SR-BI genotype. \* $P < 0.05$  compared with controls.

(*SR-BI*<sup>-/-</sup> ES clones) (Figure 1B). *SR-BI*<sup>flax/+</sup> mice were crossed with Alb-Cre transgenic mice (29), which express the Cre transgene under the albumin promoter for liver-specific expression, in order to generate *SR-BI*<sup>flax/+</sup>/Cre progeny. These animals were then backcrossed for 6 generations against C57BL/6J mice and subsequently interbred to yield *SR-BI*<sup>+/+</sup>, *SR-BI*<sup>+/+</sup>/Cre, *SR-BI*<sup>flax/flax</sup>, and *SR-BI*<sup>flax/flax</sup>/Cre mice. The Alb-Cre transgene was systematically maintained in a hemizygous state throughout the study. *SR-BI*<sup>-/-</sup> mice used in this study were also backcrossed on the C57BL/6J genetic background for 6 generations.

Alb-Cre transgenic mice have been previously described to provide complete and specific Cre-mediated recombination of floxed genes in adult hepatocytes (29, 30). PCR analysis of tail genomic DNA of *SR-BI*<sup>flax/flax</sup>/Cre mice showed the presence of only floxed alleles, whereas both floxed (to a minor degree) and knockout alleles were detected by PCR amplification of liver genomic DNA preparation (Figure 1C). We attribute the presence of the PCR product corresponding to the floxed allele in PCR amplifications from liver DNA of *SR-BI*<sup>flax/flax</sup>/Cre mice to genomic DNA from nonhepatic cells, including endothelial and Kupffer cells, that are naturally present in liver tissue. In *SR-BI*<sup>-/-</sup> mice, only the KO allele was amplified by PCR from both tail and liver tissues (Figure 1C). Western blot analysis of liver extracts of *SR-BI*<sup>flax/flax</sup>/Cre mice showed essentially undetectable levels of SR-BI protein. In addition, the C-terminal variant of SR-BI, the SR-BII isoform, was not detectable in liver extracts (Figure 2A). qRT-PCR analysis dem-

onstrated a decrease in SR-BI mRNA in the liver of *SR-BI*<sup>flax/flax</sup>/Cre mice to levels corresponding to 1% of those measured in *SR-BI*<sup>+/+</sup> mice (Figure 2B). No significant SR-BI signal was revealed by immunoblotting or by qRT-PCR upon analysis of tissues prepared from *SR-BI*<sup>-/-</sup> mice (Figure 2). Immunoblotting also clearly demonstrated that SR-BI expression was decreased significantly in the livers of *SR-BI*<sup>flax/flax</sup> mice as compared with controls (Figure 2A). This decrement in SR-BI expression was confirmed by qRT-PCR analysis (~88% versus controls; Figure 2B). Analyses of other tissues confirmed that the expression of SR-BI was decreased in both *SR-BI*<sup>flax/flax</sup> and *SR-BI*<sup>flax/flax</sup>/Cre mice in a similar manner, but to a different degree as a function of the tissue analyzed (Figure 2). These results therefore suggested that *loxP* targeting led to an attenuation of SR-BI mRNA and protein levels, thereby generating an hypomorphic SR-BI allele (hypomSR-BI allele). *SR-BI*<sup>flax/flax</sup> mice were consequently termed hypomSR-BI throughout this study. *SR-BI*<sup>flax/flax</sup>/Cre mice, which displayed a similar pattern of attenuated SR-BI expression in peripheral tissues compared with hypomSR-BI mice (Figure 2) but which were deficient for SR-BI in hepatocytes, were termed hypomSR-BI-KO<sup>liver</sup> mice. Although we did not determine the origin of the reduced expression of the floxed SR-BI allele, the *loxP* site located in the 5'-UTR region of the SR-BI gene introduces a hairpin structure in the transcribed RNA that could explain attenuated downstream gene expression. However, we cannot exclude the possibility that expression of SR-BI may be influenced by the neomycin cassette.



**Table 1**  
Plasma lipid levels in mice fed a chow diet

Genotype	Sex	n	TC (mg/dl)	FC (mg/dl)	FC/TC (%)	TG (mg/dl)
Controls	F	20	72 ± 10	17 ± 4	23 ± 3	74 ± 24
	M	16	90 ± 12	26 ± 3	29 ± 2	69 ± 18
hypomSR-BI	F	11	135 ± 20 <sup>A</sup>	34 ± 4 <sup>A</sup>	26 ± 4 <sup>B</sup>	73 ± 19
	M	10	175 ± 33 <sup>A</sup>	56 ± 9 <sup>A</sup>	32 ± 5	85 ± 35
hypomSR-BI-KO <sup>liver</sup>	F	12	168 ± 22 <sup>A</sup>	62 ± 8 <sup>A</sup>	37 ± 6 <sup>A</sup>	86 ± 26
	M	11	194 ± 27 <sup>A</sup>	87 ± 12 <sup>A</sup>	45 ± 5 <sup>A</sup>	77 ± 40
SR-BI <sup>-/-</sup>	F	10	137 ± 13 <sup>A,C</sup>	53 ± 8 <sup>A,D</sup>	39 ± 9 <sup>A,E</sup>	72 ± 26
	M	8	156 ± 5 <sup>A,E</sup>	87 ± 4 <sup>A,E</sup>	55 ± 3 <sup>A,C</sup>	79 ± 29 <sup>F</sup>

Plasma TC, FC, and TG levels were measured in 2-month-old female (F) and male (M) mice fed a chow diet. Data represent mean ± SD. <sup>A</sup>*P* < 0.001 versus control mice. <sup>B</sup>*P* < 0.04 versus control mice. <sup>C</sup>*P* < 0.002 versus hypomSR-BI-KO<sup>liver</sup> mice. <sup>D</sup>*P* < 0.03 versus hypomSR-BI-KO<sup>liver</sup> mice. <sup>E</sup>Not statistically different from values for hypomSR-BI-KO<sup>liver</sup> mice.

It has been previously reported that matings of heterozygous or homozygous SR-BI-KO males with SR-BI-KO female mice are nonproductive due to female sterility (16). Moreover, intercrosses of SR-BI<sup>+/-</sup> mice on a mixed C57BL6/129 background result in the transmission of the SR-BI-KO allele in a non-Mendelian ratio, with a low frequency for the production of SR-BI<sup>-/-</sup> mice (10). Generation of homozygous SR-BI-KO mice on a pure C57BL/6 background has equally been reported to be difficult (31). We observed similar results with our SR-BI-KO mouse line, as female SR-BI<sup>-/-</sup> mice were sterile, and we could not generate SR-BI-KO mice in a C57BL/6 background following the mating of SR-BI<sup>+/-</sup> female and male mice fed a normal chow diet. Fertility in SR-BI-KO females was restored and SR-BI-KO pups were obtained from heterozygous breeding pairs when animals were fed a chow diet supplemented with the lipid-lowering drug probucol (0.5%), as previously reported (21, 31). The frequency of the genotypes derived from mating of SR-BI<sup>fllox/+</sup> and SR-BI<sup>fllox/+</sup>/Cre mice fed a normal chow diet was close to that expected for Mendelian inheritance (SR-BI<sup>+/+</sup>, 16%; SR-BI<sup>+/-</sup>/Cre, 11%; SR-BI<sup>fllox/+</sup>, 24%; SR-BI<sup>fllox/+</sup>/Cre, 30%; SR-BI<sup>fllox/fllox</sup> [hypomSR-BI], 10%; and SR-BI<sup>fllox/fllox</sup>/Cre [hypomSR-BI-KO<sup>liver</sup>], 9%; *n* = 210). Additionally, hypomSR-BI-KO<sup>liver</sup> female mice produced normal progeny without diet supplementation with probucol. These observations indicate that extrahepatic expression of SR-BI, most likely in ovaries or in developing oocytes (16, 28, 31), is required for female fertility in mice.

**SR-BI dose-dependent effect on plasma cholesterol levels.** Plasma lipids were analyzed in mice on a chow diet at 2 months of age. As reported previously, targeted inactivation (SR-BI<sup>-/-</sup>), hemizygous expression (SR-BI<sup>+/-</sup>), or attenuated expression of SR-BI in mice results in a gene dose-dependent increase in plasma levels of HDL-C

(10, 11). Thus, significantly reduced expression of SR-BI in hypomSR-BI mice, and in particular in the liver, resulted in a marked increase in plasma total cholesterol (TC) concentrations in both males and females (Table 1). Indeed, TC levels in these mice were increased to the same order of magnitude as those in SR-BI<sup>-/-</sup> mice, the latter being almost 2-fold higher compared with the levels in controls. This 2-fold increase in plasma TC levels was similar to that reported in an SR-BI-KO mouse line described earlier (10, 15). Plasma TC concentrations in hypomSR-BI-KO<sup>liver</sup> mice tended to be higher. Interestingly, the 2-fold elevation of plasma TC levels in hypomSR-BI mice was associated with a corresponding 2-fold increase in FC, whereas plasma FC levels were increased more than 3-fold in both SR-BI<sup>-/-</sup> and hypomSR-BI-KO<sup>liver</sup> mice (Table 1). As a consequence, both SR-BI<sup>-/-</sup> and hypomSR-BI-KO<sup>liver</sup>

lines exhibited a high plasma FC/TC ratio; by contrast, this ratio was either moderately increased or similar in hypomSR-BI females and males, respectively, compared with controls (Table 1). These data clearly demonstrate that hepatic SR-BI deficiency results in a specific accumulation of FC in plasma. As shown in Figure 2, and as previously reported (10), changes in plasma cholesterol levels reflected a marked elevation of HDL-C in SR-BI<sup>-/-</sup> mice with abnormally large HDL particles. A similar lipoprotein cholesterol profile was observed in hypomSR-BI-KO<sup>liver</sup> mice, particularly with respect to the cholesterol content of large HDL particles. apoE was more abundant in these particles as compared with HDL of normal size (data not shown), as previously reported for large HDL present in SR-BI<sup>-/-</sup> mice (10). Analysis of the cholesterol elution profile of plasma from hypomSR-BI mice also revealed elevation in HDL-C levels, as expected, although large HDL particles appeared consistently more heterogeneous in size as compared with those apparent in both SR-BI<sup>-/-</sup> and hypomSR-BI-KO<sup>liver</sup> profiles (Figure 3A). Lipoprotein cholesterol distribution was similar in male and

**Figure 3**  
Impact of changes in SR-BI expression on plasma lipoprotein cholesterol profiles. (A) Fasting plasma samples (pooled plasma from 6–10 mice) from 2-month-old female mice fed a chow diet were fractionated by size-exclusion chromatography. TC was measured in each fraction to determine lipoprotein cholesterol profiles. Approximate elution volumes for particles in the size ranges of VLDL, LDL, and HDL are indicated. (B) Electrophoretic mobilities of plasma lipoproteins. Plasma samples (10 μl) were subjected to agarose gel electrophoresis and lipoproteins revealed by Sudan black staining. α, pre-β, and β positions corresponding to migrations of HDL, VLDL, and LDL particles, respectively, are indicated.

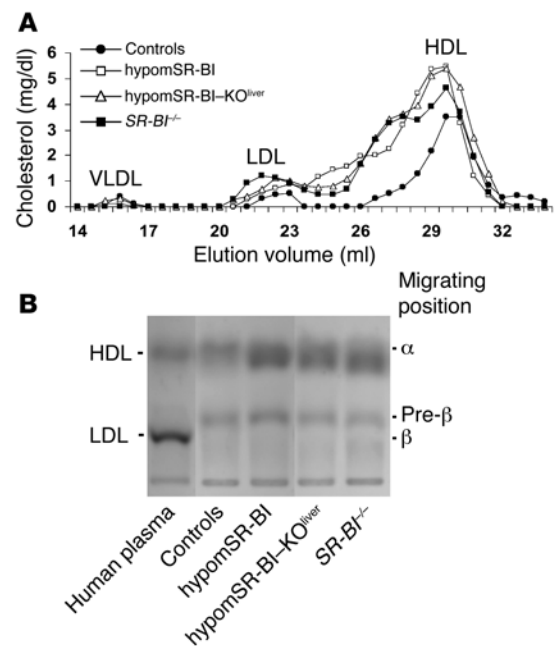






**Table 2**  
Plasma lipid levels in female mice fed the atherogenic HFC diet

Genotype	n	TC (mg/dl)	FC (mg/dl)	FC/TC (%)	TG (mg/dl)
Controls	20	160 ± 38	51 ± 15	32 ± 5	27 ± 6
hypomSR-BI	11	374 ± 97 <sup>A</sup>	183 ± 61 <sup>A</sup>	48 ± 8 <sup>A</sup>	33 ± 10
hypomSR-BI-KO <sup>liver</sup>	12	1,119 ± 252 <sup>A</sup>	839 ± 224 <sup>A</sup>	75 ± 10 <sup>A</sup>	60 ± 21 <sup>A</sup>
SR-BI <sup>-/-</sup>	10	969 ± 151 <sup>A,B</sup>	707 ± 128 <sup>A,B</sup>	73 ± 8 <sup>A,B</sup>	48 ± 8 <sup>A,B</sup>

Plasma TC, FC, and TG levels were measured in female mice after feeding an HFC diet for 11 weeks. Data represent mean ± SD. <sup>A</sup>*P* < 0.001 versus control mice. <sup>B</sup>Not statistically different from hypomSR-BI-KO<sup>liver</sup> mice.

female groups. Interestingly, analysis of electrophoretic mobilities revealed that larger HDL particles in hypomSR-BI, hypomSR-BI-KO<sup>liver</sup>, and SR-BI<sup>-/-</sup> mice displayed slightly lower electronegativity compared with the normal-sized HDL present in control mice, potentially reflecting differences in apolipoprotein content (Figure 3B). Finally, no differences in plasma triglyceride (TG) levels were observed among SR-BI genotypes (Table 1).

*SR-BI dose-dependent effect on cholesterol homeostasis in liver.* As reported previously (15), the hepatic content of FC and esterified cholesterol in SR-BI<sup>-/-</sup> mice did not differ from those in controls. Similar results were also observed for both hypomSR-BI and hypomSR-BI-KO<sup>liver</sup> mice. In addition, no significant difference was observed among SR-BI genotypes in hepatic mRNA levels of LDL-r, ABCA1, apoB-100, SR-BI-interacting scaffold protein PDZK1, and transcriptional regulators of hepatic lipid metabolism,

such as SREBP1, SREBP2, LXR, FXR, and LRH-1 (data not shown). However, we confirmed an increase in hepatic mRNA levels for the ABCG1 subfamily member ABCG1 in SR-BI<sup>-/-</sup> mice (15) (1.9-fold increase versus controls; *P* < 0.0001). An increase of similar magnitude was observed in the livers of hypomSR-BI-KO<sup>liver</sup> mice (1.7-fold versus controls; *P* < 0.001) but not in that of hypomSR-BI animals. Interestingly, both SR-BI<sup>-/-</sup> and hypomSR-BI-KO<sup>liver</sup> mice exhibited a 1.5-fold elevation (*P* < 0.001 vs controls) in hepatic mRNA levels for the macrophage marker F4/80, while no change could be detected in liver RNA prepared from hypomSR-BI mice. Taken together, these observations suggest that elevated ABCG1 expression in livers of SR-BI<sup>-/-</sup> and hypomSR-BI-KO<sup>liver</sup> mice may result from increased numbers and/or activation of resident hepatic macrophages.

*SR-BI dose-dependent effect on the development of atherosclerosis.* To evaluate the impact of general knockdown expression of SR-BI on atherosclerosis susceptibility and, in addition, to assess the potential supplementary effect triggered by complete deletion of hepatic SR-BI in this context, the various mouse lines were fed a high-fat, high-cholesterol, and cholic acid-containing (HFC) diet for 11 weeks. This diet resulted in an elevation in plasma TC (>2-fold) and a decrease in TG levels (>2.5-fold) of similar magnitude in hypomSR-BI and control mice (Tables 1 and 2). Plasma TC levels were significantly raised in both hypomSR-BI-KO<sup>liver</sup> and SR-BI<sup>-/-</sup> mice, mostly as a consequence of elevated concentrations

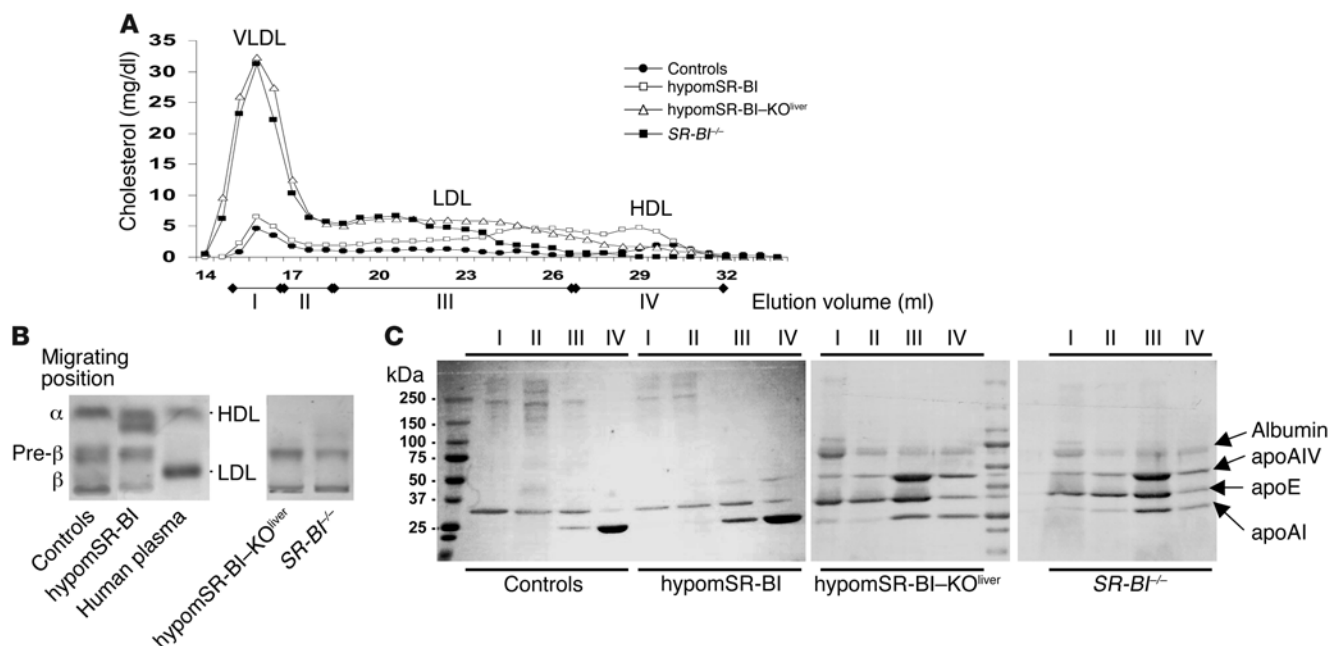


**Figure 4**  
Analysis of the distribution of plasma lipoprotein cholesterol in female mice fed an atherogenic diet. **(A)** Lipoprotein cholesterol profiles. Fasting plasma samples were prepared from female mice fed an atherogenic (HFC) diet for 11 weeks. For each genotype, plasma samples from individual mice were pooled and loaded on Superose 6 columns, and cholesterol was measured in collected fractions. **(B)** Electrophoretic mobilities of plasma lipoproteins. Plasma samples (10 μl) were subjected to agarose gel electrophoresis and lipoproteins revealed by Sudan black staining. **(C)** Apolipoprotein composition of lipoprotein fractions. Lipoproteins were first isolated from pooled plasmas (*n* = 5–10) by ultracentrifugation at a density of 1.21 g/ml and then fractionated by size-exclusion chromatography. Collected fractions were pooled as indicated in **(A)** (I, II, III, and IV), concentrated, and subjected (20–30 μg protein loaded per lane) to SDS-PAGE on gradient gels. Proteins were visualized by Coomassie blue staining. Bands corresponding to apoAI, apoE, and apoAIV, as confirmed by immunoblotting (data not shown), are indicated.

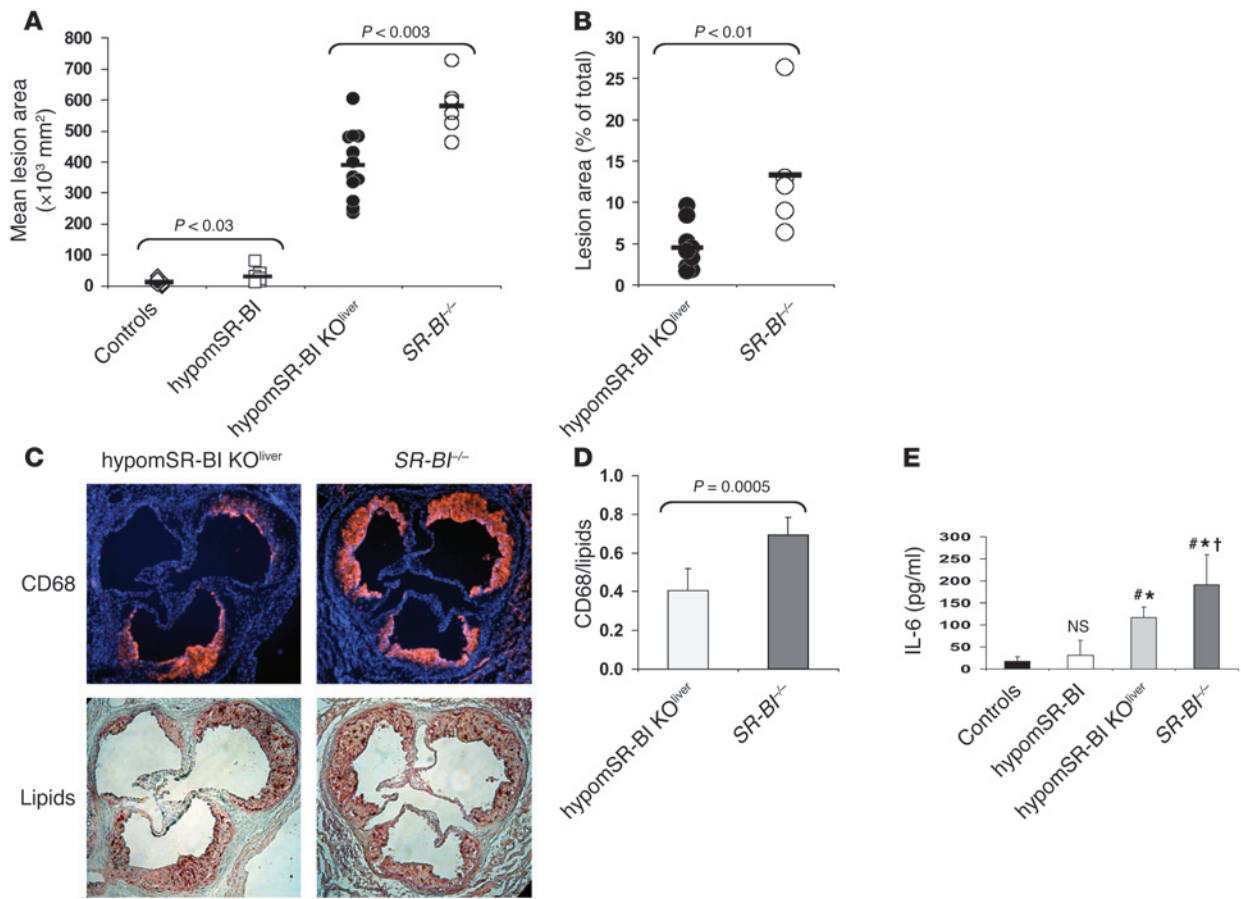


**Figure 5**

Quantification of atherosclerosis and inflammation in mice fed the atherogenic HFC diet. **(A)** Degree of atherosclerosis in the aortic root area. Lipid deposits were visualized by oil red O staining of aortic root sections. Each symbol represents the mean lesion area in a single mouse. The horizontal bar indicates the mean value for the group. Statistically significant differences between groups are indicated. **(B)** Quantification of lipid lesions in the aortic arch and thoracic aorta of hypomSR-BI-KO<sup>liver</sup> and SR-BI<sup>-/-</sup> mice. Each symbol represents the percentage of the aorta stained for lipid with Sudan IV in a single mouse. The horizontal bar indicates the mean value for each group. Statistically significant differences between the 2 groups are indicated. No lipid staining could be detected in controls and in hypomSR-BI mice. **(C)** Increased monocyte/macrophage accumulation in atherosclerotic lesions of SR-BI<sup>-/-</sup> mice as compared with hypomSR-BI-KO<sup>liver</sup> mice. Aortic atherosclerotic lesions were immunostained for monocyte/macrophage CD68 antigen (upper panels; nuclei are visualized in blue with DAPI staining) and subsequently processed for lipid staining with oil red O (lower panels). **(D)** The surface ratio of CD68<sup>+</sup> staining to oil red O<sup>+</sup> staining was calculated for both groups. Values represent the mean ± SD of 6 size-matched lesions analyzed per group. **(E)** IL-6 plasma levels in HFC diet-fed mice. #*P* < 0.03 compared with controls; \**P* < 0.05 compared with hypomSR-BI mice; †*P* < 0.05 compared with hypomSR-BI-KO<sup>liver</sup> mice. NS, not statistically different compared with values for controls.

of plasma FC. Indeed, the plasma FC/TC ratio was increased 2-fold as compared with the chow-fed condition in both lines and was 1.5- and 2.3-fold greater relative to that observed in hypomSR-BI and control female mice fed the atherogenic diet, respectively. Plasma TG levels were equally elevated in both HFC diet-fed hypomSR-BI-KO<sup>liver</sup> and SR-BI<sup>-/-</sup> mice as compared with controls. Importantly, plasma TC, FC, and TG concentrations, as well as the FC/TC ratio, were not statistically different between hypomSR-BI-KO<sup>liver</sup> and SR-BI<sup>-/-</sup> mice after the atherogenic diet (Table 2). Analysis of plasma lipoprotein cholesterol profiles revealed that the amount of cholesterol associated with VLDL-sized particles was similarly increased in both control and hypomSR-BI mice when fed the HFC diet. However, higher levels of plasma TC in hypomSR-BI mice as compared with controls was primarily due to greater amounts of cholesterol associated with both large and normal-sized HDL

(Figure 4A). As seen under normal chow diet feeding (Figure 3B), large HDL particles present in HFC diet-fed hypomSR-BI mice exhibited a lower electronegativity on agarose gels as compared with normal HDL (Figure 4B). Lipoprotein cholesterol profiles of hypomSR-BI-KO<sup>liver</sup> and SR-BI<sup>-/-</sup> mice fed the HFC diet were similar, cholesterol being mainly associated with VLDL-sized particles. Analysis of these particles from both lines revealed that they exhibited similar characteristics, as they migrated to the pre-β position in agarose gels (Figure 4B) and were rich in apoE and, to a lesser extent, in apoAIV (Figure 4C). The FC/TC ratios in these particles were also similar (73% and 78% for hypomSR-BI-KO<sup>liver</sup> and SR-BI<sup>-/-</sup> mice, respectively) and reflected those measured in the plasma of both lines (Table 2). By comparison, FC/TC ratios in isolated VLDL-sized particles from hypomSR-BI and control mice were 34% and 21%, respectively. To further characterize the



apoE-rich VLDL-sized particles migrating to the pre- $\beta$  position present in the plasma of both HFC diet-fed hypomSR-BI-KO<sup>liver</sup> and *SR-BI*<sup>-/-</sup> mice, we compared their capacity to induce cholesterol loading in the murine macrophage RAW cell line. The increase in cellular esterified cholesterol and FC content following incubation of RAW cells with these particles was similar for both mouse lines (see Supplemental Figure 1; supplemental material available online with this article; doi:10.1172/JCI26893DS1). Finally, analysis of the lipoprotein cholesterol profiles of hypomSR-BI-KO<sup>liver</sup> and *SR-BI*<sup>-/-</sup> mice fed the HFC diet also revealed that HDL-C levels were markedly reduced in both lines as compared with that present in hypomSR-BI mice; such reduction occurred primarily in normal-sized HDL (Figure 4A). This observation was confirmed by agarose gel analysis (Figure 4B). In addition, SDS-PAGE analysis of lipoproteins showed significantly increased amounts of both apoE and apoAIV in the protein moieties of HDL particles in both hypomSR-BI-KO<sup>liver</sup> and *SR-BI*<sup>-/-</sup> mice (Figure 4C).

SR-BI knockdown expression in hypomSR-BI mice led to a 2.5-fold ( $P < 0.03$ ) increase in mean atherosclerotic lesion area as compared with that in wild-type mice ( $12 \times 10^3 \pm 10 \times 10^3 \mu\text{m}^2$  and  $30 \times 10^3 \pm 22 \times 10^3 \mu\text{m}^2$ , respectively; Figure 5A). A further 13-fold increase in the size of lipid lesions ( $389 \times 10^3 \pm 112 \times 10^3 \mu\text{m}^2$ ) was observed in hypomSR-BI-KO<sup>liver</sup> mice, thus confirming the atheroprotective role of hepatic SR-BI expression, as previously reported (6, 17), but equally emphasizing its importance. Finally, analysis of *SR-BI*<sup>-/-</sup> mice revealed increased susceptibility to atherosclerotic lesion development as compared with hypomSR-BI-KO<sup>liver</sup> animals, with a mean lesion area of  $579 \pm 89 \times 10^3 \mu\text{m}^2$  (1.5-fold increase compared with hypomSR-BI-KO<sup>liver</sup> mice;  $P < 0.003$ ; Figure 5A). These findings were confirmed by lesion size quantification with en face analysis of thoracic and abdominal aortas (Figure 5B). Lipid lesions covered an average of  $4.5\% \pm 2.8\%$  and  $13.3\% \pm 7.7\%$  of the total aortic surface analyzed in hypomSR-BI-KO<sup>liver</sup> and *SR-BI*<sup>-/-</sup> mice, respectively; this difference was statistically significant ( $-66\%$  in hypomSR-BI-KO<sup>liver</sup> versus *SR-BI*<sup>-/-</sup> mice;  $P < 0.01$ ).

To examine the cellular content of aortic root lesions, and in particular macrophage abundance, we stained selected sections adjacent to size-matched lesions of hypomSR-BI-KO<sup>liver</sup> and *SR-BI*<sup>-/-</sup> mice (as determined by oil red O staining) for CD68 antigen and then further processed them for oil red O lipid staining (Figure 5C). Surprisingly, the average surface ratio of CD68<sup>+</sup> staining to lipid-positive staining was statistically significantly lower ( $-40\%$ ) in hypomSR-BI-KO<sup>liver</sup> mice than in *SR-BI*<sup>-/-</sup> mice ( $0.4 \pm 0.1$  vs.  $0.7 \pm 0.1$ , respectively;  $P = 0.0005$ ) (Figure 5D). These data suggested an increased accumulation of macrophages, reflecting increased vascular inflammation in lesions of *SR-BI*<sup>-/-</sup> mice as compared with hypomSR-BI-KO<sup>liver</sup> mice. Concomitantly, plasma concentrations of the proinflammatory cytokine IL-6 were elevated to a greater degree in *SR-BI*<sup>-/-</sup> mice than in hypomSR-BI-KO<sup>liver</sup> mice fed the HFC diet (Figure 5E). Indeed, IL-6 plasma levels were increased 10.8- and 6.6-fold in *SR-BI*<sup>-/-</sup> and hypomSR-BI-KO<sup>liver</sup> mice, respectively, as compared with control mice. HypomSR-BI mice also displayed a trend toward higher IL-6 levels (1.8-fold increase versus controls); however, such concentrations were not statistically different from those in controls.

## Discussion

Our present investigations have revealed that whereas marked reduction in the expression of SR-BI in hypomSR-BI mice was associated with increased diet-induced atherosclerosis, complete hepatic SR-BI deficiency in hypomSR-BI-KO<sup>liver</sup> mice strongly impacted

lipoprotein cholesterol distribution and massively accelerated atherosclerosis. Furthermore, comparison of hypomSR-BI-KO<sup>liver</sup> mice and *SR-BI*<sup>-/-</sup> mice demonstrated that, in a similar atherogenic lipoprotein environment, residual peripheral SR-BI expression contributed to significant atheroprotection in hypomSR-BI-KO<sup>liver</sup> mice. These data suggest that whereas the major atheroprotective role of hepatic SR-BI is tightly associated with its impact on plasma lipoprotein cholesterol levels, peripheral SR-BI expression may protect against atherosclerosis through mechanisms that are independent of changes in plasma lipid parameters.

Diet-induced atherogenesis in *SR-BI*<sup>-/-</sup> mice (15) or mice with attenuated expression of SR-BI (32) revealed either no difference or a 2- to 3-fold increase in atherosclerosis development as compared with their respective SR-BI-expressing controls. In contrast, complete deficiency of SR-BI in mice was consistently associated with a major increase in atherosclerosis development (15, 21). This observation is consistent with the modest (2.5-fold) and significant increases (48-fold) in atherosclerosis that we observed in hypomSR-BI and *SR-BI*<sup>-/-</sup> mice, respectively, as compared with controls. Residual SR-BI expression in mice may therefore ensure partial to complete atheroprotection. In contrast, the marked increase in atherosclerotic lesion size in hypomSR-BI-KO<sup>liver</sup> mice, as compared with hypomSR-BI and control mice, further confirms the critical role of hepatic SR-BI in atherogenesis (6, 17, 18), albeit under conditions of reduced expression of SR-BI in peripheral tissues, as in this study. Comparison of plasma lipoprotein cholesterol profiles indicates that such protection probably involves the contribution of hepatic SR-BI to the prevention of the accumulation of atherogenic plasma lipoproteins of VLDL size rich in FC. The specific increase in plasma FC/TC ratio observed in hypomSR-BI-KO<sup>liver</sup> and *SR-BI*<sup>-/-</sup> mice fed a chow diet suggests that hepatic SR-BI is a key determinant in maintaining plasma cholesterol homeostasis, most likely through its contribution to the delivery of HDL-CE (33, 34) and/or of HDL-FC (8) to the liver. Expression of SR-BI, albeit at low levels, in livers of hypomSR-BI mice may have ensured such activities. Interestingly, PDZK1-deficient mice, which display a profound reduction in hepatic SR-BI protein expression ( $\sim 95\%$ ), possess elevated HDL-C plasma concentrations but do not exhibit high plasma FC/TC ratios (28). Residual expression of SR-BI and/or expression of the SR-BII isoform in the livers of PDZK1-KO mice may explain phenotypic similarities of the PDZK1-deficient mice to our hypomSR-BI mouse line. Accumulation of VLDL-sized lipoproteins in HFC diet-fed hypomSR-BI-KO<sup>liver</sup> and *SR-BI*<sup>-/-</sup> mice may also result from other activities attributed to SR-BI. Indeed, in vivo studies implicate SR-BI in the removal of apoB-containing lipoproteins from the circulation (7, 35) and in postprandial chylomicron metabolism (36). Interestingly, however, we observed that these VLDL-sized lipoproteins contained primarily apoE rather than apoB100/B48. Whether such factors may contribute to the atherogenic plasma lipoprotein profile present in HFC diet-fed hypomSR-BI-KO<sup>liver</sup> and *SR-BI*<sup>-/-</sup> mice has yet to be determined.

Strikingly, hypomSR-BI-KO<sup>liver</sup> mice displayed less extensive atherosclerosis than *SR-BI*<sup>-/-</sup> mice, despite the fact that the 2 mouse models exhibited similar plasma lipid levels, lipoprotein cholesterol distribution, and apolipoprotein composition. Moreover, VLDL-sized lipoproteins isolated from these models induced cholesterol loading of macrophage RAW cells to a similar degree. Thus, differences in the extent of atherosclerosis between the models appeared to reflect a plasma lipoprotein/cholesterol-independent mechanism. Reduced CD68 immunostaining in the plaques



of hypomSR-BI-KO<sup>liver</sup> mice may indicate attenuated vascular inflammation in this model, suggesting that extrahepatic SR-BI may exert antioxidant or/and antiinflammatory activities that attenuate atherosclerosis progression. Such activities may depend on the contribution of SR-BI to the uptake or metabolism of specific components transported by lipoproteins, such as the cellular antioxidant  $\alpha$ -tocopherol (26, 27) or the proinflammatory protein serum amyloid A (37), both of which may actively participate in atherogenesis (38, 39). Alternatively, *in vivo* evidence for a role of macrophage SR-BI expression in atherosclerosis has also been suggested by BM transplantation studies in mice (21–23). However, SR-BI in BM-derived cells could exert pro- or antiatherogenic activities depending on the specific stage of atherosclerosis development (23). Although these studies are not fully conclusive, as cell types other than macrophages may be derived from BM cells in vascular lesions (e.g., smooth muscle cells and endothelial cells; ref. 40), *in vitro* studies suggest that macrophage SR-BI could participate in atherogenesis via a spectrum of activities. Thus, SR-BI could be implicated in the clearance of apoptotic cells (25) or of atherogenic oxidized lipoproteins (41), activities that may contribute to prevention of the accumulation of inflammatory material in the arterial wall. SR-BI may also stimulate macrophage cholesterol efflux (23, 42) and thereby prevent foam cell formation. In this regard, it is noteworthy that production of the inflammatory cytokine IL-6 is induced in macrophages as a consequence of cellular FC loading (43). Although plasma FC levels were dramatically and similarly increased in both HFC diet-fed hypomSR-BI-KO<sup>liver</sup> and SR-BI<sup>-/-</sup> mice, IL-6 plasma levels were elevated to a greater extent in the latter. Determining whether complete absence of SR-BI in macrophages of SR-BI<sup>-/-</sup> mice resulted in perturbation of cholesterol flux in lesion macrophages, which in turn contributed to higher IL-6 levels in these mice as compared with those measured in hypomSR-BI-KO<sup>liver</sup> mice, will be an important goal for future investigation.

In conclusion, this study not only further documents the involvement of hepatic and extrahepatic SR-BI expression *in vivo* in cholesterol homeostasis, but also provides new insight into the relationship between SR-BI and atherosclerosis susceptibility. Further experimentation using the SR-BI conditional-KO mouse model (hypomSR-BI mice) to define the relative contribution of SR-BI expressed by arterial wall cells, including endothelial cells and macrophages, to atherosclerotic lesion development may, however, be limited due to reduced expression of SR-BI in all tissues in this model. However, the significant difference between hypomSR-BI-KO<sup>liver</sup> and SR-BI<sup>-/-</sup> mice in atherosclerosis development at similar plasma lipid levels suggests that such mouse models may nonetheless represent a valuable tool with which to evaluate potential tissue-specific effects of SR-BI.

## Methods

**Generation of SR-BI conditional KO and SR-BI<sup>-/-</sup> mouse models.** The left homology arm of the targeting vector was generated by PCR amplification using SRBI.f1 5'-TGAAGTGGTCTTCAAGAGCAGTCCT-3' and SRBI.r1 5'-ACCTACACGGGGATCACGTTTC-3' located 1.2 kb upstream and 3.5 kb downstream of SR-BI exon 1, respectively (Figure 1). A *loxP* sequence, 5'-GCAACTTCGTATAGCATAACATTATACGAAGTTAT-3' (the outer 2 underlined bases were modified from the original *loxP* sequence in order to destabilize the *loxP* hairpin structure), was then introduced at position -85 bp (relative to the initiation translation codon). The left arm cassette containing the *loxP* site was then cloned into the pPN2T vector to yield the pPN2T-Larm plasmid. The right homology arm was PCR amplified

using an approximately 8-kb SR-BI/*Bam*HI fragment cloned in pBlue-script as template and the following primer pair: SRBI/*Xho*I.*loxP*.f2 primer 5'-GCCGctcggagATAACTTCGTATAGCATAACATTATACGAAGTTATGACAGTTTTTCAGAGCTCAGGG-3' (complementary sequence adjacent to the SRBI.r1 primer sequence in intron 1), containing an introduced 5' restriction site for *Xho*I (lowercase letters) and a 5'-*loxP* sequence (underlined), and M13 reverse primer 5'-CAGGAAACAGCTATGACC-3'. The resulting PCR product was then subcloned into the pPN2T-Larm plasmid to yield the final vector pPN2T-floxSRBI.

Mouse ES cells (129/SvJ; GoGermline; Genome Systems Inc.) were electroporated with 20–40  $\mu$ g of pPN2T-floxSRBI construct and plated onto neomycin-resistant mouse embryonic fibroblast feeder layers. Selective medium was applied 2 days later. Individual clones were isolated after 10–12 days, expanded, and screened by Southern blot analysis of *Xba*I-digested DNA using probe A (Figure 1). Several targeted clones containing an SR-BI allele with a floxed exon 1 (SR-BI<sup>flox/+</sup> ES) were further transfected with pBS185 Cre plasmid (Invitrogen) modified to contain the hygromycin B resistance gene and subsequently selected in hygromycin B-containing medium. Cre-mediated deletion of exon 1 of the floxed SR-BI allele in hygromycin B-resistant ES clones (SR-BI<sup>-/-</sup> ES) was confirmed by PCR and Southern blot analysis. SR-BI<sup>flox/+</sup> ES and derived SR-BI<sup>-/-</sup> ES clones were injected into C57BL/6 blastocysts, and chimeric offspring were bred to C57BL/6 mice to test for germline transmission of the floxed SR-BI allele or the exon 1-deleted SR-BI allele, respectively. SR-BI<sup>flox/+</sup> and SR-BI<sup>-/-</sup> mouse lines selected for the study were derived from the same ES clone (i.e., one SR-BI<sup>flox/+</sup> ES clone and a derived SR-BI<sup>-/-</sup> ES clone). Alb-Cre transgenic mice (29) were bred with mice carrying the SR-BI floxed allele to obtain animals with liver-specific deficiency of the SR-BI gene. SR-BI<sup>-/-</sup> mice were generated by breeding heterozygous or homozygous animals fed a chow diet containing 0.5% probucol (Sigma-Aldrich). See Supplemental Methods for more detailed information on generation of the mouse models. The animals were housed in a conventional animal facility on a 6 am to 6 pm dark/light cycle. They were weaned at 21 days and fed *ad libitum* a normal mouse chow diet (RM1; Dietex France). For the high-fat diet experiment, 2-month-old female mice were switched to a diet consisting of 1.25% cholesterol, 0.5% cholic acid, and 20% fat for 11 weeks. All animal procedures were performed at the Central Animal Facility of the Medical Faculty of La Pitié Hospital with approval from the Direction Départementale des Services Vétérinaires, Paris, France, under strict compliance with European Community Regulations.

**Plasma and tissue analyses.** Blood samples were collected in Microvette tubes (Sarstedt) before and after the high-fat diet following an overnight fast by retro-orbital bleeding using heparinized microhematocrit tubes. Plasma samples were stored frozen at -80°C. TC (Roche Diagnostics), FC (Wako), and TG (bioMérieux) concentrations were measured by enzymatic colorimetric assays. IL-6 plasma concentrations were measured with the ProteoPlex mouse cytokine kit (Novagen; EMD Biosciences). Plasma lipoproteins were fractionated by gel filtration on 2 Superose 6 (Amersham Biosciences) columns connected in series using a BioLogic DuoFlow Chromatography System (Bio-Rad). For apolipoprotein analysis by SDS-PAGE, plasmas were first ultracentrifuged (100,000 *g* for 5.5 hours at 15°C in a fixed-angle rotor in a TL100 ultracentrifuge [Beckman Coulter]) at a density of 1.21 g/ml. Lipoproteins in the supernatant were then fractionated by gel filtration on Superose 6 columns and collected into 4 fractions (I–IV). These fractions were concentrated on a Microcon YM-30 centrifugal filter unit (Millipore) and samples electrophoresed on 4%–18% SDS-polyacrylamide gels under reducing conditions. To determine cholesterol content in liver, total lipids were extracted from frozen livers (~30 mg) using the Folch extraction procedure (44). Cholesterol concentration was determined with a commercial enzymatic assay (Roche Diagnostics). Electrophoretic mobility of mouse lipoproteins was assessed on HYDRAGEL 7 LIPO + Lp(a) gels (Sebia).



**Immunoblot analysis.** Mice were sacrificed by cervical dislocation. Organs were collected, rinsed in ice-cold PBS, and snap-frozen in liquid nitrogen. Frozen tissue specimens were disrupted and homogenized with a rotor-stator homogenizer in ice-cold PBS containing 1% Triton and a protease inhibitor cocktail (Complete Mini protease inhibitor tablets; Roche Diagnostics). Samples were centrifuged at 10,000 g for 15 minutes at 4°C and protein content determined in the supernatant with the bicinchoninic acid assay reagent (Pierce). Equal amounts of protein extracts were separated by electrophoresis on 8% SDS-polyacrylamide gels under reducing conditions and then blotted onto a Hybond-C super nitrocellulose membrane (Amersham Biosciences). SR-BI and SR-BII proteins were detected using a rabbit polyclonal antibody raised against a peptide corresponding to amino acids 496–509 of the murine SR-BI sequence (45) and a specific anti-SR-BII rabbit polyclonal antibody (NB 400-102; Novus Biologicals), respectively. Primary antibodies were detected using a peroxidase-conjugated anti-rabbit antibody and revealed by chemiluminescence (ECL Plus reagent; Amersham Biosciences).

**Analysis of gene expression by qRT-PCR.** RNAs were prepared from frozen tissue specimens using TRIzol reagent (Invitrogen) and further purified with a NucleoSpin RNA II kit (Macherey-Nagel). cDNA preparation and quantitative PCR analysis were performed as previously described (45). The specific primers used are described in Supplemental Table 1.

**Analysis of atherosclerotic plaques.** Mice were sacrificed under isoflurane anesthesia and perfused with ice-cold PBS. Hearts were collected and fixed (Accustain 10% formalin solution [Sigma-Aldrich] supplemented with 2 mM EDTA and 20 μM butylated hydroxytoluene at pH 7.4) for 30 minutes followed by overnight incubation in phosphate-buffered 20% sucrose solution at 4°C; hearts were subsequently embedded in Tissue-Tek OCT compound (Sakura). The entire aortas were fixed, cleaned of adipose and connective tissues, opened longitudinally, and pinned out on a wax surface. Atherosclerotic lesions were quantified both on pinned-open aortas

by Sudan IV staining (thoracic and abdominal part of the aorta) and on serial cross-sections (10 μm) through the aortic root by oil red O staining as previously described (46).

**Immunohistochemistry.** Ten-micrometer aortic root cryosections were air dried and fixed in formalin (10%) for 30 minutes. Sections were then blocked for 60 minutes with 3% BSA in PBS and then incubated with anti-CD68 antibody or control antibodies (1:300 dilution in PBS with 20 mM glycine; Serotec) overnight at 4°C. After washing, a goat anti-rat Ig biotinylated secondary antibody (1:300 dilution; BD Biosciences – Pharmingen) was added, followed by streptavidin–horseradish peroxidase. The signal was enhanced using the tyramide signal amplification (TSA) kit (NEL 702; PerkinElmer), and the sections were counterstained for nuclei with DAPI (Molecular Probes; Invitrogen).

**Statistics.** The statistical significance of the differences between groups was evaluated using 2-tailed Student's *t* test for unpaired comparisons. *P* < 0.05 was considered significant. Values are expressed as mean ± SD.

## Acknowledgments

This study was supported by the French National Institute for Health and Medical Research (INSERM) and by an International HDL Research Award from Pfizer to P. Lesnik and T. Huby. M.J. Chapman and P. Lesnik gratefully acknowledge the award of a “Contrat d’Interface” by the Assistance Publique – Hôpitaux de Paris/INSERM.

Received for publication September 16, 2005, and accepted in revised form July 18, 2006.

Address correspondence to: Thierry Huby, INSERM U551, Hôpital de la Pitié, 83 Bd de l’hôpital, 75651 Paris 13, France. Phone: 33-142-17-78-60; Fax: 33-145-82-81-98; E-mail: huby@chups.jussieu.fr.

- Marsche, G., et al. 2001. Identification of the human analog of SR-BI and LOX-1 as receptors for hypochlorite-modified high density lipoprotein on human umbilical venous endothelial cells. *FASEB J.* **15**:1095–1097.
- Yuhanna, I.S., et al. 2001. High-density lipoprotein binding to scavenger receptor-BI activates endothelial nitric oxide synthase. *Nat. Med.* **7**:853–857.
- Yeh, Y.C., Hwang, G.Y., Liu, I.P., and Yang, V.C. 2002. Identification and expression of scavenger receptor SR-BI in endothelial cells and smooth muscle cells of rat aorta in vitro and in vivo. *Atherosclerosis.* **161**:95–103.
- Chinetti, G., et al. 2000. CLA-1/SR-BI is expressed in atherosclerotic lesion macrophages and regulated by activators of peroxisome proliferator-activated receptors. *Circulation.* **101**:2411–2417.
- Rhoads, D., and Brissette, L. 2004. The role of scavenger receptor class B type I (SR-BI) in lipid trafficking. Defining the rules for lipid traders. *Int. J. Biochem. Cell Biol.* **36**:39–77.
- Kozarsky, K.F., Donahee, M.H., Glick, J.M., Krieger, M., and Rader, D.J. 2000. Gene transfer and hepatic overexpression of the HDL receptor SR-BI reduces atherosclerosis in the cholesterol-fed LDL receptor-deficient mouse. *Arterioscler. Thromb. Vasc. Biol.* **20**:721–727.
- Ueda, Y., et al. 1999. Lower plasma levels and accelerated clearance of high density lipoprotein (HDL) and non-HDL cholesterol in scavenger receptor class B type I transgenic mice. *J. Biol. Chem.* **274**:7165–7171.
- Ji, Y., et al. 1999. Hepatic scavenger receptor BI promotes rapid clearance of high density lipoprotein free cholesterol and its transport into bile. *J. Biol. Chem.* **274**:33398–33402.
- Kozarsky, K.F., et al. 1997. Overexpression of the HDL receptor SR-BI alters plasma HDL and bile cholesterol levels. *Nature.* **387**:414–417.
- Rigotti, A., et al. 1997. A targeted mutation in the murine gene encoding the high density lipoprotein (HDL) receptor scavenger receptor class B type I reveals its key role in HDL metabolism. *Proc. Natl. Acad. Sci. U. S. A.* **94**:12610–12615.
- Varban, M.L., et al. 1998. Targeted mutation reveals a central role for SR-BI in hepatic selective uptake of high density lipoprotein cholesterol. *Proc. Natl. Acad. Sci. U. S. A.* **95**:4619–4624.
- Osgood, D., et al. 2003. Genetic variation at the scavenger receptor class B type I gene locus determines plasma lipoprotein concentrations and particle size and interacts with type 2 diabetes: the Framingham study. *J. Clin. Endocrinol. Metab.* **88**:2869–2879.
- Hong, S.H., et al. 2002. Association between HaeIII polymorphism of scavenger receptor class B type I gene and plasma HDL-cholesterol concentration. *Ann. Clin. Biochem.* **39**:478–481.
- Acton, S., et al. 1999. Association of polymorphisms at the SR-BI gene locus with plasma lipid levels and body mass index in a white population. *Arterioscler. Thromb. Vasc. Biol.* **19**:1734–1743.
- Van Eck, M., et al. 2003. Differential effects of scavenger receptor BI deficiency on lipid metabolism in cells of the arterial wall and in the liver. *J. Biol. Chem.* **278**:23699–23705.
- Trigatti, B., et al. 1999. Influence of the high density lipoprotein receptor SR-BI on reproductive and cardiovascular pathophysiology. *Proc. Natl. Acad. Sci. U. S. A.* **96**:9322–9327.
- Ueda, Y., et al. 2000. Relationship between expression levels and atherogenesis in scavenger receptor class B, type I transgenics. *J. Biol. Chem.* **275**:20368–20373.
- Arai, T., Wang, N., Bezouevski, M., Welch, C., and Tall, A.R. 1999. Decreased atherosclerosis in heterozygous low density lipoprotein receptor-deficient mice expressing the scavenger receptor BI transgene. *J. Biol. Chem.* **274**:2366–2371.
- Zhang, Y., et al. 2005. Hepatic expression of scavenger receptor class B type I (SR-BI) is a positive regulator of macrophage reverse cholesterol transport in vivo. *J. Clin. Invest.* **115**:2870–2874. doi:10.1172/JCI25327.
- Li, X.A., et al. 2002. High density lipoprotein binding to scavenger receptor, class B, type I activates endothelial nitric-oxide synthase in a ceramide-dependent manner. *J. Biol. Chem.* **277**:11058–11063.
- Covey, S.D., Krieger, M., Wang, W., Penman, M., and Trigatti, B.L. 2003. Scavenger receptor class B type I-mediated protection against atherosclerosis in LDL receptor-negative mice involves its expression in bone marrow-derived cells. *Arterioscler. Thromb. Vasc. Biol.* **23**:1589–1594.
- Zhang, W., et al. 2003. Inactivation of macrophage scavenger receptor class B type I promotes atherosclerotic lesion development in apolipoprotein E-deficient mice. *Circulation.* **108**:2258–2263.
- Van Eck, M., Bos, I.S., Hildebrand, R.B., Van Rij, B.T., and Van Berkel, T.J. 2004. Dual role for scavenger receptor class B, type I on bone marrow-derived cells in atherosclerotic lesion development. *Am. J. Pathol.* **165**:785–794.
- Li, X.A., Guo, L., Dressman, J.L., Asmis, R., and Smart, E.J. 2005. A novel ligand-independent apoptotic pathway induced by scavenger receptor class B, type I and suppressed by endothelial nitric-oxide synthase and high density lipoprotein. *J. Biol. Chem.* **280**:19087–19096.
- Nakagawa, A., Shiratsuchi, A., Tsuda, K., and Nakanishi, Y. 2005. In vivo analysis of phagocytosis



- of apoptotic cells by testicular Sertoli cells. *Mol. Reprod. Dev.* **71**:166–177.
26. Goti, D., et al. 2001. Scavenger receptor class B, type I is expressed in porcine brain capillary endothelial cells and contributes to selective uptake of HDL-associated vitamin E. *J. Neurochem.* **76**:498–508.
27. Mardones, P., et al. 2002. Alpha-tocopherol metabolism is abnormal in scavenger receptor class B type I (SR-BI)-deficient mice. *J. Nutr.* **132**:443–449.
28. Kocher, O., et al. 2003. Targeted disruption of the PDZK1 gene in mice causes tissue-specific depletion of the high density lipoprotein receptor scavenger receptor class B type I and altered lipoprotein metabolism. *J. Biol. Chem.* **278**:52820–52825.
29. Postic, C., and Magnuson, M.A. 2000. DNA excision in liver by an albumin-Cre transgene occurs progressively with age. *Genesis.* **26**:149–150.
30. Timmins, J.M., et al. 2005. Targeted inactivation of hepatic Abca1 causes profound hypoalphalipoproteinemia and kidney hypercatabolism of apoA-I. *J. Clin. Invest.* **115**:1333–1342. doi:10.1172/JCI200523915.
31. Miettinen, H.E., Rayburn, H., and Krieger, M. 2001. Abnormal lipoprotein metabolism and reversible female infertility in HDL receptor (SR-BI)-deficient mice. *J. Clin. Invest.* **108**:1717–1722. doi:10.1172/JCI200113288.
32. Huszar, D., et al. 2000. Increased LDL cholesterol and atherosclerosis in LDL receptor-deficient mice with attenuated expression of scavenger receptor B1. *Arterioscler. Thromb. Vasc. Biol.* **20**:1068–1073.
33. Brundert, M., et al. 2005. Scavenger receptor class B type I mediates the selective uptake of high-density lipoprotein-associated cholesteryl ester by the liver in mice. *Arterioscler. Thromb. Vasc. Biol.* **25**:143–148.
34. Out, R., et al. 2004. Scavenger receptor class B type I is solely responsible for the selective uptake of cholesteryl esters from HDL by the liver and the adrenals in mice. *J. Lipid Res.* **45**:2088–2095.
35. Wang, N., Arai, T., Ji, Y., Rinninger, F., and Tall, A.R. 1998. Liver-specific overexpression of scavenger receptor BI decreases levels of very low density lipoprotein ApoB, low density lipoprotein ApoB, and high density lipoprotein in transgenic mice. *J. Biol. Chem.* **273**:32920–32926.
36. Out, R., et al. 2005. Adenovirus-mediated hepatic overexpression of scavenger receptor class B type I accelerates chylomicron metabolism in C57BL/6J mice. *J. Lipid Res.* **46**:1172–1181.
37. Baranova, I.N., et al. 2005. Serum amyloid A binding to CLA-1 (CD36 and LIMPII analogous-1) mediates serum amyloid A protein-induced activation of ERK1/2 and p38 mitogen-activated protein kinases. *J. Biol. Chem.* **280**:8031–8040.
38. O'Brien, K.D., et al. 2005. Serum amyloid A and lipoprotein retention in murine models of atherosclerosis. *Arterioscler. Thromb. Vasc. Biol.* **25**:785–790.
39. Terasawa, Y., et al. 2000. Increased atherosclerosis in hyperlipidemic mice deficient in alpha-tocopherol transfer protein and vitamin E. *Proc. Natl. Acad. Sci. U. S. A.* **97**:13830–13834.
40. Sata, M., et al. 2002. Hematopoietic stem cells differentiate into vascular cells that participate in the pathogenesis of atherosclerosis. *Nat. Med.* **8**:403–409.
41. Gillotte-Taylor, K., Boullier, A., Witztum, J.L., Steinberg, D., and Quehenberger, O. 2001. Scavenger receptor class B type I as a receptor for oxidized low density lipoprotein. *J. Lipid Res.* **42**:1474–1482.
42. Ji, Y., et al. 1997. Scavenger receptor BI promotes high density lipoprotein-mediated cellular cholesterol efflux. *J. Biol. Chem.* **272**:20982–20985.
43. Li, Y., et al. 2005. Free cholesterol-loaded macrophages are an abundant source of tumor necrosis factor-alpha and interleukin-6: model of NF-kappaB- and map kinase-dependent inflammation in advanced atherosclerosis. *J. Biol. Chem.* **280**:21763–21772.
44. Folch, J., Lees, M., and Sloane Stanley, G.H. 1957. A simple method for the isolation and purification of total lipides from animal tissues. *J. Biol. Chem.* **226**:497–509.
45. Treguier, M., et al. 2004. Transcription factor sterol regulatory element binding protein 2 regulates scavenger receptor Cla-1 gene expression. *Arterioscler. Thromb. Vasc. Biol.* **24**:2358–2364.
46. Lesnik, P., Haskell, C.A., and Charo, I.F. 2003. Decreased atherosclerosis in *CX3CR1*<sup>-/-</sup> mice reveals a role for fractalkine in atherogenesis. *J. Clin. Invest.* **111**:333–340. doi:10.1172/JCI200315555.

# LDL particle subspecies are distinct in their capacity to mediate free cholesterol efflux via the SR-BI/Cla-1 receptor

Morgan Tréguier, Martine Moreau, Andrei Sposito, M. John Chapman, Thierry Huby\*

*INSERM U551, Dyslipoproteinemia and Atherosclerosis Research Unit, Hôpital de la Pitié, 83 Boulevard de l'Hôpital, 75651 Paris Cedex 13, France  
Université Pierre et Marie Curie-Paris6, UMR 551, Paris, F-75013, France*

Received 16 May 2006; received in revised form 25 November 2006; accepted 14 December 2006  
Available online 20 December 2006

## Abstract

The human scavenger receptor SR-BI/Cla-1 promotes efflux of free cholesterol from cells to both high-density and low-density lipoproteins (HDL, LDL). SR-BI/Cla-1-mediated cholesterol efflux to HDL is dependent on particle size, lipid content and apolipoprotein conformation; in contrast, the capacity of LDL subspecies to accept cellular cholesterol via this receptor is indeterminate. Cholesterol efflux assays were performed with CHO cells stably transfected with Cla-1 cDNA. Expression of Cla-1 in CHO cells induced elevation in total cholesterol efflux to plasma, LDL and HDL. Such Cla-1-specific efflux was abrogated by addition of anti-Cla-1 antibody. LDL were fractionated into five subspecies either on the basis of hydrated density or size. Among LDL subfractions, small dense LDL (sdLDL) were 1.5- to 3-fold less active acceptors for Cla-1-mediated cellular cholesterol efflux. Equally, sdLDL markedly reduced Cla-1-specific cholesterol efflux to large buoyant LDL in a dose-dependent manner. Conversely, sdLDL did not influence efflux to HDL<sub>2</sub>. These findings provide evidence that LDL particles are heterogeneous in their capacity to promote Cla-1-mediated cholesterol efflux. Relative to HDL<sub>2</sub>, large buoyant LDL may constitute physiologically-relevant acceptors for cholesterol efflux via Cla-1.

© 2006 Elsevier B.V. All rights reserved.

*Keywords:* SR-BI; Cholesterol efflux; LDL subfractions

## 1. Introduction

The scavenger receptor SR-BI is a multi-ligand receptor which facilitates the bi-directional movement of cholesterol between plasma cell membranes and lipoprotein particles and thus SR-BI is thought to play a central role in cholesterol homeostasis. Indeed, epidemiological studies have demonstrated associations between single-nucleotide polymorphisms (SNPs) in the human SR-BI (Cla-1) gene and circulating concentrations of high density lipoproteins-cholesterol (HDL-C) and of low density lipoproteins-cholesterol (LDL-C) as well as particle size of both lipoproteins [1,2]. Those data suggest that SR-BI is implicated in the metabolism of both atherogenic (LDL) and non-atherogenic (HDL) lipoprotein classes in man. On the one hand, SR-BI mediates the selective cellular uptake of cholesteryl esters (CE) from LDL and HDL and on the other, SR-BI promotes the cellular efflux of free cholesterol (FC) to a

spectrum of lipoprotein acceptor particles [3,4]. The SR-BI receptor has therefore been proposed to play a role in both the initial and final steps of the reverse cholesterol transport (RCT) pathway. This concerted biological pathway consists essentially of the removal of excess cholesterol from peripheral tissues and the arterial wall, with transport back to the liver either for excretion in bile or for recycling in nascent lipoprotein particles. Indeed, recent studies have revealed that hepatic SR-BI expression plays a key regulatory role in the flux of cholesterol through the RCT pathway in mouse [5].

Accumulation of cholesterol and other lipids in macrophages of the arterial wall is a central feature of the development of atherosclerotic plaques, as it can induce foam cell formation, thereby favouring vascular inflammation. The stimulation of cholesterol efflux from arterial macrophages by primary acceptors such as apolipoprotein-AI (apoA-I) or HDL may attenuate this process. The ABCA1 and ABCG1 transporters are most likely involved in cholesterol efflux from macrophages by interacting with lipid-poor apoA-I [6] or more mature HDL particles [7] respectively; but their relative contributions to lipid

\* Corresponding author.

E-mail address: [Thierry.huby@chups.jussieu.fr](mailto:Thierry.huby@chups.jussieu.fr) (T. Huby).

efflux remain to be determined. In addition, cholesterol can be effluxed from macrophages by aqueous diffusion or by a pathway implicating SR-BI [8]. Although, SR-BI is expressed in macrophages in both murine [9] and human [10,11] atherosclerotic lesions, its role in mediating cellular cholesterol efflux in macrophages is controversial. While some authors have reported that SR-BI deficiency was associated with a reduced capacity of the macrophage to promote cellular cholesterol efflux to HDL [8], other studies have observed similar cholesterol efflux in WT and SR-BI KO macrophages using HDL as acceptor [12,13]. Nevertheless, the role of SR-BI in cellular cholesterol efflux may potentially occur in any type of cell since SR-BI expression is rather ubiquitous.

In addition to cardioprotective HDL, the SR-BI receptor can bind and mediate efflux to LDL particles [14,15]. It cannot therefore be excluded that LDL, together with HDL, are implicated in the SR-BI-mediated efflux pathway as a function not only of cellular cholesterol status, but also of their relative concentrations in a local physiological (peripheral cells) or pathophysiological (macrophages and foam cells) context.

It is especially relevant that both LDL and HDL particles are heterogeneous in their structure, intracellular metabolism and biological functions. In particular, some studies have reported that distinct HDL particle subpopulations vary in their capacity to promote SR-BI-mediated cholesterol efflux, and notably that HDL particle composition, apoA-I conformation, apoA-I / apoA-II ratio may influence free cholesterol efflux via this mechanism [16,17]. Like HDL, plasma LDL is composed of several discrete subspecies which can be distinguished on the basis of their structural, metabolic and functional characteristics [18,19]. Among them, small dense LDL (sdLDL), which display enhanced penetration of the arterial wall, high affinity binding to glycosaminoglycans of the intimal extracellular matrix and elevated susceptibility to oxidative stress [20] are considered to possess elevated atherogenicity. In addition, sdLDL exhibit lower binding affinity *in vitro* to the LDL receptor (LDL-R) than LDL subspecies of larger size and lower hydrated density [21], thereby suggesting that interactions with membrane receptors, such as SR-BI, may differ among LDL particle subspecies. We therefore evaluated the relative capacities of distinct subspecies of LDL particles to facilitate cholesterol efflux using an experimental system of CHO cells stably expressing human SR-BI/Cla-1. Our findings suggest that sdLDL particles are not only poor acceptors of cellular cholesterol transported by Cla-1, but equally that they can inhibit cholesterol efflux to other LDL subclasses. By contrast, sdLDL did not interfere with Cla-1-mediated efflux to HDL, thereby providing additional support for the proposal that distinct binding sites on SR-BI are implicated in interaction of the extracellular domain of this receptor with LDL and HDL particles [22,23].

## 2. Materials and methods

### 2.1. Reagents

The Acyl-CoA:cholesterol acyltransferase (ACAT) inhibitor, CP113,818 was a generous gift from Pfizer. Polyclonal antibodies directed against native

human SR-BI/Cla-1 were generated by genetic immunization of rabbits (Mirus Corporation, Madison USA) with a pcDNA-hSR-BI expression vector encoding full-length hSR-BI cDNA [24].

### 2.2. Cells

CHO-K1 (ATCC#CCL-61) cells were obtained from LGC Promochem (Molsheim, France) and cultivated under standard conditions in F12 (HAM) medium (Invitrogen) containing glutamine and supplemented with 10% foetal calf serum (FCS). Human SR-BI/Cla-1 transfected CHO cells were maintained in the same medium containing 0.8 mg/ml geneticin.

### 2.3. Blood samples

After an overnight fast, blood from healthy normolipidemic individuals was drawn on EDTA (final concentration 0.1%), centrifuged and plasma was collected and stored at  $-80^{\circ}\text{C}$ .

### 2.4. Isolation of plasma lipoprotein subfractions

Plasma lipoproteins used in cholesterol efflux assays were fractionated either by isopycnic density gradient ultracentrifugation or gel filtration. Ultracentrifugation — Five distinct LDL subfractions (large buoyant LDL: LDL-1:  $d$  1.019–1.023 g/ml and LDL-2:  $d$  1.023–1.029 g/ml; LDL of intermediate density: LDL-3:  $d$  1.029–1.039 g/ml and small dense LDL: LDL-4:  $d$  1.039–1.050 g/ml and LDL-5:  $d$  1.050–1.063 g/ml), and two HDL subfractions (HDL2:  $d$  1.063–1.125 g/ml, and HDL3:  $d$  1.125–1.21 g/ml) were isolated as previously described [25]. On completion of centrifugation, all lipoprotein subfractions were collected in aliquots of 0.8 ml, with the exception of the LDL-5 subfraction (0.6 ml) in order to avoid any contribution of HDL to LDL preparations. Gel filtration—Total lipoproteins ( $d < 1.21$  g/ml) were first isolated from plasma by flotation ultracentrifugation (100,000 $\times$ g, 5 h in TL100-Beckman), and then size-fractionated by gel filtration on two Superose-6 columns (Amersham Biosciences) connected in series using a BioLogic DuoFlow Chromatography system (BioRad). Based on the absorbance profile, the LDL peak was arbitrarily subdivided into five LDL fractions (LDL-1F,-2F,-3F,-4F and-5F) as shown in Fig. 4.

The isolated LDL and HDL fractions were dialyzed at  $4^{\circ}\text{C}$  in Spectrapor membrane tubing (Spectrum Medical Industries) against 0.01 mol/L PBS containing 0.3 mmol/L EDTA (pH 7.4) and subsequently filtered through a 0.22- $\mu\text{m}$  filter (Costar) and stored at  $4^{\circ}\text{C}$ . The protein and lipid contents of isolated lipoprotein fractions were quantified using Boehringer Mannheim kits (Meylan, France), for total cholesterol (TC) and free cholesterol. Bio-Mérieux kits (Marcy-l'Etoile, France) were used for determination of triglycerides and phospholipids and the bicinchoninic acid assay reagent (Pierce, Rockford, IL) was used for protein quantification.

### 2.5. Free cholesterol efflux studies

Stably transfected CHO-Cla-1 clones and parental CHO-K1 cells were seeded in 96-well plates (4 000 cells/well) and incubated for 24 h in complete F12 medium containing 10% (V/V) FCS and 2  $\mu\text{g/ml}$  of ACAT inhibitor (CP113,818). The medium was then replaced with medium containing 3  $\mu\text{Ci/ml}$  of [ $^3\text{H}$ ] cholesterol, 20% (V/V) FCS and 2  $\mu\text{g/ml}$  of ACAT inhibitor. After 24 h of incubation, cells were washed with 1% BSA/F12 and then with serum-free F12 medium. Cellular cholesterol efflux was stimulated by adding 100  $\mu\text{l}$  of serum-free medium containing different concentrations of lipoproteins (concentration range: 5 to 50  $\mu\text{g}$  protein/ml). After 2 h, medium was collected and filtered through Multiscreen 0.45  $\mu\text{m}$  filtration plates (Millipore). The cells were washed with 0.1% BSA/PBS and then with PBS. Cell lipids were subsequently extracted with 100  $\mu\text{l}$  isopropyl alcohol. For each well, [ $^3\text{H}$ ] cholesterol released in the medium and present in the total cell lipid extract was measured by liquid scintillation counting. The percentage of cholesterol efflux was calculated as the amount of [ $^3\text{H}$ ]cholesterol recovered in the medium divided by the total label (cells+medium) in the wells multiplied by 100. Cla-1-mediated cholesterol efflux was calculated by subtraction of CHO-K1 efflux from CHO-Cla-1 efflux.



For cholesterol efflux studies performed in the presence of rabbit antiserum directed to human SR-BI (or the corresponding pre-immune serum), the assay was carried out as described above but the cells were pre-incubated with a 1/50 dilution of whole rabbit antiserum for 30 min prior to the efflux period.

## 2.6. Immunoblot

Western blot analysis was performed as previously described [26]. Cellular extracts (20  $\mu$ g of protein) of CHO cells were separated by SDS-PAGE. SR-BI was detected using a rabbit polyclonal antibody raised against mouse C-terminus domain of the protein [26]. For normalization of Western blots,  $\beta$ -Actin protein was detected with a mouse monoclonal antibody (clone AC15-Sigma). Primary antibodies were detected using a peroxidase-conjugated anti-rabbit and anti-mouse IgG.

## 2.7. Flow cytometry

Stably transfected CHO-Cla-1 cells and control CHO-K1 cells were incubated with the anti-Cla-1 primary antibody (1:50 dilution) followed by detection with a fluorescein-labelled anti-rabbit IgG antibody (1:200 dilution) (Vector Laboratories). FITC fluorescence was measured in cell suspension using 488 nm for excitation with emission detected between 520 and 530 nm (Epics XL-Beckman Coulter).

## 2.8. RNA preparation and real time quantitative PCRs

DNA-free total RNA was prepared from cells using NucleoSpin RNA II (Macherey-Nagel) according to the manufacturer's instructions. RT-PCR were performed as previously described [26]. Briefly, 25 ng of reverse transcribed total RNA were used for real time quantitative PCR reactions performed using a LightCycler PCR system (Roche) with the following specific primer pairs: hamster SR-BI (haSR-BI) forward (5'-GTTTACCCACCCAATGAAGG-3') and reverse (5'-GGATGGATGTCAAGGAACAAA-3'), and Cla-1 forward (5'-GAGCTTTGGCCTTGGTCTACCT-3') and reverse (5'-TCTTGTGCTCAC-TCCATGTTTTTC-3'). Expression data were based on the crossing points calculated with the LightCycler data analysis software and corrected for PCR efficiencies of the target and reference genes.

## 2.9. Statistical analyses

Parametric values are expressed as mean standard deviation (SD) and non-parametric values as median 25th percentile. Values of  $p > 0.05$  were considered to be non-significant. Univariate analyses were performed by paired *t* test for parametric continuous data, and by Mann–Whitney test for non-parametric.

## 3. Results

### 3.1. Characterization of Cla-1 stably transfected CHO clones.

In order to assay the capacity of Cla-1 to mediate the efflux of cholesterol to distinct lipoprotein subclasses, we used CHO cells stably transfected with Cla-1 cDNA which have been described recently [24]. Stable CHO clone was assayed for the level of Cla-1 mRNA expression by quantitative RT-PCR using primer pairs that discriminate Cla-1 cDNA from endogenous hamster SR-BI (haSR-BI) cDNA. Fig. 1A compares the Cla-1-transfected CHO clone with the parental CHO-K1 cells for the haSR-BI and Cla-1 expression. The CHO-Cla-1 clone expressed high levels of Cla-1 mRNA whereas endogenous haSR-BI mRNA expression did not differ significantly between the Cla-1-expressing cells and the control cell line. Expression of Cla-1 protein was assessed by Western blot on total cell protein extracts (Fig. 1B). Use of a polyclonal antibody directed

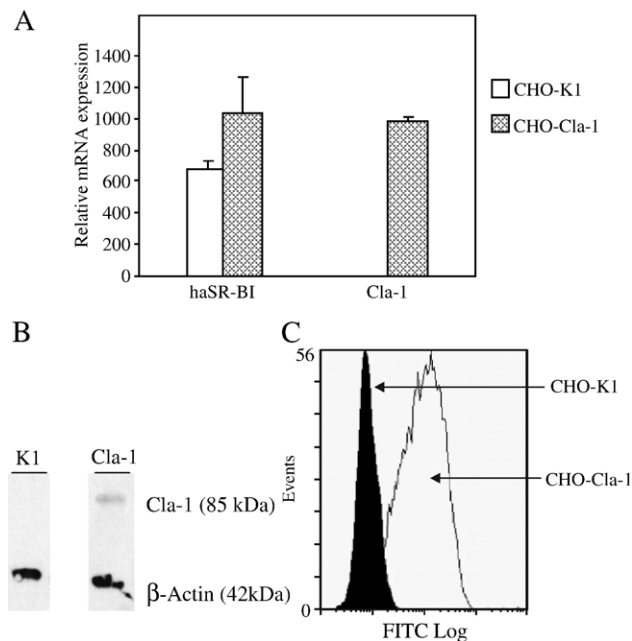


Fig. 1. Characterization of Cla-1 expression in CHO clone stably expressing Cla-1. A—Total RNA from stably transfected Cla-1 CHO clones and from CHO-K1 control cells was extracted and subjected to quantitative RT-PCR using specific primers for Cla-1 and for hamster SR-BI (haSR-BI). Relative expression is shown in arbitrary units and represents the means ( $\pm$ SD) of three independent experiments. B—Total protein extracts prepared from the two cell lines were analysed by Western blotting. Immunoblot was performed with anti-SR-BI and anti- $\beta$ -actin. Data are representative of three independent experiments. C—CHO-K1 and CHO-Cla-1 were incubated with anti-Cla-1 primary antibody, followed by FITC-conjugated secondary antibody. The FITC fluorescence of 10,000 intact gated cells was detected using flow cytometry and is shown as a histogram against fluorescence scale. The histogram shown is representative of three independent determinations.

against the SR-BI C-terminal domain revealed Cla-1 in CHO-Cla-1 clone while haSR-BI was only faintly detectable in CHO-K1 parental cells. Surface expression in CHO-Cla-1 cells was confirmed by flow cytometry analysis. Cla-1 expressing cell line incubated with an antibody directed against Cla-1 extracellular domain showed significant increase in fluorescence intensity as compared to control CHO cells (Fig. 1C).

As reported previously [3,9,27], overexpression of SR-BI in transfected cells is associated with concomitant increase in cholesterol efflux. In our experiments, the CHO-Cla-1 clone mediated 113% greater efflux to total plasma as compared to control cells ( $p < 0.01$ ) (Fig. 2A). Calculation of the difference in cholesterol efflux between CHO-Cla-1 and control cells (e.g. CHO-Cla-1-mediated efflux-CHO-K1-mediated efflux) corresponds to Cla-1-specific efflux. We confirmed the specificity of such efflux using a blocking antibody to Cla-1. As shown in Fig. 2B, incubation of Cla-1 expressing clone CHO-Cla-1 and CHO-K1 with anti-Cla-1 antibody, resulted in almost complete abrogation of Cla-1 specific efflux whether LDL or HDL particles were used as cholesterol acceptors. As a control, we used the corresponding pre-immune serum, which did not reduce total cholesterol efflux, and even led to a 54% increase in Cla-1-specific efflux in comparison with efflux obtained with HDL only. The presence of potential acceptors in pre-immune

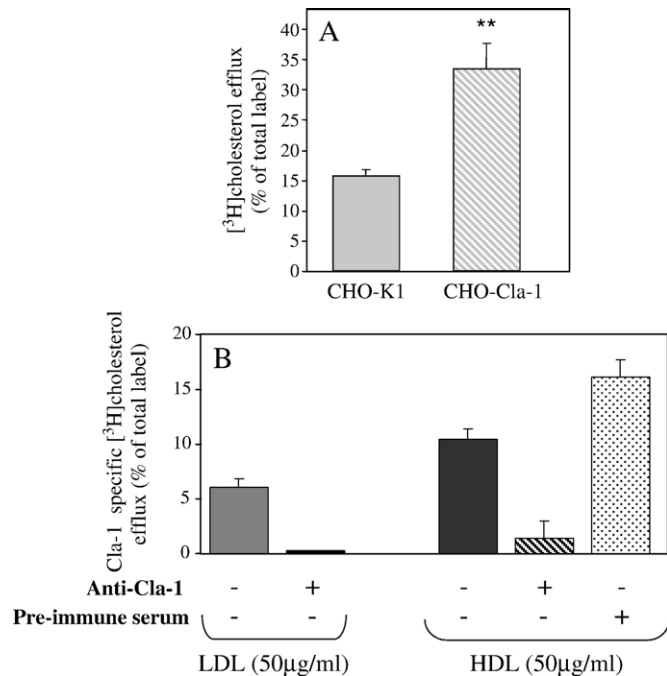


Fig. 2. Characterization of Cla-1-specific cholesterol efflux in Cla-1 expressing CHO cells. A—Control (CHO-K1) and stably transfected CHO cells (CHO-Cla-1 clone), were labelled with [<sup>3</sup>H]cholesterol and then incubated for 2 h at 37 °C in serum-free medium containing 2% plasma. Cholesterol efflux is expressed as the percentage of total [<sup>3</sup>H]cholesterol radioactivity released into the medium. Data represent the mean (±SD) of three independent experiments, and statistical differences from values obtained with CHO-K1 cells are indicated (\*\**p*<0.01). B—Inhibition of Cla-1-specific efflux to LDL and HDL particles. CHO-Cla-1 and CHO-K1 cells were labelled with [<sup>3</sup>H]cholesterol, washed and incubated for 30 min at 37 °C with serum-free medium containing a 1/50 dilution of an anti-Cla-1 serum or control pre-immune serum. After an additional 2 h incubation in the same medium in the presence of LDL or HDL (50 μg protein/ml), the amount of [<sup>3</sup>H]cholesterol present in the medium or remaining in the cells was determined. Cla-1 specific values were calculated as the difference between the efflux values determined with CHO-Cla-1 and parental CHO-K1 cells. Values±SD represent the means of quadruplicate determination. Similar results were obtained in separate experiments.

serum in addition to HDL particles could explain this increment. Together, these data indicate that stable transfection of the Cla-1 receptor in the CHO-K1 cells led to Cla-1 expression of the receptor at the cell surface and induced functional specific cholesterol efflux to both LDL and HDL particles.

### 3.2. LDL subfractions differ in their capacity to facilitate cellular cholesterol efflux via Cla-1

Fractionation of LDL based on hydrated density has previously demonstrated that LDL subfractions are heterogeneous, and indeed such subfractions differ in their binding affinity for the cellular LDL-R. Indeed, as compared to large buoyant LDL-1,-2 and-3, small dense LDL-4 and-5 exhibit lower binding affinity for the LDL-receptor [21,28] leading to a prolonged plasma half-life and a greater susceptibility to oxidation [20].

We examined the capacity of LDL subfractions to interact with Cla-1 and to facilitate cholesterol efflux from our Cla-1-expressing CHO clone loaded with [<sup>3</sup>H] cholesterol for 24 h.

Table 1

Comparison of total cholesterol/protein ratios in LDL subfractions isolated by density gradient ultracentrifugation or gel filtration

	Ultracentrifugation		Gel filtration
LDL-1	1.04±0.23	LDL-1F	1.15±0.37
LDL-2	1.39±0.29	LDL-2F	1.42±0.84
LDL-3	1.61±0.10	LDL-3F	1.23±0.48
LDL-4	1.19±0.12	LDL-4F	0.81±0.20
LDL-5	0.79±0.02	LDL-5F	0.68±0.14

Values are the means (±SD) of total cholesterol/protein ratios obtained by triplicates analyses of each fraction isolated from the plasma of three normolipidemic subjects.

We first assayed the efflux activity of discrete LDL subfractions obtained from seven normolipidemic patients, separated by density gradient ultracentrifugation. The lipid composition (proportion of free cholesterol (%)) were 35±9.1, 32.3±5.2, 31.6±.7, 28.6±9.9, and 27.3±7.7, respectively in LDL-1, LDL-2, LDL-3, LDL-4 and LDL-5) and the TC/protein ratios of these subfractions (Table 1) were similar to those reported earlier [29]. As the protein content of the different LDL subfractions varied from only 20 to 26%, we did not take into account this variation in efflux studies. As shown in Fig. 3A, the five LDL subspecies (50 μg protein/ml) exhibited similar

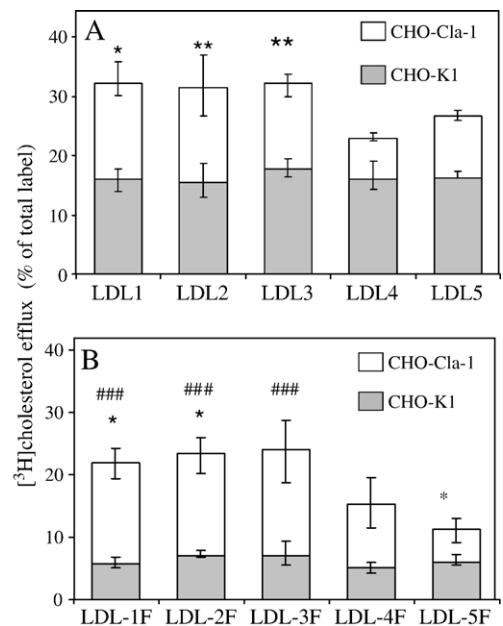


Fig. 3. Cla-1-mediated cholesterol efflux to LDL subfractions isolated by ultracentrifugation or gel filtration. CHO-K1 and stably transfected were labelled with [<sup>3</sup>H]cholesterol, washed and incubated for 2 h at 37 °C with serum-free medium containing 50 μg protein/ml of each LDL subfraction separated by gradient density ultracentrifugation (LDL-1 to LDL-5) (A) or size exclusion chromatography (LDL-1F to LDL-5F) (B). Cholesterol efflux in CHO-K1 cells (filled bars) and CHO-Cla-1 cells (full bars) is expressed as the percentage of total [<sup>3</sup>H]cholesterol radioactivity released into the medium. Cla-1 specific cholesterol efflux (open bars) correspond to the difference between the efflux values determined with CHO-Cla-1 and parental CHO-K1 cells. Values represent the median (±quartile) of three independent experiments performed with fractions isolated from the plasmas of seven (A) or three (B) normolipidemic subjects. Statistical significant differences from LDL-4 and LDL-4F (\**p*<0.05; \*\**p*<0.01) and from LDL-5F (###*p*<0.001) are indicated.

potential to accept cholesterol from control CHO-K1 cells. In contrast, incubation of each LDL subspecies at similar protein concentrations with CHO-Cla-1 cells, revealed that dense LDL (LDL-4 and-5) induced less Cla-1-specific [ $^3\text{H}$ ]cholesterol efflux (7% and 10.4% respectively) than LDL-1, LDL-2 and LDL-3; the latter subfractions promoting similar levels of cholesterol efflux via Cla-1 (16.3%, 15.9% and 14.5% efflux, respectively) (Fig. 3A). When LDL subfractions were compared as cholesterol acceptors on the basis of the ApoB concentration, the differences observed between large and dense LDL were conserved (data not shown). These data suggest that dense LDL subfractions are not avid acceptors for cellular cholesterol efflux mediated via Cla-1 as compared with large and intermediate density LDL.

In order to avoid any potential influence of the separation technique on the ability of LDL subfractions to act as cholesterol acceptors via Cla-1, we evaluated the efflux capacities of LDL subspecies fractionated on the basis of their size. Lipoproteins were first isolated from plasma proteins by ultracentrifugation ( $d < 1.21$  g/ml), and then separated by gel filtration chromatography. The elution peak corresponding to LDL particles was fractionated into five subpopulations (i.e. from larger to smaller particles: LDL-1F,-2F,-3F,-4F and-5F) (Fig. 4). Comparison of total cholesterol to protein ratios for each LDL fractions isolated from normolipidemic subjects either by gradient density or gel filtration revealed similar values for the first, second or fifth fractions. However, the TC/protein ratios were slightly different when comparing LDL-3 and-4 to LDL-3F and-4F respectively (Table 1). As previously observed for LDL fractions isolated on density gradients, percent efflux of [ $^3\text{H}$ ] cholesterol from control CHO-K1 cells to the five LDL subspecies (50  $\mu\text{g}$  protein/ml) were similar (Fig. 3B). Incubation of these LDL-F subspecies to CHO-Cla-1 cells resulted in higher levels of cholesterol efflux as compared to CHO-K1 cells. However, while the largest LDL subspecies (1F, 2F and 3F) did not differ in their capacity to promote cholesterol efflux via Cla-1 (16.2%, 16.4% and 17% respectively), values of Cla-1-specific efflux were lower with LDL-4F and-5F as compared to those obtained with LDL-1F and-2F ( $p < 0.05$

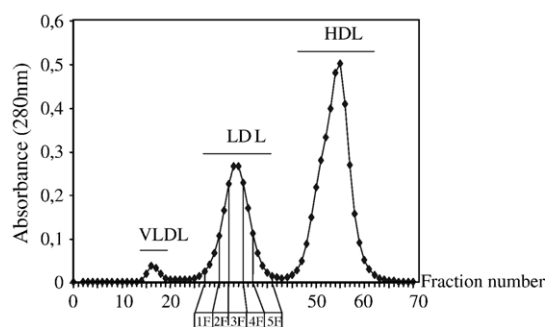


Fig. 4. Separation of LDL subfractions by gel filtration. Plasmas from normolipidemic subjects were fractionated by size-exclusion chromatography as described in Materials and methods. Fractions 12 to 20 correspond to VLDL, fractions 27 to 41 to LDL and fractions 45 to 62 to HDL. The LDL peak was sub-divided into 5 fractions: LDL-1F (fractions 27 to 30), 2F (30 to 32), 3F (32 to 35), 4F (35 to 37) and 5F (37 to 41). The chromatogram shown is representative of three independent experiments.

$p < 0.001$ , respectively) (Fig. 3B). These findings suggest that the levels of cholesterol efflux obtained for both large and small LDL subfractions were independent of the methodology used for LDL particle isolation: thus, the differential ability of LDL subspecies to promote Cla-1-mediated cellular cholesterol efflux is not dependent on the isolation method. Our results indicate that sdLDL, i.e. LDL-4 and LDL-5, are less potent acceptors for Cla-1-mediated cellular cholesterol efflux as compared to more buoyant, large LDL-1,-2 and-3.

### 3.3. LDL-4 and LDL-5 subfractions attenuate Cla-1-specific cholesterol efflux activities to larger LDL-1,-2 and-3

In order to further understand the relationship between cholesterol efflux mediated by Cla-1 and the properties of LDL subspecies as cholesterol acceptors, we evaluated Cla-1-mediated efflux activity in the presence of increasing concentrations of LDL subspecies. Cells were incubated with 25  $\mu\text{g}/\text{ml}$  of large buoyant LDL (LDL-1+2), and a dose-response study was performed by adding 25  $\mu\text{g}/\text{ml}$  of LDL-1+2, LDL-3 or sdLDL (LDL-4+5) to obtain a maximal final protein concentration of 50  $\mu\text{g}/\text{ml}$ . Indeed, as large buoyant LDL-1 and LDL-2 on the one hand and sdLDL particles, LDL-4 and LDL-5, on the other behaved similarly as cellular cholesterol acceptors, we combined subfractions LDL-1 and 2, and LDL-4 and 5. The results shown in Fig. 5A indicate that addition of LDL-1+2 or LDL-3 induced a 1.5- to 2-fold increase in Cla-1-specific efflux of labelled cholesterol, while addition of sdLDL failed to significantly enhance cholesterol efflux. When the same experiment was performed with 25  $\mu\text{g}/\text{ml}$  LDL-3, we observed that addition of LDL-1+2 or LDL-3 led to a 1.4 and 1.7-fold stimulation of cholesterol efflux, respectively (Fig. 5B). In contrast, a 1.3-fold reduction was observed when sdLDL were added to LDL-3 at a concentration of 25  $\mu\text{g}/\text{ml}$ . Thus, for both LDL-1+2 and LDL-3, addition of similar quantities of sdLDL markedly reduced the efflux capacities of lighter, larger LDL particle subfractions. As previous experiments were performed with equal amounts of LDL subfractions on a protein basis, we evaluated dose-responses by addition of increasing amounts of LDL-3 or sdLDL (5, 10, 15 and 50  $\mu\text{g}/\text{ml}$ ) to 15  $\mu\text{g}/\text{ml}$  of LDL-3. Addition of increasing amounts of LDL-3 resulted in a progressive increase in Cla-1-mediated cholesterol efflux (Fig. 6). Addition of small quantities (5  $\mu\text{g}/\text{ml}$ ) of sdLDL to 15  $\mu\text{g}/\text{ml}$  of LDL-3 slightly stimulated efflux, but larger amounts (10, 15 and 50  $\mu\text{g}$  of protein/ml) progressively decreased Cla-1-specific efflux to levels below that measured with 15  $\mu\text{g}/\text{ml}$  of LDL-3 alone. Together, these results suggest that dense LDL particles behave as poor cholesterol acceptors for Cla-1-mediated efflux and that they can attenuate the capacity of Cla-1 to promote cholesterol efflux to larger LDL subspecies (i.e. LDL-1,-2 and-3).

### 3.4. LDL-4 and LDL-5 subfractions do not influence Cla-1 specific efflux activity to HDL-2

We equally evaluated whether sdLDL could interfere with the capacity of Cla-1 to facilitate cholesterol efflux to HDL particles.

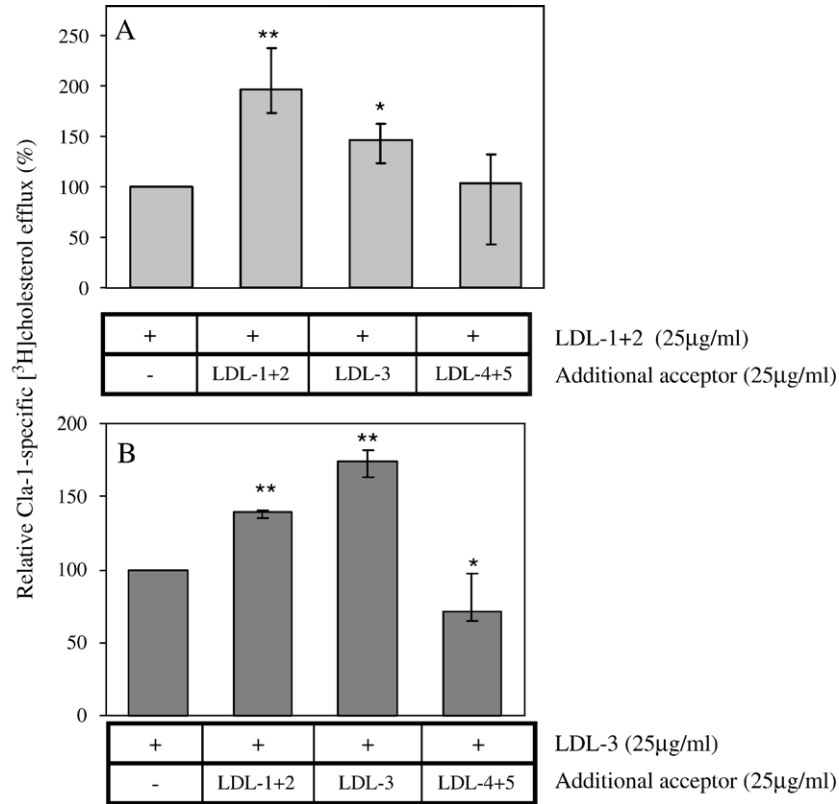


Fig. 5. Differential effects of LDL subspecies on Cla-1-specific cholesterol efflux. CHO-K1 and CHO-Cla-1 cells were labelled with [<sup>3</sup>H]cholesterol, washed and incubated for 2 h at 37 °C with serum-free medium containing 25 µg protein/ml of LDL-1 + 2 subfractions (A) or LDL-3 subfractions (B) in the absence or the presence of 25 µg protein/ml of additional acceptors: LDL-1 + 2, LDL-3 or LDL-4 + 5. Cla-1-specific cholesterol efflux values are expressed relative to that obtained with 25 µg/ml LDL-1 + 2 alone (A) or LDL-3 alone (B) set arbitrarily to 100%. Statistical differences from 25 µg/ml LDL-1/2 or LDL-3 alone are indicated (\**p* < 0.05; \*\**p* < 0.01). Data represent the median (±quartile) of three independent experiments performed in triplicate with fractions isolated by gradient density ultracentrifugation from plasmas of five normolipidemic subjects.

When the levels of cellular cholesterol efflux in presence of HDL-2 and HDL-3 were compared at similar protein concentration, HDL-2 were the more efficient acceptors of FC via Cla-1 (data not shown), in agreement with previous reports [30]. Thus, we performed the subsequent experiments with the most potent acceptor, HDL-2. Efflux assays were conducted with CHO-K1

and CHO-Cla-1 cells in the presence of 25 µg/ml of HDL2 alone, or in the presence of HDL-2 supplemented with 25 µg/ml of HDL2, LDL-1+2,-3 or sdLDL (Fig. 7). As compared with the incubation with 25 µg/ml of HDL-2, an approximate 1.6-fold increase in Cla-1-mediated cholesterol efflux was observed by doubling HDL-2 concentration at a final concentration of 50 µg/

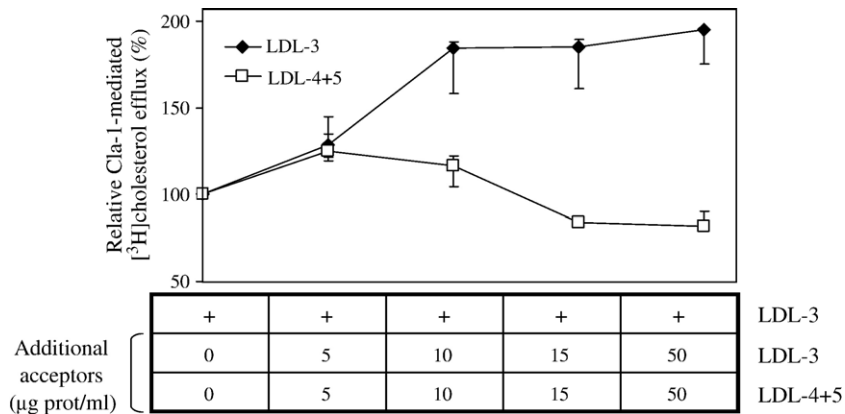


Fig. 6. Concentration dependent effect of LDL-3 or sdLDL on Cla-1-mediated efflux to LDL-3. The efflux assay was carried out with CHO-K1 and CHO-Cla-1 cells incubated with serum-free medium containing 15 µg protein/ml of LDL-3 in the absence or the presence of increasing doses (5, 10, 15, 50 µg protein/ml) of additional acceptors: LDL-3 (◆) or LDL-4 + 5 (□). Cla-1-specific cholesterol efflux values are expressed relative to that obtained with 15 µg/ml LDL-3 alone set arbitrarily to 100%. Data represent the median (±quartile) of three independent experiments performed with fractions isolated by gradient density ultracentrifugation from the plasmas of two normolipidemic subjects.

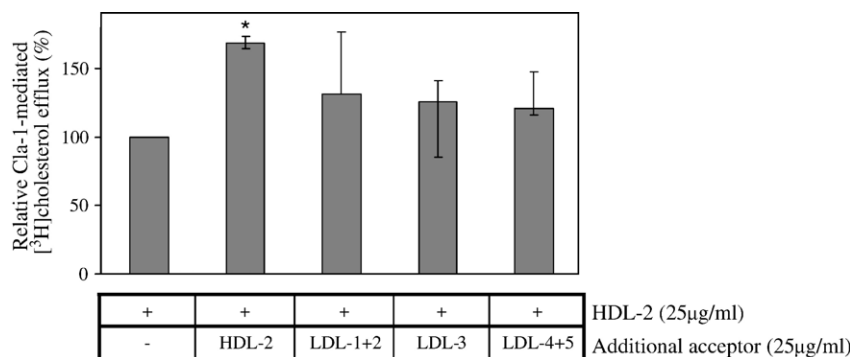


Fig. 7. Effect of additional acceptors on Cla-1 specific cholesterol efflux activities to HDL-2. CHO-K1 and stably transfected CHO-Cla-1 cells were labelled with [ $^3$ H]cholesterol, washed and incubated for 2 h at 37 °C with serum-free medium containing 25 µg protein/ml of HDL-2 in the absence or the presence of 25 µg protein/ml of additional acceptors: HDL-2, LDL-1+2, LDL-3 or LDL-4+5. Cla-1-specific cholesterol efflux values are expressed relative to that obtained with 25 µg/ml HDL-2 alone, set arbitrarily to 100%. Statistical differences from 25 µg/ml HDL-2 alone are indicated (\* $p$ <0.05). Data represent the median±quartile of three independent experiments performed with fractions isolated by gradient density ultracentrifugation from the plasmas of five normolipidemic subjects.

ml. A moderate increase of Cla-1-specific efflux and of similar magnitude was also noted when HDL-2 were mixed with either one of the LDL subspecies as compared to efflux values measured with HDL-2 alone (1.3, 1.2 and 1.2-fold increase for HDL-2/LDL-1+2, HDL-2/LDL-3 and HDL-2/sdLDL respectively). Therefore, in these experimental conditions, addition of LDL subspecies, including sdLDL, to HDL moderately enhanced cellular cholesterol efflux activities via Cla-1.

#### 4. Discussion

With the use of a defined cell system stably overexpressing the human SR-BI/Cla-1 receptor, we demonstrate for the first time that physicochemically-distinct LDL particle subspecies from normolipidemic patients differ significantly in their capacity to facilitate efflux of cellular free cholesterol through this pathway. Indeed, independently of the fractionation procedure, sdLDL exhibited a significantly lower capacity as compared to large buoyant LDL particles (at the same protein concentration) to efflux cholesterol via the SR-BI/Cla-1 pathway. By contrast, both of these LDL particle subspecies exhibited similar efflux activities in the parental CHO-K1 cell line. The poor capacity of sdLDL to mediate cholesterol efflux is therefore Cla-1-specific. Indeed, the specific contribution of the Cla-1 pathway to cellular cholesterol efflux in our cellular system was confirmed with a blocking antibody. Furthermore, sdLDL particles inhibited Cla-1-specific cholesterol efflux to large buoyant LDL in a dose-dependent manner; moreover, no effect of sdLDL particles was observed on cholesterol efflux to HDL-2, thereby suggesting that LDL and HDL interact with distinct sites on Cla-1. These findings suggest that LDL subspecies, and notably large buoyant LDL, may constitute physiologically relevant cholesterol efflux acceptors via the Cla-1 pathway. Ultimately, the ratio of the circulating concentrations of large to small dense LDL may determine the efficacy of LDL as cholesterol acceptors via SR-BI/Cla-1.

Several studies support the hypothesis that SR-BI/Cla-1-mediated bidirectional movements of cellular cholesterol are dependent on the structural characteristics, size and/or lipid content of HDL acceptor particles. Indeed, at equivalent particle

concentration, large cholesterol-rich HDL deliver more CE to cells via SR-BI-mediated selective lipid uptake and promote higher rates of FC efflux than small HDL particles [16,17]. Similarly, in the present study, sdLDL failed to promote efficient Cla-1-mediated efflux as compared to larger LDL, suggesting that particle size exerts an influence on the interaction of LDL with SR-BI/Cla-1. The enhanced FC efflux obtained with large rHDL could be due to the greater phospholipid content of these particles [17,30]. Indeed, lower PL/FC ratio in HDL could be associated with decreased efflux [31]. However, these observations do not fit with LDL data since we observed that, in agreement to previous studies [32], PL/FC ratio slightly increases in dense LDL5 compared to the larger and lighter subspecies. Furthermore, the differences in FC efflux were not eliminated by PL normalization of LDL subfractions in our cholesterol efflux assay (data not shown). These differences could also be the consequence of enzymatic differences between particles such as the LCAT activity. Controversial data have been published regarding the implication of LCAT in the mass transfer of cholesterol from cells to HDL. We did not observe statistically significant differences in LCAT activity between LDL subspecies (data not shown) suggesting that LCAT is not responsible for the observed differences in LDL subfractions capacities to accept cholesterol via Cla-1. Relatively high binding of the large rHDL particles to SR-BI could equally contribute to differences in FC efflux between HDL acceptors [17,30]. Indeed, differences in apoA-I conformation in synthetic reconstituted HDL particles of different size may influence particle interaction with SR-BI [33,34]. In this context, it is relevant that apoB conformation in sdLDL has been shown to differ from that of large LDL and to account for the reduced binding affinity of these particles to the LDL-receptor [21,28]. Thus, variability in apoB conformation among LDL particles could be responsible for their distinct capacities to interact and consequently to accept cellular cholesterol via Cla-1.

Recent reports have suggested that binding of lipoproteins to SR-BI is not sufficient to enhance cholesterol efflux and that efficient SR-BI-mediated cholesterol efflux to lipoproteins may require the formation of a “productive complex” [34,35]. Thus

we can hypothesize that sdLDL may bind to SR-BI/Cla-1, but may not form such a productive particle–receptor complex as that efficiently formed with larger LDL subspecies. Furthermore, it has been reported that the binding affinity of lipoproteins to SR-BI can affect the capacity of this receptor to facilitate cholesterol efflux. Indeed, BLTs, synthetic chemicals that block lipid transport across cell membranes, have been shown to enhance the binding affinity of HDL to SR-BI but equally to inhibit efflux of cellular cholesterol to HDL [36]. Similar observations were made upon apoA-II enrichment of HDL, which led to enhanced particle affinity for SR-BI, but inhibited specific cholesterol uptake [37]. One possible explanation may arise from the fact that BLTs or conformational modifications of HDL due to apoA-II enrichment may inhibit dissociation of HDL from SR-BI and consequently diminish potential interaction with a new HDL particle. Thus bound HDL particles would competitively inhibit the binding of others. In our experiments, the presence of sdLDL significantly reduced Cla-1-specific efflux to large buoyant LDL (Figs. 5 and 6). Small dense LDL might exhibit an elevated binding affinity for SR-BI/Cla-1, such that the availability of SR-BI to interact with other lipoprotein particles could be impaired. Such an interaction would reduce total cellular cholesterol efflux via Cla-1 to large LDL. Conversely, addition of sdLDL to HDL-2 did not modify the ability of HDL particles to accept cholesterol by Cla-1-mediated efflux (Fig. 7), indicating that SR-BI/Cla-1 may interact by mechanisms specific to individual lipoprotein subspecies. Distinct binding domains on SR-BI may therefore be potentially involved in the binding of specific lipoproteins [22,38,39]. Indeed, mutagenesis studies identified an SR-BI mutant that binds LDL but not HDL, with concomitant deficiency in SR-BI activity [22]. Thus, under our experimental conditions, addition of either large or small dense LDL to HDL led to a net increment in total SR-BI-mediated efflux to HDL in comparison with HDL alone.

In vivo studies of cholesterol efflux from cells to lipoproteins, the first step in the RCT pathway, are at early stage [5]. Under pathological conditions, the contribution of SR-BI in macrophages of the atherosclerotic lesion to this pathway is also poorly understood and still controversial [8,12,13]. Van Eck et al. [8] suggested that SR-BI in bone marrow-derived macrophages could favour either efflux of cholesterol, or selective lipid uptake as a function of the stage of atherosclerotic lesion development in mouse. In early stage lesions, macrophage SR-BI could induce accumulation of cholesterol by promoting selective cholesterol uptake, and thereby enhance development of fatty streak lesions by virtue of a pro-atherogenic role. Conversely, at later stages of plaque formation, when arterial macrophages are cholesterol loaded, SR-BI could favour net atheroprotective efflux of cholesterol to lipoproteins. The net flux of cholesterol between cells and lipoproteins would thus be dependent on cellular cholesterol status and on the presence of appropriate lipoprotein acceptors. Several studies support the contention that the net flux of cholesterol between cells and lipoproteins depends on the cholesterol concentration gradient [4,9,30]. Furthermore, *in vitro* data suggest that LDL particles could act as potent

acceptors of cellular cholesterol via the ABCG1 transporter as recently described [40] or via SR-BI/Cla-1-mediated efflux. Thus, Zimetti et al. [41] recently demonstrated that whereas cholesterol-normal macrophages undergo a net influx of cholesterol when incubated with LDL, FC loading of macrophages favours efflux of cholesterol to LDL. According to the relative amounts of HDL and LDL in the extracellular environment or the distribution of LDL subclasses, which vary among individuals, net cholesterol flux would be influenced. We observed that large LDL and HDL-2 exhibited similar Cla-1-mediated efflux activities at equal protein concentration (data not shown). Thus according to cellular cholesterol status and cellular environment, large buoyant LDL may constitute physiologically relevant cholesterol efflux acceptors. Our data also suggest that the atherogenicity attributed to sdLDL, which includes enhanced penetration of the arterial wall, high affinity binding to glycosaminoglycans of the intimal extracellular matrix and elevated susceptibility to oxidative stress, may also include a decreased capacity to contribute to overall cellular free cholesterol efflux and thus to cholesterol homeostasis.

Elevated levels of sdLDL are markers of atherogenic dyslipidemia, insulin resistance and type 2 diabetes [42–44]. Subjects with a predominance of sdLDL may therefore exhibit a reduced potential to remove excess cellular FC from cells via LDL. Whether this mechanism could partly account for the increased risk of coronary artery disease observed in these patients with an sdLDL phenotype is highly speculative and remains to be determined. Indeed, our experiments were specifically focused on the efflux of cholesterol from cells to lipoproteins and did not take into account the potential influx of cholesterol via Cla-1-mediated selective lipid uptake. Thus, further investigations to evaluate SR-BI-mediated net flux of cholesterol in the presence of LDL subspecies are necessary in order to more fully understand the impact of sdLDL on Cla-1-mediated cellular movement of cholesterol, and in particular in macrophages and foam cells.

## Acknowledgments

This study was supported by National Institute for Health and Medical Research (INSERM) and by a research grant from Bayer Healthcare (Wuppertal, Germany). M.T. was the recipient of a Doctoral Fellowship from the French Ministry of Research and Technology.

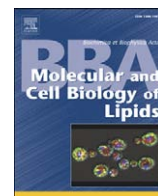
## References

- [1] S. Acton, D. Osgood, M. Donoghue, D. Corella, M. Pocioli, A. Cenarro, P. Mozas, J. Keilty, S. Squazzo, E.A. Woolf, J.M. Ordovas, Association of polymorphisms at the SR-BI gene locus with plasma lipid levels and body mass index in a white population, *Arterioscler. Thromb. Vasc. Biol.* 19 (1999) 1734–1743.
- [2] D. Osgood, D. Corella, S. Demissie, L.A. Cupples, P.W. Wilson, J.B. Meigs, E.J. Schaefer, O. Coltell, J.M. Ordovas, Genetic variation at the scavenger receptor class B type I gene locus determines plasma lipoprotein concentrations and particle size and interacts with type 2 diabetes: the Framingham study, *J. Clin. Endocrinol. Metab.* 88 (2003) 2869–2879.

- [3] B. Jian, M. de la Llera-Moya, Y. Ji, N. Wang, M.C. Phillips, J.B. Swaney, A.R. Tall, G.H. Rothblat, Scavenger receptor class B type I as a mediator of cellular cholesterol efflux to lipoproteins and phospholipid acceptors, *J. Biol. Chem.* 273 (1998) 5599–5606.
- [4] M. de la Llera-Moya, G.H. Rothblat, M.A. Connelly, G. Kellner-Weibel, S.W. Sakr, M.C. Phillips, D.L. Williams, Scavenger receptor BI (SR-BI) mediates free cholesterol flux independently of HDL tethering to the cell surface, *J. Lipid Res.* 40 (1999) 575–580.
- [5] Y. Zhang, J.R. Da Silva, M. Reilly, J.T. Billheimer, G.H. Rothblat, D.J. Rader, Hepatic expression of scavenger receptor class B type I (SR-BI) is a positive regulator of macrophage reverse cholesterol transport in vivo, *J. Clin. Invest.* 115 (2005) 2870–2874.
- [6] R.M. Lawn, D.P. Wade, M.R. Garvin, X. Wang, K. Schwartz, J.G. Porter, J.J. Seilhamer, A.M. Vaughan, J.F. Oram, The Tangier disease gene product ABC1 controls the cellular apolipoprotein-mediated lipid removal pathway, *J. Clin. Invest.* 104 (1999) R25–R31.
- [7] N. Wang, D. Lan, W. Chen, F. Matsuura, A.R. Tall, ATP-binding cassette transporters G1 and G4 mediate cellular cholesterol efflux to high-density lipoproteins, *Proc. Natl. Acad. Sci. U. S. A.* 101 (2004) 9774–9779.
- [8] M. Van Eck, I.S. Bos, R.B. Hildebrand, B.T. Van Rij, T.J. Van Berkel, Dual role for scavenger receptor class B, type I on bone marrow-derived cells in atherosclerotic lesion development, *Am. J. Pathol.* 165 (2004) 785–794.
- [9] Y. Ji, B. Jian, N. Wang, Y. Sun, M.L. Moya, M.C. Phillips, G.H. Rothblat, J.B. Swaney, A.R. Tall, Scavenger receptor BI promotes high density lipoprotein-mediated cellular cholesterol efflux, *J. Biol. Chem.* 272 (1997) 20982–20985.
- [10] G. Chinetti, F.G. Gbaguidi, S. Griglio, Z. Mallat, M. Antonucci, P. Poulain, J. Chapman, J.C. Fruchart, A. Tedgui, J. Najib-Fruchart, B. Staels, CLA-1/SR-BI is expressed in atherosclerotic lesion macrophages and regulated by activators of peroxisome proliferator-activated receptors, *Circulation* 101 (2000) 2411–2417.
- [11] K. Hirano, S. Yamashita, Y. Nakagawa, T. Ohya, F. Matsuura, K. Tsukamoto, Y. Okamoto, A. Matsuyama, K. Matsumoto, J. Miyagawa, Y. Matsuzawa, Expression of human scavenger receptor class B type I in cultured human monocyte-derived macrophages and atherosclerotic lesions, *Circ. Res.* 85 (1999) 108–116.
- [12] M. Brundert, J. Heeren, M. Bahar-Bayansar, A. Ewert, K.J. Moore, F. Rinninger, Selective uptake of HDL cholesteryl esters and cholesterol efflux from mouse peritoneal macrophages independent of SR-BI, *J. Lipid Res.* 47 (2006) 2408–2421.
- [13] W. Zhang, P.G. Yancey, Y.R. Su, V.R. Babaev, Y. Zhang, S. Fazio, M.F. Linton, Inactivation of macrophage scavenger receptor class B type I promotes atherosclerotic lesion development in apolipoprotein E-deficient mice, *Circulation* 108 (2003) 2258–2263.
- [14] X. Gu, K. Kozarsky, M. Krieger, Scavenger receptor class B, type I-mediated [3H]cholesterol efflux to high and low density lipoproteins is dependent on lipoprotein binding to the receptor, *J. Biol. Chem.* 275 (2000) 29993–30001.
- [15] H. Stangl, M. Hyatt, H.H. Hobbs, Transport of lipids from high and low density lipoproteins via scavenger receptor-BI, *J. Biol. Chem.* 274 (1999) 32692–32698.
- [16] B.F. Asztalos, M. de la Llera-Moya, G.E. Dallal, K.V. Horvath, E.J. Schaefer, G.H. Rothblat, Differential effects of HDL subpopulations on cellular ABCA1- and SR-BI-mediated cholesterol efflux, *J. Lipid Res.* 46 (2005) 2246–2253.
- [17] S.T. Thuahnai, S. Lund-Katz, P. Dhanasekaran, M. de la Llera-Moya, M.A. Connelly, D.L. Williams, G.H. Rothblat, M.C. Phillips, Scavenger receptor class B type I-mediated cholesteryl ester-selective uptake and efflux of unesterified cholesterol. Influence of high density lipoprotein size and structure, *J. Biol. Chem.* 279 (2004) 12448–12455.
- [18] M.J. Chapman, P.M. Laplaud, G. Luc, P. Forgez, E. Bruckert, S. Goulinet, D. Lagrange, Further resolution of the low density lipoprotein spectrum in normal human plasma: physicochemical characteristics of discrete subspecies separated by density gradient ultracentrifugation, *J. Lipid Res.* 29 (1988) 442–458.
- [19] R.M. Krauss, D.J. Burke, Identification of multiple subclasses of plasma low density lipoproteins in normal humans, *J. Lipid Res.* 23 (1982) 97–104.
- [20] M.J. Chapman, M. Guerin, E. Bruckert, Atherogenic, dense low-density lipoproteins. Pathophysiology and new therapeutic approaches, *Eur. Heart J.* (1998) A24–A30.
- [21] F. Nigon, P. Lesnik, M. Rouis, M.J. Chapman, Discrete subspecies of human low density lipoproteins are heterogeneous in their interaction with the cellular LDL receptor, *J. Lipid Res.* 32 (1991) 1741–1753.
- [22] X. Gu, R. Lawrence, M. Krieger, Dissociation of the high density lipoprotein and low density lipoprotein binding activities of murine scavenger receptor class B type I (mSR-BI) using retrovirus library-based activity dissection, *J. Biol. Chem.* 275 (2000) 9120–9130.
- [23] S. Parathath, D. Sahoo, Y.F. Darlington, Y. Peng, H.L. Collins, G.H. Rothblat, D.L. Williams, M.A. Connelly, Glycine 420 near the C-terminal transmembrane domain of SR-BI is critical for proper delivery and metabolism of high density lipoprotein cholesteryl ester, *J. Biol. Chem.* 279 (2004) 24976–24985.
- [24] P. Maillard, T. Huby, U. Andreo, M. Moreau, J. Chapman, A. Budkowska, The interaction of natural hepatitis C virus with human scavenger receptor SR-BI/Cla1 is mediated by ApoB-containing lipoproteins, *FASEB J.* 20 (2006) 735–737.
- [25] M. Guerin, E. Bruckert, P.J. Dolphin, G. Turpin, M.J. Chapman, Fenofibrate reduces plasma cholesteryl ester transfer from HDL to VLDL and normalizes the atherogenic, dense LDL profile in combined hyperlipidemia, *Arterioscler. Thromb. Vasc. Biol.* 16 (1996) 763–772.
- [26] M. Treguier, C. Doucet, M. Moreau, C. Dachet, J. Thillet, M.J. Chapman, T. Huby, Transcription factor sterol regulatory element binding protein 2 regulates scavenger receptor Cla-1 gene expression, *Arterioscler. Thromb. Vasc. Biol.* 24 (2004) 2358–2364.
- [27] W. Chen, D.L. Silver, J.D. Smith, A.R. Tall, Scavenger receptor-BI inhibits ATP-binding cassette transporter 1-mediated cholesterol efflux in macrophages, *J. Biol. Chem.* 275 (2000) 30794–30800.
- [28] S. Lund-Katz, P.M. Laplaud, M.C. Phillips, M.J. Chapman, Apolipoprotein B-100 conformation and particle surface charge in human LDL subspecies: implication for LDL receptor interaction, *Biochemistry* 37 (1998) 12867–12874.
- [29] P. Lesnik, A. Vonica, M. Guerin, M. Moreau, M.J. Chapman, Anticoagulant activity of tissue factor pathway inhibitor in human plasma is preferentially associated with dense subspecies of LDL and HDL and with Lp(a), *Arterioscler. Thromb.* 13 (1993) 1066–1075.
- [30] P.G. Yancey, M. de la Llera-Moya, S. Swarnakar, P. Monzo, S.M. Klein, M.A. Connelly, W.J. Johnson, D.L. Williams, G.H. Rothblat, High density lipoprotein phospholipid composition is a major determinant of the bi-directional flux and net movement of cellular free cholesterol mediated by scavenger receptor BI, *J. Biol. Chem.* 275 (2000) 36596–36604.
- [31] A. Davit-Spraul, V. Atger, M.L. Pourci, M. Hadchouel, A. Legr, N. Moatti, Cholesterol efflux from Fu5AH cells to the serum of patients with Alagille syndrome. Importance of the hdl-phospholipids/free cholesterol ratio and of the hdl size distribution, *J. Lipid Res.* 40 (1999) 328–335.
- [32] L. Chancharne, P. Therond, F. Nigon, S. Lepage, M. Couturier, M.J. Chapman, Cholesteryl ester hydroperoxide lability is a key feature of the oxidative susceptibility of small, dense LDL, *Arterioscler. Thromb. Vasc. Biol.* 19 (1999) 810–820.
- [33] M.C. de Beer, D.M. Durbin, L. Cai, A. Jonas, F.C. de Beer, D.R. van der Westhuyzen, Apolipoprotein A-I conformation markedly influences HDL interaction with scavenger receptor BI, *J. Lipid Res.* 42 (2001) 309–313.
- [34] T. Liu, M. Krieger, H.Y. Kan, V.I. Zannis, The effects of mutations in helices 4 and 6 of ApoA-I on scavenger receptor class B type I (SR-BI)-mediated cholesterol efflux suggest that formation of a productive complex between reconstituted high density lipoprotein and SR-BI is required for efficient lipid transport, *J. Biol. Chem.* 277 (2002) 21576–21584.
- [35] A. Chroni, T.J. Nieland, K.E. Kypreos, M. Krieger, V.I. Zannis, SR-BI mediates cholesterol efflux via its interactions with lipid-bound ApoE. Structural mutations in SR-BI diminish cholesterol efflux, *Biochemistry* 44 (2005) 13132–13143.
- [36] T.J. Nieland, M. Penman, L. Dori, M. Krieger, T. Kirchhausen, Discovery of chemical inhibitors of the selective transfer of lipids mediated by the

- HDL receptor SR-BI, *Proc. Natl. Acad. Sci. U. S. A.* 99 (2002) 15422–15427.
- [37] A. Pilon, O. Briand, S. Lestavel, C. Copin, Z. Majd, J.C. Fruchart, G. Castro, V. Clavey, Apolipoprotein AII enrichment of HDL enhances their affinity for class B type I scavenger receptor but inhibits specific cholesteryl ester uptake, *Arterioscler. Thromb. Vasc. Biol.* 20 (2000) 1074–1081.
- [38] S. Acton, A. Rigotti, K.T. Landschulz, S. Xu, H.H. Hobbs, M. Krieger, Identification of scavenger receptor SR-BI as a high density lipoprotein receptor, *Science* 271 (1996) 518–520.
- [39] S.T. Thuahnai, S. Lund-Katz, G.M. Anantharamaiah, D.L. Williams, M.C. Phillips, A quantitative analysis of apolipoprotein binding to SR-BI: multiple binding sites for lipid-free and lipid-associated apolipoproteins, *J. Lipid Res.* 44 (2003) 1132–1142.
- [40] N. Wang, M. Ranalletta, F. Matsuura, F. Peng, A.R. Tall, LXR-induced redistribution of ABCG1 to plasma membrane in macrophages enhances cholesterol mass efflux to HDL, *Arterioscler. Thromb. Vasc. Biol.* 26 (2006) 1310–1316.
- [41] F. Zimetti, G.K. Weibel, M. Duong, G.H. Rothblat, Measurement of cholesterol bidirectional flux between cells and lipoproteins, *J. Lipid Res.* 47 (2006) 605–613.
- [42] R.M. Krauss, Genetic, metabolic, and dietary influences on the atherogenic lipoprotein phenotype, *World Rev. Nutr. Diet.* 80 (1997) 22–43.
- [43] R.M. Krauss, Lipids and lipoproteins in patients with type 2 diabetes, *Diabetes Care* 27 (2004) 1496–1504.
- [44] M.R. Taskinen, Diabetic dyslipidaemia: from basic research to clinical practice, *Diabetologia* 46 (2003) 733–749.





## Differential regulation of the human versus the mouse apolipoprotein AV gene by PPARalpha Implications for the study of pharmaceutical modifiers of hypertriglyceridemia in mice

Xavier Prieur<sup>a,b,c,1</sup>, Philippe Lesnik<sup>a,b,d</sup>, Martine Moreau<sup>a,b</sup>, Joan C. Rodríguez<sup>e</sup>, Chantal Doucet<sup>a,b</sup>, M. John Chapman<sup>a,b,d</sup>, Thierry Huby<sup>a,b,d,\*</sup>

<sup>a</sup> INSERM UMR-S 939, Hôpital de la Pitié, F-75013, Paris, France

<sup>b</sup> UPMC Univ Paris 06, UMR-S 939 Paris, F-75013, France

<sup>c</sup> GlaxoSmithKline, 25 avenue du Québec, 91951 Les Ulis cedex, France

<sup>d</sup> AP-HP, Groupe hospitalier Pitié-Salpêtrière, Service d'Endocrinologie-Métabolisme, Paris, France

<sup>e</sup> Department of Biochemistry and Molecular Biology, School of Pharmacy, University of Barcelona, E-08028 Barcelona, Spain

### ARTICLE INFO

#### Article history:

Received 19 November 2008

Received in revised form 11 March 2009

Accepted 30 March 2009

Available online xxxxx

#### Keywords:

Apolipoprotein A5

PPAR

Gene expression

Triglyceride

### ABSTRACT

Mice have been used widely to define the mechanism of action of fibric acid derivatives. The fibrates are pharmacological agonists of the peroxisome proliferator-activated receptor  $\alpha$  (PPAR $\alpha$ ), whose activation in human subjects promotes potent reduction in plasma levels of triglycerides (TG) with concomitant increase in those of HDL-cholesterol. The impact of PPAR $\alpha$  agonists on gene expression in humans and rodents is however distinct; such distinctions include differential regulation of key genes of lipid metabolism. We evaluated the question as to whether the human and murine genes encoding apolipoprotein apoAV, a regulator of plasma concentrations of TG-rich lipoproteins, might be differentially regulated in response to fibrates. Fenofibrate, a classic PPAR $\alpha$  agonist, repressed expression of mouse *Apoa5* *in vivo* in a mouse model transgenic for the human *APOA5* gene; by contrast, expression of the human ortholog was up-regulated. Our findings are consistent with the presence of a functional PPAR-binding element in the promoter of the human *APOA5* gene; this element is however degenerate and non-functional in the corresponding mouse *Apoa5* sequence, as demonstrated by reporter assays and gel shift analyses. These data further highlights the distinct mechanisms which are implicated in the metabolism of TG-rich lipoproteins in mice as compared to man. They equally emphasize the importance of the choice of a mouse model for investigation of the impact of pharmaceutical modifiers on hypertriglyceridemia.

© 2009 Elsevier B.V. All rights reserved.

### 1. Introduction

Hypertriglyceridemia is an independent and predictive risk factor for atherosclerosis and a key feature of the metabolic syndrome [1–3].

The gene encoding apolipoprotein (apo) *APOA5* is recognized as a potential determinant of plasma levels of triglyceride (TG) and TG-rich lipoproteins in mice [4]. Indeed, overexpression of *APOA5* in genetically-modified mouse models consistently leads to reduction in circulating TG concentrations, whereas apoAV deficiency is associated with hypertriglyceridemia [5,6]. *In vitro* and *in vivo* experiments in

mice support a role for apoAV in the potentiation of lipoprotein lipase (LPL) activity [7–9]. LPL is a central player in determining plasma TG levels, as LPL catalyses the hydrolysis of the hydrophobic core of TG-rich lipoproteins (TRL), including chylomicrons and VLDL. In addition, apoAV has been proposed to enhance VLDL remnant removal by facilitating particle binding to the LDL receptor and interaction of these particles with the LDL receptor-related protein (LRP) and mosaic type-1 receptor (SorLA) [10,11].

Fibrates are lipid-modifying agents which are widely employed in the treatment of hypertriglyceridemia. Thus, pharmacological activation of the nuclear receptor peroxisome proliferator-activated receptor- $\alpha$  (PPAR $\alpha$ , NR1C1) by fibrates lowers plasma TG levels not only by increasing conversion of fatty acids to acyl-CoA derivatives and fatty acid oxidation ( $\beta$ -oxidation), but in addition, by stimulating intravascular LPL-mediated lipolysis of TRL [12–14]. Following heterodimerization of activated PPAR $\alpha$  with the retinoid X receptor (RXR), the nuclear

\* Corresponding author. INSERM UMR-S 939, Hôpital de la Pitié, 83 Bd de l'hôpital, 75651 Paris 13, France. Tel.: +33 1 42177878; fax: +33 1 45828198.

E-mail address: [thierry.huby@upmc.fr](mailto:thierry.huby@upmc.fr) (T. Huby).

<sup>1</sup> Current address: University of Cambridge Metabolic Research Laboratories, Institute of Metabolic Science, Addenbrooke's Hospital, Cambridge CB2 0QQ, UK.

receptor complex binds to peroxisome proliferator response elements (PPREs). As a direct consequence, expression of target genes implicated in fatty acid metabolism (L-FABP, mitochondrial 3-hydroxy-3-methylglutaryl-Coenzyme A synthase) and  $\beta$ -oxidation (acyl-CoA oxidase, ACOX) [15–18] is regulated. In addition, fibrates activate the expression of the *LPL* gene while concomitantly repressing that of the *LPL* inhibitor, *APOC3* [19,20].

Recent studies have shown that primate *APOA5* expression is regulated by PPAR $\alpha$ . In human hepatic cells, activation of PPAR $\alpha$  by several agonists induces elevation in *APOA5* mRNA levels. Indeed, analysis of the human *APOA5* promoter region revealed the presence of a functional PPRE, consisting of a direct repeat (DR1) motif 5'-AGGTTAAAGGTCA-3' located at -271 nt from the transcription start site [21,22]. Consistent with this finding, 14 days of treatment with 0.3 mg/kg/day of the PPAR agonist LY570977 L-lysine in the cynomolgus monkey resulted in a 2-fold increase in plasma apoAV concentration and a 50% decrease in TG levels [23]. These findings demonstrated that pharmacological activation of PPAR $\alpha$  can lead to increase in plasma apoAV levels, thereby shedding new light on the molecular mechanisms whereby PPAR $\alpha$  agonists lower plasma TG levels in primates. It can therefore be proposed that apoAV contributes to the hypotriglyceridemic effect of PPAR $\alpha$  agonists by enhancing *LPL* activity upon PPAR $\alpha$  activation.

Peroxisome proliferators were originally characterized in rodents as agents that cause peroxisome proliferation and hepatocarcinoma when chronically administered [24]. On the other hand, PPAR agonists are not associated with an elevated risk of liver cancer or peroxisome proliferation in humans, indicating a species difference in the effects of fibrates in hepatic tissue [25]. Differential regulation of genes involved in lipid metabolism by pharmacological activation of PPAR $\alpha$  has equally been reported between species. Thus, whereas the major HDL apolipoprotein gene *APOA1* is induced by PPAR $\alpha$  in humans, the mouse orthologous gene is down-regulated [26]. Recently, Dorfmeister et al. have shown that a fish oil diet rich in polyunsaturated fatty acids or rosiglitazone, both of which are PPAR $\gamma$  activators, increased *Apoa5* mRNA levels in livers of obese and insulin-resistant Zucker rats, but tended to diminish both liver and plasma apoAV. However, they also observed a lack of increase in mRNA levels in primary rat hepatocytes treated with PPAR- $\alpha$  or - $\gamma$  specific agonists, thereby suggesting that rat *Apoa5* may be insensitive to stimulation by PPAR agonists, and that the effects of rosiglitazone in Zucker rats are not directly mediated by PPAR $\gamma$  [27].

In the present study, we evaluated the question as to whether the human and murine *APOA5* genes could be differentially regulated by fibrates. We confirmed that the human *APOA5* promoter activity is up-regulated following PPAR $\alpha$  and fenofibrate treatment in a hepatic cell line. In contrast, the proximal promoter region of the mouse *Apoa5* gene was not responsive. *In vivo* analysis of mice transgenic for the human *APOA5* gene (h*APOA5*-mice) confirmed these results. Indeed, short term oral gavage of h*APOA5*-mice with fenofibrate resulted in a dose-dependent increase of human *APOA5* mRNA levels in the liver, whereas those of mouse *Apoa5* were concomitantly slightly down-regulated. These data establish that hepatic expression of the mouse and human *APOA5* genes is regulated in an opposing manner by fibrates *in vivo*, and further highlight a critical difference in the regulation of TRL metabolism between mice and humans.

## 2. Materials and methods

### 2.1. Animal protocols

All animal procedures were performed with approval from the Direction Départementale des Services Vétérinaires, Paris, France, under strict compliance with European Community Regulations. The animals were housed in a conventional animal facility on a 6 am to 6 pm dark/light cycle. They were weaned at 21 days and fed a normal mouse chow diet *ad libitum* (RM1; Dietex France). Human *APOA5* transgenic mice in an FVB genetic background were generously provided by Dr E.M. Rubin (Genome Sciences Department, Lawrence Berkeley National Lab, CA). The *APOA5* transgene was maintained in a hemizygous state by breeding transgenic animals with wild-type FVB mice. Genotyping of the mice were performed as previously described [5].

2–3 month old h*APOA5* male mice and wild-type control male littermates were given an oral gavage of 0.2 ml fenofibrate (Sigma) for five days, either once daily at a dose of 100 mg/kg or twice a day at a dose of 125 mg/kg. h*APOA5* transgenic and control non-treated groups received 0.2 ml of vehicle only (0.5% hydroxypropyl methylcellulose, 1% Tween 80). Four hours after the last dose, blood was collected under isoflurane anaesthesia. The animals were then sacrificed by cervical dislocation and livers were collected, rinsed in ice-cold PBS, and snap-frozen in liquid nitrogen. RNAs were prepared from frozen tissue specimens using TRIzol reagent (Invitrogen).

### 2.2. Plasma and lipid analyses

Blood samples were collected in EDTA-coated Microvette tubes (Sarstedt) by retro-orbital bleeding using heparinized micro-hematocrit capillary tubes. Plasma samples were stored frozen at -80 °C. Total cholesterol (Roche Diagnostics) and triglyceride (Biomérieux) concentrations were measured by enzymatic colorimetric assays. Plasma lipoproteins were fractionated by gel filtration on two Superose 6 (Amersham Biosciences) columns connected in series using a BioLogic DuoFlow Chromatography System (BioRad) [28].

### 2.3. Real time PCR quantification of mRNAs

cDNA preparation and quantitative PCR analysis were performed as previously described [29]. The sequences of forward and reverse primers are shown in Table 1. The specificity of the primers was verified by showing that the real time reverse transcriptase (RT)-PCR reaction product generated a single band after agarose gel electrophoresis. In addition, each couple of primers was tested in successive dilutions of cDNA to analyze and validate its efficiency. The levels of expression of the target genes were normalized to mouse ribosomal protein S3 (*Rps3*) expression to compensate for variations in input RNA amounts (*Rps3* levels were unaffected by fenofibrate treatment).

### 2.4. Plasmids

p-617/+18 hAvLUC containing the 5' flanking region of the human *APOA5* gene (-617 to +18) cloned in front of the promoter-

Table 1

Gene	Accession number	Full name	Sense primer	Antisense primer	Amplicon
<i>hAPOAV</i>	NM_052968.3	Human apolipoprotein	A-V 5'-AGCTGGTGGGCTGGAATTT-3'	5'-GGCCACCTGCTCCATCAG-3'	77 bp
<i>mAPOAV</i>	NM_080434.3	Mouse apolipoprotein A-V	5'-CCTTACGCAGAAAGCTTGGT-3'	5'-TCCTTCGCCTTACGTGTGAGT-3'	146 bp
<i>mLPL</i>	NM_008509.2	Mouse Lipoprotein Lipase	5'-GAGCCAAGAGAGCAGCAAG-3'	5'-CCATCCTCAGTCCAGAAAA-3'	103 bp
<i>mAPOA1</i>	NM_009692.3	Mouse apolipoprotein A-I	5'-AGCGGCAGAGACTATGTGTC-3'	5'-ACGGTTGAACCCAGAGTGTGTC-3'	98 bp
<i>mAPOC3</i>	NM_023114.3	Mouse apolipoprotein C-III	5'-GTACAGGGCTACATGGAACAA-3'	5'-TATCGGACTCTGCACGCTACT-3'	70 bp
<i>mAcox1</i>	NM_015729.2	Mouse acyl-Coenzyme A oxidase 1	5'-GGGAGTGCTACGGGTTACATG-3'	5'-CCGATATCCCCAACAGTGATG-3'	91 bp
<i>mGUSb</i>	NM_010368.1	Mouse glucuronidase, beta	5'-CTCATCTGGAATTCGCCGA-3'	5'-GGCGAGTGAAGATCCCCCTC-3'	82 bp

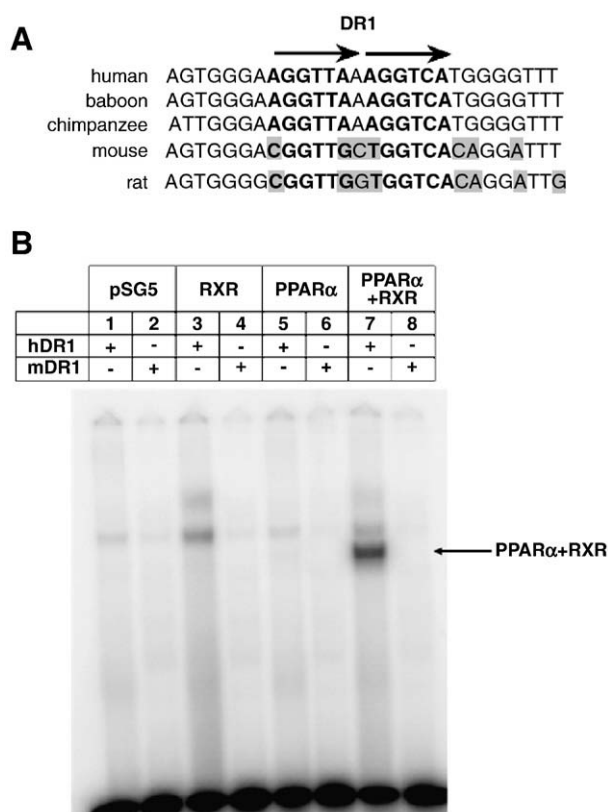


**Fig. 1.** The human *APOA5*, but not mouse *Apoa5*, 5' flanking region contains a functional PPRE (A), sequence comparison of the human DR1/PPRE element present in the 5' flanking region of the human *APOA5* gene to the corresponding baboon, chimpanzee, mouse and rat sequences. The gray boxes denote the nucleotide differences between the primate and rodent sequences. The hexameric sites are in boldface type and their orientations are indicated by arrows. (B) EMSAs were performed using labelled double-stranded oligonucleotides corresponding to the human *APOA5* gene sequence spanning nt -275 to -247 (hDR1) or the corresponding sequence in mouse *Apoa5* gene (mDR1). Oligonucleotides were incubated with either *in vitro* transcribed/translated PPAR $\alpha$ , or RXR $\alpha$ , or PPAR $\alpha$  and RXR $\alpha$ , or with unprogrammed reticulocyte lysates (pSG5). The PPAR $\alpha$ /RXR $\alpha$ -hDR1 complex is indicated by an arrow.

less luciferase gene has been previously described [21]. To generate the luciferase reporter plasmids p-1831/+17 and p-617/+17 mAvLUC, C57BL/6 mouse genomic DNA was amplified by PCR using the primer pairs mAPOAV-1831f 5'-AGT CCG TAC CCG CGT GGC TCA

CTG TTT TTA-3' and mAPOAV+17r 5'-AGT CAG ATC TCA CCT GCT CGG TTC TGG G-3', and mAPOAV-617f 5'-AGT CCG TAC CTG TGA GGG AAG ACT CTT GAG G-3' and mAPOAV+17r, respectively. The PCR products were digested at their 5' and 3' ends by KpnI and BglII restriction enzymes, respectively (restriction sites underlined in the primer sequences), and subsequently cloned in KpnI/BglII-digested pGL3 basic vector (Promega). The sequences were verified in the final constructs by DNA sequencing. Expression plasmid for PPAR $\alpha$  has been previously described [21].

## 2.5. Cell transfection and reporter assays

Human hepatoblastoma Hep3B cell lines were cultured in Dulbecco's modified Eagle medium (Invitrogen) supplemented with 10% (v/v) foetal calf serum. On day 0, cells were seeded on 24-well plates at a density of  $10^5$  cells/well. On day 1, cells were transfected with FuGENE 6 transfection reagent (Roche Applied Science) according to the manufacturer's instructions. Typically, each well of a 24 well plate received 250 ng of human or mouse *APOA5* promoter constructs, 15 ng of a  $\beta$ -galactosidase expression plasmid and, either 85 ng of the pSG5-PPAR $\alpha$  expression plasmid or a corresponding amount of empty pSG5 vector. After incubation for 5 h, the medium was replaced by fresh complete medium in the presence of either 5  $\mu$ M fenofibrate (Sigma) or vehicle (DMSO). On day 4, cell extracts were prepared in lysis buffer (Promega) and  $\beta$ -galactosidase and luciferase activities were determined as described previously [30]. Luciferase values were normalized to  $\beta$ -galactosidase activities. Transfection data represent the mean ( $\pm$  standard deviation) of four independent experiments each performed in triplicate.

## 2.6. *In vitro* transcription/translation and electro mobility shift assays (EMSAs)

Human PPAR $\alpha$  and RXR $\alpha$  proteins were synthesized *in vitro* from the expression plasmid using TNT<sup>®</sup> Quick Coupled transcription/translation system (Promega) according to the instructions of the manufacturer. In order to obtain an unprogrammed lysate as a negative control for EMSA, a reaction was performed with the empty vector pSG5. Double-stranded oligonucleotides were radiolabelled by fill-in with the Klenow fragment of DNA polymerase I and used as probes. Samples were electrophoresed at 4 °C on a 4.5% polyacrylamide gel in 0.5X TBE buffer (45 mM Tris, 45 mM boric acid, 1 mM EDTA, pH 8.0). Gels were dried and analyzed using PhosphorImager STORM 860 and ImageQuant software (Amersham Biosciences).

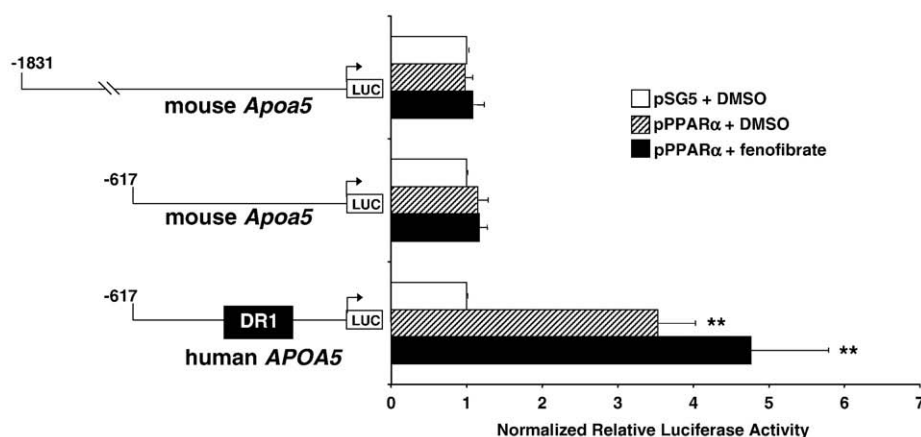


**Fig. 2.** Transactivation of the human but not the mouse *APOA5* gene promoter by PPAR $\alpha$  and fenofibrate. Hep3B cells were transfected with plasmids containing a luciferase reporter gene driven by either the -617/+18 5'-flanking region of the human *APOA5* gene or the -617/+18 or -1831/+18 5'-flanking regions of the mouse *Apoa5* gene. The *APOA5* promoter constructs were co-transfected with the PPAR $\alpha$  expression vector (or corresponding control vector pSG5) in the presence of either 5  $\mu$ M fenofibrate or vehicle (DMSO). Results are expressed as -fold induction over control. \*\*,  $p < 0.001$ .

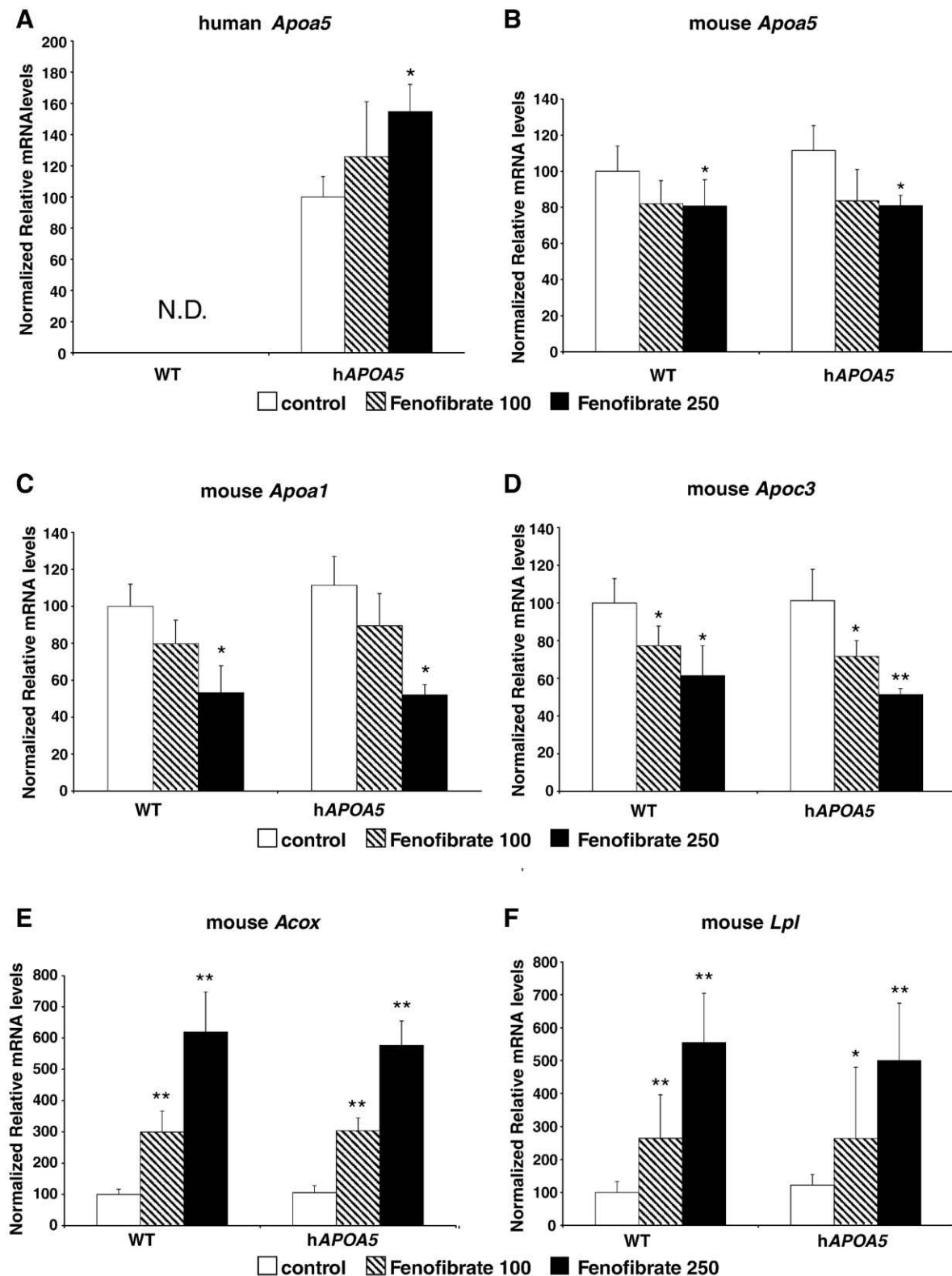


**Fig. 3.** Gene activation in livers of wild-type and hAPOA5-mice treated with fenofibrate. Wild-type (WT) and hAPOA5 transgenic mice were treated with vehicle (control), 100 mg/kg/day (fenofibrate-100 group), or 250 mg/kg/day (fenofibrate-250 group) of fenofibrate for 5 days. (A) Total RNA was extracted for analysis by real time RT-PCR as described under "Materials and methods". human APOA5 (A), mouse *ApoA5* (B), mouse *ApoA1* (C), mouse *Apoc3* (D), mouse *Acox* (E) and mouse *Lpl* (F) mRNA levels, normalized to mouse *Rps3* content, are expressed relative to untreated WT animals set as 100% (except for the hAPOA5 gene whose 100% reference corresponds to untreated-hAPOA5-mice) (mean  $\pm$  S.D.). Only data for control animals of the fenofibrate-250 group study are shown for more clarity. Significant differences compared with the corresponding untreated controls are as follows: \*,  $p < 0.05$ ; \*\*,  $p < 0.001$ . N.D., not detected.

## 2.7. Statistical analysis

The statistical significance of the differences between groups was evaluated using the unpaired two-tailed Student *t*-test.  $p < 0.05$  was considered significant.

## 3. Results

### 3.1. Presence of a functional PPRE in the proximal flanking region of the human APOA5 5' gene, but not in the mouse ApoA5 gene

Previously, we identified two PuGGTCA hexamers binding sites separated by a single nucleotide (DR1) between nt –271 and –259 in the promoter sequence of the human APOA5 gene. Luciferase assay and gel shift assays allowed us to demonstrate that this APOA5 DR1 is a genuine PPRE [21]. Interestingly, comparison of the corresponding human, baboon, chimpanzee, mouse and rat 5' flanking sequences surrounding the DR1/PPRE element revealed that the human APOA5 DR1 element is highly conserved among primates, but not in the rat or mouse gene promoters (Fig. 1A). Indeed, alignment of the sequences reveals four nucleotide differences in the latter species as compared to the human APOA5 DR1 (hDR1) sequence. Electrophoretic mobility shift assay analysis revealed that these nucleotide changes in the mouse *Apoa5* sequence abolished binding of the PPAR-RXR heterodimer (Fig. 1B, lane 8), whereas a specific protein–DNA complex was clearly detected when a probe for the human APOA5-DR1 sequence was incubated in the presence of the recombinant PPAR $\alpha$  and RXR proteins (Fig. 1B, lane 7). These data are in agreement with recent studies demonstrating that both HNF-4 [31] and ROR $\alpha$  [32], nuclear factors which bind to response elements consisting of the core recognition sequence AGGTCA, bound to the human APOA5-DR1 sequence, but not to the corresponding mouse sequence.

### 3.2. Mouse APOA5 promoter is not regulated by PPAR $\alpha$

To search for other potential PPRES in mouse *Apoa5* promoter, we cloned 1.8 kb (–1831/+18mAvLUC) and 0.6 kb (–617/+18mAvLUC) of the 5' flanking region upstream of the transcription start site of the murine *Apoa5* gene sequence into the firefly luciferase pGL3-basic vector. In Hep3B cells, the luciferase activities of these constructs remain unchanged when co-transfected with PPAR $\alpha$  expression vector alone or in combination with the PPAR $\alpha$  agonist fenofibrate (Fig. 2). Conversely, in the same experiment, a human promoter construct previously demonstrated to respond to PPAR $\alpha$  activation [21] displayed a statistically significant increase in activity of approximately 3.5- and more than 4.5-fold when co-transfected with a PPAR $\alpha$  expression vector in absence or presence of fenofibrate, respectively. Of note, in contrast to what we previously described with the PPAR $\alpha$  agonist GW9003 using similar experimental conditions [21], the enhanced effect of fenofibrate on the induction of human APOA5 promoter activity by the overexpression of PPAR $\alpha$  was only modest and did not reach statistical significance. This discrepancy may be due to the difference of affinity between the two agonists for PPAR $\alpha$  and/or the amount of effective drug available in the cell. Taken together, these data demonstrate that the proximal 5' region in the mouse gene is not responsive to PPAR $\alpha$  *in vitro*.

### 3.3. Fibrate treatment up-regulates human APOA5 gene expression, but down-regulates that of mouse ApoA5 gene *in vivo*

To determine whether the mouse *Apoa5* gene could respond to PPAR $\alpha$  agonists through distant regulatory regions, we treated mice for a short period with fenofibrate at two different dosages, and evaluated mouse *Apoa5* mRNA levels in the liver. These studies were performed concomitantly in wild-type (WT) mice and in mice

transgenic for a 26-kbp fragment of human chromosome XI solely containing the entire APOA5 gene, including its flanking regulatory regions [5]. Under the conditions tested, human APOA5 mRNA levels measured by Q-PCR were increased modestly, and dose dependently (1.3- and 1.6-fold), when hAPOA5-mice received an oral daily gavage of fenofibrate (100 or 250 mg) (Fig. 3A). Comparatively, mouse *Apoa5*

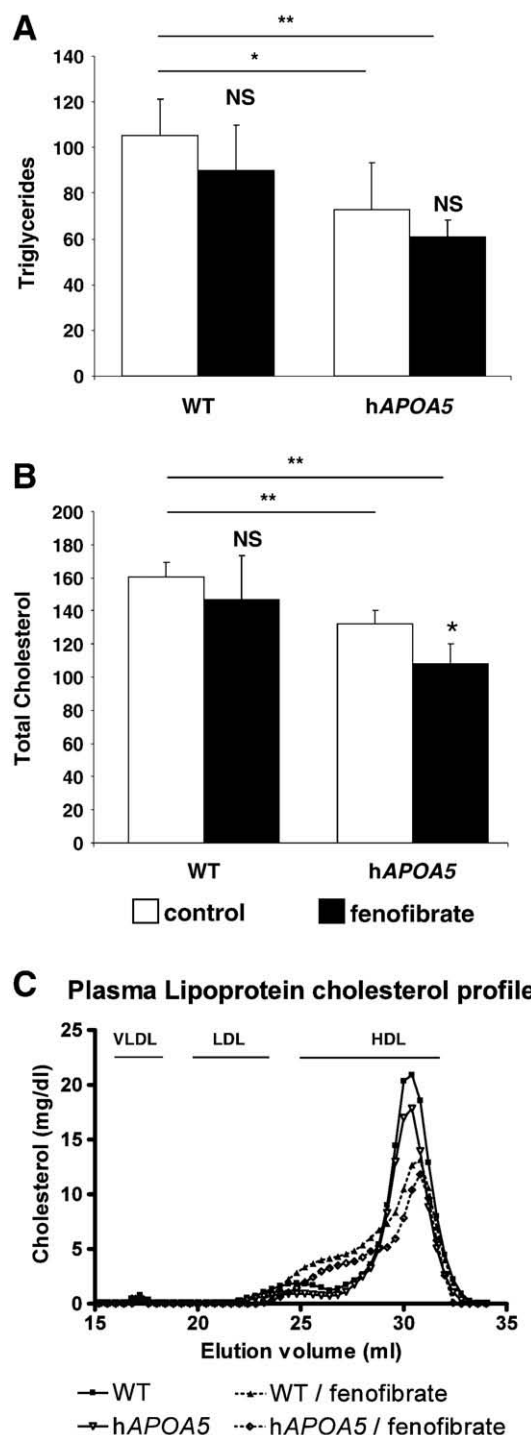


**Fig. 4.** Plasma lipid parameters in fenofibrate-treated mice: levels (mg/dl) of triglycerides (A) and total cholesterol (B) and lipoprotein cholesterol distribution (C) were determined in plasma from non-fasted wild-type (WT) or hAPOA5 mice treated with vehicle (control) or 250 mg/kg/day of fenofibrate for 5 days. Approximate elution volumes for particles in the size ranges of VLDL, LDL, and HDL are indicated in (C). Significant differences are as follows: \*,  $p < 0.05$ ; \*\*,  $p < 0.001$ ; NS: not significantly different from respective controls.

gene expression was decreased similarly (20%) at the two fenofibrate doses in both WT and hAPOA5-mice (Fig. 3B). As a control for the efficacy for short term fenofibrate treatment, we quantified the level of expression of genes known to be either repressed or activated by PPAR $\alpha$ . Thus, we observed that fenofibrate treatment decreased the steady state mRNA levels of both m*Apoa1* (Fig. 3C) and m*Apoc3* (Fig. 3D). In contrast, m*Lpl* (Fig. 3F) and m*Acox* (Fig. 3E) mRNA levels were strongly up-regulated in fenofibrate-fed mice. For all these genes, the effects were comparable in both WT and hAPOA5-mice.

Taken together, these results demonstrate an inverse response of the mouse and human APOA5 genes to PPAR $\alpha$  agonist treatment, in which transcription of the human gene is activated *in vivo*, whereas hepatic mRNA levels of the murine ortholog are down-regulated in response to fenofibrate treatment.

#### 3.4. Impact of fenofibrate treatment on plasma lipid and lipoprotein levels in WT and hAPOA5 mice

The impact of a 5-day fibrate treatment in both WT and hAPOA5-mice on plasma lipid and lipoprotein levels was evaluated at the 250 mg/kg dosage. Lipid concentrations were determined at the time of sacrifice, which was performed 4-h after the final gavage of non-fasted mice. Plasma TG levels were lower in hAPOA5-mice as compared to WT mice (Fig. 4A), as previously reported [5]. In addition, a slight and similar reduction in plasma TG levels was observed in both drug treated-groups, but this reduction did not reach statistical significance. Surprisingly, plasma total cholesterol (TC) (Fig. 4B) levels were found to be statistically lower in hAPOA5-mice than in WT untreated-mice. Plasma TC was equally found to be lower in fenofibrate-fed hAPOA5-mice as compared to untreated-hAPOA5-mice; such a reduction was not observed in the WT group. However, fenofibrate treatment markedly and similarly modified the distribution of lipoprotein cholesterol in both WT and hAPOA5-mice. Indeed, cholesterol content was reduced in fractions corresponding to HDL particles of normal size, with appearance of larger HDL particles (Fig. 4C). Such specific change in HDL particle distribution is, in all likelihood, a direct consequence of down-regulation of hepatic scavenger receptor SR-BI expression at the protein level by fibrates which has been previously reported in mice [33]. Indeed, reduced expression of SR-BI consistently results in the appearance of larger HDL, rich in cholesterol, but equally in elevation of plasma levels of HDL-C (and plasma TC) in mice [28]. In the present study, the concomitant marked reduction of mouse *Apoa1* gene expression following fenofibrate-250 treatment in the WT group (Fig. 3C) most likely masked the HDL-C raising effect of knockdown expression of SR-BI; thus resulting in no net change in plasma TC levels (Fig. 4B) but in the presence of large HDL particles and a decrease in the level of regularly sized HDLs (Fig. 4C).

#### 4. Discussion

It is well established that PPAR $\alpha$  activation has distinct effects in human and mice, especially on peroxisome proliferation [25]. In addition, with respect to lipid metabolism, it is established that PPAR $\alpha$  agonists differentially regulate genes between humans and rodents including, for example, the APOA1 or PLTP genes. Here, we demonstrate that mouse *Apoa5* is repressed by fenofibrate treatment in a mouse model transgenic for the human APOA5 gene, whereas the human ortholog is up-regulated. These findings are consistent with the presence of a functional PPRE in the human APOA5 promoter, which is degenerate in the corresponding mouse *Apoa5* sequence. These observations substantiate the differential impact of PPAR $\alpha$  activators on lipid metabolism in human and rodents.

Fibrates are potent pharmacological agents for reduction of plasma levels of triglycerides and TG-rich lipoproteins in humans, as they notably induce elevation in LPL activity through PPAR-mediated

activation of LPL gene expression, but equally repress expression of the APOC3 gene, an inhibitor of LPL activity. Although we observed a marked increase in hepatic *Lpl* expression and a concomitant decrease in *Apoc3* expression associated with fenofibrate treatment in WT mice, nonetheless there was only a trend towards fall in TG levels in these animals as compared to untreated controls. A similar observation was made in hAPOA5 mice, as we did not observe an additional reduction in plasma TG levels in hAPOA5-mice in response to drug treatment, despite evidence both of activation of human APOA5 gene expression and similar PPAR-mediated changes in expression of *Lpl* and *Apoc3* genes as seen in the WT group. The experimental conditions (non-fasting chow-fed mice, emulsifier molecules used for oral gavage) may have masked a net lowering effect of fenofibrate on plasma TG levels and in particular in hAPOA5-mice. In the latter group, one could have expected diminished TG concentrations following hAPOA5 activation. Such activation was nonetheless only moderate and the concomitant reduction in levels of mouse *Apoa5* in response to drug treatment may have introduced a confounding effect. Moreover, it should be mentioned that up-regulation of hAPOA5 was not confirmed in plasma, which represents a limitation to the present study. Nevertheless, these results may equally raise the question of the role of apoAV in the overall TG lowering action of fibrates. Notably, if apoAV and TG plasma levels were found inversely correlated in cynomolgus monkeys receiving the potent and selective PPAR $\alpha$  agonist LY570977 L-lysine, the marked fall in plasma TG preceded the elevation of plasma levels of apoAV in this study [23]. Finally, apparent contradictions are evident in the literature with respect to the relationship between plasma TG and apoAV levels. Indeed, whereas transgenic mice overexpressing hAPOA5 displayed significant reduction in plasma TG concentrations, and whereas apoAV deficient mice exhibited a net increase in plasma TG levels, it has been recently demonstrated that apoAV concentrations are positively correlated with TG levels in normolipidemic hAPOA5 mice, as reported in humans [34].

Whereas consistent associations between common polymorphisms of the APOA5 gene and plasma TG levels have been reported, the demonstration of such genetic associations with plasma cholesterol levels is less clear. Nonetheless, a number of studies have highlighted associations of genetic variants of APOA5 with circulating HDL-C levels in populations of different ethnic origin [5,6,35–39], thereby suggesting that apoAV may contribute to regulation of HDL-C levels. Indeed, apoAV is mainly present in HDL during the fasting period, which could suggest a potential role of apoAV in HDL-cholesterol metabolism. In the present study, significantly lower plasma TC and HDL-C levels were observed in chow-fed hAPOA5-mice as compared to wild-type controls. Such differences were not reported in the original publication describing the generation of hAPOA5-mice, although a trend existed [5]. However, it is of note that adenovirus-mediated overexpression of apoAV in mice resulted in a profound decrease in TG concentrations but equally plasma cholesterol levels [6]. Moreover, cross-breeding of mice overexpressing human APOA5 with either human APOC3 transgenic mice or ApoE2 knock-in mice produced a decrease in plasma cholesterol concentrations [7,40]. Further studies focusing on the role of apoAV in cholesterol and HDL metabolism are clearly needed to understand whether there exists a potential direct action of apoAV or indirect consequences of apoAV activities on HDL-C levels and HDL particle distribution. Interestingly, fenofibrate treatment resulted in significant diminution in plasma cholesterol levels in hAPOA5-mice, an effect not observed in the WT group. Whether increase in apoAV levels following fenofibrate treatment may have contributed to the diminished cholesterol levels observed in transgenic mice remains speculative and requires additional studies.

Hepatic mRNA levels of the mouse *Apoa1* and *Apoc3* genes were markedly reduced in response to oral gavage with fenofibrate. This effect, which was dose-dependent (Fig. 3C,D), may result from

PPAR $\alpha$ -mediated induction of the nuclear receptor Rev-erb $\alpha$  [20,41]. Indeed, the presence of a response element for this repressor in the promoters of rodent *Apoa1* [42] and *Apoc3* genes support this hypothesis. The sequence motifs for Rev-erb $\alpha$  and the nuclear hormone receptor ROR $\alpha$  are closely related [43] which explains that the Rev-erb $\alpha$  response element present in the *Apoa1* gene is also a ROR $\alpha$  element [42,44]. Human *APOA5* is a target gene for ROR through binding to the half-core AGGTCA DR1/PPRE site [45], whereas mouse *Apoa5* is not, due to a nucleotide difference in the half-core site which prevents ROR $\alpha$  binding to the mouse promoter [32]. Consistently, mouse *Apoa5* gene expression is not affected in the staggerer mutant mouse which carries a deletion in the gene encoding for ROR $\alpha$  [32]. Thus, the modest decrease of *mApoa5* mRNA levels that we observed in the livers of fenofibrate-fed mice is unlikely to result from PPAR-induced Rev-erb $\alpha$  repression mechanism, as most likely occurred for the *Apoa1* and *Apoc3* genes. This hypothesis is consistent with the fact that the activity of the mouse *Apoa5* promoter was not repressed by PPAR $\alpha$  and fenofibrate treatment in transient transfection assays (Fig. 2).

In conclusion, this study provides additional evidence that extrapolation from mouse to man of experimental findings involving the pharmacological action of fibric acid or their derivatives on lipid metabolism must be conducted with considerable caution. Nonetheless, comparison of hAPOA5-mice with non-transgenic controls in response to treatment with PPAR agonists may prove useful in deciphering the physiological significance of apoAV in the regulation of TG metabolism in fasting or non-fasting conditions, and equally in normo- or hyperlipidemic contexts. In the latter context, cross-breeding of hAPOA5-mice with the ApoE2 knock-in mouse model recently allowed demonstration of an atheroprotective effect of apoAV overexpression on a background of mixed dyslipidemia; this effect was further enhanced upon hAPOA5 gene activation by fenofibrate [40]. Finally, such studies may highlight a potential mechanism by which apoAV could impact HDL-C levels. In this respect, cross-breeding of hAPOA5-mice with the recently-described hyperlipidemic E3L.CETP mouse model [46], in which the dual ability of fibrates to potently reduce plasma TG and concomitantly increase HDL-C was clearly demonstrated, may constitute an interesting approach.

## Acknowledgements

These studies were supported by INSERM. PL, MJC and TH gratefully acknowledge the award of a Contrat d'Interface from Assistance Publique – Hôpitaux de Paris/INSERM (France).

## References

- [1] H.B. Brewer, Hypertriglyceridemia: changes in the plasma lipoproteins associated with an increased risk of cardiovascular disease, *Am. J. Cardiol.* 83 (1999) 3F–12F.
- [2] N. Sarwar, J. Danesh, G. Eiriksdottir, G. Sigurdsson, N. Wareham, S. Bingham, S.M. Boekholdt, K.T. Khaw, V. Gudnason, Triglycerides and the risk of coronary heart disease: 10,158 incident cases among 262,525 participants in 29 Western prospective studies, *Circulation* 115 (2007) 450–458.
- [3] M.A. Austin, J.E. Hokanson, K.L. Edwards, Hypertriglyceridemia as a cardiovascular risk factor, *Am. J. Cardiol.* 81 (1998) 7B–12B.
- [4] X. Prieur, T. Huby, J.C. Rodriguez, P. Couvert, J. Chapman, Apolipoprotein AV: gene expression, physiological role in lipid metabolism and clinical relevance, *Futur. Lipidol.* 3 (2008) 371–384.
- [5] L.A. Pennacchio, M. Olivier, J.A. Hubacek, J.C. Cohen, D.R. Cox, J.C. Fruchart, R.M. Krauss, E.M. Rubin, An apolipoprotein influencing triglycerides in humans and mice revealed by comparative sequencing, *Science* 294 (2001) 169–173.
- [6] H.N. van der Vliet, F.G. Schaap, J.H. Levels, R. Ottenhoff, N. Looije, J.G. Wesseling, A.K. Groen, R.A. Chamuleau, Adenoviral overexpression of apolipoprotein A-V reduces serum levels of triglycerides and cholesterol in mice, *Biochem. Biophys. Res. Commun.* 295 (2002) 1156–1159.
- [7] J. Fruchart-Najib, E. Bauge, L.S. Niculescu, T. Pham, B. Thomas, C. Rommens, Z. Majd, B. Brewer, L.A. Pennacchio, J.C. Fruchart, Mechanism of triglyceride lowering in mice expressing human apolipoprotein A5, *Biochem. Biophys. Res. Commun.* 319 (2004) 397–404.
- [8] F.G. Schaap, P.C. Rensen, P.J. Voshol, C. Vrins, H.N. van der Vliet, R.A. Chamuleau, L.M. Havekes, A.K. Groen, K.W. van Dijk, ApoAV reduces plasma triglycerides by inhibiting very low density lipoprotein-triglyceride (VLDL-TG) production and stimulating lipoprotein lipase-mediated VLDL-TG hydrolysis, *J. Biol. Chem.* 279 (2004) 27941–27947.
- [9] M. Merkel, B. Loeffler, M. Kluger, N. Fabig, G. Geppert, L.A. Pennacchio, A. Laatsch, J. Heeren, Apolipoprotein AV, accelerates plasma hydrolysis of triglyceride-rich lipoproteins by interaction with proteoglycan-bound lipoprotein lipase, *J. Biol. Chem.* 280 (2005) 21553–21560.
- [10] I. Grosskopf, N. Barouk, S.J. Lee, Y. Kamari, D. Harats, E.M. Rubin, L.A. Pennacchio, A.D. Cooper, Apolipoprotein A-V deficiency results in marked hypertriglyceridemia attributable to decreased lipolysis of triglyceride-rich lipoproteins and removal of their remnants, *Arterioscler. Thromb. Vasc. Biol.* 25 (2005) 2573–2579.
- [11] S.K. Nilsson, A. Lookene, J.A. Beckstead, J. Gliemann, R.O. Ryan, G. Olivecrona, Apolipoprotein A-V interaction with members of the low density lipoprotein receptor gene family, *Biochemistry* 46 (2007) 3896–3904.
- [12] B. Staels, J. Dallongeville, J. Auwerx, K. Schoonjans, E. Leitersdorf, J.C. Fruchart, Mechanism of action of fibrates on lipid and lipoprotein metabolism, *Circulation* 98 (1998) 2088–2093.
- [13] J. Auwerx, Regulation of gene expression by fatty acids and fibric acid derivatives: an integrative role for peroxisome proliferator activated receptors. The Belgian Endocrine Society Lecture 1992, *Horm. Res.* 38 (1992) 269–277.
- [14] S. Kersten, B. Desvergne, W. Wahli, Roles of PPARs in health and disease, *Nature* 405 (2000) 421–424.
- [15] J.C. Rodriguez, G. Gil-Gomez, F.G. Hegardt, D. Haro, Peroxisome proliferator-activated receptor mediates induction of the mitochondrial 3-hydroxy-3-methylglutaryl-CoA synthase gene by fatty acids, *J. Biol. Chem.* 269 (1994) 18767–18772.
- [16] K. Schoonjans, B. Staels, J. Auwerx, Role of the peroxisome proliferator-activated receptor (PPAR) in mediating the effects of fibrates and fatty acids on gene expression, *J. Lipid Res.* 37 (1996) 907–925.
- [17] J.D. Tugwood, I. Issemann, R.G. Anderson, K.R. Bundell, W.L. McPheat, S. Green, The mouse peroxisome proliferator activated receptor recognizes a response element in the 5' flanking sequence of the rat acyl CoA oxidase gene, *EMBO J.* 11 (1992) 433–439.
- [18] K. Schoonjans, B. Staels, P. Grimaldi, J. Auwerx, Acyl-CoA synthetase mRNA expression is controlled by fibric-acid derivatives, feeding and liver proliferation, *Eur. J. Biochem.* 216 (1993) 615–622.
- [19] R. Hertz, J. Bishara-Shieban, J. Bar-Tana, Mode of action of peroxisome proliferators as hypolipidemic drugs. Suppression of apolipoprotein C-III, *J. Biol. Chem.* 270 (1995) 13470–13475.
- [20] H. Coste, J.C. Rodriguez, Orphan nuclear hormone receptor Rev-erb $\alpha$  regulates the human apolipoprotein CIII promoter, *J. Biol. Chem.* 277 (2002) 27120–27129.
- [21] X. Prieur, H. Coste, J.C. Rodriguez, The human apolipoprotein AV gene is regulated by peroxisome proliferator-activated receptor- $\alpha$  and contains a novel farnesoid X-activated receptor response element, *J. Biol. Chem.* 278 (2003) 25468–25480.
- [22] N. Vu-Dac, P. Gervois, H. Jakel, M. Nowak, E. Bauge, H. Dehondt, B. Staels, L.A. Pennacchio, E.M. Rubin, J. Fruchart-Najib, J.C. Fruchart, Apolipoprotein A5, a crucial determinant of plasma triglyceride levels, is highly responsive to peroxisome proliferator-activated receptor  $\alpha$  activators, *J. Biol. Chem.* 278 (2003) 17982–17985.
- [23] A.E. Schultze, W.E. Alborn, R.K. Newton, R.J. Konrad, Administration of a PPAR $\alpha$  agonist increases serum apolipoprotein A-V levels and the apolipoprotein A-V/apolipoprotein C-III ratio, *J. Lipid Res.* 46 (2005) 1591–1595.
- [24] J.K. Reddy, M.S. Rao, D.L. Azarnoff, S. Sell, Mitogenic and carcinogenic effects of a hypolipidemic peroxisome proliferator, [4-chloro-6-(2,3-xylylidino)-2-pyrimidinylthio]acetic acid (Wy-14, 643), in rat and mouse liver, *Cancer Res.* 39 (1979) 152–161.
- [25] F.J. Gonzalez, Y.M. Shah, PPAR $\alpha$ : mechanism of species differences and hepatocarcinogenesis of peroxisome proliferators, *Toxicology* 246 (2008) 2–8.
- [26] L. Berthou, N. Duverger, F. Emmanuel, S. Langouet, J. Auwerx, A. Guillouzou, J.C. Fruchart, E. Rubin, P. Deneffe, B. Staels, D. Branellec, Opposite regulation of human versus mouse apolipoprotein A-I by fibrates in human apolipoprotein A-I transgenic mice, *J. Clin. Invest.* 97 (1996) 2408–2416.
- [27] B. Dorfmeister, S. Brandlhofer, F.G. Schaap, M. Hermann, C. Furnsinn, B.P. Hagerty, H. Stangl, W. Patsch, W. Strobl, Apolipoprotein AV does not contribute to hypertriglyceridaemia or triglyceride lowering by dietary fish oil and rosiglitazone in obese Zucker rats, *Diabetologia* 49 (2006) 1324–1332.
- [28] T. Huby, C. Doucet, C. Datchet, B. Ouzilleau, Y. Ueda, V. Afzal, E. Rubin, M.J. Chapman, P. Lesnik, Knockdown expression and hepatic deficiency reveal an atheroprotective role for SR-BI in liver and peripheral tissues, *J. Clin. Invest.* 116 (2006) 2767–2776.
- [29] M. Treguier, C. Doucet, M. Moreau, C. Datchet, J. Thillet, M.J. Chapman, T. Huby, Transcription factor sterol regulatory element binding protein 2 regulates scavenger receptor Cla-1 gene expression, *Arterioscler. Thromb. Vasc. Biol.* 24 (2004) 2358–2364.
- [30] T. Huby, C. Datchet, R.M. Lawn, J. Wickings, M.J. Chapman, J. Thillet, Functional analysis of the chimpanzee and human apo(A) promoter sequences: identification of sequence variations responsible for elevated transcriptional activity in chimpanzee, *J. Biol. Chem.* 276 (2001) 22209–22214.
- [31] X. Prieur, F.G. Schaap, H. Coste, J.C. Rodriguez, Hepatocyte nuclear factor-4 $\alpha$  regulates the human apolipoprotein AV gene: identification of a novel response element and involvement in the control by peroxisome proliferator-activated receptor- $\gamma$  coactivator-1 $\alpha$ , AMP-activated protein kinase, and mitogen-activated protein kinase pathway, *Mol. Endocrinol.* 19 (2005) 3107–3125.
- [32] A. Genoux, H. Dehondt, A. Hellebood-Chapman, C. Duhem, D.W. Hum, G. Martin, L.A. Pennacchio, B. Staels, J. Fruchart-Najib, J.C. Fruchart, Transcriptional

- regulation of apolipoprotein A5 gene expression by the nuclear receptor ROR $\alpha$ , *Arterioscler. Thromb. Vasc. Biol.* 25 (2005) 1186–1192.
- [33] P. Mardones, A. Pilon, M. Bouly, D. Duran, T. Nishimoto, H. Arai, K.F. Kozarsky, M. Altayo, J.F. Miquel, G. Luc, V. Clavey, B. Staels, A. Rigotti, Fibrates down-regulate hepatic scavenger receptor class B type I protein expression in mice, *J. Biol. Chem.* 278 (2003) 7884–7890.
- [34] L. Nelbach, X. Shu, R.J. Konrad, R.O. Ryan, T.M. Forte, Effect of apolipoprotein A-V on plasma triglyceride, lipoprotein size, and composition in genetically engineered mice, *J. Lipid Res.* 49 (2008) 572–580.
- [35] C.Q. Lai, S. Demissie, L.A. Cupples, Y. Zhu, X. Adiconis, L.D. Parnell, D. Corella, J.M. Ordovas, Influence of the APOA5 locus on plasma triglyceride, lipoprotein subclasses, and CVD risk in the Framingham Heart Study, *J. Lipid Res.* 45 (2004) 2096–2105.
- [36] Y. Lu, M.E. Dolle, S. Imholz, R.V. Slot, W.M. Verschuren, C. Wijnenga, E.J. Feskens, J.M. Boer, Multiple genetic variants along candidate pathways influence plasma high-density lipoprotein cholesterol concentrations, *J. Lipid Res.* 49 (2008) 2582–2589.
- [37] H. Grallert, E.M. Sedlmeier, C. Huth, M. Kolz, I.M. Heid, C. Meisinger, C. Herder, K. Strassburger, A. Gehringer, M. Haak, G. Giani, F. Kronenberg, H.E. Wichmann, J. Adamski, B. Paulweber, T. Illig, W. Rathmann, APOA5 variants and metabolic syndrome in Caucasians, *J. Lipid Res.* 48 (2007) 2614–2621.
- [38] Y. Yamada, H. Matsuo, S. Warita, S. Watanabe, K. Kato, M. Oguri, K. Yokoi, N. Metoki, H. Yoshida, K. Satoh, S. Ichihara, Y. Aoyagi, A. Yasunaga, H. Park, M. Tanaka, Y. Nozawa, Prediction of genetic risk for dyslipidemia, *Genomics* 90 (2007) 551–558.
- [39] K.L. Chien, M.F. Chen, H.C. Hsu, T.C. Su, W.T. Chang, C.M. Lee, Y.T. Lee, Genetic association study of APOA1/C3/A4/A5 gene cluster and haplotypes on triglyceride and HDL cholesterol in a community-based population, *Clin. Chim. Acta* 388 (2008) 78–83.
- [40] R.M. Mansouri, E. Bauge, P. Gervois, J. Fruchart-Najib, C. Fievet, B. Staels, J.C. Fruchart, Atheroprotective effect of human apolipoprotein A5 in a mouse model of mixed dyslipidemia, *Circ. Res.* 103 (2008) 450–453.
- [41] E. Raspe, H. Duez, A. Mansen, C. Fontaine, C. Fievet, J.C. Fruchart, B. Vennstrom, B. Staels, Identification of Rev-erb $\alpha$  as a physiological repressor of apoC-III gene transcription, *J. Lipid Res.* 43 (2002) 2172–2179.
- [42] N. Vu-Dac, S. Chopin-Delannoy, P. Gervois, E. Bonnelye, G. Martin, J.C. Fruchart, V. Laudet, B. Staels, The nuclear receptors peroxisome proliferator-activated receptor  $\alpha$  and Rev-erb $\alpha$  mediate the species-specific regulation of apolipoprotein A-I expression by fibrates, *J. Biol. Chem.* 273 (1998) 25713–25720.
- [43] B.M. Forman, J. Chen, B. Blumberg, S.A. Kliewer, R. Henshaw, E.S. Ong, R.M. Evans, Cross-talk among ROR  $\alpha$  1 and the Rev-erb family of orphan nuclear receptors, *Mol. Endocrinol.* 8 (1994) 1253–1261.
- [44] N. Vu-Dac, P. Gervois, T. Grotzinger, P. De Vos, K. Schoonjans, J.C. Fruchart, J. Auwerx, J. Mariani, A. Tedgui, B. Staels, Transcriptional regulation of apolipoprotein A-I gene expression by the nuclear receptor ROR $\alpha$ , *J. Biol. Chem.* 272 (1997) 22401–22404.
- [45] U. Lind, T. Nilsson, J. McPheat, P.E. Stromstedt, K. Bamberg, C. Balendran, D. Kang, Identification of the human ApoAV gene as a novel ROR $\alpha$  target gene, *Biochem. Biophys. Res. Commun.* 330 (2005) 233–241.
- [46] C.C. van der Hoogt, W. de Haan, M. Westerterp, M. Hoekstra, G.M. Dallinga-Thie, J.A. Romijn, H.M. Princen, J.W. Jukema, L.M. Havekes, P.C. Rensen, Fenofibrate increases HDL-cholesterol by reducing cholesteryl ester transfer protein expression, *J. Lipid Res.* 48 (2007) 1763–1771.



# Cholesteryl Ester Transfer Protein Expression Partially Attenuates the Adverse Effects of SR-BI Receptor Deficiency on Cholesterol Metabolism and Atherosclerosis<sup>\*[S]</sup>

Received for publication, January 11, 2011, and in revised form, March 11, 2011. Published, JBC Papers in Press, March 20, 2011, DOI 10.1074/jbc.M111.220483

Majda El Bouhassani<sup>‡S1</sup>, Sophie Gilibert<sup>‡S</sup>, Martine Moreau<sup>‡S</sup>, Flora Saint-Charles<sup>‡S</sup>, Morgan Tréguier<sup>‡S</sup>, Francesco Poti<sup>‡S</sup>, M. John Chapman<sup>‡S</sup>, Wilfried Le Goff<sup>‡S</sup>, Philippe Lesnik<sup>‡S</sup>, and Thierry Huby<sup>‡S1,2</sup>

From the <sup>‡</sup>INSERM UMR-S 939, Hôpital de la Pitié, F-75013, Paris, the <sup>S</sup>University Pierre and Marie Curie, UMR-S 939, F-75013, Paris, and the <sup>¶</sup>Assistance Publique-Hôpitaux de Paris, Groupe Hospitalier Pitié-Salpêtrière, Service d'Endocrinologie-Métabolisme, F-75013 Paris, France

Scavenger receptor SR-BI significantly contributes to HDL cholesterol metabolism and atherogenesis in mice. However, the role of SR-BI may not be as pronounced in humans due to cholesteryl ester transfer protein (CETP) activity. To address the impact of CETP expression on the adverse effects associated with SR-BI deficiency, we cross-bred our SR-BI conditional knock-out mouse model with CETP transgenic mice. CETP almost completely restored the abnormal HDL-C distribution in SR-BI-deficient mice. However, it did not normalize the elevated plasma free to total cholesterol ratio characteristic of hepatic SR-BI deficiency. Red blood cell and platelet count abnormalities observed in mice liver deficient for SR-BI were partially restored by CETP, but the elevated erythrocyte cholesterol to phospholipid ratio remained unchanged. Complete deletion of SR-BI was associated with diminished adrenal cholesterol stores, whereas hepatic SR-BI deficiency resulted in a significant increase in adrenal gland cholesterol content. In both mouse models, CETP had no impact on adrenal cholesterol metabolism. In diet-induced atherosclerosis studies, hepatic SR-BI deficiency accelerated aortic lipid lesion formation in both CETP-expressing (4-fold) and non-CETP-expressing (8-fold) mice when compared with controls. Impaired macrophage to feces reverse cholesterol transport in mice deficient for SR-BI in liver, which was not corrected by CETP, most likely contributed by such an increase in atherosclerosis susceptibility. Finally, comparison of the atherosclerosis burden in SR-BI liver-deficient and fully deficient mice demonstrated that SR-BI exerted an atheroprotective activity in extra-hepatic tissues whether CETP was present or not. These findings support the contention that the SR-BI pathway contributes in unique ways to cholesterol metabolism and atherosclerosis susceptibility even in the presence of CETP.

Epidemiological studies have demonstrated that high density lipoprotein cholesterol is a strong, independent, inverse predictor of the risk of coronary heart disease. High plasma levels of the major apolipoprotein of HDL, APOA-I, have been also shown to predict decreased risk of coronary heart disease. One major atheroprotective mechanism by which HDL/APOA-I may protect against atherosclerosis involves the transport of excess cholesterol from peripheral tissues, including macrophages, to the liver, bile, and eventually feces for excretion, a process known as reverse cholesterol transport.

The scavenger receptor SR-BI is an 82-kDa glycosylated plasma membrane protein that binds HDL/APOA-I with high affinity and stimulates the bi-directional flux of cholesterol between cells and extracellular HDL particles. In mice, SR-BI, encoded by the *Scarb1* gene, is a major determinant of HDL metabolism in mice and is protective against atherosclerosis. Indeed, hepatic overexpression of SR-BI markedly reduces plasma HDL-C levels, increases biliary secretion of cholesterol, and decreases atherosclerosis (1–3), whereas deficiency of this receptor results in elevation of plasma HDL-C with the appearance of large cholesterol rich-HDL particles and is extremely pro-atherogenic (4–7). SR-BI is an important positive regulator of the rate of *in vivo* reverse cholesterol transport (RCT)<sup>3</sup> in mice (8). Indeed, SR-BI has the capacity to mediate the selective cellular uptake of HDL-associated cholesteryl esters in liver (9), thus facilitating a critical step of RCT. SR-BI-mediated HDL-CE selective uptake activity is also important in adrenal glands where it serves to provide cholesterol for steroid hormone synthesis in mice (9). Although SR-BI promotes cellular cholesterol efflux to HDL and LDL acceptors *in vitro*, *in vivo* RCT studies using SR-BI KO macrophages did not support a role of SR-BI, at least in mice, in the initial step of RCT (10).

One important limitation of these studies in extrapolating the importance of SR-BI from murine models to human (patho)-physiology is that mice, in contrast to humans, lack the CE transfer protein (CETP). This 74-kDa hydrophobic plasma glycoprotein transfers CE from HDL to APOB-containing lipoproteins in exchange for triglyceride and therefore exerts a key role in HDL-C metabolism. Moreover, studies in mice suggest

\* This work was supported in part by the French National Institute for Health and Medical Research (INSERM).

[S] The on-line version of this article (available at <http://www.jbc.org>) contains supplemental Figs. S1–S3.

<sup>1</sup> Supported by a Fellowship from the French Ministry of Research.

<sup>2</sup> Supported by a contrat d'interface INSERM-APHP. To whom correspondence should be addressed: INSERM UMR-S 939, Hôpital de la Pitié, Pavillon Benjamin Delessert, 83 Boulevard de l'hôpital, F-75013 Paris, France. Tel.: 33-1-42177860; Fax: 33-1-45828198; E-mail: thierry.huby@upmc.fr.

<sup>3</sup> The abbreviations used are: RCT, reverse cholesterol transport; CETP, cholesteryl ester transfer protein; BMDM, bone marrow-derived macrophage; CE, cholesteryl ester; TC, total cholesterol; FC, free cholesterol.

## SR-BI-mediated Atheroprotection in Human CETP Mice

that CETP expression may increase direct removal of HDL-CE in the liver independently of known lipoprotein receptors (11, 12). Thus, CETP, directly through hepatic selective CE uptake or indirectly through transfer of HDL-CE to APOB-containing lipoproteins with subsequent receptor-mediated liver uptake, could contribute significantly to the RCT pathway in humans. A kinetic study in humans notably suggested that most of the CE output to liver occurred through APOB-containing lipoproteins, with very little from HDL (13). These data, which favor a role of CETP in promoting RCT, are supported by studies performed in mice overexpressing CETP by adenoviral- or adeno-associated virus-mediated gene transfer (14, 15). However, a lack of effect of CETP in modulating RCT in CETP-expressing mice has also been reported and is in contradiction with the latter findings (16–18). In addition, pharmacological inhibition of CETP in humans did not significantly influence fecal sterol excretion (19).

In the present study, we have investigated whether the importance of SR-BI in controlling HDL-C metabolism as previously demonstrated in the mouse, and its overall impact on atherosclerosis, could also be evidenced in the presence of the CETP pathway. Transgenic mice expressing the human CETP gene were bred with our SR-BI conditional KO mouse (4). Our results demonstrate that the quantitative role of SR-BI in regulating the plasma levels of HDL-C was greatly diminished in the presence of CETP. Indeed, HDL metabolic studies clearly revealed that CETP expression markedly accelerated HDL-derived [<sup>3</sup>H]cholesterol removal from plasma in both SR-BI liver-deficient and fully deficient mice, resulting in a significant increase of <sup>3</sup>H-labeled tracer secretion into bile and feces. However, our data also showed that whether CETP was present or not 1) SR-BI activity tightly regulates plasma free to total cholesterol (FC:TC) ratio; elevation of this ratio following liver SR-BI deficiency leading to metabolic disturbances; 2) adrenal SR-BI is critical for adrenal cholesterol content and function; and 3) hepatic SR-BI deficiency results in impaired macrophage to feces RCT. Finally, anti-atherogenic activities mediated by SR-BI in both liver and peripheral tissues could be clearly evidenced under non- and CETP-expressing conditions. Altogether, these data suggest that the SR-BI pathway may be of critical importance in cholesterol homeostasis and, potentially in atherosclerosis, in humans.

### EXPERIMENTAL PROCEDURES

**Animal Models and Diet**—The investigation conformed to the Guide for the Care and Use of Laboratory Animals published by the European Commission Directive 86/609/EEC. All animal procedures were performed at the Central Animal Facility of the Medical Faculty of La Pitié Hospital with approval from the Direction Départementale des Services Vétérinaires, Paris, France. Mice were housed in a conventional animal facility, weaned at 21 days, and fed *ad libitum* a normal mouse chow diet (RM1, Dietex France). All animal models were bred on a pure C57BL/6 background (>10 generations). The SR-BI conditional knock-out mouse model, in which *Scarb1* exon 1 targeted by the CRE recombinase loxP site insertion produced a hypomorphic allele, has been described earlier (4) and was termed the hypomSR-BI mouse. CRE-mediated *Scarb1* gene

inactivation of the hypomorphic SR-BI allele in hepatocytes (hypomSR-BI KO<sup>liver</sup> mice) was obtained through breeding with Alb-CRE transgenic mice (20). SR-BI<sup>-/-</sup> mice were described previously (4) and generated by breeding homozygous animals fed a chow diet containing 0.5% probucol (Sigma). Human CETP transgenic mice, which express CETP under control of its natural flanking regions (NFR-CETP line 5203), were obtained from Jackson Laboratories (Bar Harbor, MC). For atherosclerosis studies, 2-month-old female mice were switched to a 1.25C diet, consisting of 1.25% cholesterol and 20% fat for 20 weeks (standard A04 diet supplemented with 1.25% cholesterol and 16% cocoa butter; SAFE, Augy, France).

**Blood and Tissue Analyses**—Blood samples were collected in Microvette tubes (Sarstedt) by retro-orbital bleeding under isoflurane anesthesia (isoflurane (1.5%), oxygen (0.4 liter/min)). Plasma samples were analyzed with an Autoanalyzer using commercial reagent kits (Roche Diagnostics (total cholesterol), Diasys (free cholesterol), and ThermoElectron (glucose)). Plasma lipoproteins were fractionated by gel filtration on two Superose 6 (Amersham Biosciences) columns connected in series. Endogenous plasma lecithin:cholesterol acyltransferase activity was determined by measuring the decrease in plasma-free cholesterol following incubation at 37 °C in the presence or absence of iodoacetamide (lecithin:cholesterol acyltransferase inhibitor). To determine cholesterol and phospholipids content of red blood cells (RBC), packed RBC were mixed with an equal volume of water to achieve hemolysis. To extract lipids from RBC, a mixture of hexane:isopropyl alcohol, 3:2, was added and samples were mixed. After centrifugation, supernatants were collected, evaporated, and resuspended in isopropyl alcohol. Lipids were measured by enzymatic colorimetric methods. Plasma corticosterone levels were determined by a commercial competitive enzyme immunoassay kit (Immunodiagnostic Systems). To determine cholesterol content in adrenal glands, total lipids were extracted from frozen organs using the Folch procedure.

**Erythrocyte, Reticulocyte, and Platelet Counts**—Absolute count of erythrocytes, reticulocytes, and platelets were performed by flow cytometry (BD LSR Fortessa, BD Biosciences). Whole blood (1 μl) was incubated with either 1 μl of phycoerythrin anti-mouse CD41 (clone MWReg30, eBiosciences) for determination of platelets or 1 μl of each phycoerythrin anti-mouse Ter-119 (clone Ter-119, Miltenyi Biotec) and allophycocyanin anti-mouse CD71 (clone R17 217.1.4, eBiosciences) for determination of erythrocytes and reticulocytes, respectively. After 15 min at room temperature, samples diluted in 0.5 ml of PBS, 0.5% BSA, 2 mM EDTA, and 0.1 ml of counting beads, with an established concentration close to 1000 beads/μl<sup>-1</sup> (FlowCount Fluorospheres, Beckman Coulter), were added to express population counts as absolute number per microliter of whole blood.

**Analysis of Atherosclerotic Plaques**—Atherosclerotic lesions were quantified on serial cross-sections (10 μm) through the aortic root by oil red O staining as previously described (21), with minor modifications. Mice were sacrificed under isoflurane anesthesia and perfused with PBS. Hearts were collected and fixed (Accustain, 10% formalin solution (Sigma) supplemented with 2 mM EDTA and 20 μM butylated hydroxytoluene

at pH 7.4) for 30 min followed by overnight incubation in phosphate-buffered 20% sucrose solution at 4 °C; hearts were subsequently embedded in Tissue-Tek OCT compound (Sakura Finetek). Approximately 40 sections, 10- $\mu$ m thick, were cut through the proximal aorta, spanning the three cusps of the aortic valves. Every eighth section was fixed and stained with oil red O (0.3% in triethylphosphate) for 30 min and then counterstained with Mayer hematoxylin for 1 min. Images were captured using a Zeiss Axiovert 135 microscope and analyzed with Adobe Photoshop 7.0 software (Adobe Systems Inc., CA) and the Image Processing Tool Kit (Reindeer Graphics, NC) plugins. The extent of atherosclerosis was measured with color thresholding to delimit areas of oil red O staining and is reported as mean lesion area of the group of the sections analyzed.

**In Vivo HDL Turnover Studies**—Mouse plasma was incubated with [<sup>3</sup>H]cholesterol (4  $\mu$ Ci/ml) for 16 h at 37 °C. [<sup>3</sup>H]Cholesterol-labeled mouse HDL were then isolated from plasma by sequential ultracentrifugation in the density range of 1.063 < *d* < 1.21 g/ml, dialyzed against PBS and filter-sterilized. Labeled HDL (80  $\mu$ g of HDL protein, 0.4  $\times$  10<sup>6</sup> cpm) were injected in a volume of 200  $\mu$ l by retro-orbital injection in the right eye of the anesthetized mouse. Mice were caged separately on a wire mesh with unlimited access to food and water. Blood samples were collected by retroorbital bleeding (75  $\mu$ l) in the left eye at 3 min, 2 h, and 6 h after injection. 24 h after injection, mice were exsanguinated under isoflurane anesthesia and sacrificed by cervical dislocation. Bile was collected by direct puncture of the gall bladder with a syringe (30-gauge needle) during the initial stage of laparotomy. Mice were then perfused extensively with PBS before harvesting their organs (liver, adrenal glands, kidney, spleen, leg muscle, gonadal white adipose tissue). Bone marrow cells were flushed with PBS from femurs, and cells were depleted of erythrocytes by ACK treatment for 5 min before cell counting. Collected blood was centrifuged and plasma was collected. <sup>3</sup>H radioactivity in plasma was determined by liquid scintillation counting and plasma decay curves for <sup>3</sup>H-labeled tracer were normalized to radioactivity at the initial 3-min time point. Lipids in red blood cells were extracted as described above and [<sup>3</sup>H]cholesterol was counted in the lipid extract. Values were normalized to radioactivity present in plasma at the initial 3-min time point. Collected tissues and feces were treated as described above and counted in a liquid scintillation counter.

**In Vivo Macrophage to Feces RCT Assay**—Macrophage to feces RCT was evaluated *in vivo* using the assay developed by Zhang and colleagues (22), which measures transport of cholesterol from intraperitoneally injected [<sup>3</sup>H]cholesterol-labeled macrophages to plasma, liver, adrenals, and feces. Injected macrophages were derived from bone marrow cells (BMDM) isolated from wild-type C57BL/6 mice. BMDM were flushed with PBS from femurs of freshly euthanized mice. Cells were depleted of erythrocytes by ACK treatment for 5 min and plated for 5 days in DMEM supplemented with penicillin/streptomycin antibiotics, 1 mM glutamine, 10% heat inactivated FBS, and 30% L929 conditioned medium as a source of macrophage colony stimulating factor. BMDM were then cholesterol loaded by adding complete medium supplemented with 50  $\mu$ g/ml of

acetylated LDL protein labeled with 5  $\mu$ Ci of [<sup>3</sup>H]cholesterol/ml, and cultured for two additional days. Cholesterol-loaded and [<sup>3</sup>H]cholesterol-labeled BMDM were detached from plastic by accutase (PAA) treatment, washed, resuspended in PBS at room temperature, and injected (0.5 ml; 5  $\times$  10<sup>6</sup> cells) intraperitoneally. Mice were caged separately on a wire mesh, with unlimited access to food and water, and stools were collected continuously over the next 2 days. At 48 h post-injection, mice were exsanguinated by retro-orbital bleeding under isoflurane anesthesia, sacrificed by cervical dislocation, and then perfused extensively with PBS. Whole livers and adrenal glands were collected, weighed, and flash frozen. <sup>3</sup>H-labeled radioactivity in plasma was determined by liquid scintillation counting and expressed as counts/min/ $\mu$ l of plasma. Pooled plasmas from each group were also fractionated by gel filtration to determine cholesterol mass and <sup>3</sup>H-labeled tracer distribution into lipoproteins. For each mouse, total feces were dried, weighed, soaked in water (1 ml of water/57 mg of desiccated feces; overnight at 4 °C) and mechanically homogenized. Homogenized samples (0.2 ml) were added to 10 ml of liquid scintillation OptiPhase HiSafe 3 (PerkinElmer Life Sciences) mixture and counted in a liquid scintillation counter (Beckman LS 6000IC). <sup>3</sup>H-labeled counts in liver and adrenal glands were determined after homogenization of the tissue in water (~100 mg piece of liver tissue/ml; one adrenal gland/0.4 ml) and counting was performed in a liquid scintillation counter (0.3 and 0.4 ml of homogenized samples combined with 10 ml of OptiPhase HiSafe 3 mixture). For the RCT studies performed with ezetimibe-treated mice, the animals were first accustomed to powdered chow diet (RM1, Dietex France) for 2 weeks, and then switched to the same powdered diet supplemented with 0.005% ezetimibe (Schering-Plough) for 9 days before starting the RCT assay. During the experiment, individually housed mice were also fed the ezetimibe-supplemented diet.

**Statistical Analysis**—One-way analysis of variance and Tukey's post hoc multiple comparison tests were used to assess statistical significance between groups. All statistical analyses were performed using GraphPad Prism software (GraphPad Software, Inc., San Diego, CA). *p* < 0.05 was considered significant.

## RESULTS

**Impact of CETP Expression on Plasma Cholesterol Levels and Hematologic Parameters of SR-BI-deficient Mice**—CETP expression diminishes plasma total cholesterol levels and has a major impact on HDL cholesterol content and particle size in SR-BI<sup>-/-</sup> mice (23, 24). Under chow diet feeding, we also observed that SR-BI<sup>-/-</sup>/CETP mice exhibited a 1.5-fold decrease in plasma TC as compared with non-CETP transgenic animals (Table 1). Decreased plasma TC levels were also observed following CETP expression in mice with either attenuated SR-BI expression (hypomSR-BI) or in mice with CRE-mediated deletion of hepatic SR-BI (hypomSR-BI KO<sup>liver</sup>). Under high cholesterol feeding (1.25C diet), CETP expression also significantly reduced plasma TC in all SR-BI models with the exception of WT animals (Table 2). Analysis of lipoproteins by size exclusion chromatography (Fig. 1, A and C) or by agarose gel electrophoresis (Fig. 1, B and D) revealed that CETP

## SR-BI-mediated Atheroprotection in Human CETP Mice

**TABLE 1**

Plasma cholesterol levels, lecithin:cholesterol acyltransferase (LCAT) activity, hematocrit, and spleen weight of mice fed a chow diet

Values were determined in overnight fasted age-matched mice fed a chow diet. Data represent mean  $\pm$  S.D. Spleen mass was expressed per g of body weight. Lecithin:cholesterol acyltransferase activity is expressed as nanomol of CE transferred/h/ml.

Genotype	Gender	TC	FC:TC	LCAT activity	Hematocrit	Spleen
		mg/dl	%		%	mg/g
WT	F	73 $\pm$ 9	29 $\pm$ 2		47.4 $\pm$ 1.4	3.7 $\pm$ 0.3
	M	94 $\pm$ 3	25 $\pm$ 1	257 $\pm$ 49	48.4 $\pm$ 1.1	3.1 $\pm$ 0.5
WT/CETP	F	68 $\pm$ 13	28 $\pm$ 2		47.0 $\pm$ 2.9	4.2 $\pm$ 0.6
	M	83 $\pm$ 6	25 $\pm$ 1	224 $\pm$ 5	47.9 $\pm$ 0.9	3.0 $\pm$ 0.7
HypomSR-BI	F	130 $\pm$ 12 <sup>a</sup>	30 $\pm$ 1		47.6 $\pm$ 1.7	3.7 $\pm$ 0.3
	M	156 $\pm$ 10 <sup>a</sup>	31 $\pm$ 1 <sup>b</sup>	177 $\pm$ 51	46.9 $\pm$ 2.1	3.1 $\pm$ 0.8
HypomSR-BI/CETP	F	100 $\pm$ 15 <sup>a,c</sup>	31 $\pm$ 2		49.0 $\pm$ 2.6	3.9 $\pm$ 0.6
	M	111 $\pm$ 14 <sup>c</sup>	33 $\pm$ 2 <sup>a</sup>	233 $\pm$ 76	47.5 $\pm$ 2.2	3.1 $\pm$ 0.4
HypomSR-BI KO <sup>liver</sup>	F	176 $\pm$ 13 <sup>a</sup>	49 $\pm$ 5 <sup>a</sup>		45.5 $\pm$ 1.9	5.9 $\pm$ 0.7 <sup>a</sup>
	M	182 $\pm$ 10 <sup>a</sup>	51 $\pm$ 3 <sup>a</sup>	112 $\pm$ 30 <sup>a</sup>	44.7 $\pm$ 2.2 <sup>b</sup>	5.4 $\pm$ 1.5 <sup>a</sup>
HypomSR-BI KO <sup>liver</sup> /CETP	F	110 $\pm$ 9 <sup>a,c</sup>	49 $\pm$ 5 <sup>a</sup>		46.8 $\pm$ 1.6	4.7 $\pm$ 0.4 <sup>b,d</sup>
	M	117 $\pm$ 24 <sup>b,c</sup>	49 $\pm$ 4 <sup>a</sup>	230 $\pm$ 59 <sup>d</sup>	45.1 $\pm$ 2.1 <sup>b</sup>	3.8 $\pm$ 0.6 <sup>c</sup>
SR-BI <sup>-/-</sup>	F	147 $\pm$ 6 <sup>a</sup>	51 $\pm$ 3 <sup>a</sup>		43.1 $\pm$ 1.6 <sup>b</sup>	6.6 $\pm$ 0.6 <sup>a</sup>
	M	137 $\pm$ 14 <sup>a</sup>	52 $\pm$ 6 <sup>a</sup>	106 $\pm$ 50 <sup>b</sup>	42.3 $\pm$ 1.9 <sup>a</sup>	5.9 $\pm$ 1.6 <sup>a</sup>
SR-BI <sup>-/-</sup> /CETP	F	107 $\pm$ 9 <sup>a,c</sup>	47 $\pm$ 3 <sup>a</sup>		43.5 $\pm$ 1.9 <sup>b</sup>	6.2 $\pm$ 0.7 <sup>a</sup>
	M	94 $\pm$ 10 <sup>c</sup>	48 $\pm$ 1 <sup>a</sup>	265 $\pm$ 72 <sup>d</sup>	42.1 $\pm$ 1.6 <sup>a</sup>	4.5 $\pm$ 0.8 <sup>b,d</sup>

<sup>a</sup>  $p < 0.001$ , statistically different from values for control mice.

<sup>b</sup>  $p < 0.05$ , statistically different from values for control mice.

<sup>c</sup>  $p < 0.001$ , statistically different from values for corresponding non-CETP transgenic mice.

<sup>d</sup>  $p < 0.05$ , statistically different from values for corresponding non-CETP transgenic mice.

**TABLE 2**

Plasma lipid levels, hematocrit, and spleen weight of mice fed an atherogenic diet

Values were determined in overnight fasted female mice fed a 1.25% cholesterol diet for 20 weeks. Data represent mean  $\pm$  S.D. Spleen mass was expressed per g of body weight.

Genotype	TC	FC:TC	Hematocrit	Spleen
	mg/dl	%	%	mg/g
WT	85 $\pm$ 17	26 $\pm$ 6	44.3 $\pm$ 3.2	4.3 $\pm$ 1.3
WT/CETP	101 $\pm$ 23	24 $\pm$ 6	44.8 $\pm$ 1.7	4.6 $\pm$ 1.1
HypomSR-BI	180 $\pm$ 20 <sup>a</sup>	27 $\pm$ 2	45.8 $\pm$ 2.9	3.8 $\pm$ 1.0
HypomSR-BI/CETP	158 $\pm$ 15 <sup>a</sup>	27 $\pm$ 2	42.9 $\pm$ 3.8	4.6 $\pm$ 0.9
HypomSR-BI KO <sup>liver</sup>	331 $\pm$ 56 <sup>a</sup>	62 $\pm$ 3 <sup>a</sup>	35.9 $\pm$ 6.2 <sup>a</sup>	22.0 $\pm$ 5.9 <sup>a</sup>
HypomSR-BI KO <sup>liver</sup> /CETP	227 $\pm$ 48 <sup>a,b</sup>	61 $\pm$ 6 <sup>a</sup>	34.4 $\pm$ 3.9 <sup>a</sup>	21.3 $\pm$ 7.6 <sup>a</sup>
SR-BI <sup>-/-</sup>	311 $\pm$ 43 <sup>a</sup>	62 $\pm$ 3 <sup>a</sup>	34.3 $\pm$ 3.9 <sup>a</sup>	25.8 $\pm$ 6.7 <sup>a</sup>
SR-BI <sup>-/-</sup> /CETP	249 $\pm$ 28 <sup>a,c</sup>	62 $\pm$ 3 <sup>a</sup>	35.0 $\pm$ 4.1 <sup>a</sup>	22.2 $\pm$ 5.0 <sup>a</sup>

<sup>a</sup>  $p < 0.001$ , statistically different from values for control mice.

<sup>b</sup>  $p < 0.001$ , statistically different from values for corresponding non-CETP transgenic mice.

<sup>c</sup>  $p < 0.05$ , statistically different from values for corresponding non-CETP transgenic mice.

expression resulted in the disappearance of the large cholesterol-rich HDL particles generated by reduced/deficient hepatic SR-BI expression, thereby demonstrating the capacity of CETP to unload CE from HDL independently of the hepatic SR-BI receptor (Fig. 1). SR-BI deficiency (7, 25), and more precisely hepatic SR-BI deficiency (4), results in a specific accumulation of free cholesterol in plasma, which translates into a >1.5-fold increase in the FC:TC ratio in hypomSR-BI KO<sup>liver</sup> and SR-BI<sup>-/-</sup> mice as compared with controls (Table 1). Reduced endogenous plasma lecithin:cholesterol acyltransferase activity in both SR-BI fully and liver-deficient mouse models (Table 1) corroborated earlier findings of a significant inhibition of the endogenous cholesterol esterification rate in plasma of SR-BI<sup>-/-</sup> mice (26, 27). Interestingly, whereas CETP expression restored plasma lecithin:cholesterol acyltransferase activity to normal in both hypomSR-BI KO<sup>liver</sup> and SR-BI<sup>-/-</sup> mice, it did not change the FC:TC ratio, which remained elevated (Table 1). This observation very strongly reinforces the notion that hepatic SR-BI is a major determinant of plasma FC levels and is in agreement with earlier findings demonstrating a critical role of SR-BI in the clearance of HDL-FC from plasma (28).

It has been previously reported that SR-BI deficiency is associated with mild anemia (29), which is exacerbated by feeding mice a high cholesterol diet (30). Hematocrits were indeed significantly lower in SR-BI<sup>-/-</sup> mice but also in hypomSR-BI KO<sup>liver</sup> mice (Table 1). Upon feeding a 1.25C diet, this anemia was exacerbated in both models (Table 2). Meurs and colleagues (29) have suggested that erythrocyte cholesterol enrichment, as a result of increased plasma FC levels in SR-BI<sup>-/-</sup> mice, reduces the lifespan of erythrocytes and consequently enhances erythropoiesis, which in turn favors reticulocytosis and splenomegaly in these animals. In the present study, circulating erythrocytes in SR-BI<sup>-/-</sup> mice were decreased 1.7-fold as compared with WT controls (Fig. 2A), whereas the amount of immature erythrocytes (reticulocytes) was significantly increased to reach 6.9  $\pm$  1% of the erythrocyte population (as compared with 2.5  $\pm$  0.1% in WT) (Fig. 2B). Invalidation of SR-BI in liver resulted in a similar phenotype, with a 1.8-fold decrease in erythrocyte counts associated with a 3.6-fold elevation in the amount of reticulocytes. CETP had no major impact on the decreased hematocrit of both hypomSR-BI KO<sup>liver</sup> and SR-BI-deficient mice (Tables 1 and 2). However, its expression attenuated erythrocyte abnormalities in both models (Fig. 2, A and B). The splenomegaly present in SR-BI-deficient animals was also less pronounced when they expressed CETP in chow fed (Table 1), but not in high cholesterol fed conditions (Table 2). Thus, it appears that the increased plasma FC levels resulting from SR-BI deficiency cannot solely explain alteration in RBC metabolism. Indeed, CETP expression had no impact on the elevated plasma FC:TC ratio in these mice but partially restored RBC defects. Hypercholesterolemia must also contribute to the altered RBC metabolism in SR-BI-deficient mice. The high plasma FC:TC ratio in SR-BI<sup>-/-</sup> mice has also been correlated with thrombocytopenia (31). If fully deficient and liver-deficient mice for SR-BI similarly displayed diminished platelet counts (~2-fold), CETP expression in the latter model partially restored platelet counts, whereas no significant effect was seen in SR-BI<sup>-/-</sup> mice (Fig. 2C). These results suggest that platelet

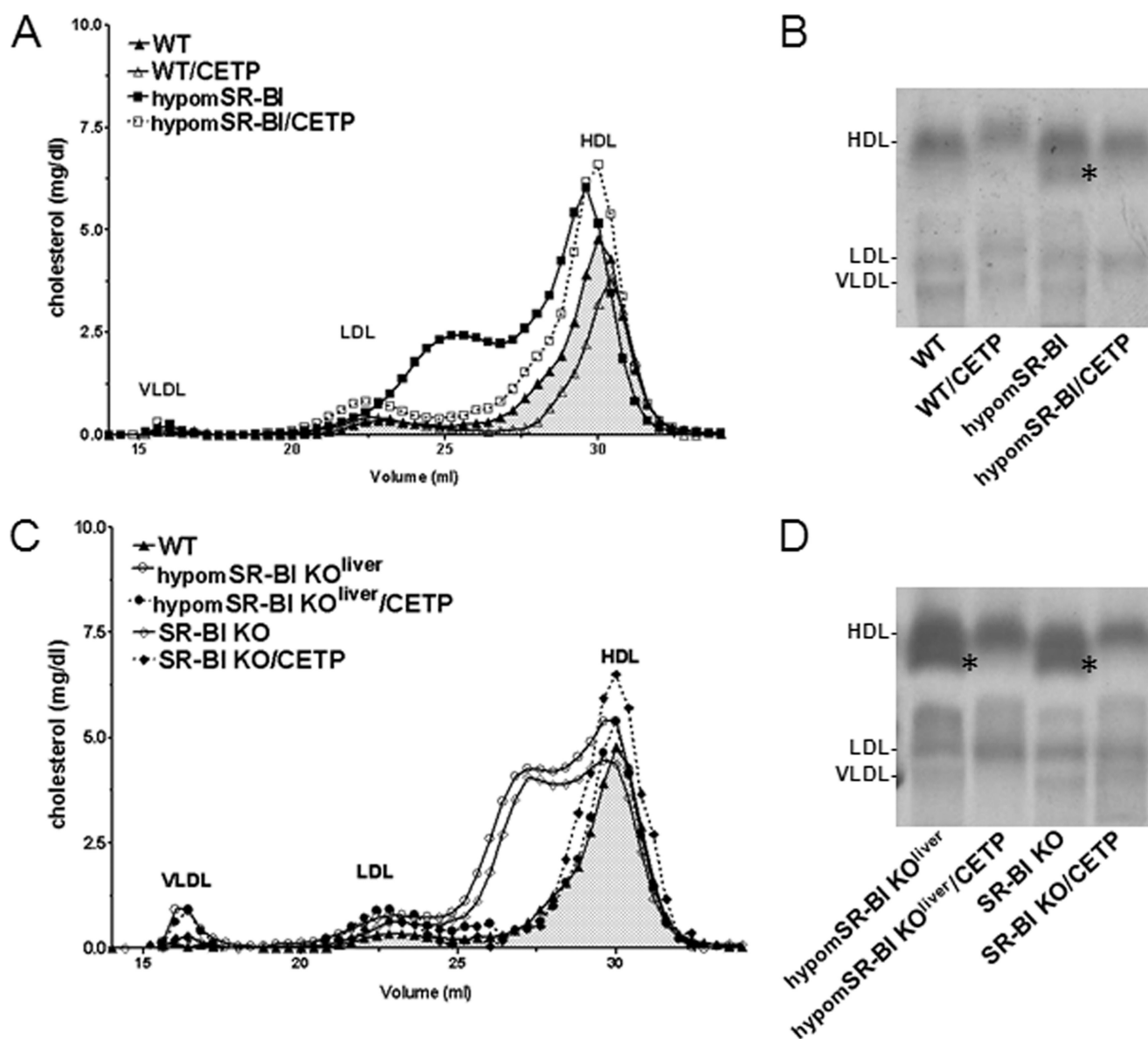


FIGURE 1. Impact of CETP and SR-BI expression on plasma lipoprotein cholesterol profiles of SR-BI-deficient mice. *A* and *C*, fasting plasma samples from 2-month-old male mice fed a chow diet were fractionated by size exclusion chromatography. Total cholesterol was measured in each fraction to determine lipoprotein cholesterol profiles. Approximate elution volumes for particles in the size ranges of VLDL, LDL, and HDL are indicated. *B* and *D*, electrophoretic mobilities of plasma lipoproteins analyzed on agarose gels. Lipoproteins were revealed by Sudan black staining. \* indicates the presence of larger HDL exhibiting a lower electronegativity.

SR-BI deficiency could contribute to thrombocytopenia in SR-BI<sup>-/-</sup>/CETP animals. Finally, it is noteworthy that hypomSR-BI mice (expressing CETP or not) displayed normal erythrocyte, reticulocyte, and platelet counts (Fig. 2) and did not possess enlarged spleens (Tables 1 and 2) as opposed to hypomSR-BI KO<sup>liver</sup> mice. These results further link hepatic SR-BI deficiency to the altered free cholesterol metabolism and as a consequence hematologic disturbances.

*CETP Expression Does Not Modulate Cholesterol Homeostasis in Adrenal Glands nor Adrenal Corticosterone Production*—SR-BI is considered to be primarily responsible for the selective uptake of HDL-CE by the adrenals in mice (9). As a consequence and as previously reported (6), the cholesterol content of adrenal glands of SR-BI<sup>-/-</sup> mice is markedly reduced (5-fold,  $p < 0.001$ ; Fig. 3A). Staining adrenal tissue for neutral lipids

clearly confirmed the presence of significantly less lipid accumulation in the adrenal cortex of these mice (Fig. 3B). Adrenal glands of SR-BI<sup>-/-</sup> mice were equally significantly enlarged (Table 3). Knock-down expression of SR-BI in hypomSR-BI mice was also associated with decreased adrenal cholesterol storage (66% of controls,  $p < 0.05$ ; Fig. 3A), but to a lower extent than that seen in SR-BI<sup>-/-</sup> mice; significantly the adrenals of these animals were of normal size (Table 3). Remarkably, analysis of the adrenal glands of hypomSR-BI KO<sup>liver</sup> mice revealed a 1.3-fold increase in cholesterol content as compared with controls ( $p < 0.05$ ; Fig. 2A) and intense lipid staining of the cortex (Fig. 3B), despite similar adrenal SR-BI expression in this line as compared with those measured in hypomSR-BI mice (Fig. 3C). Hoekstra and co-workers (32) demonstrated that adrenal glucocorticoid-mediated stress response to fasting was

## SR-BI-mediated Atheroprotection in Human CETP Mice

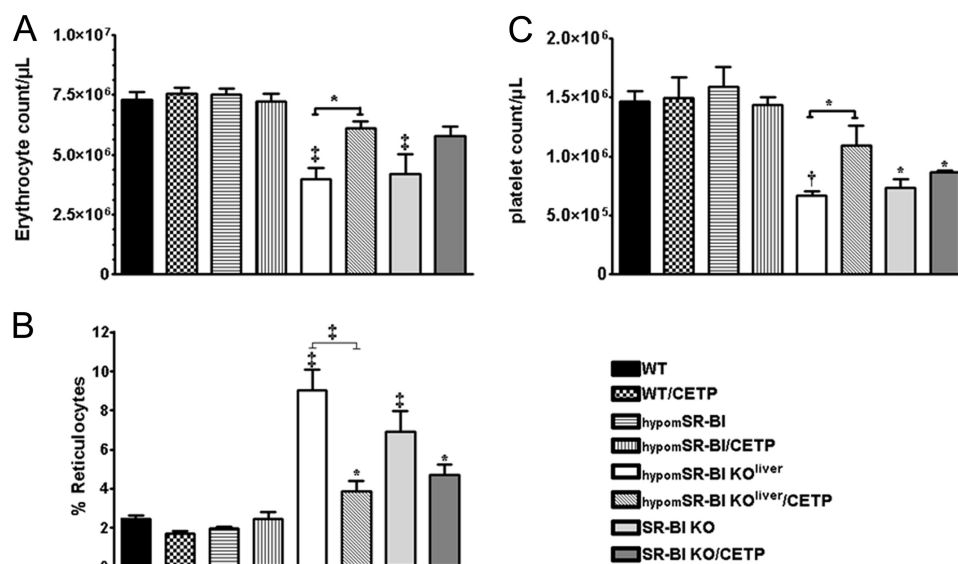


FIGURE 2. **Erythrocyte, reticulocyte, and platelet counts.** Blood isolated from male mice was analyzed by flow cytometry to determine the absolute counts of erythrocytes (A), reticulocytes (expressed as a percentage of total erythrocytes) (B), and platelets (C) ( $n = 4-9$ ; data represent mean  $\pm$  S.E.). \*, †, and ‡ denote a statistical difference versus WT mice or between indicated groups, \*,  $p < 0.05$ ; †,  $p < 0.01$ ; and ‡,  $p < 0.001$ .

impaired in SR-BI<sup>-/-</sup> mice due to adrenal glucocorticoid insufficiency, which led to hypoglycemia. We found similar results, plasma corticosterone and glucose levels being 1.9- and 1.5-fold lower in fasted SR-BI<sup>-/-</sup> female mice than in fasted WT controls, respectively (Table 3). CETP expression had no impact on cholesterol stores and weight of the adrenals of any of the mouse models studied nor did it influence plasma corticosterone and glucose levels following overnight fasting (Fig. 3 and Table 3).

To determine whether changes in adrenal cholesterol content were associated with changes in the expression of genes involved in cellular cholesterol homeostasis, we performed real time PCR quantification. The gene expression profile was consistent with a normal adaptive response of adrenal cortical cells to variation in their intracellular cholesterol status via SREBP2-mediated transcriptional gene regulation to either reduce (hypomSR-BI KO<sup>liver</sup>) or increase (hypomSR-BI, SR-BI<sup>-/-</sup>) cholesterol uptake through the LDL-r pathway and cholesterol biosynthesis and, via LXR-mediated regulation to limit (hypomSR-BI, SR-BI<sup>-/-</sup>) or enhance (hypomSR-BI KO<sup>liver</sup>) cellular cholesterol efflux (Fig. 3C). The lack of effect of CETP expression on adrenal cholesterol stores was confirmed at the mRNA level because expression levels of cholesterol-responsive genes in adrenals of WT, hypomSR-BI, hypomSR-BI KO<sup>liver</sup>, or SR-BI<sup>-/-</sup> mice were similar whether these mouse models expressed CETP or not (Fig. 3C).

**CETP Expression Fails to Restore Impaired Macrophage to Feces RCT in SR-BI-deficient Mice**—CETP reduces plasma HDL-C levels in SR-BI-deficient mice, potentially providing an alternative pathway to RCT. We therefore evaluated the impact of CETP on the metabolic fate of mouse HDL-derived cholesterol in SR-BI liver-deficient and fully deficient female mice fed a 1.25C diet for 4 weeks. As previously reported (9), [<sup>3</sup>H]cholesterol-HDL was cleared more slowly from plasma in SR-BI-deficient mice than in WT animals (Fig. 4A). CETP expression in SR-BI<sup>-/-</sup> mice accelerated clearance of the <sup>3</sup>H-labeled tracer

from plasma to an even faster rate than that observed in WT. 24 h after labeled HDL injection, <sup>3</sup>H-labeled tracer was found markedly reduced in liver and bile of SR-BI<sup>-/-</sup> mice, whereas SR-BI<sup>-/-</sup> mice expressing CETP displayed comparable <sup>3</sup>H-counts to WT controls (Fig. 4B). As expected from these results, CETP expression in SR-BI<sup>-/-</sup> mice resulted in a significant increase in <sup>3</sup>H-counts in feces (3.5-fold,  $p < 0.001$ ). However, the amount of <sup>3</sup>H-labeled tracer recovered in feces of SR-BI<sup>-/-</sup>/CETP mice was still below that found in feces of WT (1.5-fold,  $p < 0.001$ ). If no difference in <sup>3</sup>H-counts was notable between the mouse models in kidney and spleen (also in white adipose tissue, bone marrow cells, and muscle, data not shown), SR-BI-deficient mice ( $\pm$ CETP) displayed a 6-fold decrease in radioactivity in their adrenals as compared with WT (Fig. 4B). These data are in agreement with diminished adrenal cholesterol store in SR-BI<sup>-/-</sup> mice (Fig. 3) and further confirm the lack of effect of CETP expression on adrenal cholesterol homeostasis in mice. In addition, we also found that the amount of <sup>3</sup>H-labeled tracer was doubled in erythrocytes of SR-BI<sup>-/-</sup>/CETP mice, but also of SR-BI<sup>-/-</sup> mice, as compared with WT (Fig. 4B). These results are in agreement with a specific enrichment in cholesterol measured in erythrocytes of SR-BI-deficient mice expressing CETP or not ( $\sim$ 1.4-fold elevation in the cholesterol to phospholipid ratio; supplemental Fig. S1). Finally, [<sup>3</sup>H]cholesterol-HDL injection in hypomSR-BI, hypomSR-BI KO<sup>liver</sup>, and hypomSR-BI KO<sup>liver</sup>/CETP mice provided similar results as those found with the mice fully deficient for SR-BI (supplemental Fig. S2). Thus, these HDL metabolic studies confirmed the capacity of CETP to accelerate impaired RCT from plasma HDL in SR-BI-deficient mice (or SR-BI liver-deficient mice). This CETP-dependent effect most likely contributed to the net loss of plasma cholesterol observed in all SR-BI mouse models expressing CETP.

We next sought to evaluate whether CETP expression had the potential to stimulate the impaired macrophage to feces RCT associated with SR-BI deficiency. [<sup>3</sup>H]Cholesterol-labeled

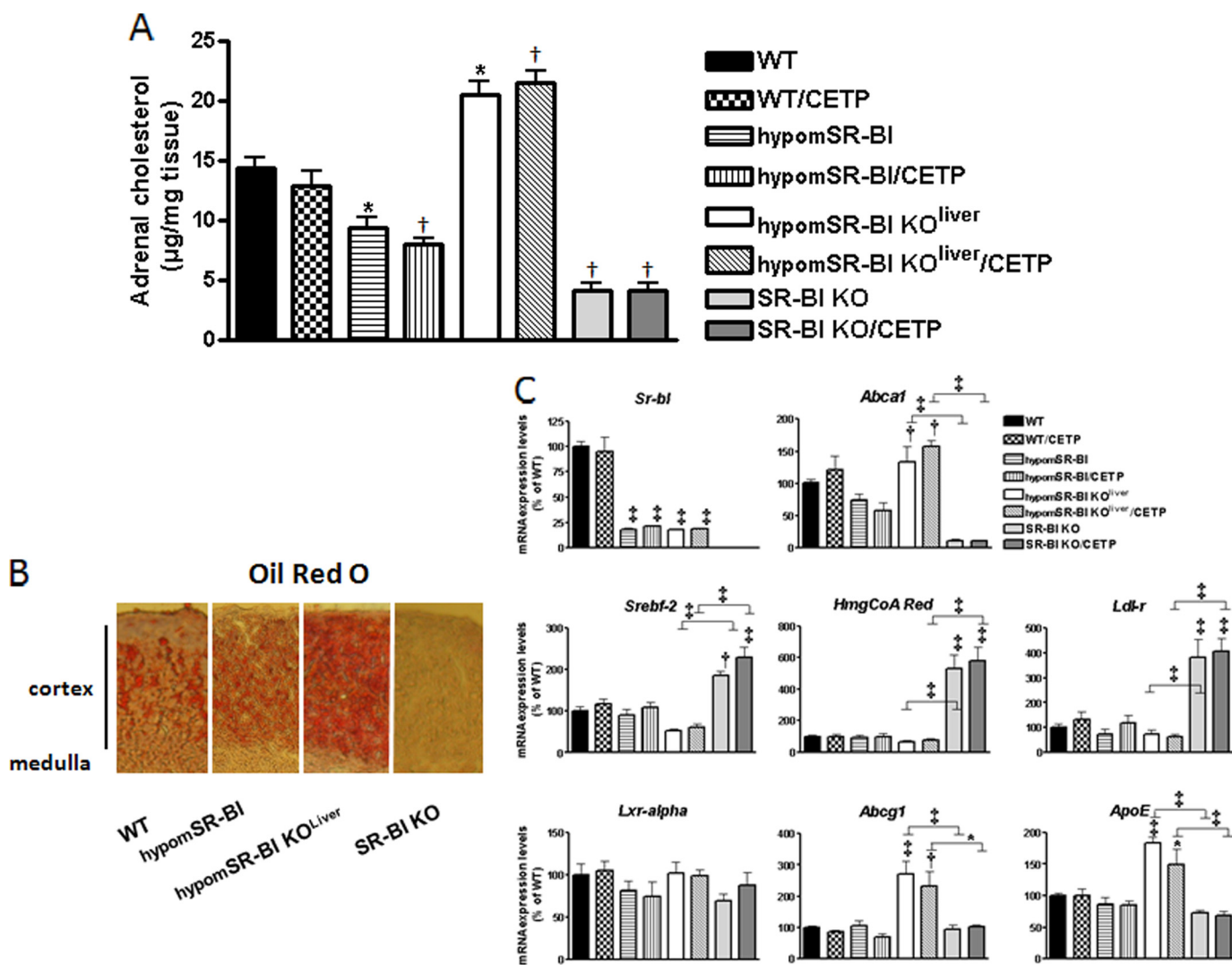


**FIGURE 3. Impact of CETP and SR-BI expression on adrenal cholesterol content and gene expression profiling.** A, cholesterol content of adrenal glands of fasting 3-month-old mice was determined after lipid extraction ( $n = 8-18$ ; data represent mean  $\pm$  S.E.). \* and † statistically different from values for WT mice, \* $p < 0.05$ ; † $p < 0.001$ . Cryosections of adrenal glands were analyzed for lipids by ORO staining (B). Adrenal gene expression profiling of mice fed a chow diet was obtained by quantitative PCR analysis. For each gene, values were normalized to hypoxanthine-guanine phosphoribosyltransferase and plotted relative to those of wild-type mice set at 100% ( $n = 5-6$ ; data represent mean  $\pm$  S.E.). \*, †, and ‡ denote a statistical difference versus WT mice or between indicated groups, \* $p < 0.05$ ; † $p < 0.01$ ; ‡ $p < 0.001$ .

**TABLE 3**

**Adrenal weight and plasma corticosterone and glucose levels of fasted mice**

Values were determined in overnight fasted 3-month-old female mice fed a chow diet. Data represent mean  $\pm$  S.D. Adrenal mass was expressed per g of body weight.

Genotype	Adrenals mg/g	Corticosterone ng/ml	Glucose mg/dl
WT	0.12 $\pm$ 0.02	164 $\pm$ 34	126 $\pm$ 31
WT/CETP	0.13 $\pm$ 0.03	151 $\pm$ 29	130 $\pm$ 14
HypomSR-BI	0.13 $\pm$ 0.02	175 $\pm$ 56	131 $\pm$ 28
HypomSR-BI/CETP	0.13 $\pm$ 0.01	149 $\pm$ 45	131 $\pm$ 33
HypomSR-BI KO <sup>liver</sup>	0.13 $\pm$ 0.01	145 $\pm$ 28	129 $\pm$ 33
HypomSR-BI KO <sup>liver</sup> /CETP	0.13 $\pm$ 0.02	157 $\pm$ 19	131 $\pm$ 33
SR-BI <sup>-/-</sup>	0.20 $\pm$ 0.03 <sup>a</sup>	88 $\pm$ 23 <sup>b</sup>	80 $\pm$ 16 <sup>b</sup>
SR-BI <sup>-/-</sup> /CETP	0.21 $\pm$ 0.03 <sup>a</sup>	87 $\pm$ 20 <sup>b</sup>	90 $\pm$ 13 <sup>b</sup>

<sup>a</sup>  $p < 0.001$ , statistically different from values for WT mice.

<sup>b</sup>  $p < 0.05$ , statistically different from values for WT mice.

bone marrow-derived macrophages were injected in WT, hypomSR-BI KO<sup>liver</sup>, and hypomSR-BI KO<sup>liver</sup>/CETP mice. Plasma [<sup>3</sup>H]cholesterol was substantially increased in hypomSR-BI KO<sup>liver</sup> mice as compared with WT, but was lowered

in CETP-expressing hypomSR-BI KO<sup>liver</sup> mice (Fig. 5A); reflecting plasma cholesterol mass in these models (Fig. 1 and Table 1). The amount of <sup>3</sup>H-sterol measured per mg of liver and feces over 48 h was significantly reduced in both hypomSR-BI KO<sup>liver</sup> and hypomSR-BI KO<sup>liver</sup>/CETP mice as compared with controls. However, <sup>3</sup>H values were not different between these two models (Fig. 5A). These data are indicative of a decreased rate of macrophage to feces RCT in SR-BI liver-deficient mice, as previously reported in the animals that were fully deficient (8). However, if CETP expression significantly accelerated RCT from plasma HDL in hypomSR-BI KO<sup>liver</sup> mice (supplemental Fig. S2), it had no effect on impaired macrophage to feces RCT (Fig. 5A). A similar result was also found in the context of a functional (WT mice) or an impaired RCT pathway due to complete SR-BI deficiency (supplemental Fig. S3A).

To further evaluate whether an impact of CETP on macrophage to feces RCT rate could be evidenced in SR-BI-deficient mice by increasing the flux of cholesterol in the animals, we fed

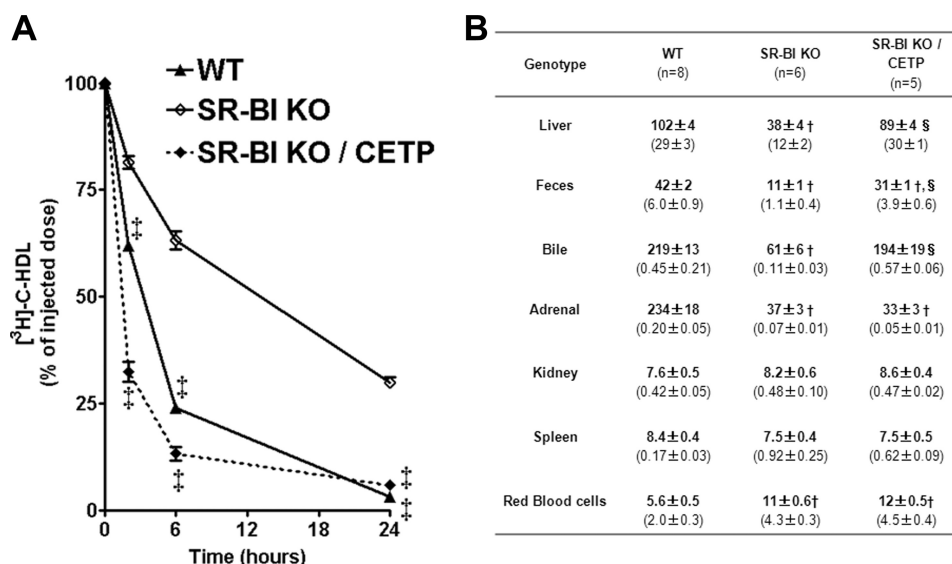


FIGURE 4. **Impact of CETP and SR-BI expression on the metabolic fate of HDL-C.** A, plasma decay over 24 h of [ $^3\text{H}$ ]cholesterol-labeled mouse HDL injected in wild-type, SR-KO, and SR-BI KO/CETP female mice fed a 1.25C diet. † statistically different from values for SR-BI KO mice at the indicated time point. B, 24 h post-injection the animals were sacrificed and the tissue distribution of radioactivity was determined. Data are expressed as cpm/mg of wet tissue or dried feces, except for bile and bone marrow cells for which values are expressed as cpm/ $\mu\text{L}$  and cpm/million cells, respectively. Values represent mean  $\pm$  S.E. Values in parentheses correspond to the percentage of the injected dose present in the organ. \* and †, statistically different from values for WT mice, \*,  $p < 0.05$ ; †,  $p < 0.001$ . ‡ and §, statistically different from values for SR-BI KO mice, ‡,  $p < 0.05$ ; §,  $p < 0.001$ .

WT and SR-BI $^{-/-}$  mice expressing or not CETP a 1.25C diet for 4 weeks before performing an *in vivo* RCT assay (Fig. 5B). [ $^3\text{H}$ ]Cholesterol was equilibrated in the plasma of cholesterol-fed mouse models in proportion to their cholesterol mass (Table 2). As expected, the amount of [ $^3\text{H}$ ]cholesterol tracer detected in liver, feces, and adrenals of SR-BI $^{-/-}$  mice was statistically significantly lower (1.6-, 2.2-, and 2.6-fold, respectively) than those measured for WT. Results obtained with WT/CETP and SR-BI $^{-/-}$ /CETP mice did not differ from those of WT and SR-BI $^{-/-}$  mice, respectively, further confirming a lack of effect of CETP in promoting macrophage to feces RCT in our experimental conditions.

Using similar *in vivo* RCT studies, Sehayek and Hazen (33) have recently reported that decreased cholesterol absorption through ezetimibe treatment significantly increases fecal cholesterol excretion; thereby supporting a major role of intestinal cholesterol absorption in RCT in mice. Thus, we evaluated whether treating our animal models with ezetimibe could reveal an effect of CETP on the RCT rate, which could have been masked in our previous experiments by elevation of intestinal cholesterol (re)-absorption in CETP-expressing mouse models. Ezetimibe treatment of WT animals resulted in an  $\sim$ 2-fold increase in fecal  $^3\text{H}$ -sterol excretion as compared with non-treated WT controls (supplemental Fig. S3B). However, CETP expression resulted in no significant change in the amount of  $^3\text{H}$ -labeled tracer measured in liver, feces, and adrenals in both ezetimibe-treated WT and SR-BI-deficient mouse models.

*The Atheroprotective Activities Mediated by SR-BI in Liver and Peripheral Tissues Are Conserved under CETP Expressing Conditions*—We previously clearly evidenced a SR-BI dose-dependent effect on the development of atherosclerosis when comparing WT, hypomSR-BI, hypomSR-BI KO $^{\text{liver}}$ , and SR-BI $^{-/-}$  mice fed an inflammatory and atherogenic (cholesterol

and cholate-containing) diet (4). The impact of CETP expression on atherogenesis in these various mouse lines was evaluated by feeding female mice a 1.25C diet for 20 weeks. This diet resulted in a moderate elevation of plasma TC as compared with chow-fed conditions (Tables 1 and 2), but more cholesterol was found associated with VLDL-sized lipoproteins in all models (Fig. 6, A and B). Expression of CETP in WT background was pro-atherogenic as previously reported (34) and resulted in a 1.7-fold increase in mean lipid lesion area (Fig. 6C). Knock-down expression of SR-BI in hypomSR-BI mice is equally pro-atherogenic (4) and led to a similar increase in atherosclerosis as compared with WT. Interestingly, the size of lipid lesions in hypomSR-BI and hypomSR-BI/CETP mice were not different ( $71 \pm 14 \times 10^3 \mu\text{m}^2$  and  $72 \pm 26 \times 10^3 \mu\text{m}^2$ , respectively), despite reduced plasma TC levels in CETP-expressing mice (Table 2). However, whereas CETP activity tended to increase HDL-C levels in normal-sized HDL particles (large HDL were not detectable in hypomSR-BI/CETP mice), it also led to a major increase in VLDL-C, suggesting dual pro- and anti-atherogenic actions of CETP in hypomSR-BI mice with a neutral effect on atherosclerosis susceptibility. Fed the 1.25C diet, SR-BI liver-deficient and fully deficient mice had a further increase in their plasma FC:TC ratio, which reached a value of  $0.62 \pm 0.03$  for both models (Table 2). Deletion of hepatic SR-BI was highly atherogenic and a further 4.1-fold increase in the size of lipid lesions ( $295 \pm 53 \times 10^3 \mu\text{m}^2$ ) was observed in hypomSR-BI KO $^{\text{liver}}$  mice as compared with hypomSR-BI mice (Fig. 6C). Despite similar lipoprotein cholesterol profiles (Fig. 6B), plasma TC and FC:TC levels (Table 2), SR-BI $^{-/-}$  mice exhibited an even greater susceptibility to atherosclerotic lesion development as compared with hypomSR-BI KO $^{\text{liver}}$  animals ( $p < 0.05$ ). These data further support the conclusions of our previous study of a peripheral atheroprotective role mediated by SR-BI (4). In these SR-BI-



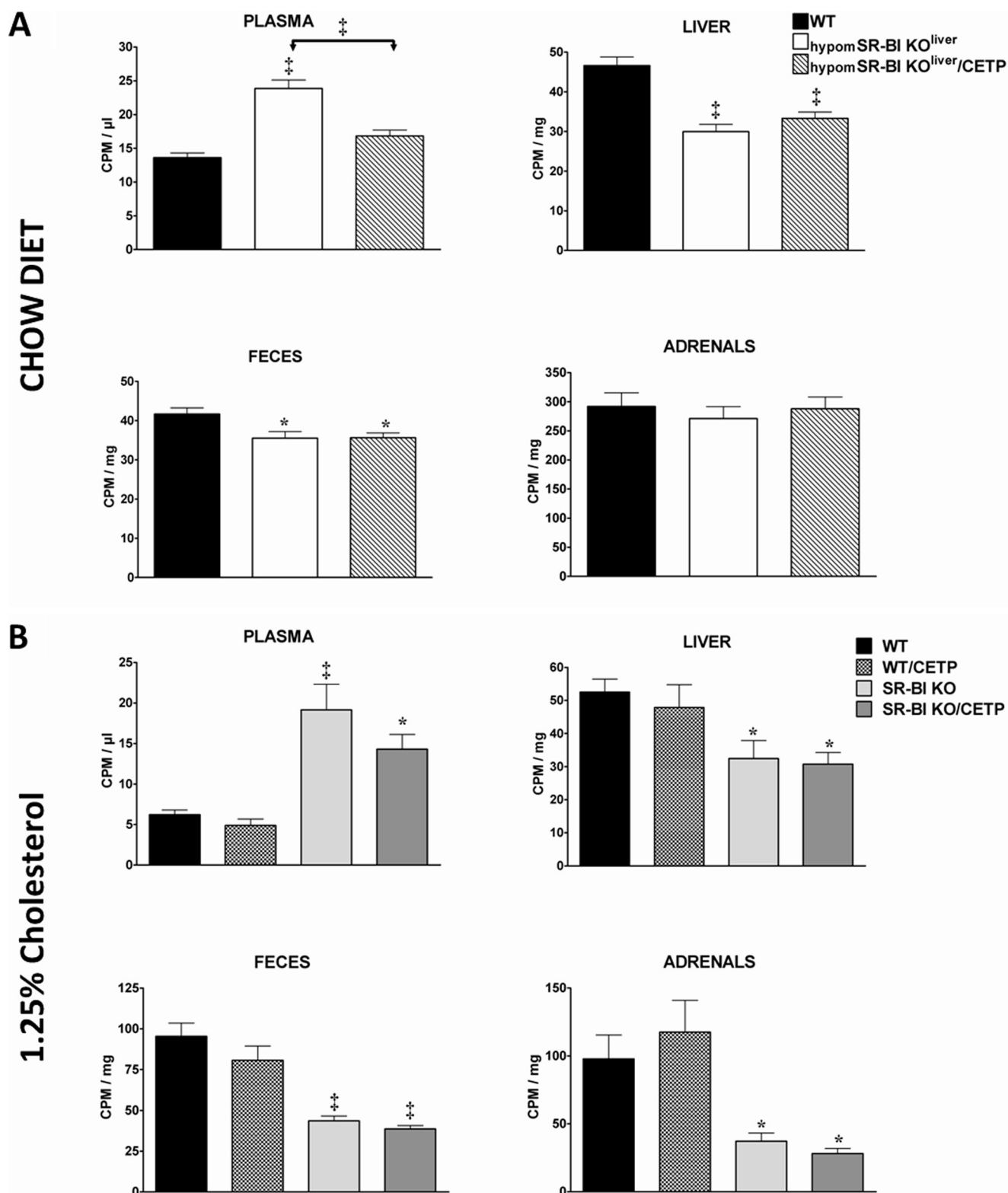
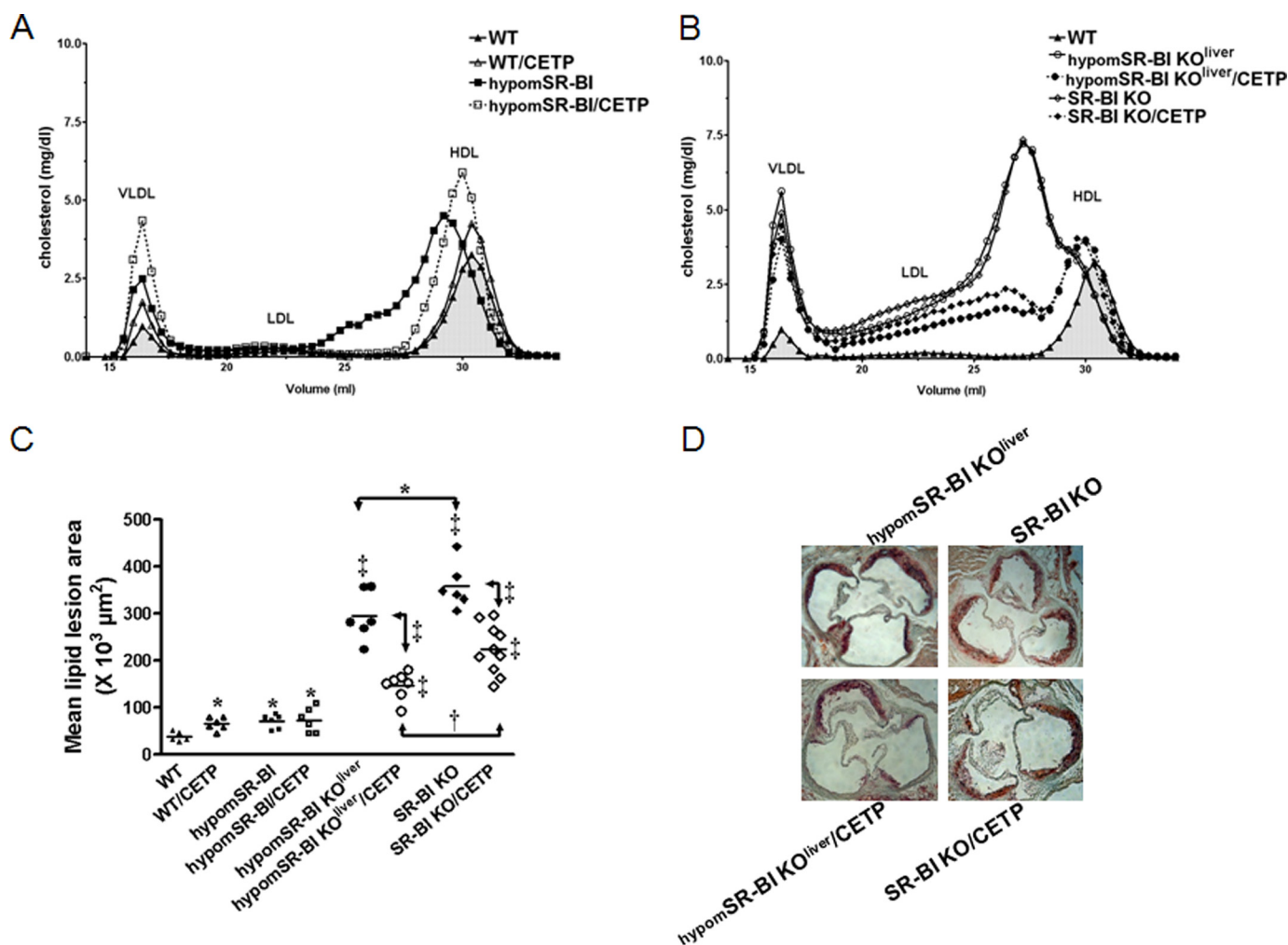


FIGURE 5. *In vivo* macrophage to feces RCT studies. Mice were injected intraperitoneally with [<sup>3</sup>H]cholesterol-labeled BM-derived macrophages and the amount of radioactivity present in plasma, liver, feces, and adrenals was determined 48 h later. RCT experiments were performed in 3–4-month-old (A) female mice ( $n = 7$ ) fed a chow diet and (B) male mice ( $n = 6$ ) fed a 1.25C diet (1.25% cholesterol, 20% fat) for 4 weeks. Data represent mean  $\pm$  S.E. \*,  $p < 0.05$ ; †,  $p < 0.01$ ; ††,  $p < 0.001$ .

deficient mouse models, CETP expression markedly lowered plasma TC levels (Table 2) by primarily reducing the amount of cholesterol present in large HDL particles, albeit without fully normalizing the HDL-C profile in both mouse models. VLDL-C

appeared also slightly diminished in CETP-expressing mice as compared with non-CETP transgenics (Fig. 6B). These changes were associated with a marked reduction in atherosclerosis susceptibility in both hypomSR-BI KO<sup>liver</sup>/CETP and SR-

## SR-BI-mediated Atheroprotection in Human CETP Mice



**FIGURE 6. Evaluation of the atheroprotective activities mediated by SR-BI in liver and peripheral tissues in mice expressing CETP or not and fed an atherogenic 1.25C diet.** A and B, plasma lipoprotein cholesterol profiles of female mice fed the 1.25C diet for 20 weeks. C, degree of atherosclerosis in the aortic root area. Lipid deposits were visualized by ORO staining of aortic root sections. Each symbol represents the mean lesion area in a single mouse. The horizontal bar indicates the mean value for the respective group. \*, †, and ‡ denote a statistical difference versus WT mice or between indicated groups, \*,  $p < 0.05$ ; †,  $p < 0.01$ ; ‡,  $p < 0.001$ . D, representative images of ORO staining of aortic root sections.

BI<sup>-/-</sup>/CETP mice as compared with hypomSR-BI KO<sup>liver</sup> ( $p < 0.001$ ) and SR-BI<sup>-/-</sup> ( $p < 0.001$ ) mice, respectively (Fig. 6, C and D). Interestingly and as observed for non-CETP transgenic models, hypomSR-BI KO<sup>liver</sup>/CETP exhibited less aortic lipid lesions than SR-BI<sup>-/-</sup>/CETP mice (1.5-fold,  $p < 0.01$ ) at comparable plasma cholesterol distribution (Fig. 6C) and levels (Table 2).

### DISCUSSION

In this study, we have shown that CETP expression in mice almost fully masked any variations in SR-BI expression and its consequences on modulating plasma HDL-C levels (and HDL particle size), most likely by promoting plasma HDL-C clearance. However, our data also highlighted that CETP expression could not compensate for the lack of SR-BI in adrenal glands to ensure cholesterol supply and normal function, and in hepatocytes to regulate the amount of plasma free cholesterol, and as a consequence erythrocyte cholesterol content, and to promote macrophage to feces RCT. These hepatic SR-BI activities most likely contributed to the major atheroprotective role of SR-BI. Importantly, we demonstrated that in a similar lipoprotein context and in the presence

or absence of the CETP pathway, residual peripheral SR-BI expression contributed to significant atheroprotection.

Complete deletion of SR-BI in mice has been associated with an impaired RCT, whereas overexpression of SR-BI in the liver promoted macrophage RCT (8). We confirmed that SR-BI<sup>-/-</sup> mice exhibited a decreased rate of cholesterol transport from plasma HDL and macrophages but, we also demonstrated that deletion of SR-BI in the liver led to similar results. These new findings strongly suggest that hepatic SR-BI expression directly regulates the rate of RCT, most probably through hepatic uptake of HDL-C. However, an indirect role of hepatic SR-BI in modulating the capacity of HDL particle to mobilize cholesterol from macrophages due to changes in their composition/structure cannot be fully excluded. In fact, if the large CE-rich HDL particles present in hypomSR-BI KO<sup>liver</sup> mice almost disappeared in CETP transgenic mice, the plasma FC:TC ratio remained elevated; a condition that may not favor peripheral cellular cholesterol efflux. Our results also support the notion that the RCT rate cannot be predicted as a function of the steady-state plasma concentration of HDL-C/APOA-I.

CETP-mediated transfer of CE from HDL to VLDL/LDL particles with subsequent uptake primarily by hepatic LDL-r constitutes a major quantitative route for delivery of cholesterol to the liver in humans. The capacity of CETP to significantly accelerate RCT from plasma HDL in liver-deficient mice clearly demonstrated that this pathway does not rely on a functional hepatic SR-BI receptor. However, animal studies that have been undertaken to demonstrate a direct contribution of CETP in accelerating macrophage to feces RCT have led to contradictory results (14–18). Studies that reported a role of CETP in RCT have used either [<sup>3</sup>H]cholesterol-labeled RAW264.7 or J774 cells in their *in vivo* RCT assay (14, 15). These macrophage cell lines do not produce APOE (35). Yet, this apolipoprotein is very abundantly secreted from macrophages (35, 36) and macrophage-derived APOE plays a critical role in promoting macrophage-RCT (37). Whether the lack of effect of CETP on the RCT rate in our studies could be due to the fact that [<sup>3</sup>H]cholesterol originating from macrophages essentially through an endogenous APOE-dependent efflux pathway is primarily directed to the liver in an APOE-dependent manner for excretion remains an intriguing possibility. In RCT studies performed with macrophage cell lines that do not express APOE, [<sup>3</sup>H]cholesterol efflux from macrophage could rely more on exogenous HDL/APOA-I acceptors and may be more directly subjected to CETP-mediated transfer to VLDL/LDL for subsequent liver uptake, allowing demonstration of a role of CETP in promoting RCT under these experimental conditions.

Circulating HDL is a major source of cholesterol for steroid synthesis in mice and SR-BI is uniquely responsible for the selective uptake of HDL-CE in this organ (9). Decreased adrenal steroidogenesis in members of a family heterozygous for a functional mutation (P297S) in the *SCARB1* gene suggests that the HDL/SR-BI tandem also plays a critical function in regulating adrenal function in humans (38). In this study, moderate and severe adrenal cholesterol depletion in hypomSR-BI mice, which exhibit reduced SR-BI expression, and SR-BI<sup>-/-</sup> mice, respectively, further support the key contribution of SR-BI to adrenal cholesterol supply. However, it is striking that hypomSR-BI KO<sup>liver</sup> mice expressing CETP or not accumulated cholesterol in their adrenal glands, whereas they also displayed attenuated adrenal SR-BI expression. As suggested above, a high plasma FC:TC ratio in these mice may alter the bidirectional cholesterol movement between adrenal cortical cell membranes and extracellular cholesterol acceptors; limiting cellular cholesterol efflux and/or favoring SR-BI-mediated cholesterol influx. Additional studies are required to investigate these potential mechanisms. Nevertheless, our results further highlight the key role of SR-BI in RCT and emphasize the fact that suppression of the hepatic step of this pathway may affect cellular cholesterol homeostasis in peripheral tissues, even when CETP is present.

In the recent report of Vergeer *et al.* (38), heterozygous carriers of the P297S SR-BI mutation, who displayed increased HDL cholesterol levels, did not seem to develop more atherosclerosis than family noncarriers (38). In this regard, it is interesting to note that if knockdown expression of SR-BI has been systematically associated with increased atherogenesis in mice (4, 5, 39), reduced levels of SR-BI in mice expressing CETP was

not pro-atherogenic despite an elevation of plasma TC (hypomSR-BI/CETP *versus* WT/CETP; Table 2). These results suggest that remodeling of HDL particles by CETP, despite being associated with an increase in circulating levels of VLDL-C (Fig. 6), may counterbalance the pro-atherogenic consequences of the attenuated levels of SR-BI. By contrast, in the context of a complete absence of hepatic SR-BI, and thus of impaired RCT, CETP activity conferred only partial atheroprotection. Most importantly, additional deletion of residual SR-BI expression in extrahepatic tissues favored atherosclerosis development in a comparable manner whether CETP was present or not. Thus, using different atherogenic diets (1.25% cholesterol-enriched diets containing cholate (4) or not (this study)) and in different contexts of cholesterol transport (presence or absence of CETP), we clearly demonstrated the peripheral atheroprotective role mediated by SR-BI. Whether such a protective role relies on the multiligands receptor nature of SR-BI, its function in steroidogenic tissues for cholesterol supply, its activities in promoting endothelial repair (40), in facilitating endothelial nitric oxide (NO) production (41), or inversely in protecting against NO cytotoxicity (42), or as a modulator of the inflammatory response in macrophages (43) remains to be established. Cross-breeding of the hypomSR-BI mouse model with cell-specific CRE transgenic lines should provide valuable mouse models to investigate these possibilities.

In conclusion, on the foreground of these studies it can be postulated that SR-BI plays a critical function in the liver in regulating the flux of circulating free cholesterol and acts as an anti-atherogenic molecule, potentially in various tissues, in species that express CETP or not. However, it can also be foreseen that variations in hepatic SR-BI activity shall not translate into major changes in the plasma concentrations of cholesterol in CETP-expressing species, and notably in humans. In this context and in the framework of the actual development of CETP inhibitors as pharmacological lipid-modulating agents, the potential use of such agents in individuals with homozygous loss-of-function mutations in the *SCARB1* gene could favor a highly atherogenic situation.

## REFERENCES

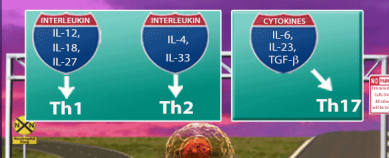
1. Kozarsky, K. F., Donahee, M. H., Rigotti, A., Iqbal, S. N., Edelman, E. R., and Krieger, M. (1997) *Nature* **387**, 414–417
2. Ueda, Y., Gong, E., Royer, L., Cooper, P. N., Francone, O. L., and Rubin, E. M. (2000) *J. Biol. Chem.* **275**, 20368–20373
3. Ueda, Y., Royer, L., Gong, E., Zhang, J., Cooper, P. N., Francone, O., and Rubin, E. M. (1999) *J. Biol. Chem.* **274**, 7165–7171
4. Huby, T., Doucet, C., Dacet, C., Ouzilleau, B., Ueda, Y., Afzal, V., Rubin, E., Chapman, M. J., and Lesnik, P. (2006) *J. Clin. Invest.* **116**, 2767–2776
5. Huszar, D., Varban, M. L., Rinninger, F., Feeley, R., Arai, T., Fairchild-Huntress, V., Donovan, M. J., and Tall, A. R. (2000) *Arterioscler. Thromb. Vasc. Biol.* **20**, 1068–1073
6. Rigotti, A., Trigatti, B. L., Penman, M., Rayburn, H., Herz, J., and Krieger, M. (1997) *Proc. Natl. Acad. Sci. U.S.A.* **94**, 12610–12615
7. Van Eck, M., Twisk, J., Hoekstra, M., Van Rij, B. T., Van der Lans, C. A., Bos, I. S., Kruijt, J. K., Kuipers, F., and Van Berkel, T. J. (2003) *J. Biol. Chem.* **278**, 23699–23705
8. Zhang, Y., Da Silva, J. R., Reilly, M., Billheimer, J. T., Rothblat, G. H., and Rader, D. J. (2005) *J. Clin. Invest.* **115**, 2870–2874
9. Out, R., Hoekstra, M., Spijkers, J. A., Kruijt, J. K., van Eck, M., Bos, I. S., Twisk, J., and Van Berkel, T. J. (2004) *J. Lipid Res.* **45**, 2088–2095

10. Wang, X., Collins, H. L., Ranalletta, M., Fuki, I. V., Billheimer, J. T., Rothblat, G. H., Tall, A. R., and Rader, D. J. (2007) *J. Clin. Invest.* **117**, 2216–2224
11. Gauthier, A., Lau, P., Zha, X., Milne, R., and McPherson, R. (2005) *Arterioscler. Thromb. Vasc. Biol.* **25**, 2177–2184
12. Zhou, H., Li, Z., Silver, D. L., and Jiang, X. C. (2006) *Biochim. Biophys. Acta* **1761**, 1482–1488
13. Schwartz, C. C., VandenBroek, J. M., and Cooper, P. S. (2004) *J. Lipid Res.* **45**, 1594–1607
14. Tchoua, U., D'Souza, W., Mukhamedova, N., Blum, D., Niesor, E., Mizrahi, J., Maugeais, C., and Sviridov, D. (2008) *Cardiovasc. Res.* **77**, 732–739
15. Tanigawa, H., Billheimer, J. T., Tohyama, J., Zhang, Y., Rothblat, G., and Rader, D. J. (2007) *Circulation* **116**, 1267–1273
16. Rotllan, N., Calpe-Berdiel, L., Guillaumet-Adkins, A., Süren-Castillo, S., Blanco-Vaca, F., and Escolà-Gil, J. C. (2008) *Atherosclerosis* **196**, 505–513
17. Harada, L. M., Amigo, L., Cazita, P. M., Salerno, A. G., Rigotti, A. A., Quintão, E. C., and Oliveira, H. C. (2007) *Atherosclerosis* **191**, 313–318
18. Stein, O., Dabach, Y., Hollander, G., Ben-Naim, M., Halperin, G., and Stein, Y. (2002) *Atherosclerosis* **164**, 73–78
19. Brousseau, M. E., Diffenderfer, M. R., Millar, J. S., Nartsupha, C., Asztalos, B. F., Welty, F. K., Wolfe, M. L., Rudling, M., Björkhem, I., Angelin, B., Mancuso, J. P., Digenio, A. G., Rader, D. J., and Schaefer, E. J. (2005) *Arterioscler. Thromb. Vasc. Biol.* **25**, 1057–1064
20. Postic, C., and Magnuson, M. A. (2000) *Genesis* **26**, 149–150
21. Lesnik, P., Haskell, C. A., and Charo, I. F. (2003) *J. Clin. Invest.* **111**, 333–340
22. Zhang, Y., Zanotti, I., Reilly, M. P., Glick, J. M., Rothblat, G. H., and Rader, D. J. (2003) *Circulation* **108**, 661–663
23. Harder, C., Lau, P., Meng, A., Whitman, S. C., and McPherson, R. (2007) *Arterioscler. Thromb. Vasc. Biol.* **27**, 858–864
24. Hildebrand, R. B., Lammers, B., Meurs, I., Korporeal, S. J., De Haan, W., Zhao, Y., Kruijt, J. K., Praticò, D., Schimmel, A. W., Holleboom, A. G., Hoekstra, M., Kuivenhoven, J. A., Van Berkel, T. J., Rensen, P. C., and Van Eck, M. (2010) *Arterioscler. Thromb. Vasc. Biol.* **30**, 1439–1445
25. Braun, A., Zhang, S., Miettinen, H. E., Ebrahim, S., Holm, T. M., Vasile, E., Post, M. J., Yoerger, D. M., Picard, M. H., Krieger, J. L., Andrews, N. C., Simons, M., and Krieger, M. (2003) *Proc. Natl. Acad. Sci. U.S.A.* **100**, 7283–7288
26. Lee, J. Y., Badeau, R. M., Mulya, A., Boudyguina, E., Gebre, A. K., Smith, T. L., and Parks, J. S. (2007) *J. Lipid Res.* **48**, 1052–1061
27. Ma, K., Forte, T., Otvos, J. D., and Chan, L. (2005) *Arterioscler. Thromb. Vasc. Biol.* **25**, 149–154
28. Ji, Y., Wang, N., Ramakrishnan, R., Sehayek, E., Huszar, D., Breslow, J. L., and Tall, A. R. (1999) *J. Biol. Chem.* **274**, 33398–33402
29. Meurs, I., Hoekstra, M., van Wanrooij, E. J., Hildebrand, R. B., Kuiper, J., Kuipers, F., Hardeman, M. R., Van Berkel, T. J., and Van Eck, M. (2005) *Exp. Hematol.* **33**, 1309–1319
30. Holm, T. M., Braun, A., Trigatti, B. L., Brugnara, C., Sakamoto, M., Krieger, M., and Andrews, N. C. (2002) *Blood* **99**, 1817–1824
31. Dole, V. S., Matuskova, J., Vasile, E., Yesilaltay, A., Bergmeier, W., Bernimoulin, M., Wagner, D. D., and Krieger, M. (2008) *Arterioscler. Thromb. Vasc. Biol.* **28**, 1111–1116
32. Hoekstra, M., Ye, D., Hildebrand, R. B., Zhao, Y., Lammers, B., Stitzinger, M., Kuiper, J., Van Berkel, T. J., and Van Eck, M. (2009) *J. Lipid Res.* **50**, 1039–1046
33. Sehayek, E., and Hazen, S. L. (2008) *Arterioscler. Thromb. Vasc. Biol.* **28**, 1296–1297
34. Marotti, K. R., Castle, C. K., Boyle, T. P., Lin, A. H., Murray, R. W., and Melchior, G. W. (1993) *Nature* **364**, 73–75
35. Werb, Z., and Chin, J. R. (1983) *J. Cell Biol.* **97**, 1113–1118
36. Kockx, M., Guo, D. L., Huby, T., Lesnik, P., Kay, J., Sabaretnam, T., Jary, E., Hill, M., Gaus, K., Chapman, J., Stow, J. L., Jessup, W., and Kritharides, L. (2007) *Circ. Res.* **101**, 607–616
37. Zanotti, I., Pedrelli, M., Poti, F., Stomeo, G., Gomaschi, M., Calabresi, L., and Bernini, F. (2011) *Arterioscler. Thromb. Vasc. Biol.* **31**, 74–80
38. Vergeer, M., Korporeal, S. J., Franssen, R., Meurs, I., Out, R., Hovingh, G. K., Hoekstra, M., Sierts, J. A., Dallinga-Thie, G. M., Motazacker, M. M., Holleboom, A. G., Van Berkel, T. J., Kastelein, J. J., Van Eck, M., and Kuivenhoven, J. A. (2011) *N. Engl. J. Med.* **364**, 136–145
39. Kocher, O., Yesilaltay, A., Shen, C. H., Zhang, S., Daniels, K., Pal, R., Chen, J., and Krieger, M. (2008) *Biochim. Biophys. Acta* **1782**, 310–316
40. Seetharam, D., Mineo, C., Gormley, A. K., Gibson, L. L., Vongpatanasin, W., Chambliss, K. L., Hahner, L. D., Cummings, M. L., Kitchens, R. L., Marcel, Y. L., Rader, D. J., and Shaul, P. W. (2006) *Circ. Res.* **98**, 63–72
41. Yuhanna, I. S., Zhu, Y., Cox, B. E., Hahner, L. D., Osborne-Lawrence, S., Lu, P., Marcel, Y. L., Anderson, R. G., Mendelsohn, M. E., Hobbs, H. H., and Shaul, P. W. (2001) *Nat. Med.* **7**, 853–857
42. Li, X. A., Guo, L., Asmis, R., Nikolova-Karakashian, M., and Smart, E. J. (2006) *Circ. Res.* **98**, e60–65
43. Guo, L., Song, Z., Li, M., Wu, Q., Wang, D., Feng, H., Bernard, P., Daugherty, A., Huang, B., and Li, X. A. (2009) *J. Biol. Chem.* **284**, 19826–19834

Take the Road Less Traveled.

**Bioactive Recombinant  
Cytokines & Chemokines**

• Manufacturer of 170+ Proteins • Functional Testing on Every Lot



 BioLegend®



## Adrenocortical Scavenger Receptor Class B Type I Deficiency Exacerbates Endotoxic Shock and Precipitates Sepsis-Induced Mortality in Mice

This information is current as of June 24, 2014.

Sophie Gilibert, Lauriane Galle-Treger, Martine Moreau, Flora Saint-Charles, Sara Costa, Raphaëlle Ballaire, Philippe Couvert, Alain Carrié, Philippe Lesnik and Thierry Huby

*J Immunol* published online 16 June 2014

<http://www.jimmunol.org/content/early/2014/06/16/jimmunol.1303164>

**Supplementary Material** <http://www.jimmunol.org/content/suppl/2014/06/16/jimmunol.1303164.DCSupplemental.html>

**Subscriptions** Information about subscribing to *The Journal of Immunology* is online at: <http://jimmunol.org/subscriptions>

**Permissions** Submit copyright permission requests at: <http://www.aai.org/ji/copyright.html>

**Email Alerts** Receive free email-alerts when new articles cite this article. Sign up at: <http://jimmunol.org/cgi/alerts/etoc>

*The Journal of Immunology* is published twice each month by  
The American Association of Immunologists, Inc.,  
9650 Rockville Pike, Bethesda, MD 20814-3994.  
Copyright © 2014 by The American Association of  
Immunologists, Inc. All rights reserved.  
Print ISSN: 0022-1767 Online ISSN: 1550-6606.



# Adrenocortical Scavenger Receptor Class B Type I Deficiency Exacerbates Endotoxic Shock and Precipitates Sepsis-Induced Mortality in Mice

Sophie Gilibert,<sup>\*,†,‡</sup> Lauriane Galle-Treger,<sup>\*,†,‡</sup> Martine Moreau,<sup>\*,†,‡</sup> Flora Saint-Charles,<sup>\*,†,‡</sup> Sara Costa,<sup>\*,†,‡</sup> Raphaëlle Ballaire,<sup>\*,†,‡</sup> Philippe Couvert,<sup>\*,†,‡,§</sup> Alain Carrié,<sup>\*,†,‡,§</sup> Philippe Lesnik,<sup>\*,†,‡,§</sup> and Thierry Huby<sup>\*,†,‡,§</sup>

Scavenger receptor class B type I (SR-BI)-deficient mice display reduced survival to endotoxic shock and sepsis. The understanding of the mechanisms underlying SR-BI protection has been hampered by the large spectrum of SR-BI functions and ligands. It notably plays an important role in the liver in high-density lipoprotein metabolism, but it is also thought to participate in innate immunity as a pattern recognition receptor for bacterial endotoxins, such as LPS. In this study, we sought to determine the tissue-specific contribution of SR-BI in the hyperinflammatory response and high mortality rates observed in SR-BI<sup>-/-</sup> mice in endotoxemia or sepsis. Restoring plasma levels of high-density lipoprotein, which are critical lipoproteins for LPS neutralization, did not improve acute outcomes of LPS injection in SR-BI<sup>-/-</sup> mice. Mice deficient for SR-BI in hepatocytes, endothelial cells, or myeloid cells were not more susceptible to LPS-induced death. However, if SR-BI ablation in hepatocytes led to a moderate increase in systemic inflammatory markers, SR-BI deficiency in myeloid cells was associated with an anti-inflammatory effect. Finally, mice deficient for SR-BI in the adrenal cortex, where the receptor provides lipoprotein-derived cholesterol, had impaired secretion of glucocorticoids in response to stress. When exposed to an endotoxin challenge, these mice exhibited an exacerbated systemic and local inflammatory response, reduced activation of atrophy genes in muscle, and high lethality rate. Furthermore, polymicrobial sepsis induced by cecal ligation and puncture resulted in early death of these animals. Our study clearly demonstrates that corticoadrenal SR-BI is a critical element of the hypothalamic-pituitary-adrenal axis to provide effective glucocorticoid-dependent host defense after an endotoxic shock or bacterial infection. *The Journal of Immunology*, 2014, 193: 000–000.

**S** scavenger receptor class B type I SCARB1, whose alias SR-BI is most commonly used, is a multiligand cell-surface receptor expressed in a large variety of tissues and most abundantly in corticoadrenal cells (1). Its role in high-density lipoprotein (HDL) metabolism has been well established in mice. SR-BI is critical in the reverse cholesterol transport process through mediating the selective uptake of cholesteryl esters from HDL in the liver. Hepatic overexpression of SR-BI markedly reduces

plasma HDL-cholesterol (HDL-C) levels (2), whereas hepatic deficiency results in elevation of plasma HDL-C with the appearance of large cholesterol-rich HDLs (3). Studies in SR-BI<sup>-/-</sup> mice have also highlighted a prominent role of the receptor in providing cholesterol to the adrenal gland. Indeed, SR-BI deficiency is associated with adrenal cholesterol store depletion (4) resulting in glucocorticoid (GC) insufficiency under stress (5). Importantly, the recent description of a family carrying a mutation provided support for similar activities played by SR-BI in adrenal steroidogenesis and HDL metabolism in humans (6).

Sepsis, which results from the spread of bacteria and their products from a focus of infection, represents a significant health problem worldwide. SR-BI<sup>-/-</sup> mice display an extreme phenotype in response to an endotoxic shock, but also to sepsis. They exhibit a hyperinflammatory systemic response to LPS (Gram-negative bacterial cell-wall component) (7, 8) when challenged with a bacterial load (7) or after cecal ligation and puncture (CLP)-induced septic peritonitis (9). Furthermore, SR-BI<sup>-/-</sup> mice exhibit very high mortality rates in LPS-induced (7, 8) or CLP-induced sepsis (9). Various mechanisms could contribute to the protective role of SR-BI against endotoxemia or septic shock. Disturbed HDL structure/composition in SR-BI<sup>-/-</sup> mice could affect the neutralization of LPS by its binding to HDL lipoproteins. SR-BI has also been shown to bind and internalize LPS in its monomerized form or associated with HDL (10). Consistently, reduced hepatic clearance of LPS has been reported in endotoxemic SR-BI<sup>-/-</sup> mice (7, 9). SR-BI, which has been shown to mediate HDL-dependent endothelial-NOS stimulation (11), could also play a protective effect in inhibiting NO-induced cellular damage (8). The capacity of SR-BI to bind LPS (10), but also lipoteichoic acid

\*INSERM Unité Mixte de Recherche\_S 1166, Hôpital de la Pitié-Salpêtrière, F-75013, Paris, France; †Université Pierre et Marie Curie 06, Unité Mixte de Recherche\_S 1166, F-75013, Paris, France; ‡Institute of Cardiometabolism and Nutrition, F-75013, Paris, France; and §Assistance Publique-Hôpitaux de Paris, Hôpital Pitié-Salpêtrière, Service d'Endocrinologie-Métabolisme, F-75013 Paris, France

Received for publication November 25, 2013. Accepted for publication May 17, 2014.

This work was supported by the French National Institute for Health and Medical Research, the University Pierre and Marie Curie, the Fondation de France (Grant 2011-20464), the French National Research Agency (Grant ANR 08-GENO-019-01 and national program "Investissements d'Avenir" ANR-10-IAHU-05), the award of a "Contrat d'Interface" by the Assistance Publique-Hôpitaux de Paris/INSERM (to T.H.), a postdoctoral fellowship from the Lefoulon-Delalande Foundation/Institut de France (to S.G.), and a doctoral fellowship from Région Île-de-France/Domaine d'Intérêt Majeur Cardiovasculaire-Obésité-Rein-Diabète (to L.G.-T.).

Address correspondence and reprint requests to Dr. Thierry Huby, INSERM Unité Mixte de Recherche\_S 1166, Pavillon Benjamin Delessert, Hôpital de la Pitié, 83 Boulevard de l'Hôpital, F-75013, Paris, France. E-mail address: thierry.huby@upmc.fr

The online version of this article contains supplemental material.

Abbreviations used in this article: BM, bone marrow; CETP, cholesteryl-ester transfer protein; CLP, cecal ligation and puncture; GC, glucocorticoid; GN, gastrocnemius; HDL, high-density lipoprotein; HDL-C, HDL-cholesterol; HSPC, hematopoietic stem and progenitor cell; *Irf*, IFN regulatory factor; KO, knockout; SR-BI, scavenger receptor class B type I.

Copyright © 2014 by The American Association of Immunologists, Inc. 0022-1767/14/\$16.00

(cell-wall component of Gram-positive bacteria) (12), bacterial Hsp60 (12), and bacteria (13–15), has led to consideration of this receptor as a pattern recognition receptor that could play a role in innate immunity. In this context, SR-BI has been shown to exert an anti-inflammatory action in LPS-stimulated macrophages, potentially dampening TLR4-mediated NF- $\kappa$ B activation (9, 16), but also interfering with the JNK and P38 signaling pathways (16). A deleterious role for SR-BI has also been reported in granulocytes. Thus, SR-BI-mediated bacterial uptake by granulocytes could facilitate bacterial escape from antibiotic treatment and their subsequent intracellular proliferation (17). Finally, SR-BI<sup>-/-</sup> mice could be more susceptible to endotoxin-induced inflammation and death as the consequence of the protective effects of adrenal SR-BI in maintaining GC production. Thus, corticosterone (predominant GC in rodents) supplementation partially reduced the high mortality rate of endotoxemic SR-BI<sup>-/-</sup> mice (7). However, it remains difficult to dissociate the protective action of administered exogenous GC that would act as an anti-inflammatory molecule per se from that of compensatory mechanisms brought by GC supplementation to adrenal insufficiency. Moreover, conflicting results were observed with SR-BI deficiency in the CLP-induced sepsis model with reports of a lack of (9) or partial protection (17) with GC supplementation.

In this work, we used an SR-BI conditional knockout (KO) mouse model (3) to directly evaluate the effect of SR-BI deletion in either the endothelium, myeloid cells, hepatocyte, or cortico-adrenal cells in the host inflammatory response and its susceptibility to death after an acute endotoxic shock (by LPS injection) or in the more complex situation of polymicrobial sepsis. We also evaluated the impact of restoring the perturbed HDL-C metabolism associated with hepatic SR-BI deficiency.

## Materials and Methods

### Animals

SR-BI KO mice were described previously (3) and were bred with human cholesteryl-ester transfer protein (CETP) transgenic mice (18), which express CETP under control of its natural flanking regions (NFR-CETP line 5203; Jackson Laboratory). Production of homozygous SR-BI KO animals was obtained by feeding breeding pairs a probucol (0.25%)-supplemented diet. SR-BI<sup>+/+</sup> controls were derived from breedings of heterozygous SR-BI<sup>+/-</sup> mice. HypomSR-BI mice, in which SR-BI exon 1 targeting by Cre recombinase loxP sites insertion produced an hypomorphic allele, have been described earlier (3). HypomSR-BI mice were crossed with: 1) Alb-Cre transgenic mice (19) to inactivate SR-BI in hepatocytes (hypomSR-BI KO<sup>liver</sup> mice); 2) LysM-cre mice expressing Cre under the endogenous lysozyme M promoter (*Ly2<sup>tm1(cre)lfo</sup>*; Jackson Laboratory) to generate animals deficient in SR-BI in the myeloid cell lineage (including monocytes, mature macrophages, and granulocytes); 3) Tie2-Cre mice (gift of Dr. Masashi Yanagisawa, University of Texas Southwestern Medical Center, Dallas, TX), which express Cre recombinase under the direction of the receptor tyrosine kinase Tek (Tie2) promoter/enhancer to delete SR-BI in endothelial cells (20); and 4) Sf1-Cre mice (21) to inactivate lox-flanked SR-BI hypomorphic allele throughout the adrenal cortex (hypomSR-BI<sup>ΔAC</sup> mice). All Cre transgenic lines and CETP-expressing animals were hemizygous for the corresponding transgene. Mice, in a C57BL/6 genetic background (>8 generations), were housed in a conventional animal facility, weaned at 21 d, and fed ad libitum a normal mouse chow diet (RM1; Dietex France). The investigation conformed to the Guide for the Care and Use of Laboratory Animals published by the European Commission Directive 86/609/EEC.

### Experimental models of endotoxemia and polymicrobial sepsis

Endotoxic shock was induced by peritoneal injection of LPS (5  $\mu$ g/g; *Escherichia coli* serotype 055:B5; Sigma-Aldrich) and mice were monitored for survival. For some experiments, the animals were anesthetized at different time points for blood sampling after LPS administration, sacrificed by cervical dislocation, and tissues were collected. In endotoxemic shock experiments with fluid resuscitation, mice received i.p. 1 ml saline at 2, 17, and 25 h after LPS injection. For induction of polymicrobial sepsis, the CLP method was performed as described previously (22). In brief, the

cecum of the animals, under isoflurane anesthesia (2% isoflurane/0.2 L O<sub>2</sub>/min), was exposed, ligatured at its external third, punctured through and through with a 22-gauge needle, and a small drop of cecal content was extruded. The cecum was returned to the peritoneal cavity, and the peritoneum and skin were sutured. The animals were resuscitated with an i.p. injection of 0.5 ml saline. Survival was monitored every 12 h for up to 8 d after induction of sepsis.

### Plasma and tissue analyses

Blood samples were collected in EDTA-coated Microvette tubes (Sarstedt) by retro-orbital bleeding using heparinized microhematocrit tubes under isoflurane anesthesia. Plasma samples were stored frozen at -80°C. Plasma corticosterone levels were determined by a competitive enzyme immunoassay kit (DetectX; Arbor Assays). Commercial ELISA kits were used to measure IL-6, IL-10, and TNF- $\alpha$  plasma concentrations (eBioscience). NO (total) plasma levels were determined by a commercial enzymatic colorimetric assay (Enzo Life Sciences), after filtration of the plasma samples through a 10,000 molecular weight cutoff filter (SpinX; Corning), as recommended by the manufacturer. To determine cholesterol content in adrenals, we extracted total lipids from one frozen gland using the method of Blich and Dyer (23). Cholesterol concentration was determined with a commercial enzymatic assay (Roche Diagnostics). Determination of plasma concentrations of endotoxins in LPS-injected mice was performed using a *Limulus* amoebocyte extract-based kit (QCL-1000 assay; Lonza) on plasma samples diluted 1/20,000 and heated during 10 min at 70°C.

### Adrenal histology and immunohistochemical analysis

Adrenals were fixed (Accustain 10% formalin solution; Sigma) for 30 min and then incubated 2 h in a phosphate-buffered 20% sucrose solution at 4°C. Adrenals were subsequently embedded in Tissue-Tek OCT compound (Sakura Finetek). For histology, formalin-fixed sections were stained for neutral lipids with Oil Red O (0.5% in triethylphosphate) for 30 min and then counterstained for nuclei with Mayer hematoxylin for 1 min. For immunohistochemical detection of SR-BI, the tyramide signal amplification fluorescence system (NEL 701; DuPont NEN Research Products) was used. In brief, ethanol-fixed sections were blocked and then incubated with a rabbit polyclonal anti-mSR-BI Ab (24) overnight at 4°C. After washing, sections were subsequently incubated with a biotinylated goat anti-rabbit IgG secondary Ab (2  $\mu$ g/ml; Vector Laboratories), with streptavidin-HRP, and then a fluorophore tyramide solution. The sections were counterstained for nuclei with DAPI included in the Vectashield mounting medium (Vector Laboratories). Images were captured using a Zeiss Axio Imager M2 fluorescence microscope.

### Flow cytometry

Blood was collected in the morning from fed animals (isoflurane anesthesia) by retro-orbital bleeding into EDTA-coated Microvette tubes (Sarstedt). RBCs were lysed in ACK buffer at room temperature, and WBCs were centrifuged, washed, and resuspended in PBS containing 1% BSA and 0.01% sodium azide. Cells were preincubated for 5 min with Fc blocker, and a mixture of Abs was subsequently added for 30 min at 4°C. An LSR Fortessa (BD) was used for multiparameter analysis of stained cell populations. mAb to mouse CD115 (AF598), mAb to mouse CD3 (145-2C11), mAb to mouse CD8 (53-6.7) and mAb to mouse CD44 (IM7) were purchased from eBioscience. mAb to mouse CD45 (30-F11), mAb to mouse CD4 (RM4-5), mAb to mouse CD62L (MEL-14), mAb to mouse CD25 (PC61), mAb to mouse FR4 (12A5), and mAb to mouse Gr1 (Ly6G/Ly6C; RB6-8C5) were purchased from BD Biosciences.

### Analysis of gene expression by real-time PCR

Mice were euthanized by cervical dislocation and perfused with saline. Spleen, adrenal glands, and gastrocnemius (GN) muscle were harvested and immediately snap frozen in liquid nitrogen. The thoracic aorta was dissected out, cleaned of fat, and cut open along its longitudinal axis. Primary endothelial cells were harvested, as previously described (25), by pressing gently the flattened vessel covered by a layer of paper onto a lysine-coated glass slide. Endothelial cells remained adhered to the glass after the vessel was removed and were immediately lysed with RLT lysis buffer (Qiagen) and frozen at -80°C. RNA from tissue specimens (mixed and dispersed in RLT buffer) and lysed endothelial cells were extracted using the RNeasy micro kit (Qiagen). cDNA was synthesized using random hexamer and SuperScript II (Life Technologies) or the transcriptor first-strand cDNA synthesis kit (Roche Applied Science). Quantitative PCR analyses were performed using a LightCycler 480 real-time PCR system and dedicated software (Roche). Initial differences in mRNA quantities were controlled using reference genes *Hprt*, *Hsp90a*, *Rpl13a*, *Nono*, and *18s*.

### Statistical analysis

The statistical significance of the differences between two groups was evaluated using the Student *t* test for unpaired comparisons. One-way ANOVA and Tukey's post hoc multiple comparison tests were used to assess statistical significance between more than two groups. Survival curves were obtained by using the Kaplan–Meier method and compared by the log-rank test. All statistical analyses were performed using GraphPad Prism software (GraphPad Software, San Diego, CA). A *p* value <0.05 was considered significant.

## Results

### Restoring abnormal HDL-C profile in SR-BI<sup>-/-</sup> mice does not protect mice against LPS-induced inflammation and death

Lipoproteins play a critical role in the host's ability to bind and neutralize LPS for subsequent hepatic clearance. We (18) and others (26) have demonstrated that expression of the CETP, which is not naturally expressed in rodents, almost completely restored the abnormal HDL-C distribution in SR-BI<sup>-/-</sup> mice. Indeed, CETP expression resulted in a major reduction in the elevated plasma total cholesterol concentrations and the disappearance of the large cholesterol-rich HDL particles observed in SR-BI<sup>-/-</sup> animals. Thus, to evaluate whether the high susceptibility of SR-BI<sup>-/-</sup> mice to LPS-induced toxic shock was a mere consequence of perturbed HDL metabolism, we challenged SR-BI<sup>-/-</sup> mice expressing or not CETP with a low dose of LPS (Fig. 1). As previously reported, such a low dose was not lethal for SR-BI<sup>+/+</sup> and SR-BI<sup>+/-</sup> animals, whereas SR-BI<sup>-/-</sup> mice died in <48 h. Expression of CETP had no major impact, as the survival curve for SR-BI<sup>-/-</sup>/CETP mice was very similar to that seen for SR-BI<sup>-/-</sup> mice. To evaluate the inflammatory response, we determined plasma levels of TNF- $\alpha$  and those of IL-6 and IL-10 at 2 and 12 h after LPS injection, respectively (Supplemental Fig. 1). SR-BI<sup>-/-</sup> mice exhibited a dramatic increase in those cytokines as previously reported (7). SR-BI<sup>-/-</sup>/CETP displayed also increased cytokine levels, but which were not statistically different from those measured in SR-BI<sup>-/-</sup> mice. Thus, these data suggested that the high susceptibility of SR-BI<sup>-/-</sup> mice to LPS-induced inflammation and death did not result from a reduced neutralization capacity of plasma HDL of these animals.

### Mice deficient for SR-BI in liver exhibit a moderately increased inflammatory response to LPS

To explore the contribution of hepatic SR-BI in protecting mice from an LPS-induced shock, we injected hypomSR-BI KO<sup>liver</sup> (SR-BI<sup>fllox/fllox</sup>; Alb-Cre) animals with a sublethal dose of LPS. Twelve hours after LPS injection, hypomSR-BI KO<sup>liver</sup> mice displayed 5-fold more plasma endotoxins as compared with SR-BI<sup>+/+</sup> and hypomSR-BI (SR-BI<sup>fllox/fllox</sup>) controls (Fig. 2A). This result directly supported previous findings (7) suggesting that hepatic SR-BI plays a role in clearance of LPS from plasma. Plasma levels of

TNF- $\alpha$  were 2- to 3-fold more elevated in hypomSR-BI KO<sup>liver</sup> mice 2 h after LPS injection than in controls (Fig. 2B). Twelve hours after LPS administration, plasma levels of IL-6 and IL-10 were also found to be more elevated (2-fold; *p* < 0.05) in the SR-BI liver-deficient mice. However, the values for the three cytokines reached in hypomSR-BI KO<sup>liver</sup> mice were far less inferior to those measured in SR-BI<sup>-/-</sup> mice, despite the fact that these two models displayed similar plasma endotoxin levels after LPS injection (Fig. 2A, 2B). The moderately increased inflammatory response observed in hypomSR-BI KO<sup>liver</sup> mice was not associated with an increased mortality. Indeed, hypomSR-BI KO<sup>liver</sup> mice survived as controls to LPS, whereas all SR-BI<sup>-/-</sup> mice died within 24 h (Fig. 2C). Administration of a higher dose of LPS resulted in an increased mortality of control (SR-BI<sup>+/+</sup> and hypomSR-BI) and hypomSR-BI KO<sup>liver</sup> mice. However, the survival rates observed were similar for the three groups (Supplemental Fig. 2). Thus, if deletion of SR-BI in the liver resulted in higher levels of circulating endotoxins after LPS challenge and in slight elevation of the inflammatory response, it did not sensitize mice to LPS-induced lethality.

### Mice deficient for SR-BI in the myeloid lineage exhibit a slightly decreased inflammatory response to LPS, whereas endothelial deletion has no impact

We next sought to evaluate the consequences of deleting SR-BI in the myeloid cell lineage or in the vascular endothelium on the inflammatory response after a LPS challenge. HypomSR-BI; LysM-Cre and hypomSR-BI; Tie2-Cre mice were generated to obtain mice deficient for SR-BI in monocyte/macrophages and granulocytes and in endothelial cells, respectively. Interestingly, deletion of SR-BI in myeloid cells resulted in slightly diminished systemic inflammation as revealed by statistically significantly lower plasma levels for TNF- $\alpha$  (1.6-fold) at 2 h and IL-6 (2.2-fold) at 15 h in hypomSR-BI; LysM-Cre mice than in hypomSR-BI matched controls. A trend for decreased levels of the anti-inflammatory cytokine IL-10 was also observed (Fig. 3A). We detected no difference for those cytokines in LPS-treated endothelial SR-BI-deficient mice as compared with controls (Fig. 3B). Both mouse models survived to this endotoxemic challenge (Fig. 3A, 3B).

To explore further the importance of SR-BI in myeloid and endothelial cells in the host's ability to survive bacterial invasion and a septic shock, we used the model of peritoneal sepsis induced by CLP. The median survival time for hypomSR-BI control mice was 81 h. A trend for higher survival rates was observed for both hypomSR-BI; LysM-Cre and hypomSR-BI; Tie2-Cre mouse models (median survival time of 122 and 106 h, respectively), but statistical significance was not reached (Fig. 3C).

### Deletion of SR-BI in the adrenal cortex results in impaired GC response to stress, changes in leukocytes populations, and uncontrolled systemic inflammation and high mortality rate after LPS injection

To directly evaluate the contribution of adrenal SR-BI in protecting mice from LPS-induced shock and death, we generated animals with a deletion of SR-BI in the adrenal cortex (hypomSR-BI<sup>ΔAC</sup>). Lack of SR-BI expression was confirmed by immunohistochemical analysis. Although an intense signal for SR-BI was clearly visible in the zona fasciculata (main site of GC production) of the adrenal cortex of hypomSR-BI mice, no signal could be detected in the adrenals of hypomSR-BI<sup>ΔAC</sup> mice (Fig. 4A). Adrenal glands of hypomSR-BI<sup>ΔAC</sup> mice displayed very similar characteristics to those of SR-BI<sup>-/-</sup> animals. The glands were enlarged (Fig. 4A) and their weight almost doubled (Fig. 4B). Staining adrenal tissue

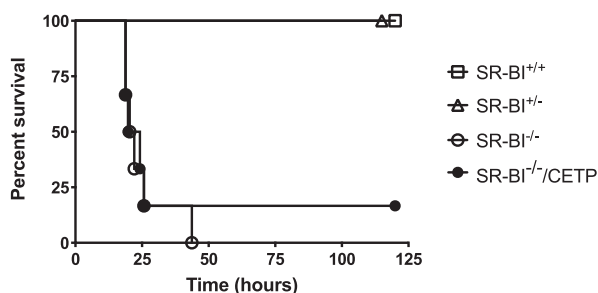


**FIGURE 1.** CETP expression has no major impact on the high susceptibility of SR-BI<sup>-/-</sup> to LPS-induced lethality. Age-matched SR-BI<sup>+/+</sup>, SR-BI<sup>+/-</sup>, SR-BI<sup>-/-</sup>, and SR-BI<sup>-/-</sup>/CETP male mice (*n* = 5–6/group) received an i.p. injection of LPS (5  $\mu$ g/g). Survival was recorded over a period of 5 d (SR-BI<sup>-/-</sup> or SR-BI<sup>-/-</sup>/CETP versus SR-BI<sup>+/+</sup>; *p* < 0.005).



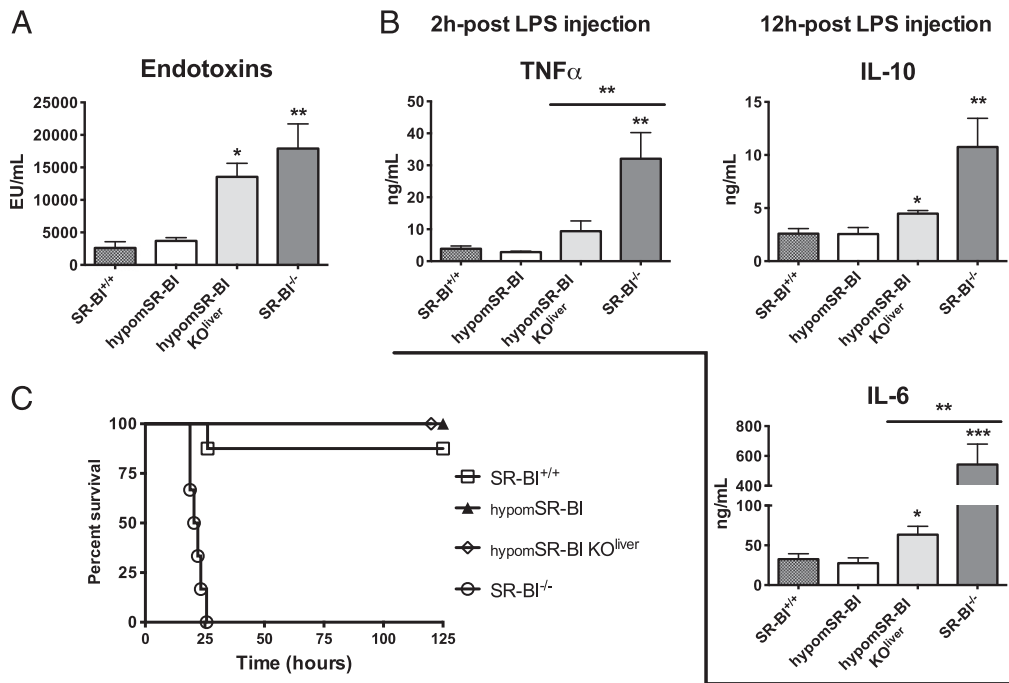


**FIGURE 2.** Hepatic SR-BI-deficient mice exhibit increased plasma endotoxins and increased systemic inflammation in response to LPS. Four-month-old SR-BI<sup>+/+</sup>, hypomSR-BI, hypomSR-BI KO<sup>liver</sup> (hypomSR-BI; Alb-Cre), and SR-BI<sup>-/-</sup> male mice received a single injection of LPS (5  $\mu$ g/g). **(A)** Determination of plasma endotoxins levels was performed at 12 h after LPS injection ( $n = 6-9$ /group). **(B)** Plasma TNF- $\alpha$  levels ( $n = 5-6$ /group) were measured 2 h after LPS injection. Plasma IL-6 and IL-10 levels were determined in a group of mice ( $n = 6-9$ /group) sacrificed 12 h after LPS injection. Values are expressed as means  $\pm$  SEM. \* $p < 0.05$ , \*\* $p < 0.01$ , \*\*\* $p < 0.001$  versus SR-BI<sup>+/+</sup> mice. If values measured for hypomSR-BI KO<sup>liver</sup> or SR-BI<sup>-/-</sup> mice were different, the statistical significance is indicated. **(C)** Survival to LPS (5  $\mu$ g/g body weight) was recorded over a period of 5 d.

for neutral lipids revealed a marked reduction in lipid content of the cortex (Fig. 4A), which likely contributed to the dark red color of the adrenals (Fig. 4A). The cholesterol content of the adrenal glands of hypomSR-BI<sup>ΔAC</sup> mice was reduced  $\sim 2$ -fold (Fig. 4B) and was comparable with that of SR-BI<sup>-/-</sup> mice (18). To evaluate whether depletion in adrenal cholesterol stores in hypomSR-BI<sup>ΔAC</sup> mice was also associated with GC insufficiency, we measured the plasma levels of corticosterone in response to an overnight fasting. If under fed conditions hypomSR-BI and hypomSR-BI<sup>ΔAC</sup> female mice displayed similar morning plasma corticosterone levels, hypomSR-BI mice responded to an overnight fast by increasing their corticosterone concentrations ( $\sim 4$ -fold; Fig. 4C). In contrast, corticosterone levels were found in a similar range under fed and fasted conditions in hypomSR-BI<sup>ΔAC</sup> female mice (Fig. 4C). Thus, hypomSR-BI<sup>ΔAC</sup> mice displayed severe GC insufficiency in response to stress.

Cytometric analysis of blood leukocytes in hypomSR-BI and hypomSR-BI<sup>ΔAC</sup> mice revealed a decrease in the proportion of monocytes in hypomSR-BI<sup>ΔAC</sup> mice (Fig. 4D). More specifically, we observed a specific reduction in the frequency of the Gr1<sup>low</sup> monocyte subset. In contrast, neutrophils were found to be increased by  $\sim 25\%$  ( $p < 0.05$ ). The proportion of CD4<sup>+</sup> and CD8<sup>+</sup> T lymphocytes was not different between hypomSR-BI and hypomSR-BI<sup>ΔAC</sup> mice. However, whereas activated T cells were found in a similar proportion in both groups, hypomSR-BI<sup>ΔAC</sup> mice exhibited a moderate expansion of regulatory T cells ( $0.08 \pm 0.05$  versus  $1.0 \pm 0.05$ ;  $p < 0.01$ ; Fig. 4D). These results suggested that adrenal SR-BI deletion may, in addition to inducing GC insufficiency in response to stress, be associated with chronic adrenal insufficiency affecting the steady-state host immune system.

The response of hypomSR-BI<sup>ΔAC</sup> mice to an endotoxic shock was evaluated as described earlier with a single low dose of LPS. Plasma levels of corticosterone 2 h after LPS administration were

6.5-fold more elevated in hypomSR-BI control mice than in hypomSR-BI<sup>ΔAC</sup> mice (Fig. 5A). Plasma levels of TNF- $\alpha$  and those of IL-6 and IL-10 were found markedly increased in LPS-injected hypomSR-BI<sup>ΔAC</sup> mice as compared with those measured in LPS-injected hypomSR-BI mice (3-, 13-, and 5-fold more elevated, respectively; Fig. 5A). Interestingly, plasma concentrations of NO were found almost 2-fold less elevated in hypomSR-BI<sup>ΔAC</sup> mice. As observed for SR-BI<sup>-/-</sup> mice (Fig. 2B), this low dose of LPS was lethal for hypomSR-BI<sup>ΔAC</sup> mice (Fig. 5B). Indeed, the mortality curves were very similar for SR-BI adrenocortical-deficient and fully deficient mice. Because cardiovascular collapse is often associated with early death when LPS injection is used as a model for endotoxic shock, fluid resuscitation was given during the first hours after LPS injection in an attempt to improve hemodynamic performance and survival of hypomSR-BI<sup>ΔAC</sup> mice. Mortality of the mice was slightly delayed, but all hypomSR-BI<sup>ΔAC</sup> mice died within 40 h (Supplemental Fig. 3). All together, these results clearly showed that mice deleted for SR-BI in the adrenal cortex showed a high susceptibility to LPS-induced inflammation and death.

#### LPS-injected hypomSR-BI<sup>ΔAC</sup> mice display multitissue inflammation and reduced muscle atrophy gene expression

We then explored at the tissue level the impact of an endotoxic shock on gene expression in hypomSR-BI<sup>ΔAC</sup> mice. In the adrenals, the transcription factor gene *Srebpf2*, a main player in the control of cellular cholesterol homeostasis, was upregulated. In agreement, genes involved in cholesterol biosynthesis (*Hmgcr*) and cholesterol uptake (*Ldl-r*), which are target genes of SREBP2 regulation, were markedly increased. *Abca1* gene, a key determinant of cellular cholesterol efflux, was inversely downregulated (Fig. 6A). This gene expression profile was very close to that observed in the adrenals of SR-BI<sup>-/-</sup> mice (18) and of those of

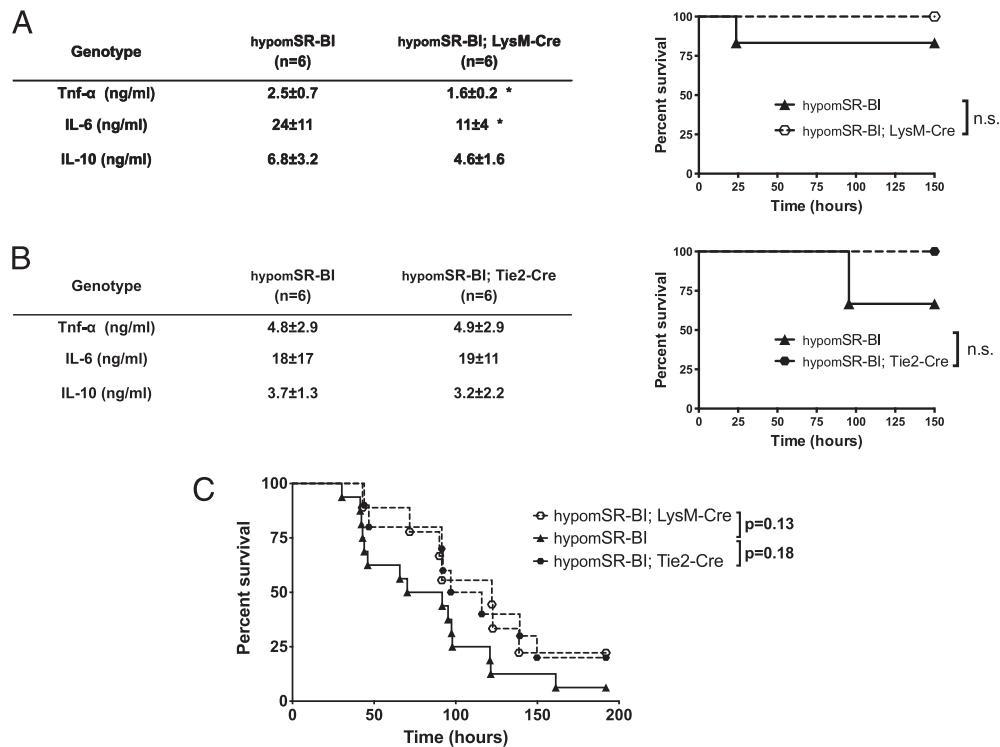


**FIGURE 3.** Deletion of SR-BI in myeloid (LysM-Cre) or endothelial (Tie2-Cre) cells has no major impact on the susceptibility of hypomSR-BI mice to LPS- and CLP-induced lethality. (**A** and **B**) Mice were injected with LPS (5  $\mu$ g/g). Two (TNF- $\alpha$ ) and 15 h (IL-6, IL-10) after LPS injection a small amount of blood was withdrawn for cytokine determination. Survival was recorded over a period of 6 d. Independent experiments were performed with (**A**) 3-month-old hypomSR-BI and hypomSR-BI; LysM-Cre female mice and (**B**) 4-month-old hypomSR-BI and hypomSR-BI; Tie2-Cre male mice. n.s., not statistically different. Values are expressed as mean  $\pm$  SD. \* $p$  < 0.05. (**C**) Three-month-old hypomSR-BI, hypomSR-BI; Tie2-Cre, and hypomSR-BI; LysM-Cre female mice underwent CLP surgery. Survival was recorded over a period of 8 d.

hypomSR-BI $^{\Delta AC}$  mice under basal conditions (data not shown), thus most likely reflecting the adaptive response of cortical cells to the major decrease of their cholesterol content. On the contrary, genes involved in the conversion of cholesterol into pregnenolone, playing a key role in acute regulation of steroid hormone synthesis (*Star*, *Cyp11a*, and *Hsd3B1*), showed similar expression levels in LPS-injected hypomSR-BI and hypomSR-BI $^{\Delta AC}$  mice. Regarding the catecholamine pathway, if the expression of the rate-limiting gene in catecholamine biosynthesis, tyrosine hydroxylase, was similar between the two models, the expression of the phenylethanolamine N-methyltransferase gene, involved in the last step of epinephrine production in chromaffin cells and which is inducible by GC, was reduced 10-fold in hypomSR-BI $^{\Delta AC}$  mice. These results suggested that an impaired response in catecholamines may also contribute to the general phenotype of hypomSR-BI $^{\Delta AC}$  mice after endotoxemia.

The hyperinflammatory state of LPS-treated hypomSR-BI $^{\Delta AC}$  mice was clearly visible at the tissue level. In the spleen, mRNA levels of *Tnf $\alpha$* , *Il-6*, and *Il-1 $\beta$* , which are normally repressed by GC, were markedly increased 15 h post LPS in hypomSR-BI $^{\Delta AC}$  mice as compared with controls (Fig. 6B). However, the proinflammatory macrophage migration inhibitory factor displayed similar levels of expression in the two models. Interestingly, among the targets and mediators of the anti-inflammatory action of GC, the genes encoding for GC-induced leucine zipper and suppressor of cytokine signaling 1 exhibited similar expression in spleens of LPS-treated hypomSR-BI and hypomSR-BI $^{\Delta AC}$  mice. A trend for diminished mRNA levels of the potent anti-inflammatory and immunosuppressive *Il-10* cytokine was observed in hypomSR-BI $^{\Delta AC}$  mice. In contrast, major differences in chemokine expression were noted. In particular, *Mcp1/Ccl2* and

*Cxcl10/Ip-10* were increased 5- to 10-fold in hypomSR-BI $^{\Delta AC}$  mice, whereas *Rantes/Ccl5* mRNA levels were found in a similar range in both mouse models. Of note, IFN regulatory factor (*Irf*) 3, a key mediator of innate immune responses and an essential transcription factor for *Cxcl10* and *Ccl5* activation downstream of TLRs, was significantly decreased in hypomSR-BI $^{\Delta AC}$  mice. This result potentially underlined that differences in the expression of some genes between controls and adrenal SR-BI-deficient mice reflected cell-specific transcriptional responses to GC insufficiency and/or changes in cellular populations in the spleens of these mouse models.

We also explored the inflammatory gene response in the adrenals that, in addition to cortical and medullary endocrine cells, are composed of endothelial, nerve, smooth muscle cells, and leukocytes. An exacerbated response was clearly visible in hypomSR-BI $^{\Delta AC}$  mice 15 h after LPS injection. Notably, *Il-6* mRNA levels were 5-fold more elevated in these animals as compared with controls (Fig. 6A). In contrast, macrophage migration inhibitory factor was found downregulated by 3.5-fold. As seen in spleen, *Ccl2* ( $\times 2.5$ ) and *Cxcl10* ( $\times 12$ ) chemokines were significantly upregulated, along with *Cxcl2/Mip-2* ( $\times 4$ ), but not *Ccl5*. Interestingly, if the mRNA levels of *Tlr2* and *Tlr3* (activated by Gram-positive bacteria and by viral dsRNA, respectively) were more elevated in the adrenals of hypomSR-BI $^{\Delta AC}$  mice, those of *Tlr4*, which plays a central role in cellular activation by LPS, were similar in both groups. Finally, the GC-induced regulatory GC-induced leucine zipper, which was unchanged in spleen, was decreased 5-fold in the adrenals of hypomSR-BI $^{\Delta AC}$  mice. Differences in gene expression profiles between spleens and adrenals were also observed for *Irf* members. If *Irf3* mRNA levels were markedly decreased in both tissues, we observed an important

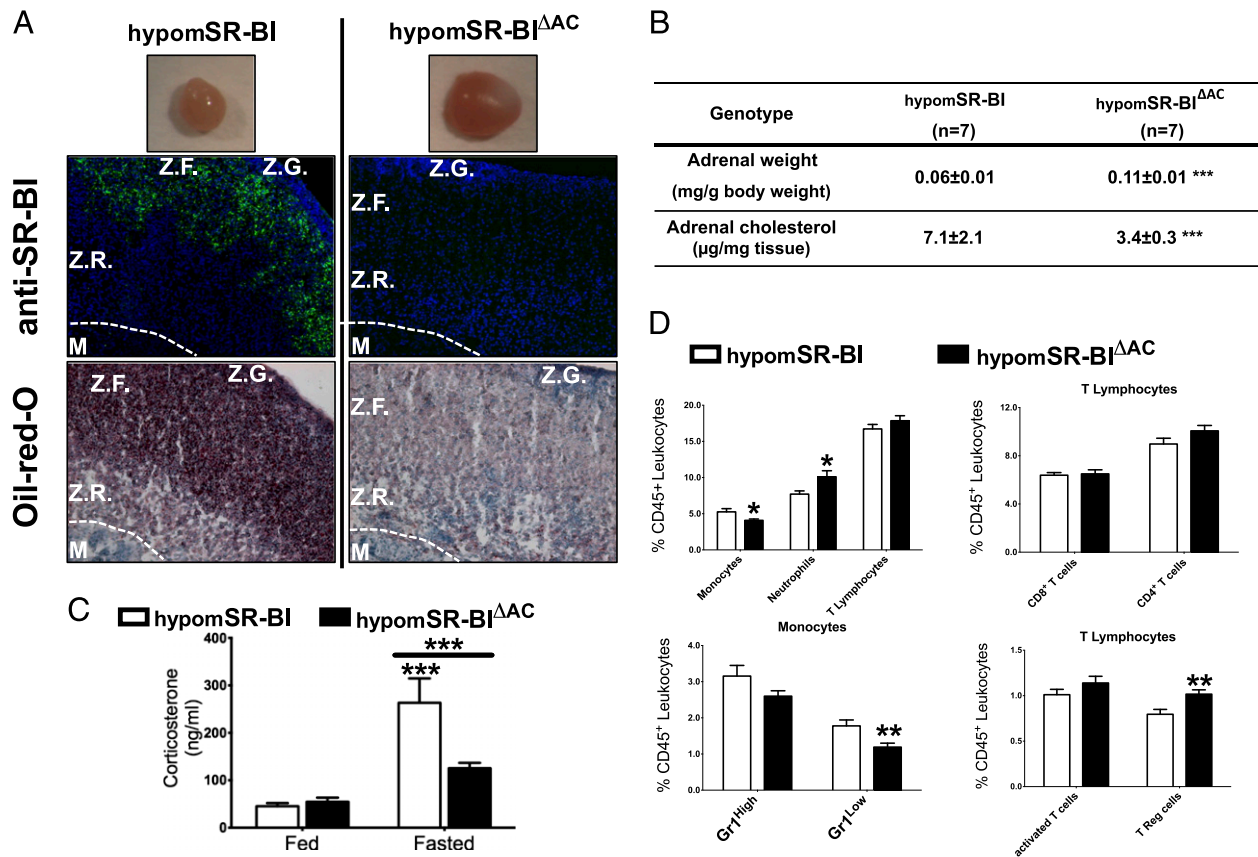


**FIGURE 4.** Phenotypic characterization of hypomSR-BI<sup>ΔAC</sup> mice deficient for SR-BI in the adrenal cortex. **(A, upper panels)** Gross morphology of adrenal glands (original magnification  $\times 10$ ). **(Middle panels)** Cryosections of adrenal glands immunostained for SR-BI (green) and counterstained for nuclei with DAPI (blue). **(Lower panels)** Cryosections of adrenal glands were analyzed for lipids by Oil Red O staining. Hematoxylin was used for nuclear counterstaining (original magnification  $\times 200$ ). Dotted line indicates the separation between the adrenal cortex (Z.R., zona reticularis; Z.F., zona fasciculata; Z.G., zona glomerulosa) and the medulla (M). **(B)** Weight and cholesterol content of adrenal glands. Values are expressed as mean  $\pm$  SD. \*\*\* $p < 0.001$  versus hypomSR-BI mice. **(C)** Plasma corticosterone concentrations were determined in blood samples collected at 10 AM. Blood was collected from hypomSR-BI ( $n = 12$ ) and hypomSR-BI<sup>ΔAC</sup> ( $n = 11$ ) female mice that were fed ad libitum or fasted overnight. **(D)** Flow cytometry analysis of blood leukocytes of 3-mo-old hypomSR-BI ( $n = 9$ ) and hypomSR-BI<sup>ΔAC</sup> ( $n = 10$ ) male mice fed a chow diet. The cell populations of monocytes (CD115<sup>+</sup>; Gr1<sup>+</sup>), neutrophils (CD115<sup>-</sup>; Gr1<sup>+</sup>), and T lymphocytes (CD3<sup>+</sup>) were identified and expressed as a percentage of total leukocytes (% CD45<sup>+</sup>). Gr1<sup>High</sup> and Gr1<sup>Low</sup> monocyte subpopulations were identified. Activated cells and Tregs were identified as CD4<sup>+</sup>CD62L<sup>-</sup>CD44<sup>High</sup> and CD4<sup>+</sup>CD25<sup>+</sup>FR4<sup>+</sup> T lymphocytes, respectively. Values are expressed as mean  $\pm$  SEM. \* $p < 0.05$ , \*\* $p < 0.01$ , \*\*\* $p < 0.001$ .

decrease and increase for *Irf4* and *Irf5*, respectively, in the adrenals of hypomSR-BI<sup>ΔAC</sup> mice, whereas their expressions were similar in the spleens of both groups (Fig. 6A, 6B).

To evaluate the state of inflammation of the vascular endothelium after LPS injection, endothelial cells harvested from the aortas of the injected mice 2 h after LPS were analyzed. mRNA levels for vascular endothelial growth factor  $\alpha$  ( $\times 1.3$ ), *Ccl2* chemokine ( $\times 1.3$ ), and *Il-1 $\beta$*  ( $\times 1.7$ ) were more elevated in hypomSR-BI<sup>ΔAC</sup> mice than in controls. These data indicated that GC insufficiency in adrenal SR-BI-deficient mice impacted very rapidly the response of the body to endotoxemia, notably in the endothelium that can be considered as the sentinel system for invading pathogens/endotoxins that have reached the bloodstream.

Finally, muscle loss as a result of increased protein degradation and a concomitant decrease in protein synthesis is also an important feature of many inflammatory conditions, including endotoxemia. We observed a markedly reduced activation of muscle atrophy Fbox (*MAFbx/atrogin1*) and muscle ring-finger protein-1, which are rate-limiting components in protein degradation, in the GN muscle of LPS-treated hypomSR-BI<sup>ΔAC</sup> mice as compared with controls (Fig. 6D). Consistently, the transcription factor *Foxo1*, a member of the forkhead box family that controls the expressions of *Atrogin1* and muscle ring-finger protein-1, was also clearly less

activated (2-fold) in hypomSR-BI<sup>ΔAC</sup> mice. mTOR signaling pathway, which plays a key role in protein synthesis, was also affected. The expression levels of mTOR-negative regulators DNA-damage-inducible transcript-4 (*Redd1/Ddit4*) and *Sestrin-1* were  $>7$ -fold less activated in hypomSR-BI<sup>ΔAC</sup> mice (Fig. 6D). Collectively, these data demonstrated that hypomSR-BI<sup>ΔAC</sup> mice displayed a reduced activation of muscle atrophy program in response to LPS despite a systemic hyperinflammatory status.

#### Adrenocortical SR-BI deficiency accelerates polymicrobial sepsis-induced death

Finally, we evaluated whether the high vulnerability of hypomSR-BI<sup>ΔAC</sup> mice to death after exposure to LPS could also be revealed in the more complex CLP animal model of polymicrobial sepsis. As observed for LPS treatment, plasma levels of corticosterone were 3.6-fold less elevated in CLP-treated hypomSR-BI<sup>ΔAC</sup> mice than in controls 20 h postsurgery (Fig. 7A). By contrast, circulating levels for IL-6 were increased 10-fold in hypomSR-BI<sup>ΔAC</sup> mice. Analysis of the survival curves revealed a median survival time of 97 h for hypomSR-BI mice and of 24 h for hypomSR-BI<sup>ΔAC</sup> ( $p = 0.008$ ; Fig. 7B). These data showed that mice deficient for SR-BI in the adrenal cortex responded to infection in a similar fashion than to an endotoxic shock, by displaying an impaired

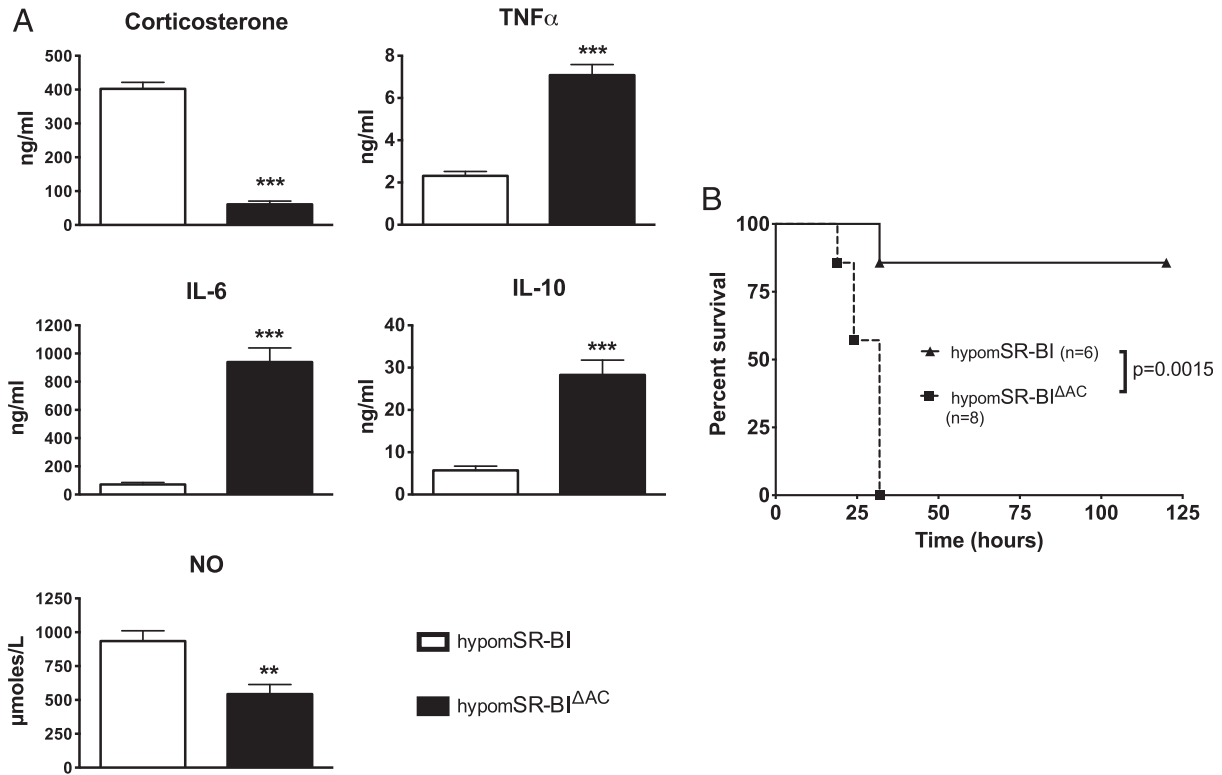


**FIGURE 5.** Mice deficient for SR-BI in the adrenal cortex demonstrate increased systemic inflammatory response and lethality after LPS injection. Four-month-old hypomSR-BI and hypomSR-BI<sup>ΔAC</sup> male mice were injected i.p. with LPS (5  $\mu$ g/g of body weight). **(A)** In a first experimental group of mice (seven mice/group), a small amount of blood was withdrawn 2 h after LPS injection for TNF- $\alpha$  and corticosterone determination. Plasma levels of IL-6, IL-10, and NO (NO total) were determined at sacrifice, 14 h after LPS injection. \*\* $p < 0.01$ , \*\*\* $p < 0.001$  versus hypomSR-BI mice. **(B)** In a second experimental group, survival was recorded over a period of 5 d.

GC response and an increased systemic inflammation. They also exhibited accelerated mortality.

## Discussion

We demonstrated in this study that SR-BI contributed to endotoxic inflammatory response at different levels and in different ways. Although absence of SR-BI in the myeloid lineage resulted in reduced inflammation after exogenous administration of LPS, hepatic SR-BI deficiency had an opposite effect, therefore highlighting a deleterious and a protective role of SR-BI in monocytes/granulocytes and liver, respectively. However, our study also revealed that the major role of SR-BI in host defense against an endotoxic shock was linked to its expression in the adrenal cortex. Indeed, SR-BI deficiency in adrenocortical cells resulted in impaired endogenous GC response with detrimental consequences in the control of inflammation, energy balance, and ultimately in host recovery leading to a high susceptibility to LPS-induced death. More importantly, results obtained in the CLP-induced septic peritonitis model provided support to the relevance of a critical role of adrenocortical SR-BI in host defense in sepsis.

Our findings that restoration of HDL-C distribution by expression of CETP in SR-BI<sup>-/-</sup> mice had no major impact on the inflammatory response, and survival of LPS-treated mice suggested that the high susceptibility of SR-BI<sup>-/-</sup> mice to LPS was not a consequence of a poor capacity of their plasma HDL to neutralize LPS. These findings are in agreement with a previous study that showed no default in plasma from SR-BI<sup>-/-</sup> mice to neutralize LPS in vitro (7). We also observed a lack of effect of CETP in the hypomSR-BI KO<sup>liver</sup> background (data not shown), also supporting that the increased LPS-induced inflammatory response in these animals was also not due to the presence of abnormal

HDL. A contribution of hepatic SR-BI in promoting plasma LPS clearance (7) might explain the moderate increase in systemic inflammation in LPS-injected hypomSR-BI KO<sup>liver</sup> mice. Indeed, we observed high concentrations of plasma endotoxins in hypomSR-BI KO<sup>liver</sup> mice treated with LPS that could likely explain a stronger inflammatory response in this mouse model. However, this effect was not associated with a higher susceptibility to death, even when higher doses of LPS were administered (Fig. 2, Supplemental Fig. 2), suggesting that alternative routes for LPS clearance remained effective in the absence of liver SR-BI.

Previous studies have suggested that expression of SR-BI in innate immune cells may also modulate the endotoxic shock response in mice. Thus, SR-BI could exert a beneficial role in macrophages by partially inhibiting the inflammatory response to LPS (9, 16). In vivo, an enhanced proinflammatory response to LPS in irradiated wild-type mice reconstituted with SR-BI<sup>-/-</sup> bone marrow (BM) cells and a diminished response in SR-BI<sup>-/-</sup> mice receiving wild-type BM cells would indeed support the existence of an anti-inflammatory activity of SR-BI in BM-derived cells (16). However, our data in the hypomSR-BI; LysM-Cre mouse model revealed a moderately reduced inflammatory response to LPS, suggesting an overall LPS-induced proinflammatory action of SR-BI expressed in monocytes/macrophages and/or granulocytes in vivo. If the mechanisms remain to be identified, the potential discrepancy between our study and BM transplantation studies (16) may reside in a role of SR-BI in BM-resident hematopoietic stem and progenitor cells (HSPC). Indeed, some recent data indicated that SR-BI might play a critical role in HSPC biology, notably in HSPC differentiation and proliferation in response to LDL and HDL (27, 28). Moreover, we observed a trend for increased survival of CLP-treated hypomSR-BI; LysM-

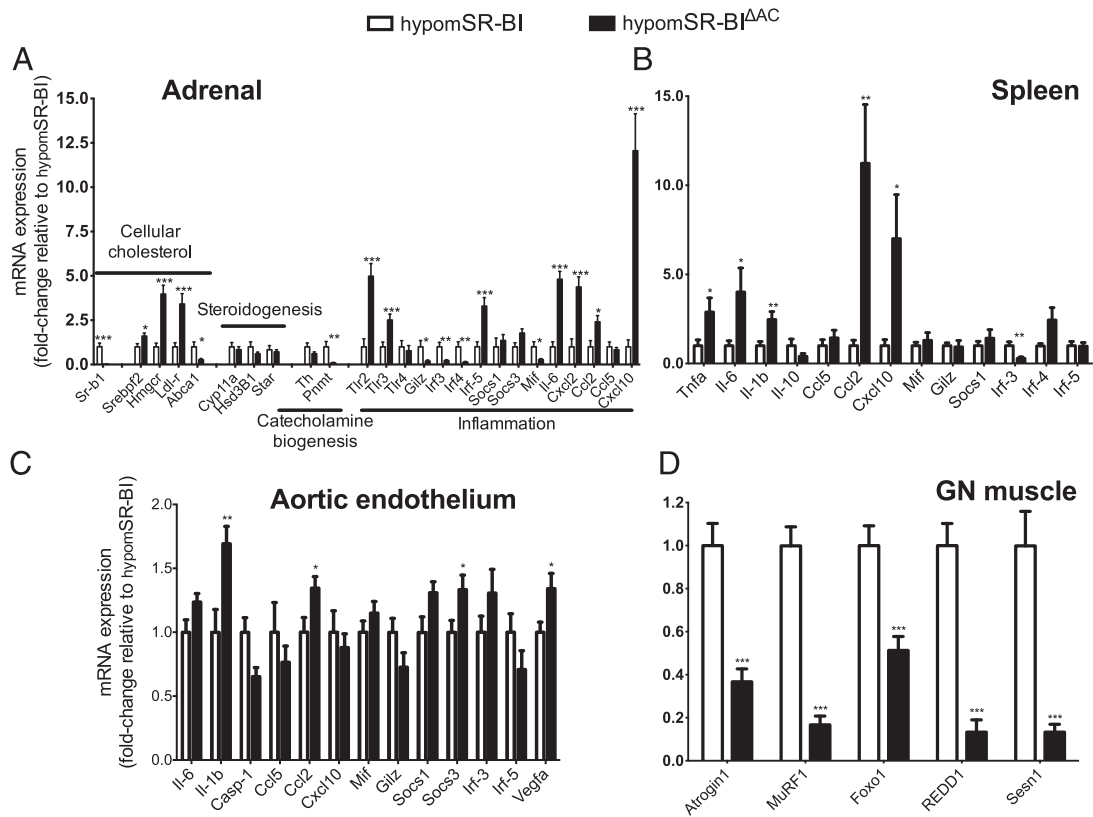


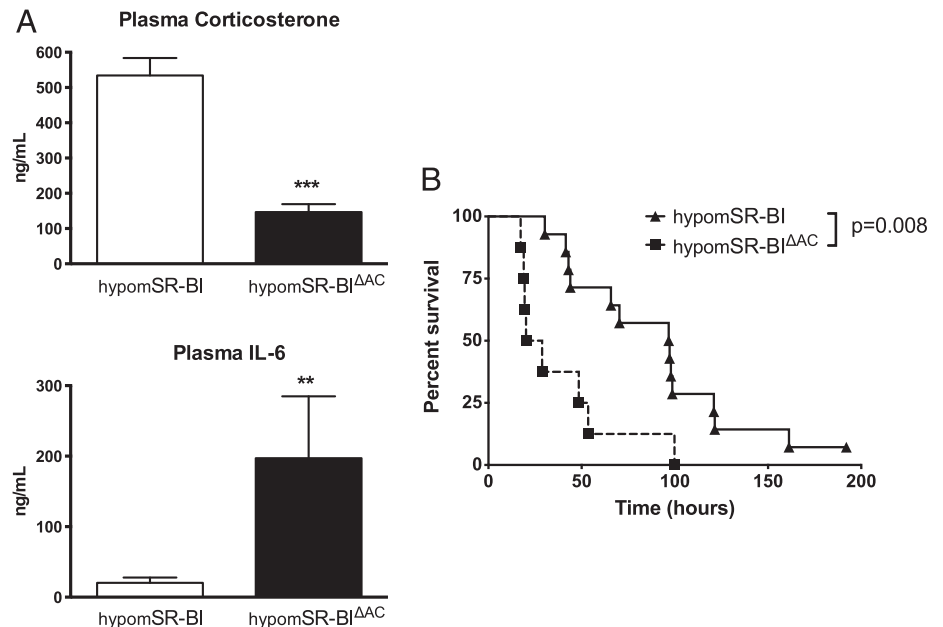
**FIGURE 6.** Mice deficient for SR-BI in the adrenal cortex exhibit increased inflammatory response in adrenals, spleen, and vascular endothelium and attenuated activation of catabolic genes in skeletal muscle after LPS injection. Gene expression was measured by real-time PCR in (A) adrenal gland, (B) spleen, and (D) GN muscle ( $n = 6-8/\text{group}$ ) 15 h after LPS injection ( $5 \mu\text{g/g}$ ) or (C) 2 h for aortic endothelial cells analyses ( $n = 8-10/\text{group}$ ). Levels of RNA were normalized to the amount of 18S RNA (spleen, adrenal) or to the mean of *Hprt*, *Hsp90*, *Nono*, and *Rpl13a* mRNA levels (muscle, endothelial cells). Data are expressed relative to those of hypomSR-BI mice, which are arbitrarily set at 1, and represented as mean  $\pm$  SEM. \* $p < 0.05$ , \*\* $p < 0.01$ , \*\*\* $p < 0.001$  versus hypomSR-BI mice.

Cre mice, which would also not support a major protective function for SR-BI expressed in cells of myeloid origin.

The contribution of adrenal SR-BI in endotoxic shock or sepsis has been evaluated indirectly through corticosterone supplementation of SR-BI<sup>-/-</sup> mice. However, controversial results have been reported (7, 9, 17). Our results in hypomSR-BI<sup>ΔAC</sup> mice clearly

demonstrated that lack of adrenocortical SR-BI expression was associated with GC insufficiency and resulted in a hyper-inflammatory state and high susceptibility or accelerated death of the mice in response to either an endotoxic shock or polymicrobial peritonitis. The impact of GC insufficiency in hypomSR-BI<sup>ΔAC</sup> mice was clearly visible in the endotoxemia model, as mRNA

**FIGURE 7.** CLP-treated mice deficient for SR-BI in the adrenal cortex exhibit increased systemic inflammation and accelerated mortality. Three-month-old hypomSR-BI and (hypomSR-BI<sup>ΔAC</sup> female mice underwent CLP surgery. (A) Twenty hours postsurgery, a small amount of blood was withdrawn for corticosterone and IL-6 determination. \*\* $p < 0.01$ , \*\*\* $p < 0.001$  versus hypomSR-BI mice. (B) Survival was recorded over a period of 8 d.



levels of proinflammatory cytokines normally repressed by GC such as *Tnfa*, *IL-1 $\beta$* , or *IL-6* were found markedly elevated. In the endothelium, we found *IL-1 $\beta$*  mRNA significantly increased only 2 h after LPS in hypomSR-BI<sup>ΔAC</sup> mice, but also *Vegfa* mRNA levels that may participate in fatal outcome by increasing vascular permeability, inducing procoagulant tissue factor, adhesion molecules, and chemokines (29). mRNA levels for *Ccl2*, *Cxcl2*, and *Cxcl10*, potent neutrophil, and monocyte chemoattractants were also found to be increased in hypomSR-BI<sup>ΔAC</sup> mice challenged with LPS. Interestingly, *Ccl5*, which is known to play a key role in recruiting leukocytes to inflammatory sites, was not differentially expressed between hypomSR-BI<sup>ΔAC</sup> mice and controls. Thus, these data further highlight the important role of GC in the regulation of specific chemokines for controlling leukocytes recruitment, which is critical for pathogen clearance but may also elicit tissue damage. Particularly in sepsis, uncontrolled activation of neutrophils has been associated with organ damage and multi-organ failure (30). Thus, excessive recruitment of neutrophils may have contributed to high mortality of hypomSR-BI<sup>ΔAC</sup> mice. Of note, lower plasma levels of NO observed in LPS-treated hypomSR-BI<sup>ΔAC</sup> mice may have also favored an overwhelming and deleterious activation of neutrophils. Indeed, NO release during acute inflammation has been shown to downmodulate neutrophil migration (31).

Increased muscle catabolism is one of the most prominent metabolic consequences of acute inflammation and sepsis. This catabolic response to endotoxic/septic shock in skeletal muscle involves increased protein breakdown, but also reduced protein synthesis and inhibition of amino acid uptake. Numerous reports have documented the potential contribution of GC (32), proinflammatory cytokines (33, 34), and LPS (35) to this effect. However, recent studies have substantially evidenced that GC were indeed requisite to this process, because activation of the genes involved in muscle atrophy after LPS-induced peripheral inflammation was essentially blocked by adrenalectomy (36). In this study, we observed a strong reduction in the activation of catabolic genes but also of repressor genes of the mTOR anabolic pathway in muscle of endotoxemic hypomSR-BI<sup>ΔAC</sup> mice. These effects were observed while these animals exhibited concomitantly markedly increased circulating cytokines levels. These results strongly support that muscle catabolism in acute inflammation does not depend exclusively on direct cytokine action on skeletal muscle, but also critically on a functional endogenous GC response produced by the host. Decreased muscle catabolic response in hypomSR-BI<sup>ΔAC</sup> mice after LPS-induced acute inflammation may have also crucially contributed to high mortality of these mice. Indeed, amino acid release after muscle breakdown may be beneficial to the organism because it provides substrates to fuel the necessary increases in immune function, but also to sustain gluconeogenesis and acute-phase protein synthesis by the liver.

The relevance of the present results in humans remains unknown. However, the human and murine orthologs share many functional properties/ligands and a tissue expression pattern to suggest that human SR-BI exerts similar functional roles than its murine counterpart. At the hepatic level, functional analyses in experimental mouse models (6, 37), genomewide association studies (38), and elevation of HDL-C in members of a family heterozygous for a functional mutation (P297S) of the hSR-BI gene (6) lend strong support to a contribution of liver SR-BI in lipoprotein/cholesterol metabolism in humans. In addition, the capacity of hSR-BI to bind and internalize monomerized and HDL-associated LPS could also support a potential contribution of the receptor in plasma detoxification of endotoxins in humans (10). At the level

of the adrenal gland, decreased adrenal steroidogenesis observed in heterozygous carriers of the hSR-BI P297S mutation suggests that SR-BI-mediated cholesterol supply to the adrenal cortex is of critical importance in regulating the endocrine function of the gland (6). Altogether, these studies underline the potential relevance of searching for mutations in the hSR-BI gene in patients diagnosed with primary adrenal insufficiency whose molecular etiology has not been identified. They also suggest that disturbance of the SR-BI pathway may also potentially participate in adrenal insufficiency reported in some critically ill patients and, in particular, in patients with septic shock.

## Disclosures

The authors have no financial conflicts of interest.

## References

- Acton, S., A. Rigotti, K. T. Landschulz, S. Xu, H. H. Hobbs, and M. Krieger. 1996. Identification of scavenger receptor SR-BI as a high density lipoprotein receptor. *Science* 271: 518–520.
- Ueda, Y., L. Royer, E. Gong, J. Zhang, P. N. Cooper, O. Francone, and E. M. Rubin. 1999. Lower plasma levels and accelerated clearance of high density lipoprotein (HDL) and non-HDL cholesterol in scavenger receptor class B type I transgenic mice. *J. Biol. Chem.* 274: 7165–7171.
- Huby, T., C. Doucet, C. Dacet, B. Ouzilleau, Y. Ueda, V. Afzal, E. Rubin, M. J. Chapman, and P. Lesnik. 2006. Knockdown expression and hepatic deficiency reveal an atheroprotective role for SR-BI in liver and peripheral tissues. *J. Clin. Invest.* 116: 2767–2776.
- Rigotti, A., B. L. Trigatti, M. Penman, H. Rayburn, J. Herz, and M. Krieger. 1997. A targeted mutation in the murine gene encoding the high density lipoprotein (HDL) receptor scavenger receptor class B type I reveals its key role in HDL metabolism. *Proc. Natl. Acad. Sci. USA* 94: 12610–12615.
- Out, R., M. Hoekstra, J. A. Spijkers, J. K. Kruijff, M. van Eck, I. S. Bos, J. Twisk, and T. J. Van Berkel. 2004. Scavenger receptor class B type I is solely responsible for the selective uptake of cholesteryl esters from HDL by the liver and the adrenals in mice. *J. Lipid Res.* 45: 2088–2095.
- Vergeer, M., S. J. Korpelaar, R. Franssen, I. Meurs, R. Out, G. K. Hovingh, M. Hoekstra, J. A. Sieris, G. M. Dallinga-Thie, M. M. Motazacker, et al. 2011. Genetic variant of the scavenger receptor BI in humans. *N. Engl. J. Med.* 364: 136–145.
- Cai, L., A. Ji, F. C. de Beer, L. R. Tannock, and D. R. van der Westhuyzen. 2008. SR-BI protects against endotoxemia in mice through its roles in glucocorticoid production and hepatic clearance. *J. Clin. Invest.* 118: 364–375.
- Li, X. A., L. Guo, R. Asmis, M. Nikolova-Karakashian, and E. J. Smart. 2006. Scavenger receptor BI prevents nitric oxide-induced cytotoxicity and endotoxin-induced death. *Circ. Res.* 98: e60–e65.
- Guo, L., Z. Song, M. Li, Q. Wu, D. Wang, H. Feng, P. Bernard, A. Daugherty, B. Huang, and X. A. Li. 2009. Scavenger receptor BI protects against septic death through its role in modulating inflammatory response. *J. Biol. Chem.* 284: 19826–19834.
- Vishnyakova, T. G., A. V. Bocharov, I. N. Baranova, Z. Chen, A. T. Remaley, G. Csako, T. L. Eggerman, and A. P. Patterson. 2003. Binding and internalization of lipopolysaccharide by Cla-1, a human orthologue of rodent scavenger receptor BI. *J. Biol. Chem.* 278: 22771–22780.
- Yuhanna, I. S., Y. Zhu, B. E. Cox, L. D. Hahner, S. Osborne-Lawrence, P. Lu, Y. L. Marcel, R. G. Anderson, M. E. Mendelsohn, H. H. Hobbs, and P. W. Shaul. 2001. High-density lipoprotein binding to scavenger receptor-BI activates endothelial nitric oxide synthase. *Nat. Med.* 7: 853–857.
- Bocharov, A. V., I. N. Baranova, T. G. Vishnyakova, A. T. Remaley, G. Csako, F. Thomas, A. P. Patterson, and T. L. Eggerman. 2004. Targeting of scavenger receptor class B type I by synthetic amphipathic alpha-helical-containing peptides blocks lipopolysaccharide (LPS) uptake and LPS-induced proinflammatory cytokine responses in THP-1 monocyte cells. *J. Biol. Chem.* 279: 36072–36082.
- Philips, J. A., E. J. Rubin, and N. Perrimon. 2005. Drosophila RNAi screen reveals CD36 family member required for mycobacterial infection. *Science* 309: 1251–1253.
- Vishnyakova, T. G., R. Kurlander, A. V. Bocharov, I. N. Baranova, Z. Chen, M. S. Abu-Asab, M. Tsokos, D. Malide, F. Basso, A. Remaley, et al. 2006. CLA-1 and its splicing variant CLA-2 mediate bacterial adhesion and cytosolic bacterial invasion in mammalian cells. *Proc. Natl. Acad. Sci. USA* 103: 16888–16893.
- Watanabe, K., E. K. Shin, M. Hashino, M. Tachibana, and M. Watarai. 2010. Toll-like receptor 2 and class B scavenger receptor type I are required for bacterial uptake by trophoblast giant cells. *Mol. Immunol.* 47: 1989–1996.
- Cai, L., Z. Wang, J. M. Meyer, A. Ji, and D. R. van der Westhuyzen. 2012. Macrophage SR-BI regulates LPS-induced pro-inflammatory signaling in mice and isolated macrophages. *J. Lipid Res.* 53: 1472–1481.
- Leelahavanichkul, A., A. V. Bocharov, R. Kurlander, I. N. Baranova, T. G. Vishnyakova, A. C. Souza, X. Hu, K. Doi, B. Vaisman, M. Amar, et al.

2012. Class B scavenger receptor types I and II and CD36 targeting improves sepsis survival and acute outcomes in mice. *J. Immunol.* 188: 2749–2758.
18. El Bouhassani, M., S. Gilibert, M. Moreau, F. Saint-Charles, M. Tréguier, F. Poti, M. J. Chapman, W. Le Goff, P. Lesnik, and T. Huby. 2011. Cholesteryl ester transfer protein expression partially attenuates the adverse effects of SR-BI receptor deficiency on cholesterol metabolism and atherosclerosis. *J. Biol. Chem.* 286: 17227–17238.
  19. Postic, C., and M. A. Magnuson. 2000. DNA excision in liver by an albumin-Cre transgene occurs progressively with age. *Genesis* 26: 149–150.
  20. Kisanuki, Y. Y., R. E. Hammer, J. Miyazaki, S. C. Williams, J. A. Richardson, and M. Yanagisawa. 2001. Tie2-Cre transgenic mice: a new model for endothelial cell-lineage analysis in vivo. *Dev. Biol.* 230: 230–242.
  21. Bingham, N. C., S. Verma-Kurvari, L. F. Parada, and K. L. Parker. 2006. Development of a steroidogenic factor 1/Cre transgenic mouse line. *Genesis* 44: 419–424.
  22. Pène, F., E. Courtine, F. Ouaz, B. Zuber, B. Sauneuf, G. Sirgo, C. Rousseau, J. Toubiana, V. Balloy, M. Chignard, et al. 2009. Toll-like receptors 2 and 4 contribute to sepsis-induced depletion of spleen dendritic cells. *Infect. Immun.* 77: 5651–5658.
  23. Bligh, E. G., and W. J. Dyer. 1959. A rapid method of total lipid extraction and purification. *Can. J. Biochem. Physiol.* 37: 911–917.
  24. Tréguier, M., C. Doucet, M. Moreau, C. Dachet, J. Thillet, M. J. Chapman, and T. Huby. 2004. Transcription factor sterol regulatory element binding protein 2 regulates scavenger receptor Cla-1 gene expression. *Arterioscler. Thromb. Vasc. Biol.* 24: 2358–2364.
  25. Lesnik, P., C. A. Haskell, and I. F. Charo. 2003. Decreased atherosclerosis in CX3CR1<sup>-/-</sup> mice reveals a role for fractalkine in atherogenesis. *J. Clin. Invest.* 111: 333–340.
  26. Hildebrand, R. B., B. Lammers, I. Meurs, S. J. Korporaal, W. De Haan, Y. Zhao, J. K. Kruijt, D. Praticò, A. W. Schimmel, A. G. Holleboom, et al. 2010. Restoration of high-density lipoprotein levels by cholesteryl ester transfer protein expression in scavenger receptor class B type I (SR-BI) knockout mice does not normalize pathologies associated with SR-BI deficiency. *Arterioscler. Thromb. Vasc. Biol.* 30: 1439–1445.
  27. Gomes, A. L., T. Carvalho, J. Serpa, C. Torre, and S. Dias. 2010. Hypercholesterolemia promotes bone marrow cell mobilization by perturbing the SDF-1: CXCR4 axis. *Blood* 115: 3886–3894.
  28. Feng, Y., S. Schouteden, R. Geenens, V. Van Duppen, P. Herijgers, P. Holvoet, P. P. Van Veldhoven, and C. M. Verfaillie. 2012. Hematopoietic stem/progenitor cell proliferation and differentiation is differentially regulated by high-density and low-density lipoproteins in mice. *PLoS ONE* 7: e47286.
  29. Suehiro, J., T. Hamakubo, T. Kodama, W. C. Aird, and T. Minami. 2010. Vascular endothelial growth factor activation of endothelial cells is mediated by early growth response-3. *Blood* 115: 2520–2532.
  30. Aldridge, A. J. 2002. Role of the neutrophil in septic shock and the adult respiratory distress syndrome. *Eur. J. Surg.* 168: 204–214.
  31. Dal Secco, D., J. A. Paron, S. H. de Oliveira, S. H. Ferreira, J. S. Silva, and Q. Cunha Fde. 2003. Neutrophil migration in inflammation: nitric oxide inhibits rolling, adhesion and induces apoptosis. *Nitric Oxide* 9: 153–164.
  32. Schakman, O., S. Kalista, C. Barbé, A. Loumaye, and J. P. Thissen. 2013. Glucocorticoid-induced skeletal muscle atrophy. *Int. J. Biochem. Cell Biol.* 45: 2163–2172.
  33. Li, W., J. S. Moylan, M. A. Chambers, J. Smith, and M. B. Reid. 2009. Interleukin-1 stimulates catabolism in C2C12 myotubes. *Am. J. Physiol. Cell Physiol.* 297: C706–C714.
  34. Li, Y. P., Y. Chen, J. John, J. Moylan, B. Jin, D. L. Mann, and M. B. Reid. 2005. TNF-alpha acts via p38 MAPK to stimulate expression of the ubiquitin ligase atrogin1/MAFbx in skeletal muscle. *FASEB J.* 19: 362–370.
  35. Doyle, A., G. Zhang, E. A. Abdel Fattah, N. T. Eissa, and Y. P. Li. 2011. Toll-like receptor 4 mediates lipopolysaccharide-induced muscle catabolism via coordinate activation of ubiquitin-proteasome and autophagy-lysosome pathways. *FASEB J.* 25: 99–110.
  36. Braun, T. P., X. Zhu, M. Szumowski, G. D. Scott, A. J. Grossberg, P. R. Levasseur, K. Graham, S. Khan, S. Damaraju, W. F. Colmers, et al. 2011. Central nervous system inflammation induces muscle atrophy via activation of the hypothalamic-pituitary-adrenal axis. *J. Exp. Med.* 208: 2449–2463.
  37. Komori, H., H. Arai, T. Kashima, T. Huby, T. Kita, and Y. Ueda. 2008. Coexpression of CLA-1 and human PDZK1 in murine liver modulates HDL cholesterol metabolism. *Arterioscler. Thromb. Vasc. Biol.* 28: 1298–1303.
  38. Teslovich, T. M., K. Musunuru, A. V. Smith, A. C. Edmondson, I. M. Stylianou, M. Koseki, J. P. Pirruccello, S. Ripatti, D. I. Chasman, C. J. Willer, et al. 2010. Biological, clinical and population relevance of 95 loci for blood lipids. *Nature* 466: 707–713.

# Targeted invalidation of SR-B1 in macrophages reduces macrophage apoptosis and accelerates atherosclerosis

Lauriane Galle-Treger<sup>1</sup>, Martine Moreau<sup>1</sup>, Raphaëlle Ballaire<sup>1†</sup>, Lucie Poupel<sup>1†</sup>, Thomas Huby<sup>1</sup>, Emanuele Sasso<sup>2,3</sup>, Fulvia Troise<sup>2</sup>, Francesco Poti<sup>4</sup>, Philippe Lesnik<sup>1</sup>, Wilfried Le Goff<sup>1</sup>, Emmanuel L. Gautier<sup>1</sup>, and Thierry Huby<sup>1\*</sup>

<sup>1</sup>Sorbonne Université, INSERM, UMR\_S 1166 ICAN, F-75013, Paris, France; <sup>2</sup>Ceinge Biotecnologie Avanzate S.C.R.L, Via Gaetano Salvatore 486, 80145, Napoli, Italy; <sup>3</sup>Dipartimento di Medicina Molecolare e Biotecnologie Mediche, Università di Napoli Federico II, 80131, Napoli, Italy; and <sup>4</sup>Department of Medicine and Surgery, Unit of Neurosciences, University of Parma, Parma, Italy

Received 30 March 2018; revised 30 January 2019; editorial decision 15 May 2019; accepted 16 May 2019; online publish-ahead-of-print 22 May 2019

Time for primary review: 25 days

## Aims

SR-B1 is a cholesterol transporter that exerts anti-atherogenic properties in liver and peripheral tissues in mice. Bone marrow (BM) transfer studies suggested an atheroprotective role in cells of haematopoietic origin. Here, we addressed the specific contribution of SR-B1 in the monocyte/macrophage.

## Methods and results

We generated mice deficient for SR-B1 in monocytes/macrophages (Lysm-Cre × SR-B1<sup>fl/fl</sup>) and transplanted their BM into Ldlr<sup>-/-</sup> mice. Fed a cholesterol-rich diet, these mice displayed accelerated aortic atherosclerosis characterized by larger macrophage-rich areas and decreased macrophage apoptosis compared with SR-B1<sup>fl/fl</sup> transplanted controls. These findings were reproduced in BM transfer studies using another atherogenic mouse recipient (SR-B1 KO<sup>liver</sup> × Cholesteryl Ester Transfer Protein). Haematopoietic reconstitution with SR-B1<sup>-/-</sup> BM conducted in parallel generated similar results to those obtained with Lysm-Cre × SR-B1<sup>fl/fl</sup> BM; thus suggesting that among haematopoietic-derived cells, SR-B1 exerts its atheroprotective role primarily in monocytes/macrophages. Consistent with our *in vivo* data, free cholesterol (FC)-induced apoptosis of macrophages was diminished in the absence of SR-B1. This effect could not be attributed to differential cellular cholesterol loading. However, we observed that expression of apoptosis inhibitor of macrophage (AIM) was induced in SR-B1-deficient macrophages, and notably upon FC-loading. Furthermore, we demonstrated that macrophages were protected from FC-induced apoptosis by AIM. Finally, AIM protein was found more present within the macrophage-rich area of the atherosclerotic lesions of SR-B1-deficient macrophages than controls.

## Conclusion

Our findings suggest that macrophage SR-B1 plays a role in plaque growth by controlling macrophage apoptosis in an AIM-dependent manner.

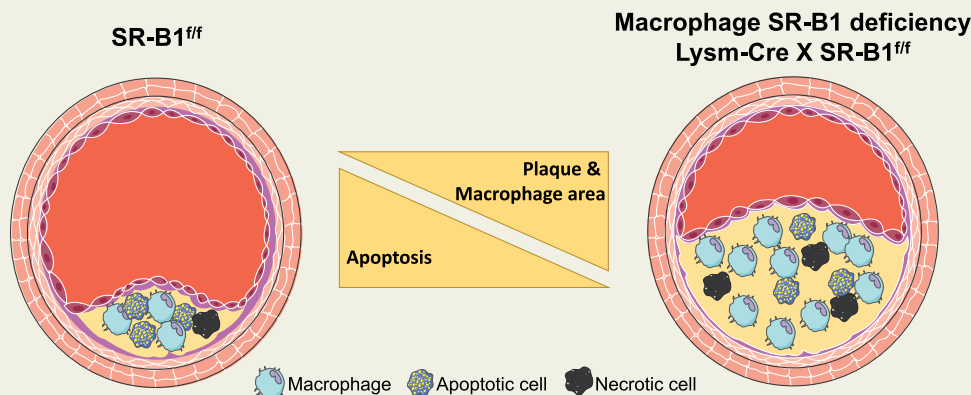
\* Corresponding author. Tel: (33)-1-40779637; E-mail: thierry.huby@sorbonne-universite.fr

† Present address. Inovarian Paris, France.



**Keywords**

SR-B1 • Atherosclerosis • Macrophage • Cholesterol • Apoptosis

**Graphical Abstract**

## 1. Introduction

A clear inverse relationship between plasma high-density lipoprotein-cholesterol (HDL-C) levels and the incidence of cardiovascular disease (CVD) in humans has been established for decades.<sup>1</sup> However, clinical trials aimed at raising HDL-C levels have failed to show CVD protection by this approach.<sup>2</sup> These results have clearly highlighted the need for a deeper understanding of the relationship between cholesterol metabolism, HDL function, and cardio(athero)-protective mechanisms.

HDL biology is highly complex.<sup>3</sup> Numerous potential anti-atherogenic effects have been attributed to HDL, among which stand out promotion of macrophage cholesterol efflux, anti-inflammatory, anti-oxidative, anti-proliferative, or anti-thrombotic activities.<sup>3–6</sup> HDL may induce changes in intracellular signalling in numerous cell types. The ATP-binding cassette (ABC) transporters ABCA1 and ABCG1 and the plasma membrane scavenger receptor SR-B1 (SCARB1) have been shown to frequently participate in these anti-atherogenic activities and cellular responses.<sup>7</sup> With regard to SR-B1, this physiological receptor for mature HDL promotes the bi-directional flux of cholesterol between cells and these lipoproteins. Notably, its capacity to mediate the selective uptake of HDL-associated cholesteryl-esters in hepatocytes promotes *in vivo* reverse cholesterol transport. As a result, hepatic overexpression of SR-B1 markedly decreases atherosclerosis while reducing plasma HDL-C levels.<sup>8,9</sup> Reciprocally, hepatic deficiency results in elevation of plasma HDL-C and favours disease development.<sup>10,11</sup> The increased HDL-C levels in a family carrying a mutation for SR-B1 suggests a similar functional role for SR-B1 in humans.<sup>12</sup>

Besides its important function in the liver, SR-B1 may also contribute to atherosclerosis in other cell types.<sup>10</sup> In the adrenal glands, SR-B1 provides lipoprotein-derived cholesterol allowing effective glucocorticoid production.<sup>13,14</sup> Though the impact of adrenocortical SR-B1 deficiency on atherosclerosis has not yet been evaluated, adrenal-specific disruption of SR-B1 modulates hepatic lipid metabolism and favours an atherogenic lipoprotein-cholesterol profile in mice.<sup>15</sup> In endothelial cells, SR-B1 serves as a plasma membrane cholesterol sensor to mediate HDL-induced signalling. Its activation leads to stimulation of endothelial nitric oxide synthase (e-NOS), subsequent production of the potent molecule

NO, as well as endothelial cell migration.<sup>16,17</sup> Finally, there is a strong evidence to support an atheroprotective function of SR-B1 in cells of haematopoietic origin. Indeed, SR-B1<sup>-/-</sup> bone marrow (BM) transplantation into *Ldlr*<sup>-/-18–20</sup> or *apoE*<sup>-/-21</sup> mice resulted in increased atherosclerosis. Combined deletion of SR-B1 and of the ABC transporter *ABCA1* (a critical player of cellular cholesterol efflux) in BM further enhanced atherosclerosis progression in transplanted *Ldlr*<sup>-/-</sup> recipients.<sup>22</sup> These studies have pinpointed that the protective role of SR-B1 could rely on its expression in the monocyte/macrophage; however, it cannot be ruled out that SR-B1 expression in other white blood cells (WBC), which also play important roles in atherosclerosis such as B or T lymphocytes,<sup>23,24</sup> may also contribute. Moreover, studies have suggested that SR-B1 could also play an important atheroprotective function in haematopoietic stem/progenitor cells (HSPC) by mediating the inhibitory effects of HDL on their proliferation and differentiation.<sup>25</sup>

In this context, we sought to directly address the role of SR-B1 in myeloid cells by cross-breeding SR-B1<sup>ff</sup> mice with the *Lysm-Cre* mouse. Characterization of SR-B1 expression in circulating WBC of SR-B1<sup>ff</sup> mice showed highest expression in monocytes, but no expression in neutrophils or eosinophils. Cre-mediated deletion of SR-B1-floxed gene in *Lysm-Cre* × SR-B1<sup>ff</sup> mice resulted in complete lack of SR-B1 expression in macrophages and partial deletion in blood monocytes. Transplantations of SR-B1<sup>ff</sup> and *Lysm-Cre* × SR-B1<sup>ff</sup> BM, but also of SR-B1<sup>-/-</sup> BM, in atherosclerotic mouse models clearly demonstrated that monocyte/macrophage SR-B1 exerts a predominant role in atherogenesis. Studies of underlying mechanisms suggested that loss of SR-B1 diminishes macrophage apoptosis susceptibility by up-regulating expression of the apoptosis inhibitor of macrophage (AIM) in a STAT3-dependent manner.

## 2. Methods

### 2.1 Animal models and diets

Animals were on a C57BL/6J background. SR-B1<sup>-/-</sup> mice and SR-B1<sup>ff</sup> conditional knock-out mice, in which SR-B1 exon 1 is flanked by Cre recombinase *loxP* sites, have been described earlier.<sup>10</sup> Cre-mediated SR-B1 gene inactivation in myeloid cells or in hepatocytes (SR-B1 KO<sup>liver</sup>) were

obtained through breeding with *Lysm-Cre* (*Lyz2<sup>tm1(cre)Jfo</sup>*; Jackson Laboratory) or *Alb-Cre* [*Tg(Alb-cre)21Mgn*; Jackson Laboratory] transgenic mice, respectively. Cre and Cholesteryl Ester Transfer Protein (CETP) [*Tg(CETP)5203Tall*]; Jackson Laboratory] expressing animals were always hemizygous for the corresponding transgene. Mice were housed in a conventional animal facility and fed *ad libitum* a normal chow diet. For BM transplant studies, 8-week-old *Ldlr<sup>-/-</sup>* (*Ldlr<sup>tm1HerJ</sup>*; Jackson Laboratories) or SR-B1 KO<sup>liver</sup> × *CETP* female mice were subjected to medullar aplasia ( $2 \times 5$  Gray total body irradiation) and then injected intravenously with  $2.5 \times 10^6$  BM cells isolated from the donor female mice. Mice were given antibiotics (penicillin, 100 U/mL and streptomycin, 100 µg/mL) for 4 weeks in drinking water. Diet-induced atherosclerosis started 3 weeks after transplantation. Transplanted *Ldlr<sup>-/-</sup>* mice were fed a normal chow diet containing 1% cholesterol for 8 weeks and transplanted SR-B1 KO<sup>liver</sup> × *CETP* were fed a diet containing 1.25% cholesterol and 16% cocoa butter for 20 weeks. All animal procedures were performed in accordance with the guidelines of the Charles Darwin Ethics Committee on animal experimentation and with the French Ministry of agriculture license. Moreover, this investigation conformed to the European directive 2010/63/EU revising directive 86/609/EEC on the protection of animals used for scientific purposes.

## 2.2 Blood and tissue analyses

Blood samples were collected in ethylenediaminetetraacetic acid (EDTA)-coated tubes (Microvette, Sarstedt) by retro-orbital bleeding under isoflurane anaesthesia (2% isoflurane/0.2 L O<sub>2</sub>/min). Plasma samples were stored frozen at -80°C. Cholesterol levels in plasma or in lipoproteins fractions were determined as previously.<sup>10</sup>

## 2.3 Analysis of atherosclerotic plaques

Atherosclerotic lipid lesions were quantified on serial cross sections (10 µm) throughout the aortic root as previously described.<sup>26</sup> Images were captured using a Zeiss AxioImager M2 microscope and plaque area measured with the AxioVision Zeiss software. To determine the macrophage area, we performed immunostainings on aortic root cryosections fixed in absolute ethanol for 10 min. Sections were then blocked for 30 min with 1% Bovine Serum Albumin (BSA) in Phosphate-Buffered Saline (PBS) containing mouse FcR Blocking Reagent (Miltenyi Biotec) and incubated with a rat anti-mouse CD68 mAb (FA-11; Serotec, 1:100) overnight at 4°C. After washing, a Cy3-labelled donkey anti-rat IgG secondary antibody (Jackson ImmunoResearch, 1:500) was added. Sections were subsequently counterstained for nuclei with 4',6-diamidino-2-phenylindole (DAPI). Co-immunostaining for AIM (CD5L/Ap16/Spα) and CD68 antigens were performed by incubating the sections with CD68 mAbs and goat anti-mouse CD5L antibody (R&D systems, 1 µg) and then, after washing, with Cy3-conjugated anti-rat IgG and fluorescein isothiocyanate (FITC)-conjugated rabbit anti-goat IgG (Vector laboratories) secondary antibodies. Necrotic areas were identified as DAPI negative areas of the intima. Detection of apoptotic cells was performed on formalin-fixed section using the In Situ Cell Death Detection Kit (TMR red, Roche) following the labelling protocol for difficult tissue.

## 2.4 Blood monocytes recruitment into lesions

Four days before sacrifice, atherosclerotic mice were anaesthetized with isoflurane and injected (200 µL, i.v.) with 1:4 diluted 1 µm fluoresbrite YG microspheres (Polysciences Europe) to label monocytes, as previously described.<sup>27</sup> Labelling efficiency of monocytes was verified by flow

cytometry 1 day after labelling. Green fluorescent beads were manually counted in the intima of 15 aortic sections per mice.

## 2.5 Flow cytometry

Blood was collected on animals under isoflurane anaesthesia by retro-orbital bleeding into EDTA-coated tubes (Microvette, Sarstedt). Red blood cells were lysed in red blood cell lysis buffer (BD Bioscience) on ice and WBC were pelleted by centrifugation, washed, and suspended in PBS containing 1% BSA and 0.5 mM EDTA. Cells were incubated with antibodies for 30 min on ice. Stained cells were analysed on LSR Fortessa (BD Bioscience) and the data were analysed with FlowJo software (TreeStar, Ashland, Oregon). Monoclonal antibodies (mAb) to mouse CD115 (AFS98), CD3 (145-2C11), CD45 (30-F11), and CD8 (53-6.7) were purchased from eBioscience. mAb to mouse CD4 (RM4-5) and Gr-1 (Ly-6G/Ly-6C; RB6-8C5) were purchased from BD Biosciences. mAb to mouse CD19 (6D5) was purchased from Biolegend. Expression of SR-B1 on WBC was detected using the human mAb C11,<sup>28</sup> followed by incubation with a Cy3-labelled donkey anti-human IgG antibody (Jackson ImmunoResearch).

## 2.6 Bone marrow-derived macrophages

SR-B1<sup>fl/fl</sup> and *Lysm-Cre* × SR-B1<sup>fl/fl</sup> mice were anaesthetized with isoflurane (2%) and then euthanized by cervical dislocation. BM cells were prepared and plated in the presence of L929 conditioned medium as a source of macrophage colony stimulating factor, as previously.<sup>26</sup> On Day 6, bone marrow-derived macrophage (BMDM) were cultured for 20 h in RPMI medium supplemented with 1% hi-FBS, or RPMI supplemented with 50 µg/mL of acetylated-LDL protein and 10 µg/mL ACAT inhibitor (Sandoz 58-035, Sigma-Aldrich). To extract lipids, isopropanol was added to the wells and plates placed on an orbital shaker for 30 s. Two additional extractions per well were performed and pooled. Samples were evaporated and suspended in 100 µL isopropanol. Total and free cholesterol (FC) were measured by enzymatic-colorimetric methods.<sup>10</sup> Desmosterol quantification in BMDM was performed by gas chromatography-mass spectrometry (GC/MS) on a DBX 5MS column. Briefly, cells were first extracted in a water:methanol:CHCl<sub>3</sub> (1:3:6) solution containing labelled internal standards (desmosterol-d6 and cholesterol-d7; Avanti Polar Lipids). After centrifugation, the lower phase was dried, sterols were suspended in KOH/methanol for saponification and then extracted in water:hexane (1:2). After centrifugation, the upper phase was dried, suspended in N,O-Bis(trimethylsilyl)trifluoroacetamide/Trimethylchlorosilane (BSTFA/TMCS) (90:10) for 1 h at 80°C and dried again before final suspension in cyclohexane containing 1% BSTFA for GC/MS injection. For western blots, wells were washed with cold PBS and cells lysed in RIPA buffer (0.5% sodium deoxycholate, 0.1% sodium dodecyl sulfate, 1% Triton X-100, 20 mM Tris, 150 mM NaCl, and 5 mM EDTA, pH8) containing protease and phosphatase inhibitors (Complete Mini protease inhibitor and PhosSTOP phosphatase inhibitor cocktail tablets; Roche Diagnostics). Samples were prepared as previously<sup>10</sup> and equal amounts of proteins were separated by electrophoresis on NuPAGE 4–12% Bis-Tris Protein Gels (Thermo Fisher Scientific) under reducing conditions and then blotted onto nitrocellulose membrane (iBlot; Thermo Fisher Scientific). Membranes were incubated with primary antibodies overnight and revealed with IR dye 800 nm-conjugated secondary antibodies. Infrared fluorescence was acquired on a Li-Cor scanner (Odyssey). Antibodies against phosphorylated and non-phosphorylated p38MAPK and STAT1 proteins were purchased from Cell Signaling Technology. To assay macrophage apoptosis, BMDM were

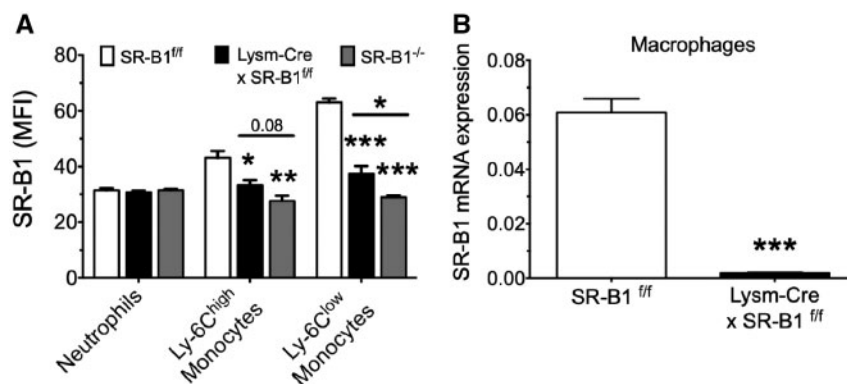


**Figure 1** Characterization of SR-B1 deletion in monocyte/macrophage. (A) SR-B1 expression was determined by flow cytometry on blood neutrophils and monocyte subsets in *SR-B1<sup>fl/fl</sup>* ( $n = 6$ ), *Lysm-Cre x SR-B1<sup>fl/fl</sup>* ( $n = 4$ ), and *SR-B1<sup>-/-</sup>* ( $n = 3$ ) mice. (B) SR-B1 mRNA levels were measured by real-time Polymerase Chain Reaction (PCR) in bone marrow-derived macrophages ( $n = 5$  mice/group). Means  $\pm$  SEM for each group are indicated. \* $P < 0.05$ , \*\* $P < 0.01$ , \*\*\* $P < 0.001$ . The statistical significance of differences was determined using one-way analysis of variance (ANOVA) followed by Tukey's *post hoc* test (A) or unpaired *t*-test (B).

detached from plates by addition of ice-cold PBS, washed and incubated with an allophycocyanin (APC)-conjugated anti-mouse F4/80 antibody (clone BM8; eBioscience) in PBS/BSA 0.5%/EDTA 2 mM for 20 min at 4°C. The cells were then washed, and incubated with recombinant annexin V-FITC (eBioscience) and propidium iodide (Sigma) in annexin V binding buffer (HEPES 10 mM, NaCl 140 mM, CaCl<sub>2</sub> 2.5 mM) for 10 min prior to flow cytometry analysis. To determine AIM protein expression, BMDM were detached from plates, washed and labelled with an APC-conjugated anti-mouse F4/80 antibody (see above). The cells were fixed and permeabilized (cytofix/cytoperm kit from BD Bioscience), and then incubated with a goat anti-mouse AIM antibody (AF2834, R&D systems), followed by an incubation with a Cy3-conjugated affiniPure F(ab')<sub>2</sub> fragment rabbit anti-goat IgG (Jackson ImmunoResearch laboratories) prior to flow cytometry analysis.

## 2.7 THP-1 macrophages

Human THP-1 monocytic cells [American Type Culture Collection (ATCC)] were cultured and differentiated into macrophages.<sup>29</sup> THP-1 macrophages were then transfected with 50 nM control siRNA (Dharmacon) or *hSR-B1*-targeting siRNA (Dharmacon) using lipofectamine RNAiMax (ThermoFisher Scientific) according to the manufacturer's instructions.

## 2.8 Analysis of gene expression

Cells were washed with PBS, lysed with RA1 lysis buffer (Macherey-Nagel) and frozen at -80°C. Total RNA was prepared using the NucleoSpin RNAII kit (Macherey-Nagel). cDNA was synthesized using random hexamer and SuperScript II (Life Technologies) or the transcriptor first strand cDNA synthesis kit (Roche Applied Science). Quantitative Polymerase Chain Reaction (PCR) analyses were performed using a LightCycler<sup>®</sup> 480 real-time PCR system and dedicated software (Roche). Initial differences in mRNA quantities were controlled using reference mouse genes *Hprt*, *Rpl13a*, and *Nono* for BMDM or human genes *HPRT*, *ALA*, *NONO*, *TUBA*, *HSP90AB1*, and *18S* rRNA for Thp1 cells.

## 2.9 Statistics

Comparisons between groups were performed using unpaired *t*-tests. One-way analysis of variance (ANOVA) and Tukey's *post hoc* analysis

was used for multiple comparison tests. All statistical analyses were performed using GraphPad Prism software (GraphPad Software, Inc., San Diego, CA, USA).  $P < 0.05$  was considered significant.

## 3. Results

### 3.1 Specific deletion of SR-B1 in monocyte/macrophage

To specifically delete SR-B1 in myeloid cells, *SR-B1<sup>fl/fl</sup>* mice were crossed with *Lysm-Cre* transgenic mice that express the recombinase Cre under control of the murine M lysozyme (*Ly2z*) gene in neutrophils, monocytes, and macrophages. Deletion specificity was evaluated on circulating WBCs by flow cytometry using the conformational C11 mAb.<sup>28</sup> Comparison of *SR-B1<sup>fl/fl</sup>*, *Lysm-Cre x SR-B1<sup>fl/fl</sup>* and fully deficient *SR-B1<sup>-/-</sup>* mice revealed that SR-B1 is present at the cell surface of monocytes, B and T lymphocytes, but absent on neutrophils and eosinophils (Figure 1A and Supplementary material online, Figure S1). As expected, *Lysm-Cre x SR-B1<sup>fl/fl</sup>* mice exhibited significantly less SR-B1 expression on monocytes (both Ly-6C<sup>low</sup> and Ly-6C<sup>hi</sup> subsets) compared with *SR-B1<sup>fl/fl</sup>* mice. However, residual SR-B1 expression was still visible when comparing with *SR-B1<sup>-/-</sup>* mice (Figure 1A). These data are in agreement with previous studies<sup>30,31</sup> in which the *Lysm-Cre* transgene was reported to lead to partial deletion of floxed genes in monocytes. Finally, analysis of BMDM from *Lysm-Cre x SR-B1<sup>fl/fl</sup>* mice confirmed complete deficiency of SR-B1 gene expression (Figure 1B).

### 3.2 SR-B1 in macrophages protects from atherosclerosis

We assessed the impact of *SR-B1* deficiency in monocytes/macrophages on atherosclerosis development in two different mouse models of the disease. First, *Ldlr<sup>-/-</sup>* mice were irradiated and transplanted with BM prepared from either *SR-B1<sup>fl/fl</sup>* mice or *Lysm-Cre x SR-B1<sup>fl/fl</sup>* mice. After recovery, mice were fed a chow diet supplemented with 1% cholesterol for 8 weeks. In response to the diet, plasma total cholesterol (TC) and FC levels increased similarly in the two groups of mice (about 950 mg/dL and 190 mg/dL, respectively; Figure 2A). Plasma cholesterol distribution into lipoprotein subclasses was also identical between the two groups

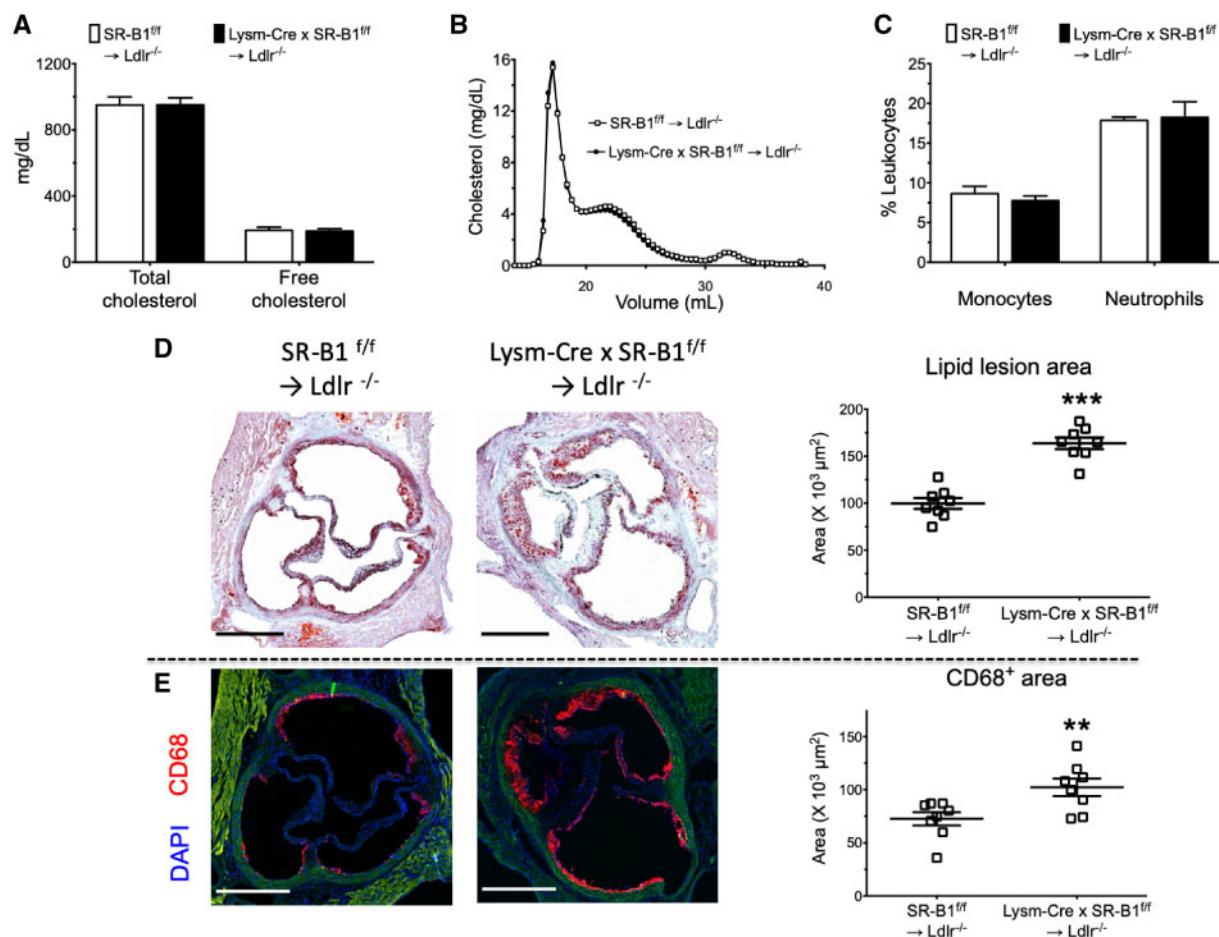


**Figure 2** SR-B1 deficiency in monocyte/macrophages favours plaque development in the *Ldlr*<sup>-/-</sup> background. (A) Plasma total cholesterol (TC) and free cholesterol (FC) were determined in overnight-fasted *SR-B1*<sup>fl/fl</sup>→*Ldlr*<sup>-/-</sup> and *Lysm-Cre* × *SR-B1*<sup>fl/fl</sup>→*Ldlr*<sup>-/-</sup> transplanted female mice (*n* = 15/group) fed a 1% cholesterol diet for 8 weeks. (B) Plasma samples were fractionated by size-exclusion chromatography. Total cholesterol was measured in each fraction to determine lipoprotein cholesterol profiles. (C) Percent of blood monocytes and neutrophils was assessed by flow cytometry (*n* = 8 mice/group). (D) Representative images of the degree of atherosclerosis in the aortic root area. Lipid lesions in the arterial intima were quantified by ORO staining of aortic root sections (×400). Scale bars, 500 μm. (E) Representative images of macrophages immunostaining in the aortic root sections. Atherosclerotic lesions were immunostained for the macrophage CD68 antigen and nuclei were visualized in blue with DAPI staining (autofluorescence in green) (×400). Scale bars, 500 μm. For (D) and (E), each symbol represents the mean area of a single mouse. Means ± SEM for each group are indicated. \*\**P* < 0.01, \*\*\**P* < 0.001 (unpaired t-test).

(Figure 2B). Circulating neutrophil and monocyte levels were also comparable (Figure 2C). Analysis of the Ly-6C<sup>hi</sup> and Ly-6C<sup>low</sup> monocyte subsets did not show any difference either (Supplementary material online, Figure S2). In this context, we observed larger atherosclerotic lesions in the aortic sinus of *Lysm-Cre* × *SR-B1*<sup>fl/fl</sup>→*Ldlr*<sup>-/-</sup> mice compared to *SR-B1*<sup>fl/fl</sup>→*Ldlr*<sup>-/-</sup> mice (Figure 2D, 164 ± 6 and 100 ± 6 × 10<sup>3</sup> μm<sup>2</sup>, respectively; *P* < 0.001). Immunostaining of CD68<sup>+</sup> lesional macrophages consistently revealed a 40% increase (102 ± 8 and 73 ± 6 × 10<sup>3</sup> μm<sup>2</sup>, respectively; *P* < 0.01) in the macrophage area in *Lysm-Cre* × *SR-B1*<sup>fl/fl</sup>-transplanted mice (Figure 2E).

To confirm these findings in a second mouse model of atherosclerosis, we chose the diet-induced atherogenic *SR-B1* KO<sup>liver</sup> × CETP mouse, in which we previously demonstrated that SR-B1 expression in peripheral, non-hepatic cells exerts atheroprotective activities.<sup>10,26</sup> Thus, irradiated *SR-B1* KO<sup>liver</sup> × CETP mice were transplanted with BM from *SR-B1*<sup>fl/fl</sup> or

*Lysm-Cre* × *SR-B1*<sup>fl/fl</sup> mice. In addition, to gain further insights into the role of SR-B1 expressed by cells of haematopoietic origin other than monocytes/macrophages, we transplanted irradiated *SR-B1* KO<sup>liver</sup> × CETP recipients with BM of *SR-B1*<sup>-/-</sup> mice. After transplantation recovery, mice were fed a high-cholesterol and high-fat diet for 20 weeks. At sacrifice, *SR-B1*<sup>fl/fl</sup>, *Lysm-Cre* × *SR-B1*<sup>fl/fl</sup>, and *SR-B1*<sup>-/-</sup> BM-transplanted *SR-B1* KO<sup>liver</sup> × CETP mice exhibited similarly elevated plasma TC levels (Figure 3A). Plasma cholesterol distribution in lipoprotein fractions was also similar between groups (Supplementary material online, Figure S3). As we previously reported,<sup>10,26</sup> hepatic SR-B1 deficiency results in elevated levels of circulating FC. Indeed, plasma FC was similarly increased (Figure 3A) and contributed to 60% of plasma TC in the three groups (as compared to 20–25% in *Ldlr*<sup>-/-</sup> mice). Similar to our findings in the *Ldlr*<sup>-/-</sup> background, *Lysm-Cre* × *SR-B1*<sup>fl/fl</sup>→*SR-B1* KO<sup>liver</sup> × CETP mice exhibited larger lesion area than control *SR-B1*<sup>fl/fl</sup>→*SR-B1* KO<sup>liver</sup> × CETP

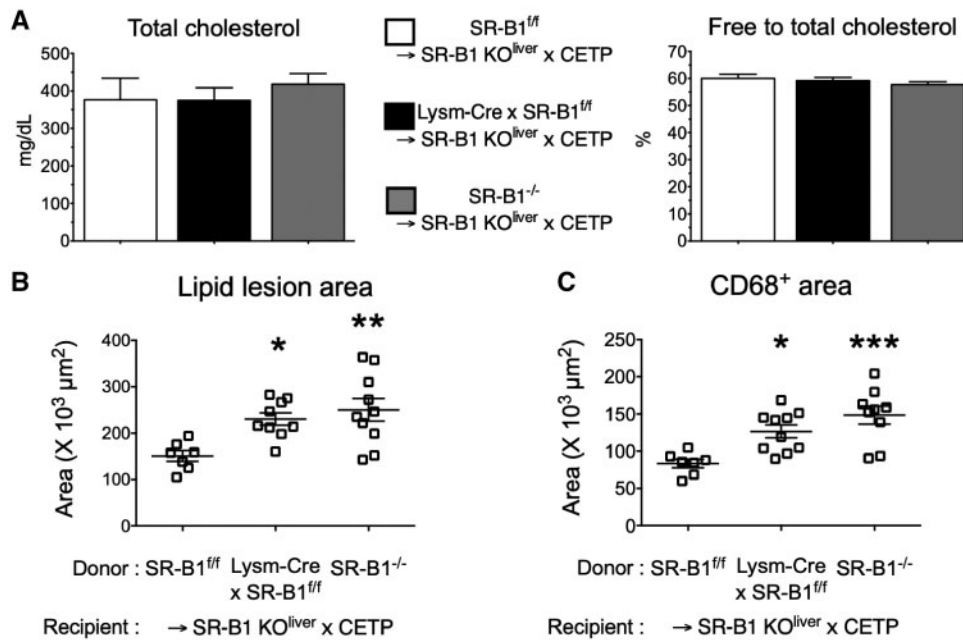


**Figure 3** SR-B1 deficiency in monocyte/macrophages favours plaque development in the atherogenic SR-B1 KO<sup>liver</sup> × CETP background. (A) Plasma TC and FC were determined in overnight-fasted SR-B1<sup>fl/fl</sup> → SR-B1 KO<sup>liver</sup> × CETP (n = 8), Lysm-Cre × SR-B1<sup>fl/fl</sup> → SR-B1 KO<sup>liver</sup> × CETP (n = 10) and SR-B1<sup>-/-</sup> → SR-B1 KO<sup>liver</sup> × CETP (n = 8) transplanted female mice fed a 1.25% cholesterol, 16% fat diet for 20 weeks. The degree of aortic root atherosclerosis was evaluated in these mice by quantifying (B) lipid lesions with ORO staining and (C) macrophage content by immunostaining for the macrophage CD68 antigen. Each symbol represents the mean area of a single mouse. Means ± SEM for each group are indicated. \*P < 0.05, \*\*P < 0.01, \*\*\*P < 0.001 (one-way ANOVA followed by Tukey's *post hoc* test).

mice (Figure 3B,  $230 \pm 13$  and  $151 \pm 11 \times 10^3 \mu\text{m}^2$ , respectively;  $P < 0.05$ ). This effect was associated with a 51% increase in the macrophage area (Figure 3C,  $127 \pm 9$  and  $84 \pm 6 \times 10^3 \mu\text{m}^2$ , respectively;  $P < 0.05$ ). Finally, analysis of aortic lesions of SR-B1<sup>-/-</sup> → SR-B1 KO<sup>liver</sup> × CETP mice showed larger lipid lesions and macrophage areas compared to control SR-B1<sup>fl/fl</sup> → SR-B1 KO<sup>liver</sup> × CETP mice, but no difference when compared to Lysm-Cre × SR-B1<sup>fl/fl</sup> → SR-B1 KO<sup>liver</sup> × CETP mice (Figure 3B, C).

### 3.3 Macrophage SR-B1-deficient mice exhibit decreased macrophage apoptosis in atherosclerotic lesions

To reveal potential mechanisms underlying increased atherosclerosis in macrophage SR-B1-deficient mice, we first monitored monocyte recruitment into plaques as described in Tacke *et al.*<sup>32</sup> Thus, SR-B1<sup>fl/fl</sup> → Ldlr<sup>-/-</sup> and Lysm-Cre × SR-B1<sup>fl/fl</sup> → Ldlr<sup>-/-</sup> mice fed for a 1% cholesterol diet for 7 weeks were intravenously injected with fluorescent latex beads to label circulating monocytes. Bead-labelling efficiency of blood monocytes was tested 1 day after beads injection and was not different between the two groups (data not shown). Quantification of bead<sup>+</sup> monocytes recruited into aortic sinus lesions 4 days later revealed a slight but non-statistical increased number of labelled cells into Lysm-Cre × SR-B1<sup>fl/fl</sup> → Ldlr<sup>-/-</sup> (Supplementary material online, Figure S4). No difference in recruited monocytes was also observed between SR-B1<sup>fl/fl</sup> and Lysm-Cre × SR-B1<sup>fl/fl</sup> BM-transplanted SR-B1 KO<sup>liver</sup> × CETP mice (data not shown).

We then assessed the effect of macrophage SR-B1 deficiency on lesional macrophage apoptosis using TUNEL staining. Quantification of

TUNEL<sup>+</sup> and DAPI<sup>+</sup> cells within the lesional macrophage area revealed an approximate 41% ( $P < 0.05$ ) decrease in the percentage of apoptotic cells in Lysm-Cre × SR-B1<sup>fl/fl</sup> → Ldlr<sup>-/-</sup> mice compared to SR-B1<sup>fl/fl</sup> → Ldlr<sup>-/-</sup> mice (Figure 4A and Supplementary material online, Figure S5A). Similar findings were also observed in the other atherogenic mouse background. Indeed, Lysm-Cre × SR-B1<sup>fl/fl</sup> → SR-B1 KO<sup>liver</sup> × CETP mice exhibited half as many apoptotic cells as SR-B1<sup>fl/fl</sup> transplanted controls (Figure 4B). Interestingly, such reduced percentage of TUNEL-positive cells in macrophage SR-B1-deficient mice was also observed in lesions of SR-B1<sup>-/-</sup> BM-transplanted mice (57% decrease compared to controls; Figure 4B and Supplementary material online, Figure S5B).

Finally, we quantified necrotic areas defined as DAPI-negative areas of the aortic intima. We found a marked increase in lesional necrotic area in Lysm-Cre × SR-B1<sup>fl/fl</sup> → Ldlr<sup>-/-</sup> mice compared to controls ( $58 \pm 4$  and  $36 \pm 4 \times 10^3 \mu\text{m}^2$ , respectively;  $P < 0.01$ ). However, this difference between the two groups was proportional to that found when comparing total lesion areas. As such, necrotic areas represented approximately 35% of the total lesion area for both groups of mice (Figure 4C). Similar findings were observed in the SR-B1 KO<sup>liver</sup> × CETP background. The percentage of necrotic areas was not different between SR-B1<sup>fl/fl</sup>, Lysm-Cre × SR-B1<sup>fl/fl</sup> and SR-B1<sup>-/-</sup> BM-transplanted mice (approximately 40% of total lesion; Figure 4D).

### 3.4 SR-B1 favours macrophage apoptosis

SR-B1 facilitates the bi-directional flux of cholesterol between cells and lipoproteins. In this context, it has also been well demonstrated that FC loading of macrophages promotes ER stress-induced apoptosis,<sup>33</sup> a process likely to contribute to plaque progression. Thus, we evaluated the

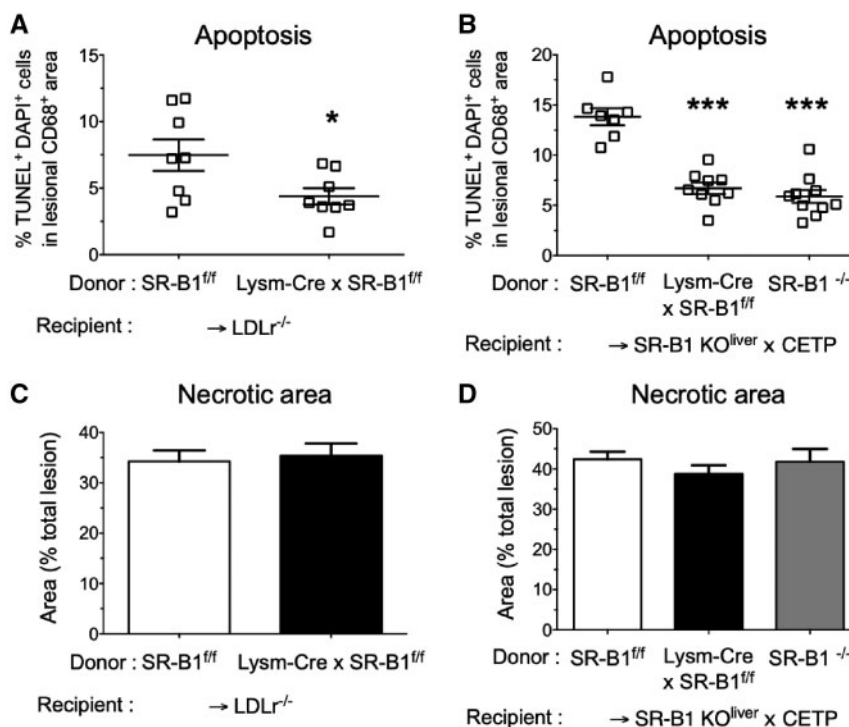


**Figure 4** Increased atherosclerosis in Lysm-Cre  $\times$  SR-B1<sup>ff</sup> transplanted mice is associated with decreased apoptosis of lesional macrophages. (A) and (B) Detection of apoptotic cells within the intimal CD68-positive area was performed with the TUNEL assay. Each symbol represents the percentage of TUNEL+ and DAPI+ cells for a single mouse. Means  $\pm$  SEM for each group are indicated. (C) and (D) Lesional necrosis in the aortic root intima was determined by quantifying ORO-positive and DAPI-negative areas. Data are expressed as percentage of the total lipid (ORO+) lesion. Means  $\pm$  SEM for each group are indicated. \* $P < 0.05$ , \*\*\* $P < 0.001$  [unpaired *t*-test (A, C) or one-way ANOVA followed by Tukey's *post hoc* test (B, D)].

consequences of SR-B1 deficiency upon FC-loading of macrophages. To do so, macrophages prepared from SR-B1<sup>ff</sup> and Lysm-Cre  $\times$  SR-B1<sup>ff</sup> BMs (BMDM) were incubated for 20 h with medium supplemented with acetylated-LDL (ac-LDL; 50  $\mu$ g/mL) in the presence of an ACAT inhibitor to block cellular cholesterol esterification and promote FC-loading. Under these conditions, the cellular cholesterol content of SR-B1<sup>ff</sup> and Lysm-Cre  $\times$  SR-B1<sup>ff</sup> BMDM, primarily present under an unesterified form (>90%), was increased three-fold compared to control medium. However, no difference in cholesterol loading, for both esterified and non-esterified forms, was observed between the two genotypes (Supplementary material online, Figure S6). In this context, analysis of apoptosis susceptibility by flow cytometry (Supplementary material online, Figure S7) revealed that FC-loading resulted in significantly less cell death in SR-B1-deficient macrophages compared to control SR-B1<sup>ff</sup> macrophages (Figure 5A and Supplementary material online, Figure S8). This finding (i.e. diminished apoptosis in SR-B1-deficient cells) was also observed when comparing FC-loaded macrophages prepared from SR-B1<sup>+/+</sup> and SR-B1<sup>-/-</sup> mice (Figure 5B).

Previous studies have clearly demonstrated that P38-MAPK<sup>34</sup> and signal transducer and activator of transcription-1 (STAT1)<sup>35</sup> are activated and play critical role in controlling macrophage apoptosis following FC-loading. Thus, we looked at the active, phosphorylated state of these two proteins in FC-loaded SR-B1<sup>ff</sup> and Lysm-Cre  $\times$  SR-B1<sup>ff</sup> BMDM. We did not detect any difference in the total amount of both proteins, but phospho-P38-MAPK and Ser-phospho-STAT1 were found moderately, but statistically decreased by 20% and 15% in Lysm-Cre  $\times$  SR-B1<sup>ff</sup>,

respectively (Figure 5C). In this setting, we analysed downstream targets of P38-MAPK signalling, and notably transcription factor C/EBP homologous protein (CHOP), a critical determinant of FC loading-induced apoptosis. However, FC-loaded SR-B1<sup>ff</sup> and Lysm-Cre  $\times$  SR-B1<sup>ff</sup> BMDM exhibited similar expression levels of CHOP (Figure 5D). Other CHOP independent, proapoptotic pathways may also contribute to macrophage apoptosis, including pathways involved in the generation of nitric oxide and reactive oxygen species. In fact, nitric oxide (NO) production by the inducible-nitric oxide synthase (*Nos2*, *iNos*) may also modulate macrophage apoptosis.<sup>36,37</sup> Interestingly, we observed significantly lower levels of *Nos2* expression in FC-loaded Lysm-Cre  $\times$  SR-B1<sup>ff</sup> BMDM compared with those measured in FC-loaded SR-B1<sup>ff</sup> BMDM (Figure 5D). However, analysis of macrophage apoptosis following FC-loading in the presence of the NOS inhibitor L-NAME did not abrogate the difference between Lysm-Cre  $\times$  SR-B1<sup>ff</sup> and SR-B1<sup>ff</sup> BMDM (Figure 5E). Thus, this finding ruled out the possibility that reduced *Nos2* expression contributed to reduced levels of apoptosis in macrophage lacking SR-B1.

### 3.5 AIM is induced in macrophages deficient for SR-B1

AIM (CD5L/Sp $\alpha$ /Api6) has previously been shown to be induced in response to oxLDL loading of macrophages, but also to protect macrophages from the apoptotic effects of oxidized-lipids.<sup>38</sup> As shown in Figure 6A, we found AIM expression increased by more than two-fold in Lysm-Cre  $\times$  SR-B1<sup>ff</sup> macrophages compared to SR-B1<sup>ff</sup> control macrophages.

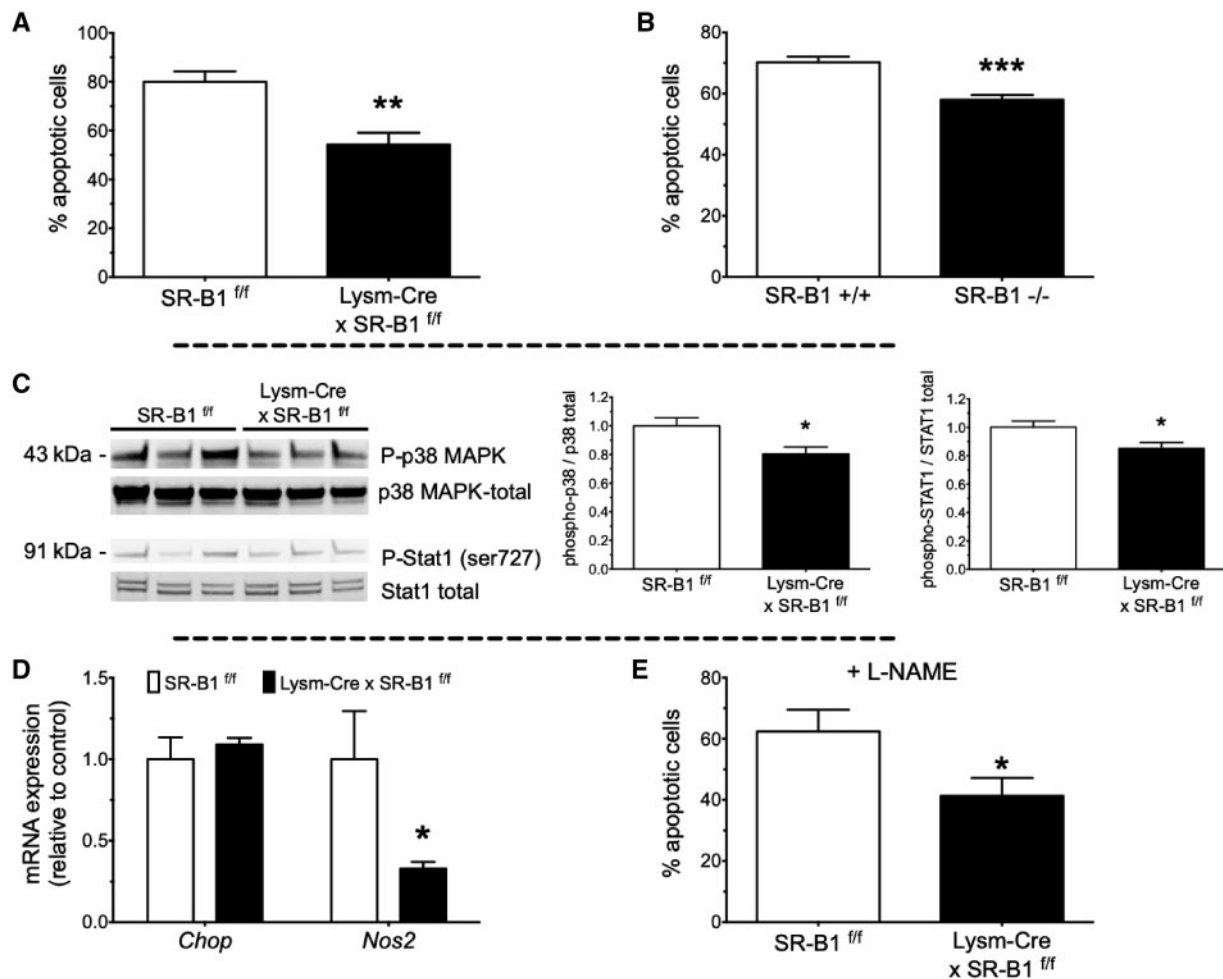


**Figure 5** SR-B1-deficient macrophages are less susceptible to free cholesterol loading-induced apoptosis. (A) *SR-B1<sup>fl/fl</sup>* and *Lysm-Cre × SR-B1<sup>fl/fl</sup>* bone marrow-derived macrophages (BMDM) and (B) *SR-B1<sup>+/+</sup>* and *SR-B1<sup>-/-</sup>* BMDM were loaded with free cholesterol (ac-LDL plus ACAT inhibitor) for 20 h and then assayed for apoptosis by flow cytometry. Data are expressed as the percentage of total cells that stained for annexin V and propidium iodide. (C) Cellular protein lysates from BMDM loaded with free cholesterol for 20 h were immunoblotted for phosphorylated and total P38-MAPK and STAT1 proteins. Representative immunoblots are shown. Histograms show means ± SEM ( $n = 5$  mice/group) of phosphorylated to total protein ratio obtained for both genotypes and proteins. Data are expressed relative to those of *SR-B1<sup>fl/fl</sup>* BMDM, which are arbitrarily set at 1. (D) Gene expression analysis for *Chop* and *Nos2* was performed under experimental conditions described in (A). (E) Macrophages were loaded with free cholesterol in presence of the NOS inhibitor L-NAME (50  $\mu$ M) and then assayed for apoptosis as in (A) ( $n = 6$  mice per group). Statistical differences between genotypes \* $P < 0.05$ , \*\* $P < 0.01$ , \*\*\* $P < 0.001$  (unpaired t-test).

Upon FC-loading, *AIM* expression was upregulated in both *Lysm-Cre × SR-B1<sup>fl/fl</sup>* and *SR-B1<sup>fl/fl</sup>* BMDM but remained significantly more elevated in *SR-B1*-deficient macrophages at all time points studied (Figure 6A). Increased expression of *AIM* in *Lysm-Cre × SR-B1<sup>fl/fl</sup>* BMDM was confirmed at the protein level (Supplementary material online, Figure S9). Higher expression of *AIM* was also observed in *SR-B1*-deficient macrophages polarized by LPS/IFN $\gamma$  (M1-polarization) (Supplementary material online, Figure S10). Neutralization of the receptor by a conformational antibody provided similar findings. Indeed, incubation of *SR-B1<sup>fl/fl</sup>* macrophages with anti-*SR-B1* antibody C11<sup>28</sup> resulted in increased *AIM* mRNA levels, whereas *AIM* expression remained unchanged in C11-treated *SR-B1*-deficient macrophages (Figure 6B). We could also demonstrate that siRNA-mediated *hSR-B1* gene silencing induced *hAIM* mRNA levels in human THP1 macrophage cell line (Figure

6C). This difference in *AIM* expression could not be explained by a difference in expression of MafB transcription factor (Supplementary material online, Figure S11) whose activity is critical for *AIM* induction in lipid-loaded macrophages.<sup>39</sup> *AIM* is also a direct target for regulation by nuclear receptors LXRs,<sup>38,40</sup> that are major players in macrophage cholesterol metabolism. However, we observed no difference in cellular desmosterol content, the dominant LXR natural agonist in cholesterol-loaded macrophages,<sup>41</sup> between *Lysm-Cre × SR-B1<sup>fl/fl</sup>* and *SR-B1<sup>fl/fl</sup>* macrophages (Supplementary material online, Figure S12). Finally, *AIM* expression can be promoted by STAT3.<sup>42</sup> Thus, we investigated the consequence of STAT3 inhibition by cucurbitacin I treatment of *Lysm-Cre × SR-B1<sup>fl/fl</sup>* and *SR-B1<sup>fl/fl</sup>* BMDM on *AIM* expression. As shown in Figure 6D, incubation of the macrophages with cucurbitacin I for 6 h abolished the differential expression of *AIM* between both cell types and suggested

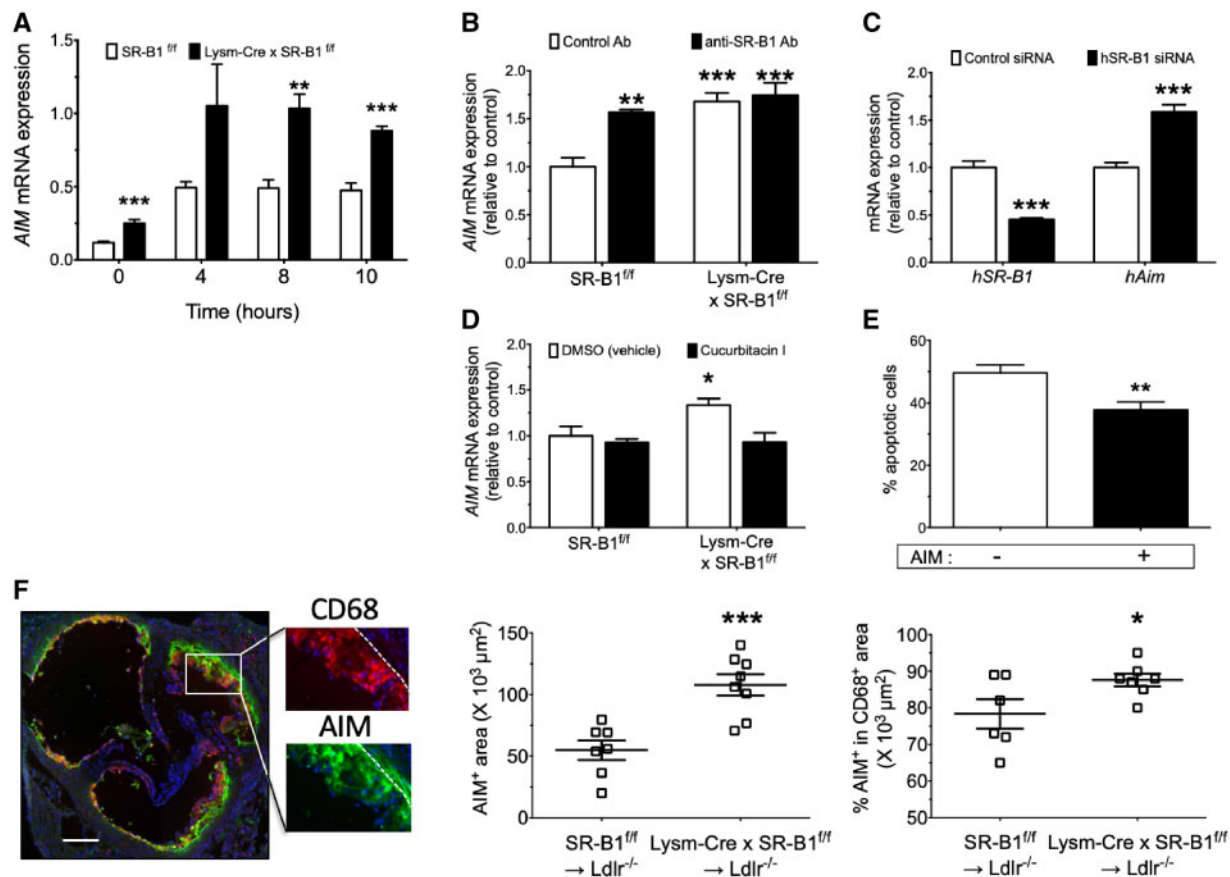


**Figure 6** Apoptosis inhibitor of macrophage (AIM) expression is increased in macrophages deficient for SR-B1 and reduces FC loading-induced macrophage apoptosis. AIM mRNA levels were determined in SR-B1<sup>fl/fl</sup> and Lysm-Cre × SR-B1<sup>fl/fl</sup> BMDM incubated (A) under free cholesterol loading conditions for the indicated times ( $n = 6$  mice per group, statistical differences between genotypes  $**P < 0.01$ ,  $***P < 0.001$  (unpaired *t*-test) or (B) in the presence of anti-SR-B1 C11 antibody (20  $\mu\text{g}/\text{mL}$ ) or control human IgG overnight ( $n = 6$  per genotype, *P*-values vs. 'SR-B1<sup>fl/fl</sup>, control Ab' [paired *t*-test (anti-SR-B1 Ab, SR-B1<sup>fl/fl</sup>) or unpaired *t*-test]). (C) Human THP-1 macrophages were transfected with hSR-B1-targeting siRNA or control siRNA. Forty-eight hours post-transfection hSR-B1 and hAIM mRNA expression levels were determined by RT-qPCR ( $n = 6$  per condition, paired *t*-test). (D) AIM mRNA expression was quantified in SR-B1<sup>fl/fl</sup> and Lysm-Cre × SR-B1<sup>fl/fl</sup> BMDM treated with STAT3 inhibitor cucurbitacin I (1  $\mu\text{M}$ ) or vehicle (DMSO) for 6 h ( $n = 6$ , statistical differences vs. control 'SR-B1<sup>fl/fl</sup>, DMSO') were calculated using paired (same genotype) or unpaired *t*-test. (E) Wild-type BMDM were pre-incubated or not with recombinant AIM (5  $\mu\text{g}/\text{mL}$ ) for 5 h and then acLDL and ACAT inhibitor were added for free cholesterol loading for 20 h. Macrophage apoptosis was determined by flow cytometry ( $n = 6$ ,  $**P < 0.01$ , paired *t*-test). (F) Atherosclerotic lesions of SR-B1<sup>fl/fl</sup> → Ldlr<sup>-/-</sup> and Lysm-Cre × SR-B1<sup>fl/fl</sup> → Ldlr<sup>-/-</sup> transplanted female mice fed a 1% cholesterol diet for 8 weeks were subjected to immunohistochemical analyses. Sections were stained with anti-CD68 (red), anti-AIM (green), and DAPI (blue) ( $\times 400$ ). Scale bar, 200  $\mu\text{m}$ . Dashed lines in insert panels delineate intima-media border. AIM positive areas were quantified and the percentage of CD68+ area that stained for AIM was determined. Each symbol represents the area of a single mouse. Means  $\pm$  SEM for each group are indicated.  $*P < 0.05$ ,  $***P < 0.001$  (unpaired *t*-test).

that activation of STAT3 signalling was involved in raised AIM expression levels in SR-B1-deficient macrophages.

Then, as AIM deficiency accelerates oxLDL-induced apoptosis in cultured macrophages,<sup>38</sup> we sought to determine whether AIM had the potential to protect ER-stressed macrophages upon FC-loading from apoptosis. BMDM were pre-incubated with recombinant mouse AIM protein for 5 h and then loaded with FC. Incubation of FC-loaded macrophages with AIM resulted in a significant anti-apoptotic protective effect (Figure 6E). Finally, we performed immunofluorescence analysis for AIM in atherosclerotic aortic lesions of both Lysm-Cre × SR-B1<sup>fl/fl</sup> and SR-B1<sup>fl/fl</sup> BM-transplanted mice (Figure 6F and Supplementary material online, Figure S13). We found that AIM-positive intima areas were significantly larger in macrophage SR-B1-deficient mice. More importantly and

consistent with our *in vitro* data, the percentage of the macrophage area that stained positive for AIM was bigger in Lysm-Cre × SR-B1<sup>fl/fl</sup> than SR-B1<sup>fl/fl</sup> controls ( $87.6 \pm 1.7$  and  $78.3 \pm 4.0\%$ , respectively;  $P < 0.05$ ; Figure 6F).

## 4. Discussion

BM transplant studies have established that SR-B1 exerts an atheroprotective function in cells of haematopoietic origin.<sup>18–22</sup> The present study is the first demonstration that this protective activity is primarily exerted by SR-B1 expression in the macrophage. These results were validated in two different diet-induced pro-atherosclerotic mouse models.



Accelerated atherosclerosis progression resulting from macrophage SR-B1 deficiency was associated with reduced numbers of apoptotic macrophages within the lesions. Available evidence suggests that increased expression of the anti-apoptotic protein AIM in SR-B1-deficient macrophages may contribute to the decreased apoptosis susceptibility and accelerated plaque growth.

In the conceptual view of reverse cholesterol transport, cellular transporters involved in cholesterol efflux from macrophage foam cells are thought to play a critical role in initiating the first step of this pathway and in protecting from atherogenesis. These transporters include the ABC transporters ABCA1 and ABCG1, but also SR-B1. Increased atherosclerosis in hypercholesterolaemic *Ldlr*<sup>-/-</sup> mice transplanted with *Abca1*<sup>-/-</sup> BM has been generally interpreted as a demonstration of such protective role for macrophage ABCA1.<sup>43</sup> However, specific deletion of *Abca1* in monocyte/macrophage using *Lysm-Cre* × *Abca1*<sup>fl/fl</sup> mice cross-bred in the *Ldlr*<sup>-/-</sup> background surprisingly revealed no effect on atherosclerosis development.<sup>44</sup> Though not tested by specific targeting, *Abcg1*<sup>-/-</sup> BM transplantation did not reveal a major impact of *Abcg1* deletion on atherosclerosis development, but rather led to controversial results.<sup>45–47</sup> These studies suggested a limited impact for macrophage cholesterol efflux in atherogenesis. However, the combined deletion of *Abca1* and *Abcg1* genes in the macrophage resulted in accelerated atherosclerosis with increased plaque inflammation.<sup>31</sup> These results underlined the importance of compensatory mechanisms in cholesterol efflux pathways. They also highlighted non-arterial indirect pro-atherogenic role, notably played by splenic macrophage foam cells deficient for *Abca1* and *Abcg1* on promoting monocytosis and neutrophilia via increased chemokine secretion.<sup>31</sup> Our results clearly established that the sole deletion of SR-B1 in the monocyte/macrophage lineage was responsible for the increased lesional macrophage burden. This effect was not associated with any change in blood monocytes and neutrophils in the *Ldlr*<sup>-/-</sup> background. Although combined deletion of SR-B1 with *Abca1* has been shown to enhance the formation of lipid-laden macrophages *in vivo*, SR-B1 deficiency by itself did not seem to favour any foam cell development.<sup>22</sup> This suggests that aberrant chemokine/cytokine secretion from foam cells unlikely participated in the atherogenic phenotype associated with monocyte/macrophage-SR-B1 deficiency in our study.

It is now well established that macrophage apoptosis plays a critical role in the progression of atherosclerosis. However, genetic modulation of macrophage apoptosis has revealed that it may act as a positive<sup>27,48–50</sup> or negative regulator<sup>27,38,39,51–53</sup> of plaque growth. The emerging view is that its impact may depend on the stage of atherosclerosis development.<sup>27,54</sup> The scavenger receptor cysteine-rich superfamily (SRCR-SF) member AIM is primarily expressed by mature tissue macrophages,<sup>55,56</sup> albeit a role in other cell types has also been documented.<sup>42</sup> The anti-apoptotic function of AIM in macrophages against various apoptosis-inducing stimuli,<sup>39,40,56–58</sup> including oxidized-LDL,<sup>38</sup> is well documented. In the context of atherosclerosis, deletion of AIM in *LDLr*<sup>-/-</sup> mice resulted in a dramatic increase in the amount of apoptotic macrophages in the lesions leading to an important reduction of plaque growth with diminished macrophage content.<sup>38</sup> Another important demonstration for a role of AIM in protecting macrophage from apoptosis and the associated consequences on atherosclerosis development has also been brought by Hamada *et al.*<sup>39</sup> in irradiated *LDLr*<sup>-/-</sup> mice reconstituted with MafB-deficient foetal liver cells. Indeed, they showed in their study that the lack of AIM induction by the LXR/RXR pathway following macrophage lipid loading in the absence of MafB was associated with accelerated macrophage apoptosis and attenuation of early atherogenesis

development. In this context, our findings bring additional support for a critical role of macrophage apoptosis in modulating atherosclerosis development. Indeed, consistent with the pro-apoptotic and atheroprotective effects reported with AIM deficiency, our results showed decreased macrophage apoptosis and accelerated plaque growth in mice exhibiting increased AIM expression in SR-B1-deficient macrophages.

Efferocytosis, the phagocytic clearance of dying cells primarily by macrophages, is an efficient process that prevents post-apoptotic necrosis. In advanced lesions, defective efferocytosis has been shown to contribute to plaque necrotic core formation, but other non-apoptotic cell death pathways can also actively participate.<sup>59,60</sup> In our study, the percentage of plaque necrosis did not differ between groups in both atherosclerotic mouse models tested (SR-B1 KO<sup>liver</sup> × CETP or *LDLr*<sup>-/-</sup> background). These findings are in agreement with a previous study using SR-B1<sup>-/-</sup> BM-transplanted *Ldlr*<sup>-/-</sup> mice,<sup>22</sup> but contrast with those of Tao *et al.*<sup>20</sup> reporting a five-fold increase in necrosis using the same experimental approach. In the latter, the authors suggested that defective macrophage SR-B1-mediated efferocytosis was responsible for the observed increase in the number of apoptotic cells in the lesions and of plaque size. Although these results seem incompatible with ours, these apparent contradictions may reflect that macrophage-SR-B1 exerts various protective activities that are differentially revealed as a function of lesion stage development. In early developing lesions, AIM-dependent protection of macrophages from apoptosis would predominate, whereas a role for SR-B1 in efferocytosis could be more pronounced in advanced lesions when efferocytosis pathways become impaired. As such an example, G2a-deficient mice displaying decreased macrophage apoptosis as well as efferocytosis demonstrated increased atherosclerosis.<sup>53</sup>

Previous studies have clearly established that the transcription factor MafB directly regulates AIM gene expression in macrophages and that lack of MafB results in lower expression level of AIM.<sup>39</sup> Moreover, AIM expression is increased upon oxLDL-induced lipid loading of macrophages or treatment with synthetic agonist of the LXR transcription factor. This activation of AIM by the LXR/RXR heterodimer complex was also shown to depend on MafB.<sup>39</sup> Consistent with these studies, we observed a rapid induction of AIM expression following FC loading of macrophages. However, AIM mRNA levels were clearly more elevated in SR-B1-deficient macrophages independently of lipid loading. Moreover, upregulation of AIM levels upon SR-B1 invalidation was confirmed by means other than genetic deletion and in macrophages of murine and human origin (i.e. SR-B1 antibody neutralization and siRNA-mediated hSR-B1 gene silencing in human THP1 cells). In our experimental conditions, increased AIM expression could not be explained by differential macrophage cholesterol content (including desmosterol cellular concentration) or enhanced MafB expression, but rather involved STAT3 signalling. Interestingly, SR-B1 has been identified earlier as a plasma membrane cholesterol sensor able to regulate kinase signalling. Such function regulates p38-MAPK dependent-APOB trafficking in enterocytes but also HDL stimulation of eNOS in endothelial cells and cell migration.<sup>16</sup> Alternatively, we previously reported that SR-B1 can modulate the cholesterol enrichment of lipid rafts in hepatocytes.<sup>61</sup> Thus, whether or not plasma membrane cholesterol sensing is relevant to SR-B1 function in macrophages to modulate AIM expression in a STAT3-dependent manner will remain to be explored.

In conclusion, this study demonstrates by specific targeting that an important extra-hepatic role of SR-B1 in atheroprotection lies in monocytes/macrophages, potentially involving a direct influence of SR-B1 on the macrophage life cycle in the developing atherosclerotic lesion.

Understanding of its beneficial action in limiting disease development will require investigating whether such effects could be controlled by SR-B1 ligands.

## Supplementary material

Supplementary material is available at *Cardiovascular Research* online.

## Acknowledgements

We thank Marie Lhomme for the lipidomic analyses performed at the ICANalytics core facility of the Institute of Cardiometabolism and Nutrition (IHU-ICAN, ANR-10-IAHU-05), Paris, France.

**Conflict of interest:** none declared.

## Funding

This work was supported by the French National Institute for Health and Medical Research (INSERM). L.G. was supported by a Fellowship from Région Île-de-France/CORDDIM.

## References

- Gordon T, Castelli WP, Hjortland MC, Kannel WB, Dawber TR. High density lipoprotein as a protective factor against coronary heart disease. The Framingham Study. *Am J Med* 1977;**62**:707–714.
- Kingwell BA, Chapman MJ, Kontush A, Miller NE. HDL-targeted therapies: progress, failures and future. *Nat Rev Drug Discov* 2014;**13**:445–464.
- Rader DJ. Molecular regulation of HDL metabolism and function: implications for novel therapies. *J Clin Invest* 2006;**116**:3090–3100.
- Barter PJ, Nicholls S, Rye K-A, Anantharamaiah GM, Navab M, Fogelman AM. Antiinflammatory properties of HDL. *Circ Res* 2004;**95**:764–772.
- Yvan-Charvet L, Pagler T, Gautier EL, Avagyan S, Siry RL, Han S, Welch CL, Wang N, Randolph GJ, Snock HW, Tall AR. ATP-binding cassette transporters and HDL suppress hematopoietic stem cell proliferation. *Science* 2010;**328**:1689–1693.
- Mineo C, Deguchi H, Griffin JH, Shaul PW. Endothelial and antithrombotic actions of HDL. *Circ Res* 2006;**98**:1352–1364.
- Mineo C, Shaul PW. Regulation of signal transduction by HDL. *J Lipid Res* 2013;**54**:2315–2324.
- Arai T, Wang N, Bezouevski M, Welch C, Tall AR. Decreased atherosclerosis in heterozygous low density lipoprotein receptor-deficient mice expressing the scavenger receptor BI transgene. *J Biol Chem* 1999;**274**:2366–2371.
- Ueda Y, Gong E, Royer L, Cooper PN, Francone OL, Rubin EM. Relationship between expression levels and atherogenesis in scavenger receptor class B, type I transgenics. *J Biol Chem* 2000;**275**:20368–20373.
- Huby T, Doucet C, Dacet C, Ouzilleau B, Ueda Y, Afzal V, Rubin E, Chapman MJ, Lesnik P. Knockdown expression and hepatic deficiency reveal an atheroprotective role for SR-BI in liver and peripheral tissues. *J Clin Invest* 2006;**116**:2767–2776.
- Huszar D, Varban ML, Rinninger F, Feeley R, Arai T, Fairchild-Huntress V, Donovan MJ, Tall AR. Increased LDL cholesterol and atherosclerosis in LDL receptor-deficient mice with attenuated expression of scavenger receptor B1. *Arterioscler Thromb Vasc Biol* 2000;**20**:1068–1073.
- Vergeer M, Korporaal SJ, Franssen R, Meurs I, Out R, Hovingh GK, Hoekstra M, Sierts JA, Dallinga-Thie GM, Motazacker MM, Holleboom AG, Van Berkel TJ, Kastelein JJ, Van Eck M, Kuivenhoven JA. Genetic variant of the scavenger receptor BI in humans. *N Engl J Med* 2011;**364**:136–145.
- Gilibert S, Galle-Treger L, Moreau M, Saint-Charles F, Costa S, Ballaire R, Couvert P, Carrié A, Lesnik P, Huby T. Adrenocortical scavenger receptor class B type I deficiency exacerbates endotoxemic shock and precipitates sepsis-induced mortality in mice. *J Immunol* 2014;**193**:817–826.
- Out R, Hoekstra M, Spijkers JA, Kruijff JK, Eck M, V, Bos IS, Twisk J, Van Berkel TJ. Scavenger receptor class B type I is solely responsible for the selective uptake of cholesteryl esters from HDL by the liver and the adrenals in mice. *J Lipid Res* 2004;**45**:2088–2095.
- Hoekstra M, Rj van der S, Van Eck M, Van Berkel TJ. Adrenal-specific scavenger receptor BI deficiency induces glucocorticoid insufficiency and lowers plasma very-low-density and low-density lipoprotein levels in mice. *Arterioscler Thromb Vasc Biol* 2013;**33**:e39–46.

- Saddar S, Carriere V, Lee WR, Tanigaki K, Yuhanna IS, Parathath S, Morel E, Warriar M, Sawyer JK, Gerard RD, Temel RE, Brown JM, Connelly M, Mineo C, Shaul PW. Scavenger receptor class B type I is a plasma membrane cholesterol sensor. *Circ Res* 2013;**112**:140–151.
- Yuhanna IS, Zhu Y, Cox BE, Hahner LD, Osborne-Lawrence S, Lu P, Marcel YL, Anderson RG, Mendelsohn ME, Hobbs HH, Shaul PW. High-density lipoprotein binding to scavenger receptor-BI activates endothelial nitric oxide synthase. *Nat Med* 2001;**7**:853–857.
- Covey SD, Krieger M, Wang W, Penman M, Trigatti BL. Scavenger receptor class B type I-mediated protection against atherosclerosis in LDL receptor-negative mice involves its expression in bone marrow-derived cells. *Arterioscler Thromb Vasc Biol* 2003;**23**:1589–1594.
- Van Eck M, Bos IS, Hildebrand RB, Van Rij BT, Van Berkel TJ. Dual role for scavenger receptor class B, type I on bone marrow-derived cells in atherosclerotic lesion development. *Am J Pathol* 2004;**165**:785–794.
- Tao H, Yancey PG, Babaev VR, Blakemore JL, Zhang Y, Ding L, Fazio S, Linton MF. Macrophage SR-BI mediates efferocytosis via Src/PI3K/Rac1 signaling and reduces atherosclerotic lesion necrosis. *J Lipid Res* 2015;**56**:1449–1460.
- Zhang W, Yancey PG, Su YR, Babaev VR, Zhang Y, Fazio S, Linton MF. Inactivation of macrophage scavenger receptor class B type I promotes atherosclerotic lesion development in apolipoprotein E-deficient mice. *Circulation* 2003;**108**:2258–2263.
- Zhao Y, Pennings M, Hildebrand RB, Ye D, Calpe-Berdiel L, Out R, Kjerrulf M, Hurt-Camejo E, Groen AK, Hoekstra M, Jessup W, Chimini G, Van Berkel TJ, Van Eck M. Enhanced foam cell formation, atherosclerotic lesion development, and inflammation by combined deletion of ABCA1 and SR-BI in bone marrow-derived cells in LDL receptor knockout mice on western-type diet. *Circ Res* 2010;**107**:e20–31.
- Sage AP, Tsiatoulas D, Binder CJ, Mallat Z. The role of B cells in atherosclerosis. *Nat Rev Cardiol* 2019;**16**:180–196.
- Tabas I, Lichtman AH. Monocyte-macrophages and T cells in atherosclerosis. *Immunity* 2017;**47**:621–634.
- Gao M, Zhao D, Schouteden S, Sorci-Thomas MG, Van Veldhoven PP, Eggermont K, Liu G, Verfaillie CM, Feng Y. Regulation of high-density lipoprotein on hematopoietic stem/progenitor cells in atherosclerosis requires scavenger receptor type BI expression. *Arterioscler Thromb Vasc Biol* 2014;**34**:1900–1909.
- El Bouhassani M, Gilibert S, Moreau M, Saint-Charles F, Tréguier M, Poti F, Chapman MJ, Le Goff W, Lesnik P, Huby T. Cholesteryl ester transfer protein expression partially attenuates the adverse effects of SR-BI receptor deficiency on cholesterol metabolism and atherosclerosis. *J Biol Chem* 2011;**286**:17227–17238.
- Gautier EL, Huby T, Witztum JL, Ouzilleau B, Miller ER, Saint-Charles F, Aucouturier P, Chapman MJ, Lesnik P. Macrophage apoptosis exerts divergent effects on atherogenesis as a function of lesion stage. *Circulation* 2009;**119**:1795–1804.
- Catanese MT, Graziani R, Hahn T, V, Moreau M, Huby T, Paonessa G, Santini C, Luzzago A, Rice CM, Cortese R, Vitelli A, Nicosia A. High-avidity monoclonal antibodies against the human scavenger class B type I receptor efficiently block hepatitis C virus infection in the presence of high-density lipoprotein. *J Virol* 2007;**81**:8063–8071.
- Frisdal E, Lesnik P, Olivier M, Robillard P, Chapman MJ, Huby T, Guerin M, Le Goff W. Interleukin-6 protects human macrophages from cellular cholesterol accumulation and attenuates the proinflammatory response. *J Biol Chem* 2011;**286**:30926–30936.
- Abram CL, Roberge GL, Hu Y, Lowell CA. Comparative analysis of the efficiency and specificity of myeloid-Cre deleting strains using ROSA-EYFP reporter mice. *J Immunol Methods* 2014;**408**:89–100.
- Westertep M, Murphy AJ, Wang M, Pagler TA, Vengrenyuk Y, Kappus MS, Gorman DJ, Nagareddy PR, Zhu X, Abramowicz S, Parks JS, Welch C, Fisher EA, Wang N, Yvan-Charvet L, Tall AR. Deficiency of ATP-binding cassette transporters A1 and G1 in macrophages increases inflammation and accelerates atherosclerosis in mice. *Circ Res* 2013;**112**:1456–1465.
- Tacke F, Alvarez D, Kaplan TJ, Jakubzick C, Spanbroek R, Llodra J, Garin A, Liu J, Mack M, Rooijen N, V, Lira SA, Habenicht AJ, Randolph GJ. Monocyte subsets differentially employ CCR2, CCR5, and CX3CR1 to accumulate within atherosclerotic plaques. *J Clin Invest* 2007;**117**:185–194.
- Devries-Seimon T, Li Y, Yao PM, Stone E, Wang Y, Davis RJ, Flavell R, Tabas I. Cholesterol-induced macrophage apoptosis requires ER stress pathways and engagement of the type A scavenger receptor. *J Cell Biol* 2005;**171**:61–73.
- Seimon TA, Wang Y, Han S, Senokuchi T, Schrijvers DM, Kuriakose G, Tall AR, Tabas IA. Macrophage deficiency of p38alpha MAPK promotes apoptosis and plaque necrosis in advanced atherosclerotic lesions in mice. *J Clin Invest* 2009;**119**:886–898.
- Lim WS, Timmins JM, Seimon TA, Sadler A, Kolodgie FD, Virmani R, Tabas I. Signal transducer and activator of transcription-1 is critical for apoptosis in macrophages subjected to endoplasmic reticulum stress in vitro and in advanced atherosclerotic lesions in vivo. *Circulation* 2008;**117**:940–951.
- Marriott HM, Hellewell PG, Cross SS, Ince PG, Whyte MK, Dockrell DH. Decreased alveolar macrophage apoptosis is associated with increased pulmonary inflammation in a murine model of pneumococcal pneumonia. *J Immunol* 2006;**177**:6480–6488.
- Weber TJ, Smallwood HS, Kathmann LE, Markillie LM, Squier TC, Thrall BD. Functional link between TNF biosynthesis and CaM-dependent activation of inducible

- nitric oxide synthase in RAW 264.7 macrophages. *Am J Physiol Cell Physiol* 2006;**290**: C1512–20.
38. Arai S, Shelton JM, Chen M, Bradley MN, Castrillo A, Bookout AL, Mak PA, Edwards PA, Mangelsdorf DJ, Tontonoz P, Miyazaki T. A role for the apoptosis inhibitory factor AIM/Spalpa/Ap16 in atherosclerosis development. *Cell Metab* 2005;**1**:201–213.
  39. Hamada M, Nakamura M, Tran MT, Moriguchi T, Hong C, Ohsumi T, Dinh TT, Kusakabe M, Hattori M, Katsumata T, Arai S, Nakashima K, Kudo T, Kuroda E, Wu CH, Kao PH, Sakai M, Shimano H, Miyazaki T, Tontonoz P, Takahashi S. MafB promotes atherosclerosis by inhibiting foam-cell apoptosis. *Nat Commun* 2014;**5**:3147.
  40. Joseph SB, Bradley MN, Castrillo A, Bruhn KW, Mak PA, Pei L, Hogenesch J, O'Connell RM, Cheng G, Saez E, Miller JF, Tontonoz P. LXR-dependent gene expression is important for macrophage survival and the innate immune response. *Cell* 2004;**119**:299–309.
  41. Spann NJ, Garmire LX, McDonald JG, Myers DS, Milne SB, Shibata N, Reichart D, Fox JN, Shaked I, Heudobler D, Raetz CR, Wang EW, Kelly SL, Sullards MC, Murphy RC, Merrill AH, Brown HA, Dennis EA, Li AC, Ley K, Tsimikas S, Fahy E, Subramaniam S, Quehenberger O, Russell DW, Glass CK. Regulated accumulation of desmosterol integrates macrophage lipid metabolism and inflammatory responses. *Cell* 2012;**151**:138–152.
  42. Wang C, Yosef N, Gaublotme J, Wu C, Lee Y, Clish CB, Kaminski J, Xiao S, Meyer Zu Horste G, Pawlak M, Kishi Y, Joller N, Karwacz K, Zhu C, Ordovas-Montanes M, Madi A, Wortman I, Miyazaki T, Sobel RA, Park H, Regev A, Kuchroo VK. CD5L/Alm regulates lipid biosynthesis and restrains Th17 cell pathogenicity. *Cell* 2015;**163**: 1413–1427.
  43. Eck M, V, Bos IS, Kaminski WE, Orso E, Rothe G, Twisk J, Botcher A, Van Amersfoort ES, Christiansen-Weber TA, Fung-Leung WP, Van Berkel TJ, Schmitz G. Leukocyte ABCA1 controls susceptibility to atherosclerosis and macrophage recruitment into tissues. *Proc Natl Acad Sci USA* 2002;**99**:6298–6303.
  44. Brunham LR, Singaraja RR, Duong M, Timmins JM, Fievet C, Bissada N, Kang MH, Samra A, Fruchart JC, McManus B, Staels B, Parks JS, Hayden MR. Tissue-specific roles of ABCA1 influence susceptibility to atherosclerosis. *Arterioscler Thromb Vasc Biol* 2009;**29**:548–554.
  45. Out R, Hoekstra M, Hildebrand RB, Kruit JK, Meurs I, Li Z, Kuipers F, Van Berkel TJ, Van Eck M. Macrophage ABCG1 deletion disrupts lipid homeostasis in alveolar macrophages and moderately influences atherosclerotic lesion development in LDL receptor-deficient mice. *Arterioscler Thromb Vasc Biol* 2006;**26**:2295–2300.
  46. Ranalletta M, Wang N, Han S, Yvan-Charvet L, Welch C, Tall AR. Decreased atherosclerosis in low-density lipoprotein receptor knockout mice transplanted with Abcg1<sup>-/-</sup> bone marrow. *Arterioscler Thromb Vasc Biol* 2006;**26**:2308–2315.
  47. Tarling EJ, Bojanic DD, Tangirala RK, Wang X, Lovgren-Sandblom A, Lusic AJ, Bjorkhem I, Edwards PA. Impaired development of atherosclerosis in Abcg1<sup>-/-</sup> Apoe<sup>-/-</sup> mice: identification of specific oxysterols that both accumulate in Abcg1<sup>-/-</sup> Apoe<sup>-/-</sup> tissues and induce apoptosis. *Arterioscler Thromb Vasc Biol* 2010;**30**:1174–1180.
  48. Feng B, Zhang D, Kuriakose G, Devlin CM, Kockx M, Tabas I. Niemann-Pick C heterozygosity confers resistance to lesion necrosis and macrophage apoptosis in murine atherosclerosis. *Proc Natl Acad Sci USA* 2003;**100**:10423–10428.
  49. Liao X, Sluimer JC, Wang Y, Subramanian M, Brown K, Pattison JS, Robbins J, Martinez J, Tabas I. Macrophage autophagy plays a protective role in advanced atherosclerosis. *Cell Metab* 2012;**15**:545–553.
  50. Thorp E, Li G, Seimon TA, Kuriakose G, Ron D, Tabas I. Reduced apoptosis and plaque necrosis in advanced atherosclerotic lesions of Apoe<sup>-/-</sup> and Ldlr<sup>-/-</sup> mice lacking CHOP. *Cell Metab* 2009;**9**:474–481.
  51. Yamada S, Ding Y, Tanimoto A, Wang KY, Guo X, Li Z, Tasaki T, Nabesima A, Murata Y, Shimajiri S, Kohno K, Ichijo H, Sasaguri Y. Apoptosis signal-regulating kinase 1 deficiency accelerates hyperlipidemia-induced atheromatous plaques via suppression of macrophage apoptosis. *Arterioscler Thromb Vasc Biol* 2011;**31**: 1555–1564.
  52. Liu J, Thewke DP, Su YR, Linton MF, Fazio S, Sinensky MS. Reduced macrophage apoptosis is associated with accelerated atherosclerosis in low-density lipoprotein receptor-null mice. *Arterioscler Thromb Vasc Biol* 2005;**25**:174–179.
  53. Bolick DT, Skafren MD, Johnson LE, Kwon SC, Howatt D, Daugherty A, Ravichandran KS, Hedrick CC. G2A deficiency in mice promotes macrophage activation and atherosclerosis. *Circ Res* 2009;**104**:318–327.
  54. Van Vre EA, Ait-Oufella H, Tedgui A, Mallat Z. Apoptotic cell death and efferocytosis in atherosclerosis. *Arterioscler Thromb Vasc Biol* 2012;**32**:887–893.
  55. Heng TSP, Painter MW, Elpek K, Lukacs-Kornek V, Mauerer N, Turley SJ, Koller D, Kim FS, Wagers AJ, Asinovsky N, Davis S, Fassett M, Feuerer M, Gray DHD, Haxhinasto S, Hill JA, Hyatt G, Laplace C, Leatherbee K, Mathis D, Benoist C, Jianu R, Laidlaw DH, Best JA, Knell J, Goldrath AW, Jarjoura J, Sun JC, Zhu Y, Lanier LL, Ergun A, Li Z, Collins JJ, Shinton SA, Hardy RR, Friedline R, Sylvia K, Kang J. The Immunological Genome Project: networks of gene expression in immune cells. *Nat Immunol* 2008;**9**:1091–1094.
  56. Miyazaki T, Hirokami Y, Matsuhashi N, Takatsuka H, Naito M. Increased susceptibility of thymocytes to apoptosis in mice lacking AIM, a novel murine macrophage-derived soluble factor belonging to the scavenger receptor cysteine-rich domain superfamily. *J Exp Med* 1999;**189**:413–422.
  57. Kuwata K, Watanabe H, Jiang SY, Yamamoto T, Tomiyama-Miyaji C, Abo T, Miyazaki T, Naito M. AIM inhibits apoptosis of T cells and NKT cells in Corynebacterium-induced granuloma formation in mice. *Am J Pathol* 2003;**162**:837–847.
  58. Valledor AF, Hsu LC, Ogawa S, Sawka-Verhelle D, Karin M, Glass CK. Activation of liver X receptors and retinoid X receptors prevents bacterial-induced macrophage apoptosis. *Proc Natl Acad Sci USA* 2004;**101**:17813–17818.
  59. Lin J, Li H, Yang M, Ren J, Huang Z, Han F, Huang J, Ma J, Zhang D, Zhang Z, Wu J, Huang D, Qiao M, Jin G, Wu Q, Huang Y, Du J, Han J. A role of RIP3-mediated macrophage necrosis in atherosclerosis development. *Cell Rep* 2013;**3**:200–210.
  60. Vanden Berghe T, Linkermann A, Jouan-Lanhouet S, Walczak H, Vandenabeele P. Regulated necrosis: the expanding network of non-apoptotic cell death pathways. *Nat Rev Mol Cell Biol* 2014;**15**:135–147.
  61. Yalaoui S, Huby T, Franetich JF, Gego A, Rametti A, Moreau M, Collet X, Siau A, Gemert G, V, Sauerwein RW, Luty AJ, Vaillant JC, Hannoun L, Chapman J, Mazier D, Froissard P. Scavenger receptor BI boosts hepatocyte permissiveness to Plasmodium infection. *Cell Host Microbe* 2008;**4**:283–292.



# Macrophage SR-B1 in atherosclerotic cardiovascular disease

*Thierry Huby and Wilfried Le Goff*

## Purpose of review

Scavenger receptor class B type 1 (SR-B1) promotes atheroprotection through its role in HDL metabolism and reverse cholesterol transport in the liver. However, evidence indicates that SR-B1 may impact atherosclerosis through nonhepatic mechanisms.

## Recent findings

Recent studies have brought to light various mechanisms by which SR-B1 affects lesional macrophage function and protects against atherosclerosis. Efferocytosis is efficient in early atherosclerotic lesions. At this stage, and beyond its role in cholesterol efflux, SR-B1 promotes free cholesterol-induced apoptosis of macrophages through its control of apoptosis inhibitor of macrophage (AIM). At more advanced stages, macrophage SR-B1 binds and mediates the removal of apoptotic cells. SR-B1 also participates in the induction of autophagy which limits necrotic core formation and increases plaque stability.

## Summary

These studies shed new light on the atheroprotective role of SR-B1 by emphasizing its essential contribution in macrophages during atherogenesis as a function of lesion stages. These new findings suggest that macrophage SR-B1 is a therapeutic target in cardiovascular disease.

## Keywords

apoptosis, atherosclerosis, cholesterol, macrophage, SR-B1

## INTRODUCTION

According to the WHO, cardiovascular disease (CVD) remains the leading cause of mortality and morbidity worldwide. The inverse correlation of circulating HDL levels with the risk of atherosclerotic cardiovascular disease (ASCVD) was first reported in the late seventies [1,2] and since confirmed by numerous epidemiological studies. Patients with low plasma concentrations of HDL cholesterol (HDL-C) exhibit a high risk of ASCVD that may reflect the protective biological activities of HDL particles [3]. Among them is the capacity of HDL to promote reverse cholesterol transport (RCT) through which cholesterol returns from peripheral tissues to the liver for elimination. This RCT pathway was proposed to underly the atheroprotective role of HDL [4]. However, intervention studies aimed at increasing HDL-C levels [5,6], infusion of recombinant HDL [7,8] and Mendelian randomization studies [9] do not support a causal role of HDL in CVD. Epidemiological studies also identified a U-shaped relationship between HDL-C and CVD wherein at both very low and very high levels, HDL-C was associated with an increased risk of CVD and mortality [10,11]. Such results have prompted questions about the role of HDL in lipid metabolism and CVD [12<sup>\*\*\*</sup>].

From biogenesis at liver and intestinal sites, remodelling in the vascular compartment, and recycling and catabolism by the kidney, numerous enzymes and receptors are involved in HDL metabolism. In this context, the scavenger receptor class B type 1 (SR-B1) is a physiological HDL receptor [13] that plays a pivotal role in HDL metabolism and signalling [14]; however, its role in CVD is probably more complex than anticipated by earlier studies.

## A BRIEF OVERVIEW OF SR-B1 STRUCTURE AND REGULATION

SR-B1 is a member of the class B scavenger receptor family that includes CD36 (or SCARB3) and lysosomal integral membrane protein 2 (LIMP-2). An SR-

Sorbonne Université, INSERM, Institute of Cardiometabolism and Nutrition (ICAN), UMR\_S1166, Paris, France

Correspondence to Thierry Huby, PhD, and Wilfried Le Goff, PhD, INSERM UMR\_S1166, Faculté de médecine Sorbonne Université, 91, boulevard de l'Hôpital, 75013 Paris, France. E-mail: thierry.huby@sorbonne-universite.fr, wilfried.le\_goff@sorbonne-universite.fr

**Curr Opin Lipidol** 2022, 33:000–000

DOI:10.1097/MOL.0000000000000822

## KEY POINTS

- Both hepatic and extrahepatic SR-B1 serve major atheroprotective roles.
- Macrophage SR-B1 exerts several protective activities during atherogenesis as a function of the lesion stage.
- Pharmacological raise of SR-B1 expression and activity in macrophages of atherosclerotic lesions is a potential mode of action targeting CVD.

B2 isoform of the receptor has been described with a divergent cytoplasmic tail due to alternative splicing [15]. Human SR-B1 is encoded by the *SCARB1* gene on chromosome 12, which contains 13 exons and 12 introns [16] and generates a protein of molecular mass 82 kDa following posttranslational modifications. SR-B1 protein is composed of two short intracellular domains at the N- and C-termini, two transmembrane domains and a large extracellular region forming an ectodomain responsible for the binding of HDL. Importantly, the C-terminal cytosolic domain contains motifs involved in SR-B1 expression (PDZ-binding domain) and activity (SIK-1 binding domain) [14]. Although SR-B1 is expressed in numerous cell types [14], the greatest expression is found in the liver, ovary and adrenal glands. Regulation of SR-B1 expression is tissue-dependent and mainly involves trophic hormones adrenocorticotropin in adrenal glands, anterior pituitary hormones in the ovary and biliary acids in the liver [14]. It is noteworthy that in the context of ASCVD, expression of SR-B1 is highly regulated by cholesterol (through SREBP-1a [17] and -2 [18] and LXR $\alpha/\beta$ ), LRH-1 [19] and PPAR agonists [20] in the liver and/or macrophages.

### SR-B1 IS AN ESSENTIAL REGULATOR OF CHOLESTEROL HOMEOSTASIS AND ATHEROSCLEROSIS

The SR-B1 receptor plays a major role in HDL metabolism by mediating both the uptake and efflux of cholesterol between cells and large mature HDL. Importantly, expression of SR-B1 in hepatocytes promotes the selective uptake of cholesteryl esters from HDL [21,22] and RCT [23] and contributes to the optimal recycling of circulatory HDL. Such a function was recently proposed to involve the multimerization of SR-B1 into large metastable clusters at the plasma membrane, thereby evading endocytic pathways in a process requiring a C-terminal leucine zipper motif within SR-B1 [24]. In genetically modified mouse models, overexpression of SR-B1 in

hepatocytes was accompanied by reduced plasma HDL-C [25,26] and decreased atherosclerosis [25]. Conversely, SR-B1 deficiency in hepatocytes led to the opposite phenotype [27], which recapitulated the detrimental effect of SR-B1 on atherosclerosis when its expression in the whole body was attenuated or ablated [27–30] (Table 1). In humans, the importance of SR-B1 in HDL metabolism was corroborated with the identification of the functional *SCARB1* variants P297S and P376L that exhibited decreased HDL cholesterol uptake in hepatocytes and increased HDL-C in plasma of carriers of the mutations [31,32]. Analysis of carotid artery intima-media thickness in a small group of heterozygous carriers of the P297S mutation revealed no difference compared to noncarriers within the family. Rare *SCARB1* variants were also not associated with coronary artery disease (CAD) despite increased HDL-C levels in the relatively homogeneous population of Iceland [33]. However, an association between P376L carrier status and coronary heart disease (CHD) in 137 995 individuals from the CARDIOGRAM Exome and the CHD Exome+ Consortia revealed that carriers of this variant display elevated HDL-C concentrations and an increased risk of CHD [odds ratio (OR) 1.79] [32]. These findings support epidemiological studies linking extremely high HDL-C with CHD risk and mouse model studies using genetically modified SR-B1. However, they must be interpreted with caution because of the very low frequency of the P376L variant in both healthy controls ( $n=52$ ) and CHD cases ( $n=34$ ) detected in this meta-analysis [32]. It must also be kept in mind that mouse and genetic studies indicate that SR-B1 not only plays a role in HDL metabolism, but it also participates in the clearance of apoB-containing lipoproteins, which may contribute to the relationship between SR-B1 and CAD [34]. Such a hypothesis is supported by recent genome-wide association studies reporting associations between the *SCARB1* locus and CAD risk independently of HDL-C [35,36].

Interestingly, study of *SCARB1* variants equally highlighted a potential impact of SR-B1 in platelet activation and glucocorticoid production. Altered platelet function and decreased adrenal steroidogenesis were also reported in carriers of the P297S mutation [31]. In support of these studies, a critical function of SR-B1 in providing lipoprotein-derived cholesterol for glucocorticoid synthesis in response to stress was clearly demonstrated in mice [37]. In addition to the pivotal role of SR-B1 in the cellular import of HDL-C, a recent study proposed that large HDL particles enriched in free cholesterol resulting from SR-B1 deficiency may mediate free cholesterol delivery into tissues. This mechanism may equally

**Table 1.** Role of *Srb1* on atherosclerosis development in genetically modified mouse models

Targeted <i>Srb1</i> expression	Major findings	Impact on atherosclerosis development	Reference
Whole body			
Attenuation	↑HDL-C, ↓liver HDL-CE uptake	n.d.	Varban <i>et al.</i> [22]
Attenuation	↑TC	↑	Huby <i>et al.</i> [27]
Attenuation	↑TC, ↑LDL-C	↑ ( <i>Ldlr</i> KO)	Huszar <i>et al.</i> [29]
KO	↑HDL-C, ↓liver HDL-CE uptake	n.d.	Brundert <i>et al.</i> [21]
KO	↑TC, ↑VLDL-C	↑	Huby <i>et al.</i> [27]
KO	↑TC, ↓biliary chol., ↓ fertility	n.d.	Trigatti <i>et al.</i> [28]
KO	↑TC, ↓biliary chol., ↓ VLDL-C	↑ ( <i>ApoE</i> KO)	Trigatti <i>et al.</i> [28]
KO	↑MI, cardiac dysfunctions	↑ ( <i>ApoE</i> KO)	Braun <i>et al.</i> [30]
KO	↑HSPC proliferation	↑	Gao <i>et al.</i> [49]
KO	↑HDL-C	↑ ( <i>Ldlr</i> KO)	Covey <i>et al.</i> [44]
dKO ( <i>Abca1</i> / <i>Srb1</i> )	↑ mΦ foam cells	↔	Zhao <i>et al.</i> [58]
Liver			
Overexpression	↑mΦ RCT	n.d.	Zhang <i>et al.</i> [23]
Overexpression	↓HDL-C, ↓VLDL-C, ↓LDL-C	↓ ( <i>Ldlr</i> KO)	Arai <i>et al.</i> [25]
KO	↑TC, ↑VLDL-C	↑	Huby <i>et al.</i> [27]
Endothelial			
KO	Loss of HDL-mediated neuroprotection	n.d.	Tran-Dinh <i>et al.</i> [41 <sup>■</sup> ]
KO	↓LDL transcytosis	↓ ( <i>ApoE</i> KO)	Huang <i>et al.</i> [43 <sup>■</sup> ]
Myeloid (BMT)			
KO	↔TC	↑ ( <i>Ldlr</i> KO)	Covey <i>et al.</i> [44]
KO	↓mΦ chol. efflux	Depends on lesion stage ( <i>Ldlr</i> KO)	Van Eck <i>et al.</i> [45]
KO	↓efferocytosis, ↑necrotic core	↑ ( <i>ApoE</i> KO, <i>Ldlr</i> KO)	Tao <i>et al.</i> [46]
KO	↓mΦ apoptosis	↑ ( <i>SR-B1</i> <sup>KO<sup>liver</sup></sup> × <i>CETP</i> )	Galle-Treger <i>et al.</i> [48 <sup>■</sup> ]
KO	↑HSPC proliferation	↑ ( <i>Ldlr</i> KO)	Gao <i>et al.</i> [49]
KO	↔TC, ↔ mΦ chol. efflux	↑ ( <i>ApoE</i> KO)	Zhang <i>et al.</i> [55]
dKO ( <i>Abca1</i> / <i>Srb1</i> )	↓TC, ↑foam cells	↑ ( <i>Ldlr</i> KO)	Zhao <i>et al.</i> [47]
KO	↓mΦ autophagy	n.d.	Tao <i>et al.</i> [56 <sup>■</sup> ]
Macrophage (BMT)			
KO	↓mΦ apoptosis	↑ ( <i>Ldlr</i> KO, <i>SR-B1</i> <sup>KO<sup>liver</sup></sup> × <i>CETP</i> )	Galle-Treger <i>et al.</i> [48 <sup>■</sup> ]

BMT, bone marrow transplantation; Chol., cholesterol; HDL, high-density lipoprotein; LDL, low-density lipoprotein; MI, myocardial infarction; mΦ, macrophage; n.d., not determined; RCT, reverse cholesterol transport; TC, total cholesterol.

contribute to their dysfunction in the absence of SR-B1 [38<sup>■</sup>]. Indeed, such elevation of free cholesterol content in ovaries, erythrocytes, heart, lung, and macrophages in *Srb1* knockout mice might also contribute to female infertility, impaired red blood cell maturation, cardiac dysfunction, and atherosclerosis development in these mice.

## SR-B1 IN ENDOTHELIAL CELLS AND ATHEROSCLEROSIS

Beyond the importance of liver SR-B1 in HDL metabolism, studies have highlighted the contribution of SR-B1 to the protective action of HDL on the vascular endothelium by propagating HDL signalling,

which stimulates endothelial nitric oxide synthase [39]. HDL-mediated intracellular signalling relies on SR-B1 receptor interaction with plasma membrane cholesterol via the SR-B1 C-terminal transmembrane domain [40]. Interestingly, the contribution of endothelial SR-B1 in promoting HDL-mediated neuroprotection was recently demonstrated in the context of acute ischemic stroke [41<sup>■</sup>]. SR-B1 may also act as a transporter in endothelial cells to facilitate the entry of lipoproteins such as HDL and LDL into the subendothelial space by transcytosis [42,43<sup>■</sup>]. Notably, a recent study demonstrated that SR-B1 binds LDL and drives their transcytosis across aortic endothelial cells by a mechanism that requires binding of dedicator of cytokinesis 4

(DOCK4) to SR-B1 and activation of the Rho GTPase ras-related C3 botulinum toxin substrate 1 (RAC1). This SR-B1-mediated active transport of LDL to the artery wall promotes atherosclerosis and is the first demonstration of a pro-atherogenic activity for the receptor [43<sup>\*\*\*</sup>].

### SR-B1 IN HAEMATOPOIETIC CELLS AND ATHEROSCLEROSIS

Comparison of liver-specific *srb1* KO mice to fully deficient mice demonstrated that, in addition to its major atheroprotective role in liver, SR-B1 exerts an antiatherogenic role in extrahepatic tissues [27]. This is in agreement with earlier studies demonstrating increased atherosclerosis in mice transplanted with *Srb1* KO bone marrow [44–47]. Importantly, modulation of atherosclerosis consecutive to the lack of SR-B1 in haematopoietic cells was independent of any alteration of plasma HDL or total cholesterol levels. Although these studies concluded that the expression of SR-B1 in macrophage underlies the atheroprotective role of SR-B1 in bone marrow derived cells, the final demonstration of a critical role of SR-B1 in macrophages was brought only recently by Galle-Treger *et al.* [48<sup>\*\*\*</sup>] through transplantation studies using bone marrow from *Lysm-Cre x Srb1<sup>fl/fl</sup>* mice. Noteworthy, earlier studies have suggested that SR-B1 could also contribute to atheroprotection by promoting HDL-mediated control of the proliferation and differentiation of haematopoietic stem/progenitor cells in the bone marrow, thus limiting leukocytosis and inflammation [49].

### SR-B1 IN MACROPHAGES AND ATHEROSCLEROSIS

#### Cholesterol efflux and reverse cholesterol transport

Among immune cells involved in atherosclerosis, macrophages exert a central role in the initiation and progression of disease [50]. One atheroprotective function of HDL is the capacity of plaque macrophages to remove excess cholesterol by promoting efflux to HDL for elimination through RCT. Thus, ex-vivo evaluation of the capacity of HDL from patients to facilitate macrophage cholesterol efflux is inversely associated with atherosclerosis [51], incident cardiovascular events [52] and mortality [53]. SR-B1 is expressed in tissue macrophages and specifically in atherosclerotic lesions in humans [20]. Because it promotes cholesterol efflux to HDL, it was initially proposed that SR-B1 expression in macrophages could enhance RCT resulting in reduced

foam cell and plaque formation. Cholesterol efflux from human macrophages to HDL *in vitro* was reduced by antibody-mediated neutralization of SR-B1 [54] or when macrophages isolated from carriers and noncarriers of the dysfunctional *SCARB1* P297S variant were compared [31]. In mice, however, the importance of macrophage SR-B1 in mediating cholesterol efflux to HDL [45,55], promoting macrophage foam cell formation [47,48<sup>\*\*\*</sup>,56<sup>\*\*\*</sup>] or participating in in-vivo RCT [57,58] is unclear due to conflicting results. It is noteworthy that the combined deletion of *Srb1* and genes known to contribute to cholesterol efflux, such as *ATP-binding cassette A1* (*Abca1*) or *apolipoprotein E* (*ApoE*), dramatically enhanced the formation of macrophage foam cells [47,59]. In double *Srb1/ApoE* knockout mice, dyslipidaemia and altered cholesterol mobilization, with an accumulation of free cholesterol into lysosomes due to SR-B1 deficiency, contribute to cholesterol accumulation in macrophages [59]. In double *Abca1/Srb1* knockout mice, massive macrophage lipid-loading occurs even under hypocholesterolaemia in these animals [47]. Interestingly, Liu *et al.* [38<sup>\*\*\*</sup>] recently reported that free cholesterol rich HDL particles generated in SR-B1 deficient mice also favour free cholesterol accumulation in macrophages.

### APOPTOSIS

Apoptosis of macrophages is a critical event during atherogenesis with divergent effects on the progression of the disease. Macrophage apoptosis is proposed to be atheroprotective in early lesions, whereas it promotes atherosclerosis development at more advanced stages [60]. The specific deletion of macrophage SR-B1 in two different atherosclerotic mouse models recently revealed a marked reduction in apoptotic macrophages in developing aortic lesions [48<sup>\*\*\*</sup>]. Galle-Treger *et al.* [48<sup>\*\*\*</sup>] observed that SR-B1 deficient macrophages were less susceptible to apoptosis induced by free cholesterol loading compared with control macrophages with reduced activation of p38MAPK and STAT1, which are critical factors in free cholesterol-driven macrophage apoptosis. SR-B1 deficient macrophage resistance to apoptosis was associated with the STAT3-mediated induction of the antiapoptotic factor AIM (CD5L, Sp $\alpha$ , Api6) [61], a member of the scavenger receptor cysteine-rich superfamily (SRCR-SF) [48<sup>\*\*\*</sup>]. Similar induction of AIM was observed in atherosclerotic macrophages [48<sup>\*\*\*</sup>]. Interestingly, reduction of macrophage apoptosis with increased atherosclerosis in macrophage SR-B1 deficient mouse models did not change the extent of plaque necrosis [48<sup>\*\*\*</sup>]. Altogether, these results suggested a pro-survival effect of AIM in SR-B1 deficient

macrophages leading to increased plaque cellularity and early expansion of lesions in the context of efficient efferocytosis. Other mechanisms may contribute to the pro-apoptotic role of SR-B1 during atherogenesis. Indeed, SR-B1 could also contribute to clearance of apoptotic cells by macrophages (efferocytosis) [46] and regulate autophagy [56<sup>¶</sup>] as recently reported in advanced atherosclerotic lesions [46,56<sup>¶</sup>].

## EFFEROCYTOSIS

Efferocytosis is an important element in plaque necrotic core formation in advanced atherosclerotic lesions because it alleviates the necrosis of apoptotic cells including macrophages [62]. In this context, Tao *et al.* [46] suggested that macrophage SR-B1 could influence efferocytosis. They reported that SR-B1 bound to phosphatidylserine at the surface of apoptotic cells resulting in the recruitment and phosphorylation of the Src tyrosine kinase and the downstream activation of phosphoinositide 3 kinase (PI3K)/Rac1 GTPase leading to membrane ruffling. In in-vitro and in-vivo assays, macrophage SR-B1 deficiency was associated with defective efferocytosis. Haematopoietic SR-B1 deficiency was also associated with an increased number of apoptotic cells, fewer events of engulfment of apoptotic cells by macrophages and more necrosis in advanced atherosclerotic lesions of bone marrow transplanted *Ldlr*<sup>-/-</sup> mice [46]. These effects were reinforced when double SR-B1 and ApoE deficient haematopoietic cells were used. The combined deficiencies were associated with evidence of plaque instability resulting from a reduction of the collagen content and fibrous cap thickness [46]. Altogether, SR-B1 appears to play an atheroprotective role by promoting efferocytosis in late-stage lesions. The results cannot exclude, however, that accelerated plaque development in macrophage SR-B1 deficient atherosclerotic mice [48<sup>¶¶</sup>] also contributed to impaired efferocytosis because efferocytosis is defective in advanced atherosclerosis [63,64].

## AUTOPHAGY

The accumulation of neutral lipids, including the esterified form of cholesterol within lipid droplets in macrophages, was proposed to induce autophagy and promote free cholesterol efflux via its trafficking from autophagosomes to lysosomes [65]. Although the relevance of this finding to atherosclerosis has not been determined, mice with deficient autophagy in macrophages displayed increased plaque necrosis, macrophage apoptosis and defective efferocytosis [66]. In this context, the regulation of

macrophage autophagy by SR-B1 was recently proposed to contribute to its atheroprotective properties [56<sup>¶</sup>]. Consistent with the proposed role of SR-B1, deletion of SR-B1 in macrophages resulted in impairment of the peroxisome proliferator-activated receptor alpha (PPAR $\alpha$ )-induced expression of transcription factor EB (TFEB), a master regulator of genes involved in lysosomal biogenesis and autophagy. Notably, expression of the autophagy genes *VPS34* and *Beclin-1* was reduced in SR-B1 deficient macrophages and led to defective autophagy, the latter being rescued by the overexpression of TFEB or *VPS34*. The role of SR-B1 in autophagy was further shown to involve the recruitment of the *VPS34* complex and *Barkor* to cholesterol domains in autophagosomes [56<sup>¶</sup>]. The impact of defective autophagy on cholesterol efflux in SR-B1 deficient macrophages was not investigated, however. Finally, reduced signs of autophagy, including reduced *VPS34* activity, in advanced atherosclerotic lesions of mice with a haematopoietic deletion of SR-B1 suggest that SR-B1 may actively contribute to the induction of autophagy at later stages of the disease.

## CONCLUSION

Beyond the well described atheroprotective role of liver SR-B1 on HDL metabolism and RCT [14], recent studies have uncovered diverse nonhepatic mechanisms by which SR-B1 may impact atherosclerosis (Table 1). Early comparison of liver SR-B1 deficient to fully SR-B1-deficient mice demonstrated that SR-B1 globally exerts an antiatherogenic role in extrahepatic tissues [27]. However, the recent discovery that SR-B1 acts in endothelial cells as a transporter facilitating lipoprotein transcytosis revealed that it could also be pro-atherogenic [43<sup>¶¶</sup>]. This deleterious role opposes those of SR-B1 in the macrophage. New findings support a model in which macrophage SR-B1 exerts several protective activities during atherogenesis as a function of the lesion stage. In the early development of atherosclerosis, SR-B1 could promote macrophage cholesterol efflux and RCT resulting in reduced macrophage foam cell formation. Importantly, SR-B1 could mediate macrophage apoptosis in response to the cholesterol burden to limit plaque growth. In advanced lesions, SR-B1 could limit the formation of the necrotic core and promote plaque stability via the clearance of apoptotic cells (Fig. 1). This newly acquired knowledge indicates that macrophage SR-B1 may be a therapeutic target in CVD. Further investigations are needed to identify pharmacological tools that induce SR-B1 expression and activity in macrophages in atherosclerotic lesions. The ongoing development of



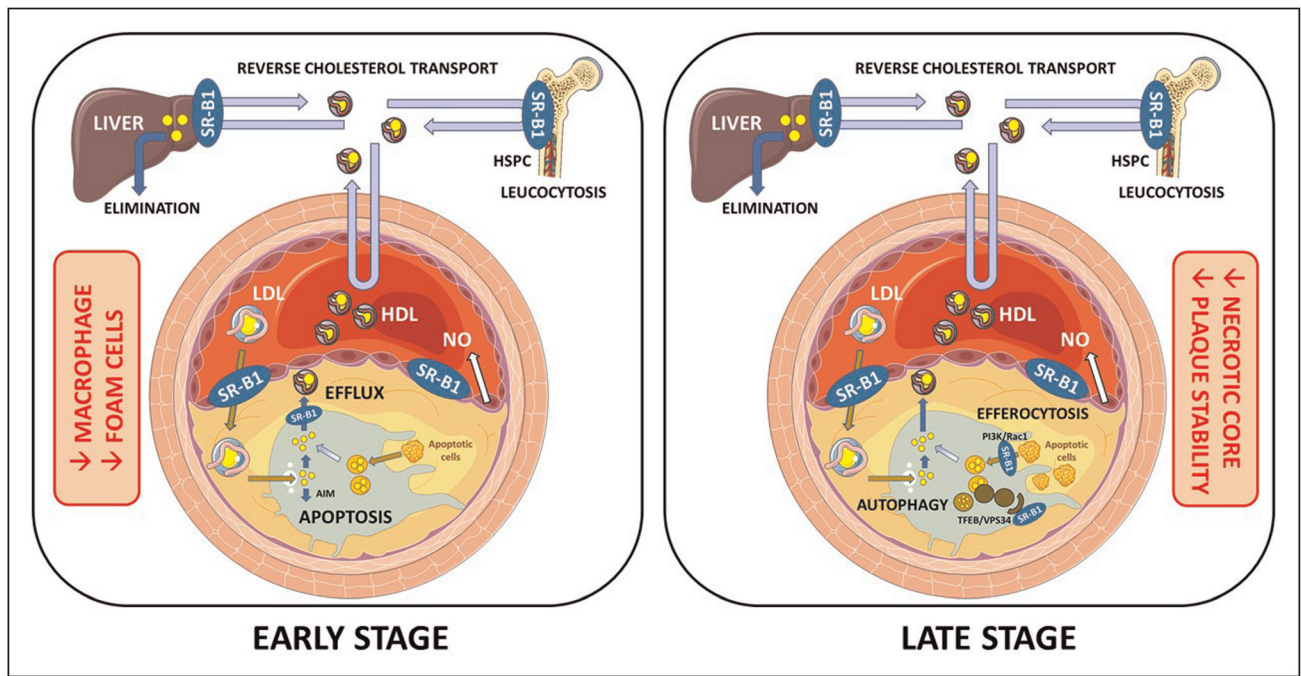


**FIGURE 1.** Protective activities of macrophage SR-B1 during atherosclerosis as a function of the lesion stage. Beyond the atheroprotective role of SR-B1 on HDL metabolism and RCT, nonhepatic SR-B1 contributes to atherosclerosis through several activities. SR-B1 alleviates leukocytosis and inflammation by controlling the proliferation and differentiation of HSPC in the bone marrow. At the vascular endothelial level, SR-B1 exerts both pro (LDL transcytosis) and antiatherogenic (NO production) activities. Left: At the early stage of atherosclerosis development, macrophage SR-B1 reduces foam cell formation and plaque macrophage content. Right: At later stages of atherosclerosis development, macrophage SR-B1 limits the formation of the necrotic core and promotes plaque stability. AIM, apoptosis inhibitor of macrophage; HDL, high-density lipoprotein; HSPC, haematopoietic stem/progenitor cells; LDL, low-density lipoprotein; NO, nitric oxide; PI3K, phosphoinositide 3 kinase; Rac1, ras-related C3 botulinum toxin substrate 1; SR-B1, scavenger receptor class B type 1; TFEB, transcription factor EB.

● Cholesterol.

macrophage-targeted nanomedicine could be a critical resource for achieving this goal [67].

## Acknowledgements

None.

## Financial support and sponsorship

This work was supported by the French National Institute for Health and Medical Research (INSERM) and Sorbonne Université.

T.H. acknowledges support from the Fondation de France (project number 00096295), Alliance Sorbonne Université (Programme Emergence) and the Agence Nationale pour la Recherche (ANR-17-CE14-0044-01 and ANR-21-CE14-0067-01). W.L.G. acknowledges support from the Fondation de France (00066330), Alliance Sorbonne Université (Programme Emergence), the Société Francophone du Diabète and the Agence Nationale pour la Recherche (ANR-19-CE14-0020).

## Conflicts of interest

There are no conflicts of interest.

## REFERENCES AND RECOMMENDED READING

Papers of particular interest, published within the annual period of review, have been highlighted as:

- of special interest
- of outstanding interest

1. Gordon T, Castelli WP, Hjortland MC, *et al.* High-density lipoprotein as a protective factor against coronary heart disease. The Framingham Study. *Am J Med* 1977; 62:707–714.
2. Castelli WP, Garrison RJ, Wilson PW, *et al.* Incidence of coronary heart disease and lipoprotein cholesterol levels. The Framingham Study. *JAMA* 1986; 256:2835–2838.
3. Camont L, Chapman MJ, Kontush A. Biological activities of HDL subpopulations and their relevance to cardiovascular disease. *Trends Mol Med* 2011; 17:594–603.
4. Pownall HJ, Rosales C, Gillard BK, Gotto AM. High-density lipoproteins, reverse cholesterol transport and atherosclerosis. *Nat Rev Cardiol* 2021; 17:594–603.
5. HPS2-THRIVE Collaborative Group. Landray MJ, Haynes R, Hopewell JC, *et al.* Effects of extended-release niacin with laropirant in high-risk patients. *N Engl J Med* 2014; 371:203–212.
6. Tall AR, Rader DJ. Trials and tribulations of CETP inhibitors. *Circ Res* 2018; 122:106–112.
7. Nicholls SJ, Puri R, Ballantyne CM, *et al.* Effect of infusion of high-density lipoprotein mimetic containing recombinant apolipoprotein A-I Milano on coronary disease in patients with an acute coronary syndrome in the MILANO-PILOT Trial: a randomized clinical trial. *JAMA Cardiol* 2018; 3:806–814.
8. Nicholls SJ, Andrews J, Kastelein JJP, *et al.* Effect of serial infusions of CER-001, a Preβ high-density lipoprotein mimetic, on coronary atherosclerosis in patients following acute coronary syndromes in the CER-001 atherosclerosis regression acute coronary syndrome trial: a randomized clinical trial. *JAMA Cardiol* 2018; 3:815–822.

9. Voight BF, Peloso GM, Orho-Melander M, *et al*. Plasma HDL cholesterol and risk of myocardial infarction: a mendelian randomization study. *Lancet* 2012; 380:572–580.
10. Madsen CM, Varbo A, Nordestgaard BG. Extreme high high-density lipoprotein cholesterol is paradoxically associated with high mortality in men and women: two prospective cohort studies. *Eur Heart J* 2017; 38:2478–2486.
11. Ko DT, Alter DA, Guo H, *et al*. High-density lipoprotein cholesterol and cause-specific mortality in individuals without previous cardiovascular conditions: the CANHEART study. *J Am Coll Cardiol* 2016; 68:2073–2083.
12. Kontush A. HDL and reverse remnant-cholesterol transport (RRT): relevance to cardiovascular disease. *Trends Mol Med* 2020; 26:1086–1100.
- This article discusses the importance of HDL in the acquisition of free cholesterol released upon triglyceride-rich lipoproteins lipolysis in the context of atherosclerosis.
13. Acton S, Rigotti A, Landschulz KT, *et al*. Identification of scavenger receptor SR-BI as a high-density lipoprotein receptor. *Science* 1996; 271:518–520.
14. Shen W-J, Azhar S, Kraemer FB. SR-B1: a unique multifunctional receptor for cholesterol influx and efflux. *Annu Rev Physiol* 2018; 80:95–116.
15. Webb NR, Connell PM, Graf GA, *et al*. SR-BII, an isoform of the scavenger receptor BI containing an alternate cytoplasmic tail Mediates Lipid Transfer between High-Density Lipoprotein and Cells. *J Biol Chem* 1998; 273:15241–15248.
16. Webb NR, de Villiers WJ, Connell PM, *et al*. Alternative forms of the scavenger receptor BI (SR-BI). *J Lipid Res* 1997; 38:1490–1495.
17. Lopez D, McLean MP. Sterol regulatory element-binding protein-1a binds to cis-elements in the promoter of the rat high-density lipoprotein receptor SR-BI gene. *Endocrinology* 1999; 140:5669–5681.
18. Tréguier M, Doucet C, Moreau M, *et al*. Transcription factor sterol regulatory element-binding protein 2 regulates scavenger receptor Cla-1 gene expression. *Arterioscler Thromb Vasc Biol* 2004; 24:2358–2364.
19. Schoonjans K, Annicotte J-S, Huby T, *et al*. Liver receptor homolog 1 controls the expression of the scavenger receptor class B type I. *EMBO Rep* 2002; 3:1181–1187.
20. Chinetti G, Gbaguidi FG, Griglio S, *et al*. CLA-1/SR-BI is expressed in atherosclerotic lesion macrophages and regulated by activators of peroxisome proliferator-activated receptors. *Circulation* 2000; 101:2411–2417.
21. Brundert M, Ewert A, Heeren J, *et al*. Scavenger receptor class B type I mediates the selective uptake of high-density lipoprotein-associated cholesteryl ester by the liver in mice. *Arterioscler Thromb Vasc Biol* 2005; 25:143–148.
22. Varban ML, Rinninger F, Wang N, *et al*. Targeted mutation reveals a central role for SR-BI in hepatic selective uptake of high-density lipoprotein cholesterol. *Proc Natl Acad Sci U S A* 1998; 95:4619–4624.
23. Zhang Y, Da Silva JR, Reilly M, *et al*. Hepatic expression of scavenger receptor class B type I (SR-BI) is a positive regulator of macrophage reverse cholesterol transport in vivo. *J Clin Invest* 2005; 115:2870–2874.
24. Marques PE, Nyegaard S, Collins RF, *et al*. Multimerization and retention of the scavenger receptor SR-B1 in the plasma membrane. *Dev Cell* 2019; 50:283–295. e5.
25. Arai T, Wang N, Bezouevski M, *et al*. Decreased atherosclerosis in heterozygous low-density lipoprotein receptor-deficient mice expressing the scavenger receptor BI transgene. *J Biol Chem* 1999; 274:2366–2371.
26. Komori H, Arai H, Kashima T, *et al*. Coexpression of CLA-1 and human PDZK1 in murine liver modulates HDL cholesterol metabolism. *Arterioscler Thromb Vasc Biol* 2008; 28:1298–1303.
27. Huby T, Doucet C, Dacet C, *et al*. Knockdown expression and hepatic deficiency reveal an atheroprotective role for SR-BI in liver and peripheral tissues. *J Clin Invest* 2006; 116:2767–2776.
28. Trigatti B, Rayburn H, Viñals M, *et al*. Influence of the high-density lipoprotein receptor SR-BI on reproductive and cardiovascular pathophysiology. *Proc Natl Acad Sci U S A* 1999; 96:9322–9327.
29. Huszar D, Varban ML, Rinninger F, *et al*. Increased LDL cholesterol and atherosclerosis in LDL receptor-deficient mice with attenuated expression of scavenger receptor B1. *Arterioscler Thromb Vasc Biol* 2000; 20:1068–1073.
30. Braun A, Trigatti BL, Post MJ, *et al*. Loss of SR-BI expression leads to the early onset of occlusive atherosclerotic coronary artery disease, spontaneous myocardial infarctions, severe cardiac dysfunction, and premature death in apolipoprotein E-deficient mice. *Circ Res* 2002; 90:270–276.
31. Vergeer M, Korpelaar SJA, Franssen R, *et al*. Genetic variant of the scavenger receptor BI in humans. *N Engl J Med* 2011; 364:136–145.
32. Zanoni P, Khetarpal SA, Larach DB, *et al*. Rare variant in scavenger receptor BI raises HDL cholesterol and increases risk of coronary heart disease. *Science* 2016; 351:1166–1171.
33. Helgadottir A, Sulem P, Thorgerirsson G, *et al*. Rare SCARB1 mutations associate with high-density lipoprotein cholesterol but not with coronary artery disease. *Eur Heart J* 2018; 39:2172–2178.
34. Irene G-R, César M, Fernando C, *et al*. A key receptor involved in the progression of cardiovascular disease: a perspective from mice and human genetic studies. *Biomedicines* 2021; 9:612.
- A comprehensive article reviewing data from mice and human genetic studies regarding the association between SR-B1 and CVDs.
35. Webb TR, Erdmann J, Stirrups KE, *et al*. Systematic evaluation of pleiotropy identifies 6 further loci associated with coronary artery disease. *J Am Coll Cardiol* 2017; 69:823–836.
36. Howson JMM, Zhao W, Barnes DR, *et al*. Fifteen new risk loci for coronary artery disease highlight arterial-wall-specific mechanisms. *Nat Genet* 2017; 49:1113–1119.
37. Gilibert S, Galle-Treger L, Moreau M, *et al*. Adrenocortical scavenger receptor class B type I deficiency exacerbates endotoxin shock and precipitates sepsis-induced mortality in mice. *J Immunol* 2014; 193:817–826.
38. Liu J, Gillard BK, Yelamanchili D, *et al*. High free cholesterol bioavailability drives the tissue pathologies in Scarb1<sup>-/-</sup> mice. *Arterioscler Thromb Vasc Biol* 2021; 41:e453–e467.
- This study proposes that elevated free cholesterol content of HDL, as observed in Scarb1 deficiency, promotes accumulation of free cholesterol in tissues and may represent a biomarker in multiple pathologies.
39. Yu L, Dai Y, Mineo C. Novel functions of endothelial scavenger receptor class B type I. *Curr Atheroscler Rep* 2021; 23:6.
40. Sadder S, Carriere V, Lee W-R, *et al*. Scavenger receptor class B type I is a plasma membrane cholesterol sensor. *Circ Res* 2013; 112:140–151.
41. Tran-Dinh A, Levoe A, Couret D, *et al*. High-density lipoprotein therapy in stroke: evaluation of endothelial SR-BI-dependent neuroprotective effects. *Int J Mol Sci* 2020; 22:E106.
- This study puts forward the pivotal role of endothelial SR-B1 in the neuroprotective effect of HDL in the preservation of the blood-brain barrier in stroke.
42. Rohrer L, Ohnsorg PM, Lehner M, *et al*. High-density lipoprotein transport through aortic endothelial cells involves scavenger receptor BI and ATP-binding cassette transporter G1. *Circ Res* 2009; 104:1142–1150.
43. Huang L, Chambliss KL, Gao X, *et al*. SR-B1 drives endothelial cell LDL transcytosis via DOCK4 to promote atherosclerosis. *Nature* 2019; 569:565–569.
- The first study of a proatherogenic role for SR-B1 by promoting LDL transcytosis in endothelial cells.
44. Covey SD, Krieger M, Wang W, *et al*. Scavenger receptor class B type I-mediated protection against atherosclerosis in LDL receptor-negative mice involves its expression in bone marrow-derived cells. *Arterioscler Thromb Vasc Biol* 2003; 23:1589–1594.
45. Van Eck M, Bos IST, Hildebrand RB, *et al*. Dual role for scavenger receptor class B, type I on bone marrow-derived cells in atherosclerotic lesion development. *Am J Pathol* 2004; 165:785–794.
46. Tao H, Yancey PG, Babaev VR, *et al*. Macrophage SR-BI mediates efferocytosis via Src/PI3K/Rac1 signaling and reduces atherosclerotic lesion necrosis. *J Lipid Res* 2015; 56:1449–1460.
47. Zhao Y, Pennings M, Hildebrand RB, *et al*. Enhanced foam cell formation, atherosclerotic lesion development, and inflammation by combined deletion of ABCA1 and SR-BI in bone marrow-derived cells in LDL receptor knockout mice on western-type diet. *Circ Res* 2010; 107:e20–e31.
48. Galle-Treger L, Moreau M, Ballaire R, *et al*. Targeted inactivation of SR-B1 in macrophages reduces macrophage apoptosis and accelerates atherosclerosis. *Cardiovasc Res* 2020; 116:554–565.
- This study provides the first evidence of the atheroprotective role of SR-B1 in macrophages by promoting macrophage apoptosis in early atherosclerosis lesions.
49. Gao M, Zhao D, Schouteden S, *et al*. Regulation of high-density lipoprotein on hematopoietic stem/progenitor cells in atherosclerosis requires scavenger receptor type BI expression. *Arterioscler Thromb Vasc Biol* 2014; 34:1900–1909.
50. Koelwyn GJ, Corr EM, Erbay E, Moore KJ. Regulation of macrophage immunometabolism in atherosclerosis. *Nat Immunol* 2018; 19:526–537.
51. Khera AV, Cuchel M, de la Llera-Moya M, *et al*. Cholesterol efflux capacity, high-density lipoprotein function, and atherosclerosis. *N Engl J Med* 2011; 364:127–135.
52. Rohatgi A, Khera A, Berry JD, *et al*. HDL cholesterol efflux capacity and incident cardiovascular events. *N Engl J Med* 2014; 371:2383–2393.
53. Guerin M, Silvain J, Gall J, *et al*. Association of serum cholesterol efflux capacity with mortality in patients with ST-segment elevation myocardial infarction. *J Am Coll Cardiol* 2018; 72:3259–3269.
54. Larrede S, Quinn CM, Jessup W, *et al*. Stimulation of cholesterol efflux by LXR agonists in cholesterol-loaded human macrophages is ABCA1-dependent but ABCG1-independent. *Arterioscler Thromb Vasc Biol* 2009; 29:1930–1936.
55. Zhang W, Yancey PG, Su YR, *et al*. Inactivation of macrophage scavenger receptor class B type I promotes atherosclerotic lesion development in apolipoprotein E-deficient mice. *Circulation* 2003; 108:2258–2263.
56. Tao H, Yancey PG, Blakemore JL, *et al*. Macrophage SR-BI modulates autophagy via VPS34 complex and PPAR $\alpha$  transcription of TfEB in atherosclerosis. *J Clin Invest* 2021; 131:94229.
- This study uncovers a role of macrophage SR-B1 in autophagy in advanced atherosclerotic lesions.
57. Wang X, Collins HL, Ranalletta M, *et al*. Macrophage ABCA1 and ABCG1, but not SR-BI, promote macrophage reverse cholesterol transport in vivo. *J Clin Invest* 2007; 117:2216–2224.
58. Zhao Y, Pennings M, Vrins CLJ, *et al*. Hypocholesterolemia, foam cell accumulation, but no atherosclerosis in mice lacking ABC-transporter A1 and scavenger receptor BI. *Atherosclerosis* 2011; 218:314–322.
59. Yancey PG, Jerome WG, Yu H, *et al*. Severely altered cholesterol homeostasis in macrophages lacking apoE and SR-BI. *J Lipid Res* 2007; 48:1140–1149.

60. Gautier EL, Huby T, Witztum JL, *et al.* Macrophage apoptosis exerts divergent effects on atherogenesis as a function of lesion stage. *Circulation* 2009; 119:1795–1804.
61. Arai S, Shelton JM, Chen M, *et al.* A role for the apoptosis inhibitory factor AIM/Spalpha/Ap16 in atherosclerosis development. *Cell Metab* 2005; 1:201–213.
62. Yurdagul A, Doran AC, Cai B, *et al.* Mechanisms and consequences of defective efferocytosis in atherosclerosis. *Front Cardiovasc Med* 2017; 4:86.
63. Schrijvers DM, De Meyer GRY, Kockx MM, *et al.* Phagocytosis of apoptotic cells by macrophages is impaired in atherosclerosis. *Arterioscler Thromb Vasc Biol* 2005; 25:1256–1261.
64. Tabas I. Macrophage death and defective inflammation resolution in atherosclerosis. *Nat Rev Immunol* 2010; 10:36–46.
65. Ouimet M, Franklin V, Mak E, *et al.* Autophagy regulates cholesterol efflux from macrophage foam cells via lysosomal acid lipase. *Cell Metab* 2011; 13:655–667.
66. Liao X, Sluimer JC, Wang Y, *et al.* Macrophage autophagy plays a protective role in advanced atherosclerosis. *Cell Metab* 2012; 15:545–553.
67. Chen W, Schilperoort M, Cao Y, *et al.* Macrophage-targeted nanomedicine for the diagnosis and treatment of atherosclerosis. *Nat Rev Cardiol* 2021; 10:1–22.